ANGLIA RUSKIN UNIVERSITY

NEURAL MAPPING OF BINOCULAR AND AMBLYOPIC SUPPRESSION

AKASH SINGH CHIMA

A Thesis in partial fulfilment of the requirements of Anglia Ruskin University for the degree of

Doctor of Philosophy

Submitted:
April 2015

DEDICATION

To Sandy Gunn, without the persistence of whom this PhD may not have started, and to Lucy Catherine Hill for her boundless love and support throughout.

ACKNOWLEDGEMENTS

My sincere and immeasurable gratitude goes to my supervisory team, Dr Sarah Waugh and Dr Monika Formankiewicz, for the unending assistance, extensive hours spent on this project, including personal time, concern for my academic career, and importantly, introducing me to the fascinating world of vision science. I am indebted to you for all of your help. I also thank Robert Hess for helpful and stimulating discussions in the early stages of the project. I would also like to thank both the College of Optometrists and Anglia Ruskin University for funding the project, all of the staff in the Department of Vision and Hearing Sciences and Anglia Ruskin University Eye Clinic for their assistance, and the Faculty of Science and Technology administrators.

I am extremely grateful to the tireless participants, whose psychophysical prowess I salute. Special thanks to participant SP who exceeded requirements and was always agreed to take part in another control experiment.

I am very grateful for the people with whom I've shared a lab at some point, (Norsham Ahmad, Izzu Hairol, Sarah Lalor, and Vineela Varikuti) for the stimulating discussions and a pleasant work environment. My extended gratitude to lab mates and good friends Josselin Gautier, Stephen Ocansey and Jan Skerswetat, who knew when I needed a break even when I did not.

I would also like to express general thanks to my family, especially to Nya Pari Patel and Zorawar Matharu, for being born and being inherently wonderful. My deepest gratitude goes to Lucy Catherine Hill, for the encouragement and support, and always knowing what to say (we're doing it!). Finally, thanks to all of my friends, for reminding me that there is also life outside of work.

ANGLIA RUSKIN UNIVERSITY

ABSTRACT

FACULTY OF SCIENCE AND TECHNOLOGY

DOCTOR OF PHILOSOPHY (PhD)

NEURAL MAPPING OF BINOCULAR AND AMBLYOPIC SUPPRESSION

By AKASH SINGH CHIMA

2015

Inter-ocular suppression occurs when very different images are presented to each eye. Diplopia ensues if different images are superimposed and perceived. The brain removes this unfavourable viewing experience by suppressing one eye's input to enable clear single vision. Inter-ocular suppression during visual development occurs in response to sufficiently disparate images caused by strabismus (misalignment of the visual axis) or anisometropia (uncorrected difference in refractive error), and if persistent may result in amblyopia. This is reduced visual sensitivity, usually in one eye, to a range of visual functions that cannot be corrected by refraction. Furthermore, binocular vision is reduced or absent.

Depth and extent of suppression is measured across the central visual field in healthy participants with monocularly blurred vision, healthy participants with monocularly reduced luminance using neutral density (ND) filters, and participants with naturally disrupted binocular vision and/or amblyopia. Suppression of spatial stimuli defined by luminance (L) and luminance-modulated noise (LM) was compared to that measured for stimuli defined by contrast-modulated noise (CM), for which there is no change in mean luminance. For all stimuli suppression depth increased with increased imbalance of binocular input. Suppression was of a similar depth across the visual field with imposed blur and localised central suppression was found with ND filters. Microstrabismics showed central suppression, while strabismic amblyopes showed central in addition to hemifield suppression.

Suppression for all participants was measured to be deeper for CM spatial stimuli than for LM spatial stimuli. This is suggested to be a result of CM stimuli engaging more binocular mechanisms of processing, than LM stimuli, thereby becoming more sensitive to disruptions of binocularity such as those produced in the participants in the present study. CM stimuli are therefore more sensitive to detecting suppression, which is associated with amblyopia.

Keywords: inter-ocular suppression, amblyopia, luminance-modulated, contrast-modulated, blur, neutral density filters

TABLE OF CONTENTS

LIST OF FIGURES

LIST OF TABLES

CHAPTER 1

LITERATURE REVIEW

1.1 Introduction to inter-ocular suppression

Binocular vision is a prominent feature of mammalian visual systems, using two eyes to produce perception of a single image. In addition to providing another eye if one is damaged and a wider visual field, the overlap of each eye's visual field affords the advantages of binocular summation and stereopsis. Binocular summation is the increase in binocular over monocular sensitivity when both eyes are presented with matching stimuli to corresponding retinal points. Stereopsis is a visual system's ability to extract relative field depth information from two slightly disparate views of the same visual scene.

Inter-ocular suppression elicits repression of the visual field of one eye, so that these advantages of binocular vision are lost. Mehdorn (1989) clarifies the use of inter-ocular suppression as the description for when "a stimulus projected onto the retina of one eye is perceived with less intensity under binocular conditions than under monocular conditions". When sufficiently disparate images are presented to corresponding retinal points, diplopia results, which is the simultaneous perception of two dissimilar images. Inter-ocular suppression occurs in turn as a sensory response to the reception of incongruous images by each eye that cannot be fused (Travers, 1938; Jampolsky, 1955; Harrad, Sengpiel and Blakemore, 1996; Sengpiel and Blakemore, 1996).

Long-term inter-ocular suppression during visual development may lead to amblyopia (Sireteanu and Fronius, 1981; Harrad, 1996; Sengpiel and Blakemore, 1996). The degree of amblyopia is defined as a decrease in visual acuity in (usually) one eye with no other ocular abnormalities (Flom and Neumaier, 1966). Amblyopia is also characterised by reduced contrast sensitivity (Abrahamsson and Sjöstrand, 1988; Zhou et al., 2006; Hess et al., 2009a) more so at high spatial frequencies (Hess and Howell, 1977; Bradley

and Freeman, 1981), impaired hyperacuity and Vernier performance (Bedell and Flom, 1981; Levi, Klein and Aitsebaomo, 1985; Wilson, 1991), abnormal contour interaction (Flom, Weymoth and Kahneman, 1963; Hess and Jacobs, 1979; Levi, Hariharan and Klein, 2002), reduced binocular function including stereopsis (McKee, Levi and Movshon, 2003; Levi, McKee and Movshon, 2011; Wallace et al., 2011) and suppression of all or parts of the amblyopic eye's image (Harms, 1937; Travers, 1938; Jampolsky, 1955; Herzau, 1980; Sireteanu and Fronius, 1981; Campos, 1982; Pratt-Johnson and Tillson, 1983; Joosse et al., 1999; Hess, Mansouri and Thompson, 2010b; Li et al., 2011; Narasimhan, Harrison and Giaschi, 2012). One study reports deeper suppression with less amblyopia, i.e. smaller inter-ocular acuity difference (Holopigian, Blake and Greenwald, 1988). Other studies conclude the opposite (Sireteanu and Fronius, 1981; Li et al., 2011), such that deeper suppression is associated with greater degrees of amblyopia. Inter-ocular suppression also occurs in those with normal vision with the presentation of sufficiently different images to corresponding retinal points in each eye. The subsequent alternation in perception and suppression of images received by each eye, despite unchanging physical stimulation, is known as binocular rivalry (Levelt, 1965).

In brief, this thesis describes a novel way of measuring both the depth and extent of inter-ocular suppression across the binocular visual field in compromised normal vision and in amblyopia. Previous studies have used standard luminance stimuli to assess depth and extent of suppression. In addition to this in this study, the use of more complex stimuli defined by contrast differences is employed. These stimuli will be employed for the first time, allowing for the assessment of suppression of more complex stimuli thought to undergo extra stages of cortical processing. Inter-ocular suppression will be induced in normal participants by compromising monocular vision using either dioptric blur or neutral density filters. Monocular dioptric blur (Barbeito, Bedell, Flom and Simpson, 1987; Levi and Klein, 1990b, 1982a; b; Pianta and Kalloniatis, 1998; Song, Levi and Pelli, 2014) and neutral density filters (Pugh, 1954; von Noorden and Leffler, 1966; de Belsunce and Sireteanu, 1991; Leonards and Sireteanu, 1993; Baker, Meese and Georgeson, 2007; Baker,

Meese and Hess, 2008; Zhang, Bobier, Thompson and Hess, 2011; Zhou, Jia, Huang and Hess, 2013) have previously been found to simulate both monocular and binocular viewing in amblyopia. Using these simulations, I hope to evaluate this new suppression mapping tool for both standard and more complex visual stimuli, as a potential clinical tool. Results will also give an indication of suppressive mechanisms on binocular perception in patients with compromised monocular vision such as in monovision contact lens wear, or in patients with diseases affecting one eye more than the other, e.g. cataract, age-related macular degeneration and optic neuritis.

Initially, current literature on inter-ocular suppression will be reviewed to justify my choice of suitable stimuli and experimental paradigm for the experiments described further on in this thesis. The ultimate aim of this thesis is to carefully evaluate a new tool for quantifying depth and extent of inter-ocular suppression.

1.1.1 Suppression and amblyopia

The etymology of the word amblyopia is widely described as a derivative of the Greek *amblyos*- 'blunt', and *opia*- 'vision'. The degree of amblyopia is defined as the reduction in acuity, or inter-ocular visual acuity difference (Flom and Neumaier, 1966). An early account (Bethune, 1846) gives the broad definition of "weakness of sight", and indeed describes the amblyopic eye as being partially blind. Bethune (1846) attributed this weakness of sight to a variety of non-ocular causes, including lack of "pleasant" weather, literacy, and the poor quality of printed literature. However, these claims were anecdotal and no data were shown to support these assumptions. The total or partial blindness, without any reasons attributed to changes in ocular anatomy seen with ophthalmoscopy described by Bethune (1846), implies that the affected eye does not contribute to binocular vision, a view shared by Johnson (1893). A few years after Bethune, Albrecht von Graefe (von Graefe, 1856) described a contrasting opinion of how a strabismic eye *does* contribute to binocular perception and also the expansion of the binocular, versus the monocular visual field in exotropes. In the first recorded measure of amblyopic suppression, he used a simple apparatus: red

glass, prisms and a candle. The amblyopic eye was suppressed if the participant viewed the candle flame as red when the red glass was in front of the fixing eye. If a red and a yellow candle flame were seen, diplopia was present. Prisms were used to align the images on each fovea and measure the angle of squint. Although von Graefe demonstrated the presence of suppression in strabismus, there has subsequently been some controversy regarding the relationship between suppression and amblyopia, which will be explored presently.

Suppression is widely accepted as the visual system's way to cope with confusion or diplopia, i.e. the simultaneous perception of two non-fusable retinal images. Contrasting beliefs as to the role of suppression in amblyopia have been offered. On the one hand, strong suppression has been found with small inter-ocular acuity differences (Holopigian et al., 1988). On the other hand, positive correlations between depth of suppression and degree of amblyopia have been reported (Sireteanu and Fronius, 1981; Li et al., 2011, 2013; Narasimhan, Harrison and Giaschi, 2012), and some authors have suggested a causal relationship between suppression and amblyopia (Sireteanu and Fronius, 1981), as discussed further on in this review.

Holopigian et al. (1988) examined the relationship between the inter-ocular suppression and the degree of amblyopia in five strabismics (two of whom were clinically amblyopic, defined as two or more lines of inter-ocular acuity difference) and three anisometropes (all of whom were amblyopic). Four normal observers also took part in the experiments. Amblyopia was quantified as the elevation of amblyopic relative to non-amblyopic eye contrast detection thresholds, measured with sinusoidal gratings of 3.3 c/deg, as this spatial frequency is close to the peak of the human contrast sensitivity function (Campbell and Robson, 1968). Suppression was estimated dichoptically using contrast increment thresholds. Here two identical horizontal sinusoidal gratings were presented to each eye (10% pedestal contrast). A contrast increment was added to either the top or bottom half of the suppressed eye grating only (during dichoptic viewing) and participants indicated which half contained the increment.

The larger the difference in contrast sensitivity between the amblyopic and non-amblyopic eyes, the smaller the increment threshold added to the amblyopic eye's stimulus was required for a change in the stimulus to be detected, i.e. to break down the suppression. This is illustrated as a negative correlation between depth of inter-ocular suppression and the difference in monocular contrast thresholds in amblyopic eyes (Figure 1.1 - top).

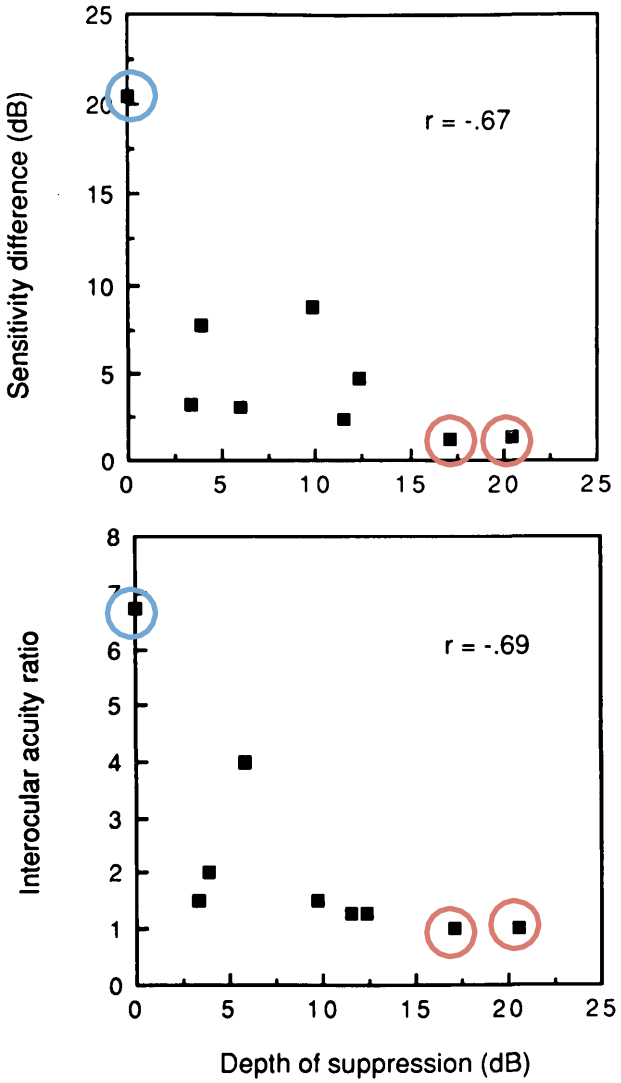

Figure 1.1. Top: Difference in monocular contrast sensitivities of the amblyopic and non-amblyopic eyes of nine amblyopes compared with depth of suppression. **Bottom**: Comparing the inter-ocular acuity ratio and the depth of suppression for the same participants. Red circles denote non-amblyopic participants, blue circle denotes participant LP (see text). Correlation values are shown in insets. From Holopigian et al. (1988).

The authors conclude that with greater degrees of amblyopia comes less suppression. However, the data circled in red denotes participants that are non-amblyopic, i.e. no inter-ocular difference in visual acuity, with alternating esotropia. The blue circle represents an *intermittent* esotrope with a large (7 D) difference in refractive error and a difference in visual acuity (right eye: equivalent to 6/40; left eye: 6/6), though with measurable stereopsis (400 arc secs - Titmus stereotest). This level of stereopsis indicates that information between the eyes is combined reasonably well, and therefore lack of suppression measured may be expected. If one excludes those participants who have minimal inter-ocular visual acuity difference (red circles), or clinically measurable stereopsis indicating good binocular fusion (blue circles), then the strong correlation is severely weakened (-0.07 for inter-ocular acuity difference and -0.02 for monocular sensitivity). Furthermore, the contrast of the pedestal grating in the suppression depth measurements of 10% is relatively low for amblyopes. It has previously been shown that ability to detect an increment improves with lower pedestal contrasts closer to detection threshold (e.g. Kingdom and Whittle, 1996). As thresholds are higher for amblyopic eyes, these eyes may have improved increment detection thresholds at 10% pedestal contrast relative to non-amblyopic eyes. This may account for deeper suppression found with lower degrees of amblyopia.

More recently, Li et al. (2011) used a dichoptic global motion paradigm to investigate the relationship between depth of suppression and degree of amblyopia. Amblyopic participants (n=43) aged between 9 and 56 years (mean age 21±12 years) were involved in the study. Strabismic amblyopes had an angle of less than 35 prism dioptres and anisometropic amblyopes a difference in refractive error greater than 1 D (spherical equivalent) with no strabismus. Acuity was different inter-ocularly by at least one line on a visual acuity chart, with worst acuity of 6/30. For the dichoptic motion coherence threshold determination, random-dot kinetograms were displayed in head-mounted displays with one screen for each eye. Separate images were presented to each eye. Stimuli were signal dots that all moved in the same direction, and

noise dots that moved in random directions, and each population of dots were presented to one eye at a time. Images to each eye were fused, and participants indicated the coherent direction of motion. In order to measure depth of suppression, the contrast of dots presented to the amblyopic eye (either signal or noise) was fixed at 100% and the dots shown to the non-amblyopic eye were varied in contrast. A “balance point” was determined which was the non-amblyopic eye dot contrast at which the ratio of signal to noise dots was the same regardless of which eye the signal dots were presented to. This balance point gave a measure of depth of suppression, as it represents contrast attenuation in the non-amblyopic eye until both eyes performed equally. Balance points for each of the participants are plotted against inter-ocular acuity ratio, i.e. degree of amblyopia (Figure 1.2).

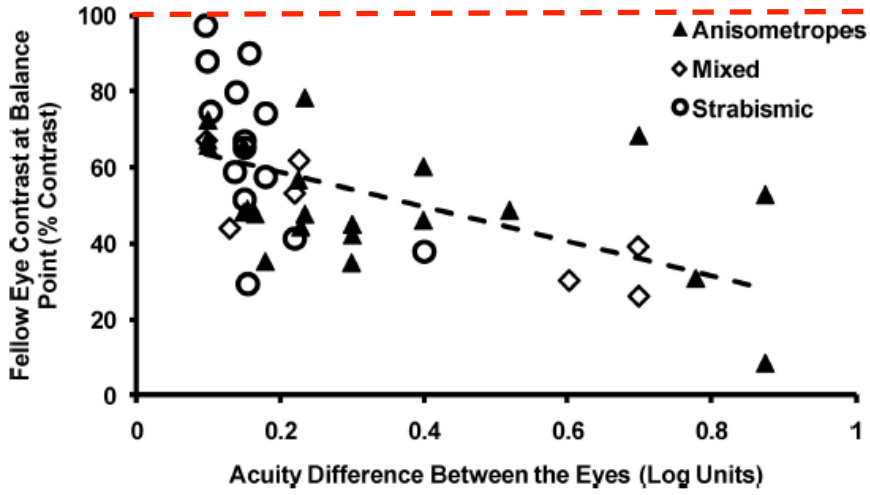

Figure 1.2: Amount of contrast adjustment to the fixing eye to allow normal binocular combination of information between the two eyes, compared with the acuity difference. Dashed red line shows no suppression measured. Adapted from Li et al. (2011)

Contrary to Holopigian et al. (1988), Li et al. (2011) showed deeper suppression with greater degrees of amblyopia. Strabismic and mixed amblyopes (both strabismic and anisometropic as defined by the authors) showed significant negative correlations: ρ = -0.62 and ρ = -0.82, respectively. Anisometropic amblyopes showed a non-significant negative correlation ρ = -0.42, suggesting

that the presence of strabismus influenced the strength of the relationship between acuity difference and balance point for the mixed amblyopes. Data in Figure 1.2 suggest that larger degrees of amblyopia (i.e. inter-ocular acuity difference) result in deeper suppression. If no suppression were present, no contrast attenuation would be required to equate performance between the eyes, shown as the dashed red line in Figure 1.2. Li et al. (2013) adjusted the global motion coherence paradigm for assessment of anisometropic suppression. Aniseikonia associated with anisometropia was shown to affect signal and noise segregation, and to remove this cue all dots were randomised in size. With this adjusted technique, depth of suppression again correlated with degree of amblyopia.

Narasimhan et al. (2012) also claim that stronger suppression is associated with deeper amblyopia. A similar dichoptic global motion task was employed to measure suppression, although participants were strabismic or anisometropic amblyopic children (5-16 years) and their data were compared with those from age-matched normals. Although no significant correlation was found between the inter-ocular difference in acuity and suppression, amblyopic children who have previously responded positively to amblyopia treatment gave measures that were significantly lower for suppression than those that had a negative response to treatment (calculated as visual acuity before and after treatment). This may provide indirect evidence of a positive link between suppression and amblyopia, i.e. if amblyopia is still present suppression was not broken down during treatment. The most widely-used current treatment of amblyopia is occlusion therapy. It focuses on monocular improvement of amblyopic eye vision. As harmonious interaction between the two eyes is not encouraged in occlusion therapy, binocularity may not be expected to improve, due to residual suppression.

More indirect evidence for a positive correlation between amblyopia and suppression comes in the form of recent amblyopia treatments being aimed at suppression. Hess, Mansouri and Thompson (2010a) showed in their case-study that repeatedly measuring suppression (with a dichoptic global motion

coherence paradigm, as explained above) showed a reduction in suppression (and therefore improvement in binocular combination) with a concurrent improvement in both stereopsis and visual acuity. Other recent studies that aim to improve binocular combination by reducing suppression also find improvements in visual acuity and stereopsis (Hess, Mansouri and Thompson, 2010b; Black, Thompson, Maehara and Hess, 2011; To et al., 2011; Knox, Simmers, Gray and Cleary, 2012).

In conclusion, stronger evidence exists to support a positive than negative correlation between suppression depth and degree of amblyopia. Being able to accurately quantify suppression in amblyopia is required, both as an indicator of degree of amblyopia and also to assess treatment success. The main focus of this thesis is the quantification of inter-ocular suppression and its relevance to monitoring suppression in amblyopia. Inter-ocular blur suppression will first be investigated, as monocular blur in normal eyes has been shown to simulate spatial vision in amblyopia (see Section 1.5.1). It is also of direct clinical relevance to anisometropia, monovision contact lens correction for presbyopia, and any pathology resulting in differential inter-ocular blur.

1.1.2 Blur suppression

Although suppression cannot be directly controlled, image dissimilarity that leads to suppression can. One way to do this is by using different levels of inter-ocular blur (Section 1.5.1 provides a review of blur as a model for amblyopia).

Inter-ocular blur suppression can be used advantageously in those with normal binocular vision. Monovision contact lens wear for presbyopia involves the refractive correction of one eye for distance viewing, and the other eye for near vision (for reviews, see Johannsdottir and Stelmach, 2001; Evans, 2007). At either distance, one eye's image is blurred relative to the other. Rather than experiencing diplopia due to image dissimilarity, or blurred fusion at any distance, the image of one eye is suppressed. Although affording clear single vision at different distances without the need to change refractive correction,

stereopsis is degraded, even when compared to blurring both eyes equally (e.g. Wood, 1983; Lovasik and Szymkiw, 1985; Back, Grant and Hine, 1992; Kirschen, Hung and Nakano, 1999)

Simpson (1991) investigated depth and extent of inter-ocular blur suppression. Stimuli are shown in Figure 1.3, and are dark triangles on a high luminance background (175 cd/m^2), with a contrast of 30%. Presented to one eye were two squares (68.75 arcmin side length) that each contained two triangles (34.38 arcmin). Stimuli to each eye were dissociated with a vertical prism. The fused percept in the absence of suppression would be three stacked squares as in Figure 1.3.

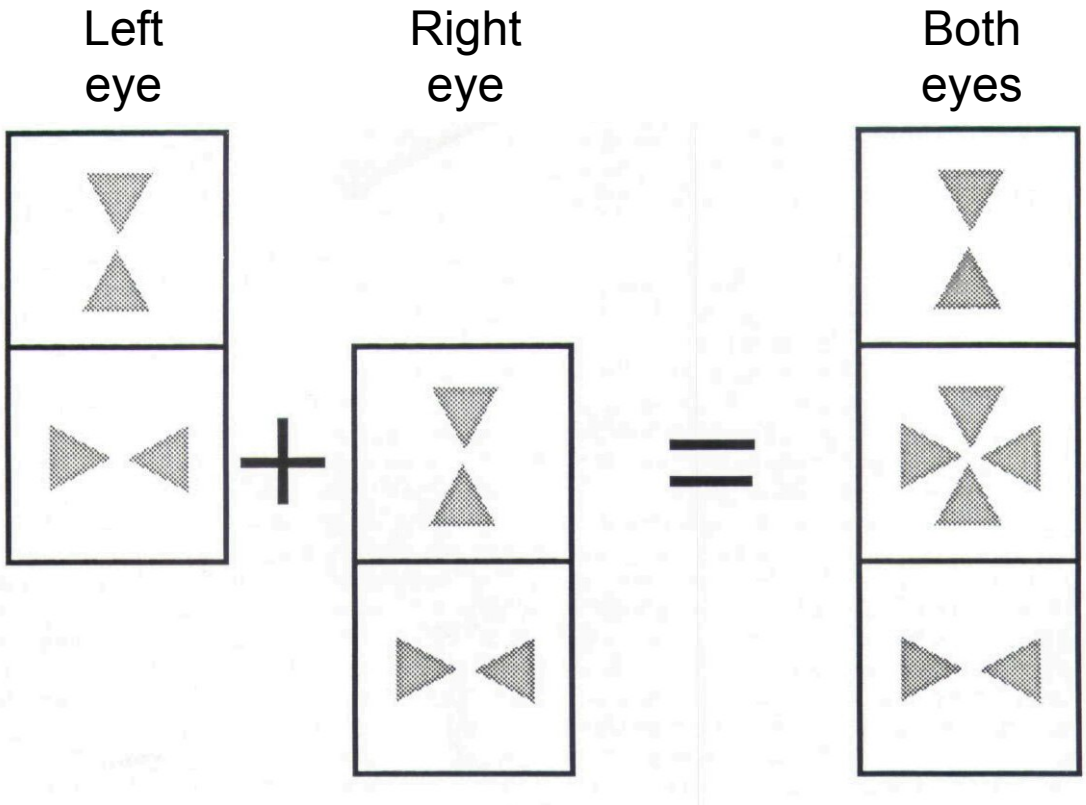

Figure 1.3: Dichoptic stimuli presented to each eye individually and fused to make the percept on the right of the Figure. Adapted from Simpson (1991)

The stimuli were varied in three ways: 1) the size of the original stimulus was

made a factor of two smaller, 2) the contrast of the triangles was increased by a factor of approximately two, and 3) the background with and without more fusional elements present (i.e. square-wave grating background). Blur was presented in front of right and left eyes monocularly, with a positive lens providing effective blur from 0 D to +3 D in 0.25 D steps. Testing distance was 4m. Using a two alternative forced-choice task, five binocularly normal participants decided whether the Maltese cross in the middle square was incomplete or complete (i.e. suppression or no suppression, respectively). Suppression thresholds were calculated as the level of monocular defocus that produced a 50% chance of suppression. Histograms with the blur levels for different participants and conditions can be seen in Figure 1.4.

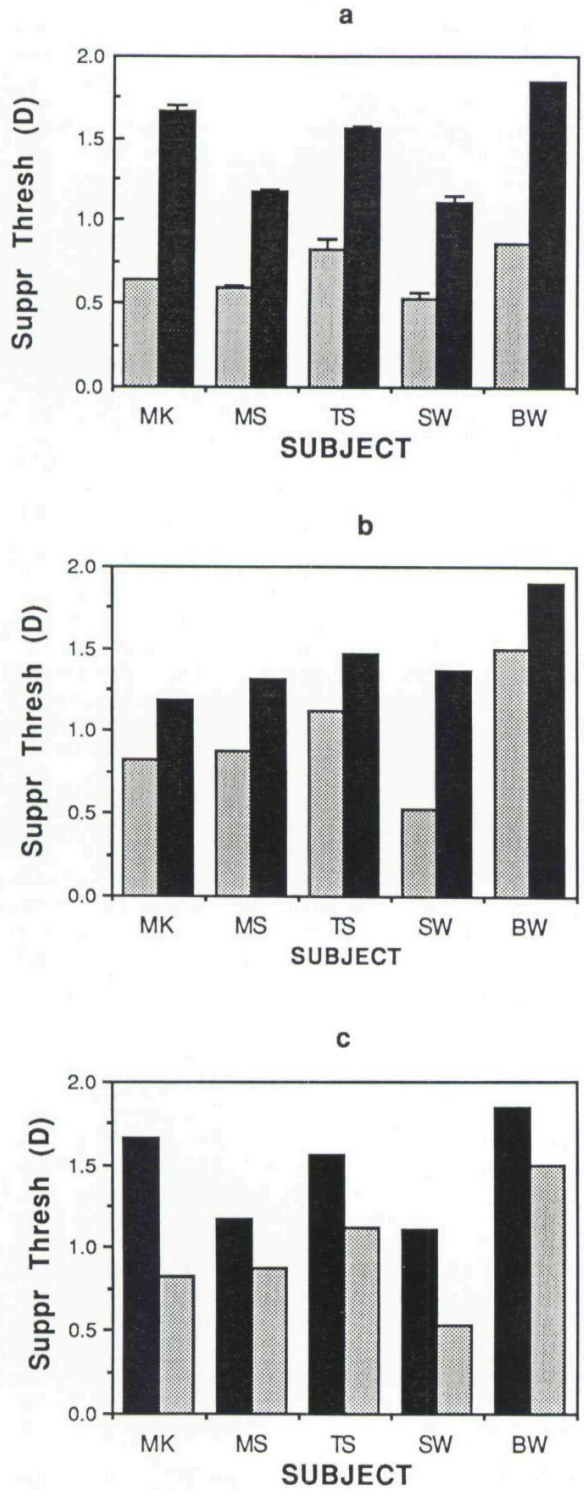

Larger stimuli (dark bars – 68.75 arcmin) and smaller stimuli (light bars – 34.38 arcmin)

High contrast (dark bars – 63%) and low contrast (light bars – 30%)

More fusional elements (dark bars) and fewer fusional elements (light bars)

Figure 1.4: Suppression thresholds defined by the amount of monocular defocus for A) larger (dark bars) and smaller (light bars) targets. B) High contrast (dark bars) compared with lower contrast (light bars) targets. C) More fusional elements (dark bars) compared with fewer fusional (light bars) targets, where the former stimuli were more spatially correlated.

Simpson's (1991) results for the differently sized suppression stimuli are shown in Figure 1.4A. For all participants the larger stimuli required a significantly higher level of monocular blur before it was suppressed (1-1.75 D for 34 arc min compared with 0.5-0.75 D for 17 arc min stimuli), where both sizes fall within the foveal area. Significantly higher levels of monocular blur were required to suppress higher compared to lower contrast stimuli (Figure 1.4B). Stimuli with more compare to fewer fusional elements required significantly more monocular blur to be suppressed (Figure 1.4C). Taken together, these results suggest that stronger stimuli (i.e. larger, higher contrast, more binocular elements) require greater inter-ocular blur to be suppressed.

Presence of inter-ocular blur suppression was inferred with another type of stimulus by Sireteanu, Fronius and Singer (1981), who measured local stereopsis at different locations across the visual field of strabismic and anisometropic amblyopes. The authors used a dynamic motion-in-depth paradigm to measure stereopsis. Two squares (side length 2.5 deg) were presented dichoptically using polarising filters, which resulted in the luminance of the stimuli being 3 cd/m^2. The luminance of the stimulus presented on the screen of 1 cd/m^2 resulted in a stimulus contrast of 67%. The squares moved smoothly in opposite horizontal directions until their centres were separated by 2.5 deg, over a period of 2 s. The authors chose these parameters to produce a "powerful impression" of motion-in-depth. Crossed disparities were used so that when fused, a square was perceived to be moving towards the participant. Monocular blur was also induced in one normal participant. A lack of measurable stereopsis at any location suggested that suppression was present.

Figure 1.5 shows the results for the blurred normal participant. Each diagram represents the binocular visual field (80 deg horizontally by 40 deg vertically) for a different level of monocular blur. Each of the 19 points measured on the visual field have either one, two or three dots, representing a subjective measure of the intensity of the effect, fewer dots being lower intensities. An arrow denotes a horizontal direction of perceived movement, implying that in this case, slight suppression rather than fusion may have occurred. A black area indicates no

perceived stereopsis, again implying suppression.

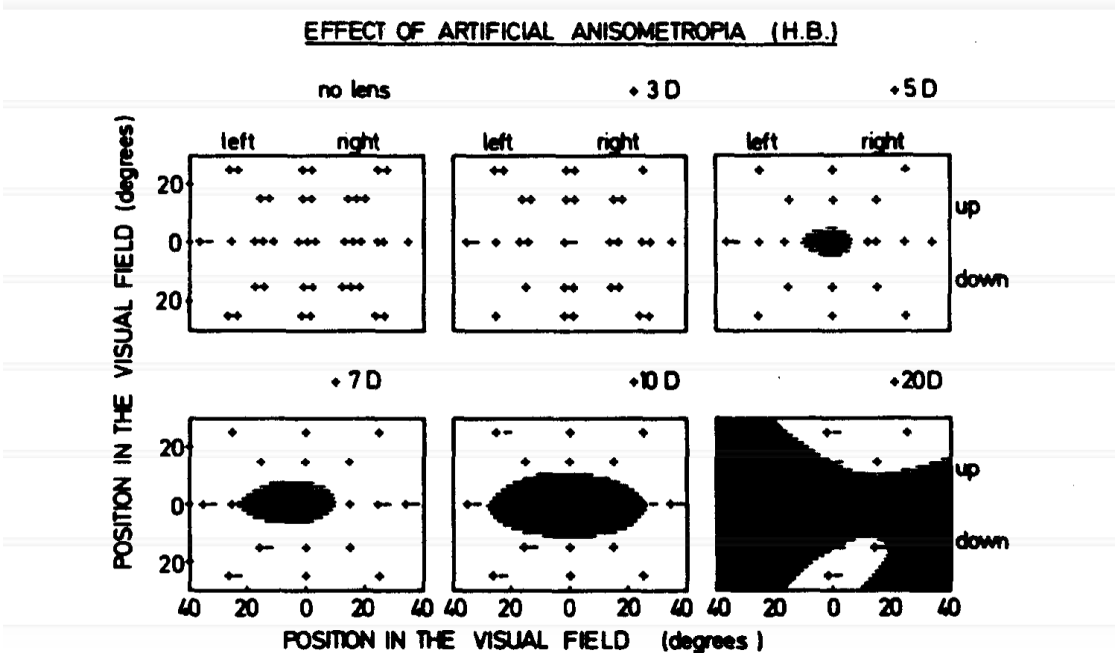

Figure 1.5: Effect of blur on local stereopsis measurements across the visual field with increasing amounts of dioptric monocular blur. From Sireteanu, Fronius, and Singer (1981)

The results in Figure 1.5 show that increasing monocular blur results in larger areas of no stereopsis, which could be interpreted as areas of suppression. If this is the case, central localised areas of suppression that increase with increasing levels of blur are found. Other studies have also found reduced stereopsis with monocular blur (Wood, 1983; Goodwin and Romano, 1985; Lovasik and Szymkiw, 1985). Stereopsis is also reduced with monovision contact lens correction for presbyopia (Back, Grant and Hine, 1992; Kirschen, Hung and Nakano, 1999). These reductions in stereopsis worsen with increased inter-ocular blur, and could be due to inter-ocular suppression of the more blurred image.

Blur suppression may also depend on stimulus visibility. Pardhan and Gilchrist (1990) investigated the effect of monocular blur on visual contrast sensitivity in binocular conditions, i.e. binocular summation. Participants viewed a vertical sinusoidal grating (6 c/deg, 8 deg diameter circular mask) on two screens

through a stereoscope. Monocular blur was achieved with plus lenses in front of one eye. Contrast sensitivity thresholds were measured in three scenarios: monocularly with left eye only (right eye viewed isoluminant screen), monocularly with right eye viewing through a blurring lens (left eye occluded), and binocularly with the right eye blurred.

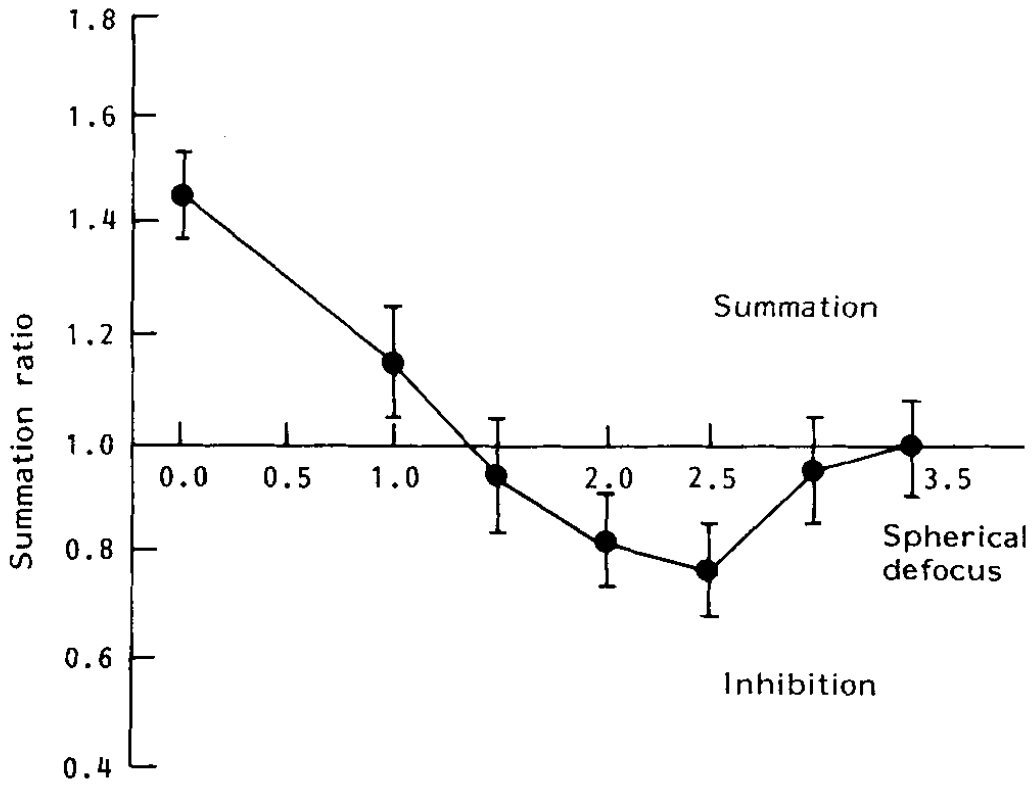

Figure 1.6: Binocular summation ratios averaged across 10 participants, with different levels of monocular defocus. From Pardhan and Gilchrist (1990)

Figure 1.6 shows the results from the experiment. The ratio of binocular/monocular sensitivity (binocular summation) was averaged across 10 normal participants plotted for each level of monocular blur. With no blur, binocular summation was above √2, as found previously (e.g. Harwerth, Smith and Levi, 1980; Legge, 1984). Increasing monocular blur decreased the level of binocular summation until +1.5 D blur, where binocular sensitivity becomes worse than monocular sensitivity. Binocular inhibition is strongest at +2.5 D monocular blur, above which it starts to decrease until +3.5 D blur where monocular and binocular contrast sensitivity is again equal. This return to

monocular sensitivity is not discussed by the authors, however it may be due to binocular contrast averaging at +2.5 D, progressing to complete suppression of the blurred eye image at +3.5 D. Legge and Rubin (1981) also demonstrated binocular contrast averaging of gratings of two different contrasts presented to each eye. This follows a distinctly different pattern to the effect of increasing inter-ocular blur on stereopsis just described (Sireteanu et al., 1981), demonstrating that the link between inter-ocular suppression and stereopsis is unclear, and therefore may not be directly related.

An electrophysiological study measuring dichoptic cortical visual evoked potentials (VEP) with one eye dioptrically blurred (0 – 2.5 D blur, in 0.5 D steps) found a lack of the normal increased binocular compared with monocular response to viewed phase-alternating gratings (Fiorentini, Maffei, Pirchio and Spinelli, 1978). Participants also indicated perceptual suppression with dichoptic suppression markers. This reduced dichoptic compared with binocular (not blurred) evoked potential amplitude occurred simultaneously with perceptual suppression of the blurred stimuli during binocular viewing. As the highest blur level was 2.5 D, whether binocular inhibition reduced when increasing to 3.5 D (as in Pardhan and Gilchrist, 1990) was not assessed. A more recent study found similar results across different eccentricities (Leaney, Klistorner, Arvind and Graham, 2010) ranging from the fovea to 24 deg. In that study, stimuli were reversing checkerboards at different locations of the visual field (spatially scaled with eccentricity). Suppression was measured as the reduction in binocular compared with monocular VEP amplitude without blur and with effective inter-ocular blur of 1 and 3 D, and was deeper centrally with both blur levels, though to a greater extent with 3 D blur. Release of suppression in the non-blurred eye, as measured by increase in VEP amplitude, also increased with increasing blur in a similar pattern across the visual field.

In summary, the aforementioned studies show that increasing dioptric blur monocularly reduces binocular visual function. Successful monovision contact lens wear relies on the presence of suppression. Therefore controlled levels of monocular blur during binocular viewing can be used to trigger suppression of

the more blurred image, and model monovision contact lens wear, as well as pathological conditions where differential inter-ocular blur is present. Dioptric blur has also been used to model amblyopia in normals, which is discussed later in this review (Section 1.5.1). The presentation of differentially blurred, non-fusable images to each eye of normal observers can also lead to the continuous alternation in perception between each image individually (Fahle, 1983), known as binocular rivalry (Levelt, 1968). The following section acknowledges that binocular rivalry could be induced in normals with monocular blur, and explores whether this could affect the measurement of inter-ocular blur suppression, or indeed amblyopic suppression.

1.1.3 Binocular rivalry suppression

The presentation of two very different images to each eye of participants with normal binocular vision leads to an alternation in perception between the two images. Whilst one image is dominant, the other is being suppressed. During blur suppression, the imposition of monocular blur during binocular viewing may cause images to be sufficiently different to cause rivalry. Taken with the suggestion of some studies that amblyopic suppression is a one-sided form of binocular rivalry (Sireteanu and Fronius, 1981; Harrad, 1996), a review of binocular rivalry is important to understand amblyopic suppression.

Binocular rivalry was first described by the polymath Giambattista della Porta in 1593 when he placed a partition between the eyes and presented two different pages of a book to each eye simultaneously. He stated that only the page presented to the right eye could be seen, unless “visual virtue” was drawn from the right to the left eye. Rivalry was induced by the presentation of different images to each eye; when one image is being perceived the other is being suppressed. Le Clerc in 1712 aligned the rivalrous images by over-converging his eyes so the centre of each different stimulus was imaged on the separate foveae. Dutour in 1761 stimulated rivalry by the use of a prism in front of one eye to align two rivalrous images (Wade, 1998).

Amblyopic and rivalry suppression are similar in that one eye's image does not reach perception, despite an unchanging physical stimulus. However, there are several differences in these types of suppression such as: 1) suppression of similar stimuli presented to each eye does not occur in normal vision (with no inter-ocular blur), but does in strabismics (Schor, 1977); 2) strabismic amblyopic suppression depth reduces with physical dissimilarity of images presented to corresponding retinal points (Kilwinger, Spekreijse and Simonsz, 2002); 3) wavelength-specific loss occurs during rivalry suppression, but not during strabismic suppression (Smith, Levi, Manny and Harwerth, 1985); 4) each type of suppression has different time courses of alternation (de Belsunce and Sireteanu, 1991), i.e. strabismic suppression is constant. Depth of suppression of horizontal sinusoidal gratings was the same for clinical suppressors and normals during binocular rivalry (Holopigian, 1989), again suggesting that they may be processed by a similar neural process, which is therefore important to try to understand.

A 'hybrid model' of binocular rivalry (Tong, Meng and Blake, 2006) is depicted in Figure 1.7. The model is so-called as it accounts for rivalry at different levels of visual processing; between monocular neurons (e.g. striate cortex or the lateral geniculate nucleus), and between binocular neurons involved with the processing of coherent patterns. Blue lines with dots represent inhibitory neuronal connections, and the red lines with arrows excitatory connections. Left eye and right eye columns in Figure 1.7A represent a lower level, such as V1 where monocular neurones from left and right eyes, respectively, inhibit each other. Blake, O'Shea and Mueller (1992), for example, demonstrated that this inter-ocular competition could occur with small (100 arc min^2) diagonally orientated sinusoidal gratings (6 c/deg, 80% contrast), as there are periods of exclusive dominance of each of the left and right eye images over a 240 s period. As grating size increased, a mixed perception of a patchwork of the two gratings was perceived.

Figure 1.7B depicts two adjacent neurones that receive input from each eye. Among the lower-level monocular neurones (e.g. V1 or indeed the LGN),

reciprocal excitatory connections can promote grouping by eye, or inter-ocularly by orientation preferences of the adjacent monocular neurones. Excitatory connections between higher-level binocular neurones also lead to pattern-based grouping of similar stimulus attributes. Figure 1.7C illustrates how feedback connections could modulate the strength of suppression of one of the eyes or indeed a coherent complex visual stimulus (Tong et al., 1998). Therefore, stimuli processed in extra-striate areas (e.g. coherent patterns) can also undergo rivalry suppression. If the same is true for amblyopic suppression, stimuli of different complexity can also be used to explore the amblyopic deficit at different stages of visual processing. The neural locus, or loci, of amblyopic suppression may then be uncovered. This concept is discussed in Section 1.3, whilst Section 1.2 describes the functional physiology of an amblyopic visual system.

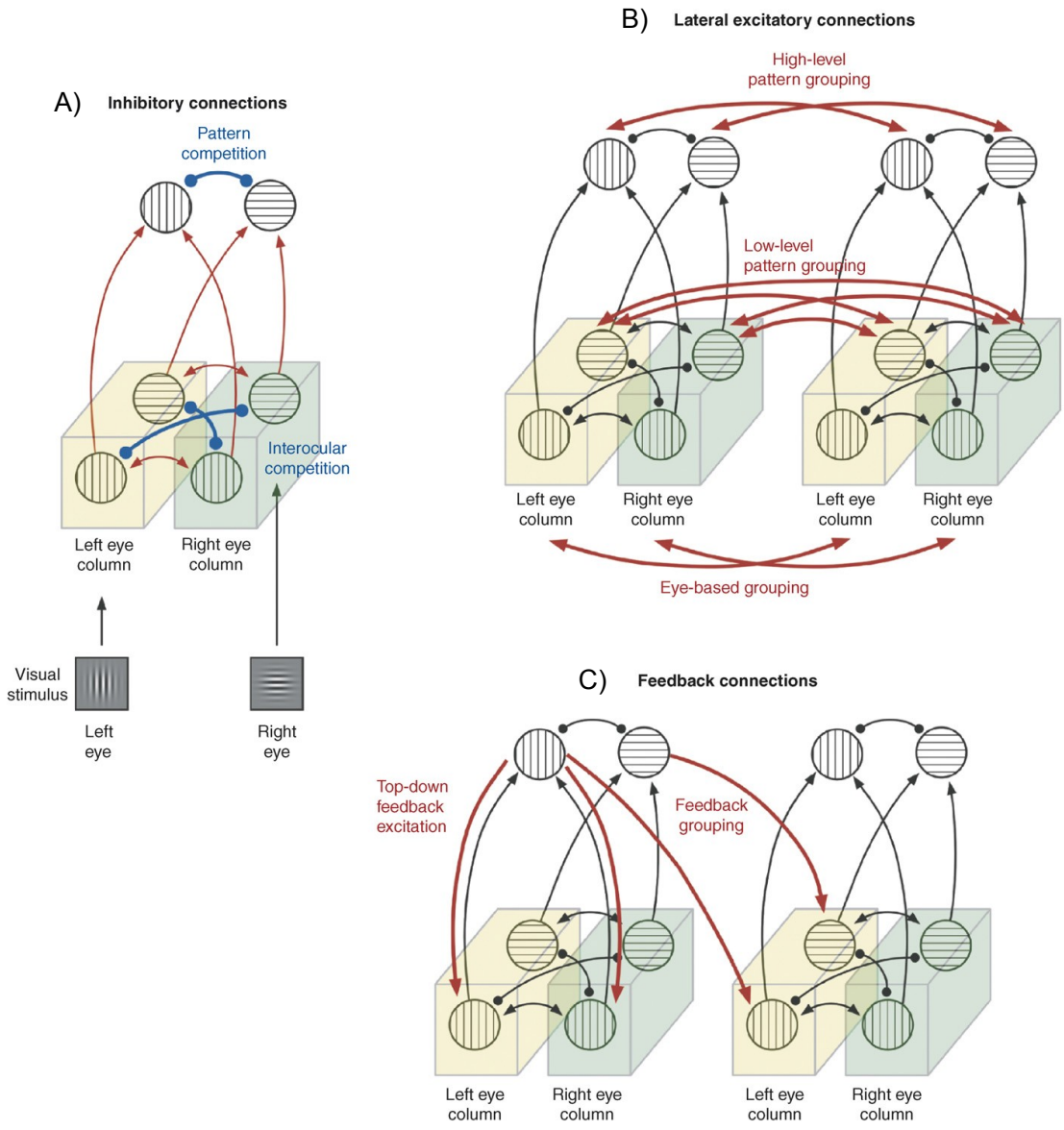

Figure 1.7: Schematic diagram of inhibitory (lines with filled circles) and excitatory (lines with arrows) connections in the hybrid model of binocular rivalry. A) Reciprocal inhibitory connections (blue lines with circles) that may account for eye dominance suppression and pattern dominance suppression. B) Reciprocal excitatory connections (blue lines with arrows) that account for eye-based grouping, low-level grouping between monocular neurones with similar pattern preferences, and high-level pattern-based grouping between binocular neurones. C) Excitatory feedback projections (red lines with arrows) that may account for top-down influence of visual attention. From Tong, Meng, and Blake (2006).

1.2 Physiology of amblyopia

Determining the neural locus of the deficit in amblyopia has been greatly aided by single neuron recordings performed in the 20th century on awake, behaving non-human animals. The site of the deficit in amblyopia is accepted to be further along the visual pathway than the retina (for review, see Hess, 2001). As fMRI becomes more available to researchers, the correlation between brain activity and perception can also be used to elucidate parts that function abnormally in the human amblyopic visual cortex. Understanding the parts of the cortex that are affected in amblyopia can be combined with the knowledge of the loci of visual processing of different stimuli. This will benefit the design of stimuli to target inter-ocular suppression of specific areas of the visual cortex.

1.2.1 Lateral geniculate nucleus

One lateral geniculate nucleus (LGN) is found in each cerebral hemisphere and it is made up of six layers of neurones. Layers 2, 3 and 5 receive input from the temporal fibres of the ipsilateral retina, and the nasal retinal fibres of the contralateral retina feed to the remaining three layers (Le Gros Clark and Penman, 1934), although input from corresponding retinal points in each eye is not yet combined. Additionally, the LGN receives input from the visual cortex. Guillery (1967) showed that damaging the cat cortex resulted in degeneration of coarse fibres between the LGN and the visual cortex.

The four dorsal layers of the LGN are part of the parvocellular pathway, which responds selectively to form and colour, whilst the remaining two layers are part of the magnocellular pathway concerned with depth and motion (for a concise review see Livingstone and Hubel, 1988). More recently, the koniocellular pathway has been demonstrated to exist in thin inter-layers of the LGN, with a role in carrying short-wavelength colour information to cytochrome-oxidase blobs of V1 (Hendry and Reid, 2000). The receptive fields of monkey LGN cells were found by Wiesel and Hubel's (1966) seminal series of single unit recording studies, to have antagonistic centre-surround concentric organisations, similar to the receptive fields of retinal ganglion cells.

Hess, Thompson, Gole and Mullen (2009) investigated the activity of the human LGN in amblyopia using functional magnetic resonance imaging. As the visual cortex is the area where information from the two eyes is combined, the visual deficit in amblyopia was thought to occur here. Hess et al. (2009) presented high contrast square-wave checkerboard stimuli (check size, 1.5 deg; field size, 12 by 10 deg) to the amblyopic and non-amblyopic eyes of six amblyopic participants: three strabismic; one anisometropic; and two form deprivation amblyopes. The results suggest that the LGN has reduced function in amblyopes. However, LGN changes are likely to be affected by cortical deficits via corticogeniculate feedback connections. As information is not combined between the two eyes at the LGN, it is unlikely that the LGN is where the amblyopia deficit originates.

1.2.2 Visual cortex

After the LGN, the next stage in the visual pathway is the primary visual cortex. The architecture of the human visual cortex was investigated in 1910 by Korbinian Brodmann (Zilles and Amunts, 2010). He believed that the brain was separated into localised functional areas, as a result of lesion studies on humans and investigating animal brains. He also found that the visual cortex (Brodmann area 17) was subdivided into six layers. The Russo-Japanese war saw many brain injuries that exhibited visual field defects. Tatsuji Inouye (1909, as cited by Glickstein and Whitteridge, 1987) compared lesions of the visual cortex with visual field defects in 29 cases of brain injury during this time, and interestingly found, amongst many other things, that a larger area of cortex was dedicated to the central representation of the visual field, and furthermore that this area was located in the cortex most posteriorly.

Throughout the 20th century, techniques of cell recording advanced, allowing the recording of responses from one neuron, as opposed to a group of neurons (Barlow, 2003). This led to further description and elucidation of the architecture of the visual cortex in non-human animals (e.g. Barlow, 1953; Hubel and Wiesel, 1959, 1960; Daniel and Whitteridge, 1961). Another way has been to correlate

activity of specific areas of the human brain in vivo (Rorden and Karnath, 2004) using electrophysiological and functional imaging methods. One advantage of these modern techniques over single cell recording or lesion studies, is that the inference of a specific function can be attributed to more than one area of the brain that is active when viewing a specific stimulus. With respect to the investigation of neural loci for processing of different visual stimuli, many areas may contribute to the visual percept.

Hubel and Wiesel (1965) surgically induced divergent strabismus (by medial rectus section) in four post-natal kittens during the period at which their eyes were beginning to open. Single-unit recordings at the visual cortex at 3 months of age found that most cells were driven by one eye only, but that there were regions where either only the contralateral eye activated the cells, as well as a few cells that were driven binocularly. Distribution of ocular dominance columns was abnormal. In one particular cat, 60% of cells were driven by one eye only, as opposed to 20% in binocularly normal kittens. This classical finding suggested that there is a loss of binocular cells after disruption to binocularity by the induction of a squint. In a more extreme example, in which one eye of a group of macaque monkeys was enucleated (Hubel, Wiesel and LeVay, 1977), a decrease in size of the columns driven by the enucleated eye was accompanied by an expansion in the columns driven by the remaining eye.

Data from studies such as these, suggest that binocularly-driven cells are lost in monocular animals, and that potentially this is what happens in human amblyopia. However, animal studies that induced anisometropia, strabismus, or form deprivation did so in extreme ways, which may not mimic the case for humans with amblyogenic factors. In one study on a human amblyope, a 79-year old female with left esotropia and visual acuity in the amblyopic eye of 6/240, Horton and Hocking (1996) carried out post-mortem cytochrome oxidase staining (which is correlated to functional neuronal activity) on the LGN and visual cortex. Staining revealed no shrinkage of ocular dominance columns as would be expected from the results of Hubel et al. (1977). This discrepancy may be due to differences in species, but also could be due to the naturally occurring

amblyopia in this human, rather than the experimentally induced amblyopia, in the strabismic monkey.

Crawford, Smith, Harwerth and Von Noorden (1984) prevented the formation of binocular interactions by the continuous use of prisms in three rhesus monkeys between 30 and 60 days of age. Three years of normal binocular experience followed, and then recordings were made from 880 neurones. This experimental design may be more akin to human amblyopia development than surgical induction of a strabismus. No stereopsis was measurable with Randot stereo testing prior to electrophysiological experiments. Neurons located in V1 and V2 were recorded for orientation selectivity, grating sensitivity and eye dominance.

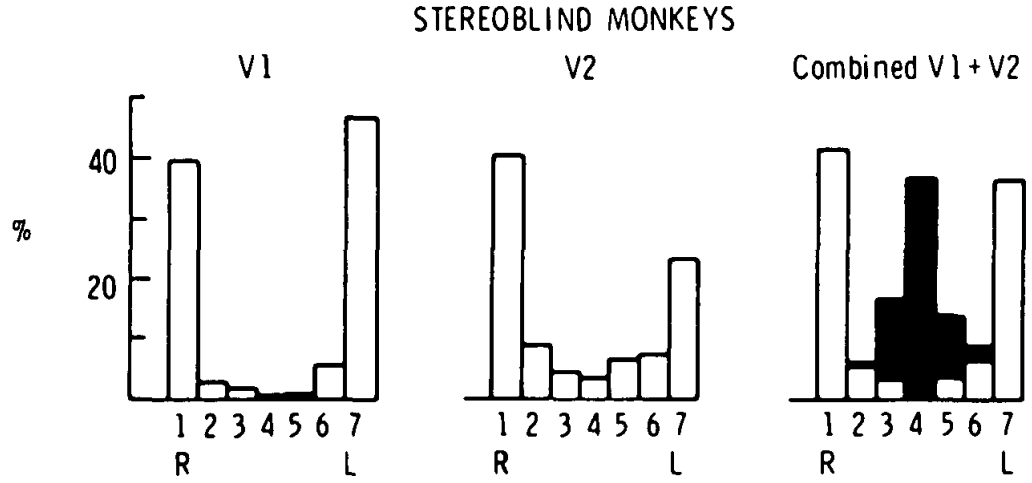

Figure 1.8: Eye dominance histograms for stereoblind monkeys. The first two histograms are comprised of the percentage of the neurons from V1, V2, and the third an average of the first two. The dark bars in the third histogram show the results for the control monkeys, who had measurable stereopsis with random dot stereograms. Reproduced from Crawford et al. (1984).

Figure 1.8 shows the percentage of neurons activated by either the left or right eyes ('7' and '1' on the histograms, respectively). Numbers 2-6 on the abscissas are classes of binocular neurons. Of V2 neurons, 98% were binocular in the four control monkeys, and of 66% of V1 neurons were binocular. In contrast, 30% of V2 neurones of the stereoblind monkeys were measured as binocular and 13%

in V1. The black bars in Figure 1.8 show data for control monkeys, and represent how in these stereo-normal monkeys, the majority of the neurons are binocular, which is in stark contrast to data for stereoblind monkeys. These results show how the deficit in amblyopia extends to extra-striate cortical areas, namely V2 in this case.

With respect to the investigation of neural loci for processing of different visual stimuli, many areas may contribute to the visual percept. Figure 1.9 illustrates schematically the different areas of the visual pathway and cortex that are involved with the processing of different aspects of vision: colour, form, motion and depth.

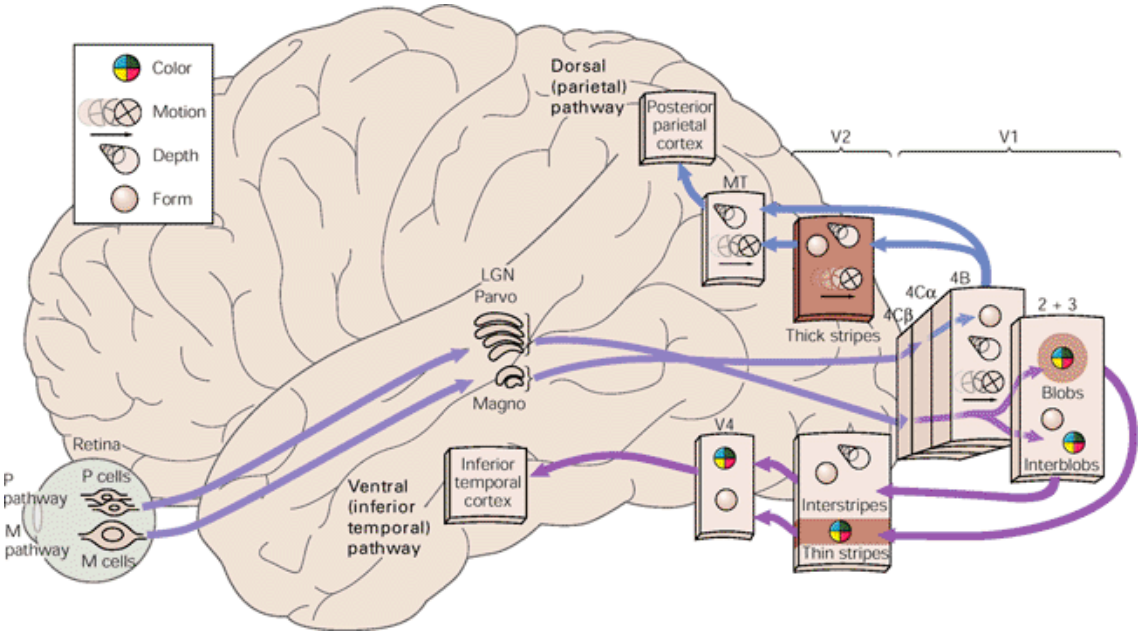

Figure 1.9: Schematic diagram of the dorsal (magnocellular) and ventral (parvocellular) pathways of the visual pathway and the aspect of perception each are concerned with. The legend in the top left corner shows the key for each of four aspects of perception – colour, motion, depth and form. The ventral stream is concerned with the processing of form and colour, with the inferotemporal cortex involved in recognising faces. The dorsal stream is associated with the perception of motion and depth. Taken from Kandel, Schwartz, and Jessell (2000).

Barnes et al. (2001) used fMRI to correlate the amblyopic eye contrast sensitivity, determined psychophysically, with activation of various areas of the visual cortex of 11 amblyopes. Stimuli were radial suprathreshold sinusoidal gratings. Retinotopic stimuli were also used comprising a radial checkerboard at 80% contrast. Blood oxygen level dependent (BOLD) percentage change was monitored in those areas of cortex that were responsive to visible stimuli presented to either or both eyes.

Stimuli that were invisible to the amblyopic visual system were used intentionally to test whether the striate cortex was normal in strabismic amblyopes. For stimuli that were above the high spatial frequency cut-off of the amblyopic eye, there were larger differences between normal eye and amblyopic eye brain activation. These results also indicate that V1 and other extra-striate areas show reduced levels of activation in amblyopia. They also suggest that V1 is the earliest site of the neural deficit in amblyopia. In light of the active inter-ocular suppression that occurs in the striate cortex (Mower et al., 1984; Sengpiel et al., 2006), this conclusion gains yet more credibility, as neighbouring ocular dominance columns may have inhibitory connections. Barnes et al. do, however, postulate that the lack of response to the high spatial frequency stimuli measured in V1 could be a result of extra-striate feedback connections to the striate cortex, which may be inhibiting V1.

Li, Dumoulin, Mansouri and Hess (2007) sought to find the site, or sites, of the cortical deficit in amblyopia. Participants were 11 strabismic amblyopes, of which five were also anisometropic, all with esotropia less than 15 deg, and amblyopic eye acuity ranging from 6/12 to 6/120. Stimuli were the standard retinotopic wedge and annulus checkerboard as used by Barnes et al. (2001). With fMRI recording, the six control (binocularly normal) participants showed functional activation of the visual cortex at similar levels for each eye. For amblyopic participants, data analysed in the same way revealed a reduction in activation when the amblyopic eye viewed the stimuli compared to the non-amblyopic eye. Reduction in activation worsened for extrastriate areas measured (V2, V3, Vp, V3a, and V4) compared with striate V1. With fMRI

therefore, the amblyopic deficit is found initially in V1. Moving to areas of the cortex where more specialised features of vision are processed (see Figure 1.9), the deficit is deeper. Recent studies corroborate this finding in primary and secondary visual areas and also find deficits in higher areas associated with processing of depth perception from binocular cues (Joly and Frankó, 2014). This is reflected by decreased sensitivity to second-order visual stimuli, as is discussed in the following section.

1.3 Psychophysics of amblyopia

Neuroscience constantly traverses the frontiers of understanding how parts of the brain work, more specifically in vision science with determining specific parts of the visual cortex involved with the processing of certain aspects of vision. In the case of visual perception, how does each part of the visual pathway and the visual cortex contribute to a participant perceiving something? This alludes to the “hard problem” (Chalmers, 1995), and brings an age-old philosophical endeavour into the realm of science. Psychophysical investigation quantifies the perceptual response to a physical stimulus. In amblyopic participants, the deficit in perception relative to normal vision can be quantified.

1.3.1 Perception in amblyopia

Spatial stimuli used to measure vision have often been defined by differences in luminance, i.e. first-order stimuli. However, the visual system is also able to detect stimuli due to differences in texture or contrast, i.e. second order stimuli (Baker and Mareschal, 2001). This section describes deficits to these types of stimuli in amblyopia, giving an idea of how the deficit in amblyopia is spread through the hierarchy of visual processing.

1.3.1.1 First-order loss

Levi and Harwerth (1977) compared spatial deficits to luminance-based stimuli in amblyopic and non-amblyopic (or preferred) eyes of amblyopic participants. Contrast sensitivity functions were measured for two strabismic and two anisometropic amblyopes. Luminance contrast for a range of sinusoidal grating spatial frequencies was increased until the stimulus was just detectable.

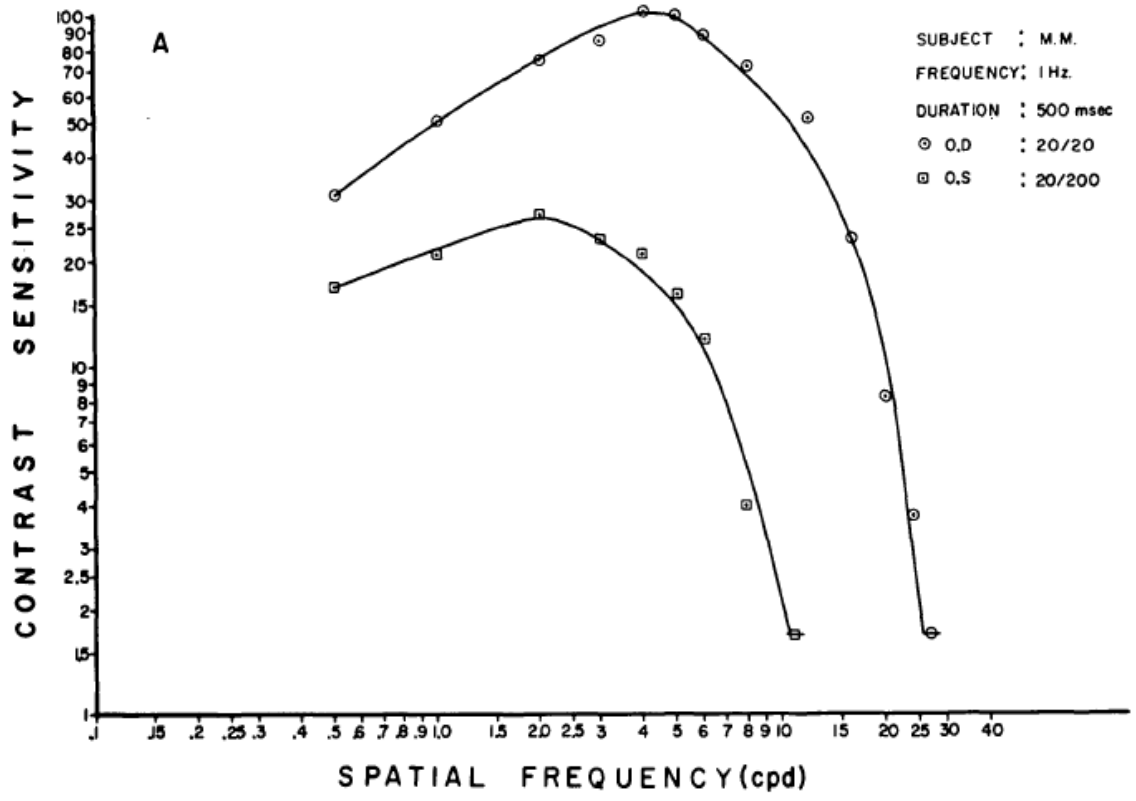

Figure 1.10: Contrast sensitivity function for the amblyopic (lower) and non-amblyopic (upper) eye of a strabismic participant. Ordinate axis shows 1/contrast, abscissa shows spatial frequency. From Levi and Harwerth (1977)

Figure 1.10 shows the contrast sensitivity function for the amblyopic and the non-amblyopic eyes of a strabismic participant. The lower function is for the amblyopic eye and shows a reduction in sensitivity for all spatial frequencies. For all participants the high spatial frequency cut-off was reduced in the amblyopic eye, as was the peak spatial frequency, and there was no difference in the contrast sensitivity functions found for strabismic amblyopes or anisometropic amblyopes (not shown). Hess and Howell (1977) found a similar result for 10 strabismic amblyopes, with slightly different methods and vertical sinusoidal gratings.

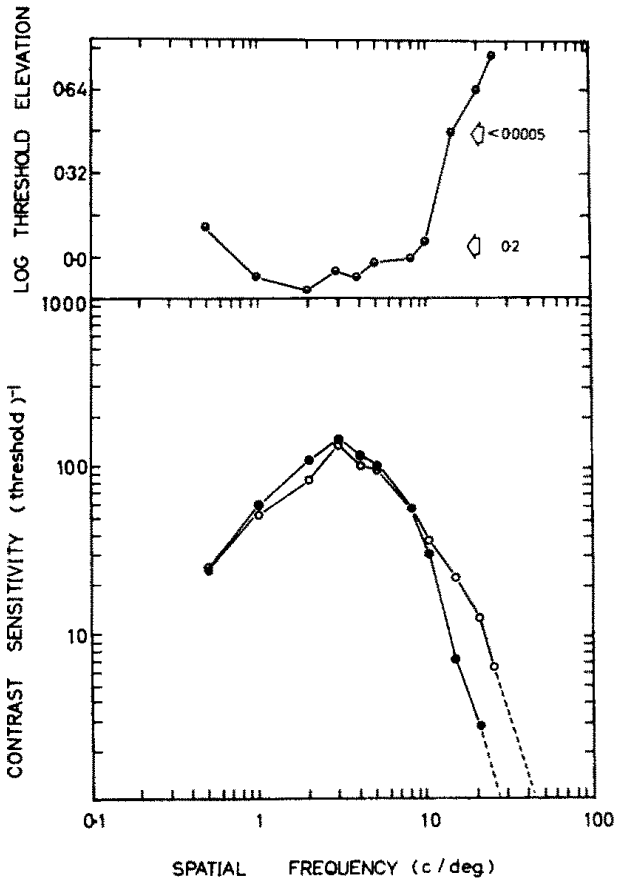

Figure 1.11: Threshold elevation between non-amblyopic and amblyopic eyes of a strabismic amblyope (top). Contrast sensitivity functions for amblyopic and non-amblyopic eye the same participant. From Hess and Howell (1977)

Figure 1.11 shows the results of Hess and Howell's (1977) experiment. Similar to Levi and Harwerth (1977), the strabismic amblyope shows a reduced high spatial frequency cut-off. However, the lower spatial frequencies appear to be similar between the amblyopic and non-amblyopic eyes, as can be seen at the top of the Figure. This is likely due to the degrees of amblyopia demonstrated by the participants. Figure 1.10's participant had visual acuity 6/60 in the amblyopic eye compared to the 6/15 in the amblyopic eye of Figure 1.11's participant.

Abrahamsson and Sjöstrand (1988) also found greater contrast sensitivity deficits for strabismic than anisometropic amblyopes, although this difference could also

be explained by greater visual acuity loss in the strabismic amblyope group. Kiorpes et al. (1998), found that aetiology of amblyopia did not affect the contrast sensitivity deficits of monkeys with induced anisometropia (n=3) or induced strabismus (n=3). Single unit recordings of V1 neurones were taken to obtain the proportion of units that were sensitive to a particular spatial frequency and contrast. Behavioural contrast sensitivity functions (CSF) for a normal control monkey were similar to that of a normal human, agreeing with previous studies (e.g. De Valois, Morgan and Snodderly, 1974), with similar peak sensitivities at 3-5 c/deg, though the monkey CSF had a lower high spatial frequency cut-off at 20 c/deg. Rather than the CSF deficit being related to amblyopia aetiology *per se*, the severity of amblyopia (calculated as difference between the area under the curve of the amblyopic and non-amblyopic eye CSFs) measured behaviourally, was related to the changes found in cortical neuron spatial responses compared with the normal control monkey.

The age of amblyopia onset must also be considered. As contrast sensitivity to low spatial frequencies develops sooner than it does for high spatial frequencies (e.g. Banks and Salapatek, 1978), if the amblyogenic factor, be it anisometropia or strabismus, occurred earlier on, then the range of spatial frequency deficits may be the same irrespective of the aetiology of the amblyopia and is likely to show for low as well as high spatial frequencies.

Levi and Klein (1982a; b), however, showed that anisometropic and strabismic amblyopes do indeed have different deficits of other spatial acuity types. In those studies, vertical grating acuity, Vernier acuity measured using two rows of offset vertical gratings, and Snellen acuity was compared. Observers were five anisometropic, four strabismic, and three mixed (strabismic and anisometropic) amblyopes. Results are shown in Figure 1.12A. Snellen acuity loss is similar to grating acuity loss, as data points lay close to the 1:1 line. For strabismics, Snellen acuity is worse than that predicted by grating acuity loss. Levi and Klein (1985) showed that grating acuity loss was proportional to Vernier acuity loss in anisometropic amblyopes and that Vernier acuity loss was greater than that predicted by grating acuity loss for strabismics (Figure 1.12B). A more recent larger scale study (McKee et al., 2003) confirmed these results with 84

anisometropes (43% amblyopic) and 40 strabismics (48% amblyopic). These results show that spatial acuity deficits are worse for strabismic than anisometropic amblyopes, suggesting a difference between these types of amblyopia.

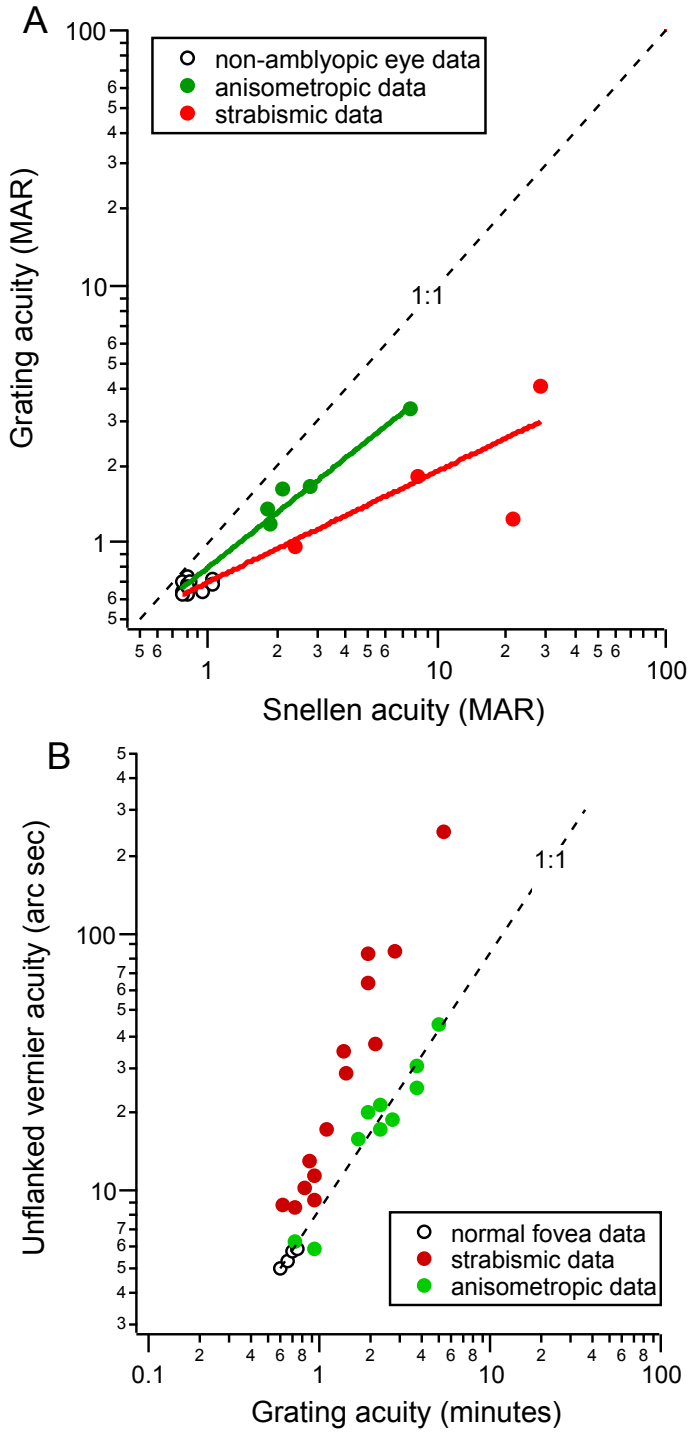

Figure 1.12: A) grating vs. Snellen acuity (redrawn from Levi and Klein, 1982b), B) Vernier vs. grating acuity (redrawn from Levi and Klein, 1985). Open symbols show non-amblyopic eyes, green symbols – anisometropes, red symbols – strabismics.

Furthermore, Song, Levi and Pelli (2014) recently compared flanked (by other letters) and unflanked letter optotype acuity of blurred normals, normal eccentric viewing, anisometropic amblyopes (n=6), strabismic amblyopes (n=6), and mixed amblyopes (n=6). Letter size was reduced until threshold was reached for both unflanked and flanked letters. The flanked letters were a constant distance away from the target letter, 0.1 of total letter size. Strabismics (with and without anisometropia) showed worse crowded letter acuity than predicted by unflanked acuity, compared to pure anisometropes.

McKee et al. (2003) also found a difference between anisometropic and strabismic participants with respect to binocularity in their large-scale study on different types of amblyopes. A range of visual functions were measured for all participants. A “pass” in the binocular tests was defined if the participants had some stereopsis (Randot circles) or achieved some binocular motion integration (binocular motion integration test). Of the strabismic participants 10% passed the test, 64% of anisometropes passed, and 100% of normal passed. A larger proportion of anisometropes than strabismics had some measurable binocular function, further illustrating the difference in strabismic amblyope and anisometropic amblyope characteristics. This finding has been repeated by others (Agrawal et al., 2006; Narasimhan, Harrison and Giaschi, 2012).

In summary, strabismics and anisometropic amblyopes show different monocular and binocular visual deficits, as well as different patterns of suppression (see Section 1.4.2, Table 1.2), for the same degree of amblyopia (as measured by visual acuity difference). This finding suggests that different mechanisms underlie each type of amblyopia. Furthermore, a method of measuring suppression is required that is sensitive enough to elucidate different anisometropic and strabismic suppression patterns. Simulating these different types of suppression will be useful to refine the method, and this is the subject of Section 1.1.5.

1.3.2.1 Second-order loss

Stimuli that are not defined by luminance (or colour) are termed ‘second-order stimuli’. An example of the different proposed processing pathways of first- and second-order stimuli are shown in Figure 1.13. The first-order stimulus is a sinusoidal grating defined by luminance, while the second-order stimulus has the same mean luminance but the envelope and carrier differ in orientation and spatial frequency. The “early filter” comprises detectors stimulated by the high spatial frequency carrier. Responses are pooled and rectified ensuring that positive and negative information (in this example, lower envelope spatial frequency) do not cancel each other out, and therefore can be detected by the “late filter” (Baker and Mareschal, 2001).

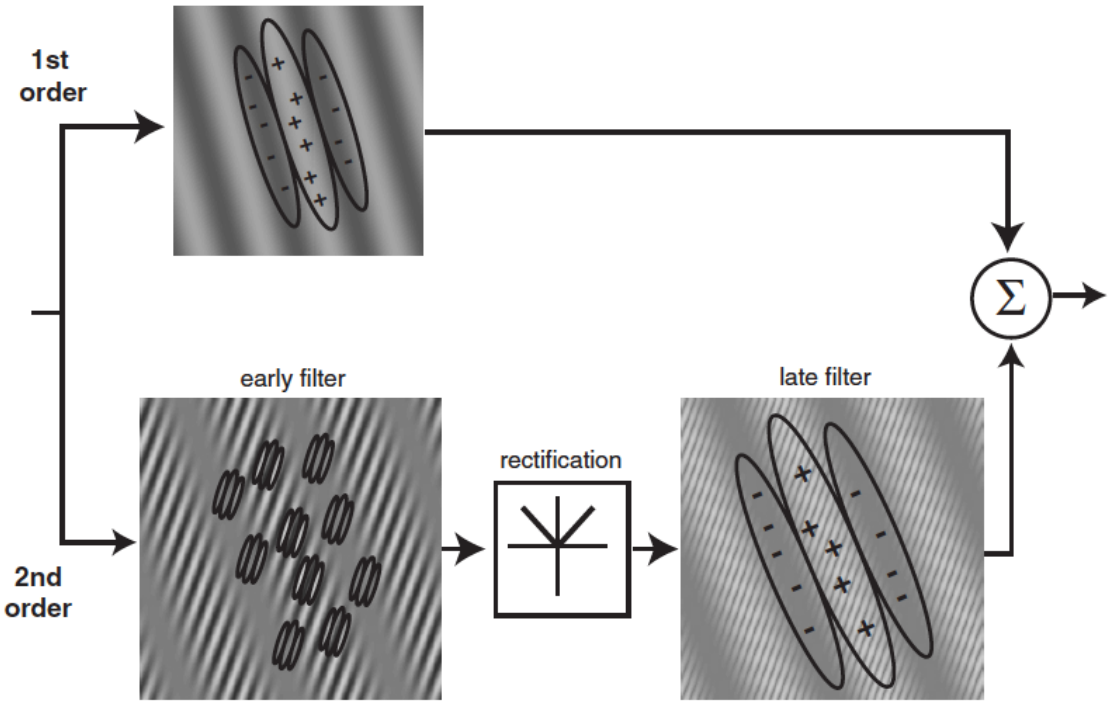

Figure 1.13: Model of a cortical neuron (Σ) response as a result of either a first- or second-order pathway. From Baker and Mareschal (2001)

Earlier work in motion perception (Albright, 1992) describes “form-cue invariance” where an MT cell of a monkey was responsive to a moving bar defined by luminance, and this same neuron was also responsive to dynamic

noise on a static noise background with the same direction preference, without luminance cues. This result suggests different pathways for the processing of first- and second-order stimuli before reaching the recorded area (MT). A similar suggestion was offered by Schofield and Georgeson (1999) for spatial stimuli. Luminance-modulated noise (LM – first-order) or contrast-modulated noise (CM – second-order) gratings were used to measure modulation sensitivity functions, and compared to those measured for standard luminance (L) gratings. Static binary noise (luminance amplitude of 0.4) was added to a sinusoidal grating for LM stimuli, and multiplied by a sinusoidal grating to generate CM stimuli. Sensitivity to standard noiseless (L) gratings showed a characteristic band-pass modulation (contrast) sensitivity shape. The addition of noise (i.e. LM stimuli) showed a flatter, lower function, whilst the multiplication of noise (i.e. CM stimuli) showed further lowering of visual sensitivity.

A further experiment by Schofield and Goergeson quantified modulation discrimination “dipper” functions (Legge and Foley, 1980) for each stimulus type. Modulation increments were added to pedestal L gratings of different baseline modulations until a change in the stimulus was perceived. With first-order (luminance-defined) stimuli, at low modulations (or contrasts) the pedestal facilitates discrimination. As pedestal modulation is increased, discrimination thresholds (as a percentage of the pedestal modulation) also increase (Legge and Foley, 1980), also known as masking. This was also true for both LM and CM stimuli in Schofield and Georgeson’s (1999) study. However, there was no cross-facilitation (i.e. improvement) or masking when LM and CM stimuli were combined. This suggests that different pathways exist for the detection of LM and CM stimuli. Allard and Faubert (2007) measured detection thresholds for LM and CM Gabors (sinusoidal gratings with a Gaussian window) and found that LM stimuli in LM noise, and CM stimuli in CM noise, were less detectable than LM stimuli in CM noise, and vice versa. This also provides evidence for different processing mechanisms, at least for the detection stage, of LM and CM stimuli.

Do amblyopic visual systems show different deficits for first- and second-order stimuli? Investigation of this question aids in understanding the nature of the

amblyopia deficit at different processing stages. Wong, Levi and McGraw (2001) investigated the visual sensitivity deficit in amblyopia, comparing first- and second-order sensitivity losses in the amblyopic versus the preferred eyes. First-order stimuli were vertical sinusoidal gratings. Second-order stimuli were amplitude-modulated vertical gratings consisting of a high spatial frequency carrier, whose contrast was modulated by a low spatial frequency envelope. The envelope and the carrier both had the same mean luminance and therefore varied in spatial frequency and contrast only, and could not be distinguished by differences in luminance.

Modulation detection thresholds were measured for the two types of stimuli, for amblyopic and non-amblyopic eyes of five amblyopic participants, and the dominant eyes of three binocularly normal participants. Second-order carrier visibility was equated with first-order thresholds, to isolate the second-order detection deficit. Amblyopes showed similar first-order deficits to those determined by previous studies. Four of five amblyopes showed specific second-order losses with their amblyopic eyes, and three with their non-amblyopic (preferred) eyes, when comparing thresholds with the dominant eyes of non-amblyopic control participants. As most amblyopes experienced raised thresholds compared to control eyes with their non-amblyopic (or preferred) eyes, a possible binocular locus for the processing of second-order, contrast-defined stimuli was suggested. Binocularity in amblyopes is disrupted and as the processing of second-order or contrast-defined stimuli may be served by mechanisms receiving strong binocular input, reduced sensitivity to these types of stimuli may extend to the non-amblyopic eye also.

Mansouri, Allen and Hess (2005) investigated the processing of second-order stimuli in eight amblyopic participants and eight normal participants. First-order stimuli were Gaussian windowed noise patches, and observers' detection thresholds were measured with a 2AFC procedure. Second-order stimuli were also Gaussian windowed noise patches, but detection thresholds were measured with a 2AFC task using horizontally or vertically orientated patches. Results showed that normal participants had comparable first-order thresholds

in their dominant and non-dominant eyes. Non-amblyopic eyes of amblyopic participants had lower thresholds (averaged across all normal and all amblyopic participants), and expectedly amblyopic eyes had the highest thresholds of all. For second-order stimuli, both non-dominant and dominant eyes had similar modulation thresholds, as well as amblyopic and non-amblyopic eyes of amblyopic participants. However, the amblyopic participants' eyes both had significantly higher thresholds than either of the normal participants' eyes. This result suggests that there are second-order processing deficits that cannot be explained in terms of first-order loss, and agrees with the aforementioned supposition of a binocular locus for some stage of second-order processing.

Chung, Li and Levi (2006) measured recognition thresholds of second-order contrast defined stimuli in their study using any of the 26 lower case Times-Roman characters. Initially, the size threshold for identifying letters for each individual amblyope was determined with letters of a high contrast. Stimuli were presented monocularly to the amblyopic or the non-amblyopic eye, whilst the other was patched. Figure 1.14 shows the results from measuring letter recognition thresholds.

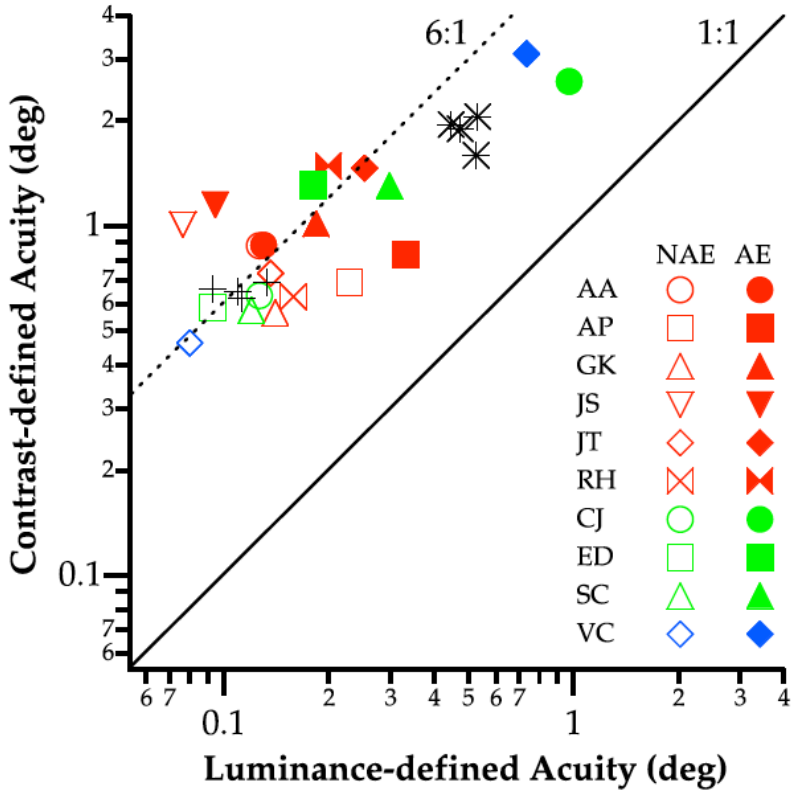

Figure 1.14: Acuity (letter size threshold) for first- against second-order stimuli acuity. Red symbols represent strabismics; green for anisometropes, and blue for a mixed amblyope. Filled symbols denote amblyopic eyes, and open symbols the non-amblyopic eye. Cross and asterisk symbols show data from normals at the fovea and 10 deg in the periphery, respectively. From Chung et al. (2006)

Contrary to the previous two studies the similarity between contrast-defined letter size thresholds in the non-amblyopic and amblyopic eyes is not as evident. Luminance-defined letter size threshold is generally, as expected, worse in the amblyopic eye. Non-amblyopic eye contrast-defined letter size threshold is similar to normals (denoted by the '+' symbols) in 8 of 10 amblyopes. This finding is contrary to the previous studies that second-order deficits extend to amblyopic and non-amblyopic eyes. However, the use of different stimuli and with a recognition rather than resolution or detection task may have caused this lack of agreement.

The above studies generally point towards the notion that second-order stimulus processing, at least at some stage, involves neurons receiving input from both eyes, as the non-amblyopic eye also shows a deficit. The use of these types of stimuli may therefore give a more sensitive measure of inter-ocular suppression, as there is a disruption to normal binocularity in amblyopia. As previously depicted in Figure 1.9, there are different processing streams for different aspects of visual processing. Using different types of stimuli to measure suppression, e.g. moving, contrast-defined, or luminance-defined stimuli, will allow the mapping of the deficit in amblyopia along different stages of visual processing, and give an idea of performance in normal and disrupted (e.g. amblyopic) vision. The following section elaborates on this, with particular focus on binocular combination of monocular images.

1.3.2 Binocular combination in amblyopia

1.3.2.1 Combination of first-order stimuli

As the experiments detailed in this thesis are concerned with inter-ocular suppression, a purely binocular phenomenon, theories of binocular combination in normal and disrupted binocular vision may be helpful in predicting results. Binocular summation is the improvement of binocular sensitivity over monocular sensitivity, greater than the improvement predicted by the probability of having two detectors, i.e. two eyes, rather than one (Campbell and Green, 1965; Westendorf and Fox, 1977; Harwerth, Smith and Levi, 1980). Levi, Harwerth and Smith (1980) failed to find improved binocular over monocular contrast detection thresholds in one anisometropic amblyope, one strabismic amblyopic, or one alternating strabismic. Furthermore, the presentation of a subthreshold grating to one eye improved detection thresholds (i.e. facilitation) to the other eye of normal observers. This was not seen in the clinically anomalous participants, suggesting that there is no excitatory binocular combination (i.e. binocular summation) present in those with abnormal binocular vision. The finding that there is no improvement in reaction time to the presentation of suprathreshold grating viewed binocularly compared to monocularly in strabismic or anisometropic amblyopes, corroborates this suggestion (Levi, Harwerth and Manny, 1979).

However, Baker et al. (2007) demonstrated binocular summation in strabismic amblyopes if contrast was increased to the amblyopic eye, relative to the non-amblyopic (or preferred) eye. This led to the proposition that binocular interactions are still present in amblyopes, opening a new path in investigation, and perhaps treatment of amblyopia (Hess, Mansouri and Thompson, 2010b; a; Black et al., 2011; To et al., 2011; Knox et al., 2012; Hess et al., 2014). The two stage model of binocular combination developed by Meese et al. (2006) to explain binocular summation in normal vision has also been applied to amblyopic vision to explain binocular summation achievable in amblyopes. Inhibitory and excitatory interactions both within (masking and facilitation, respectively) and

across eyes (inter-ocular suppression and excitation, respectively) in that model are also common to the inter-ocular contrast gain model of Ding, Klein, and Levi, (2013b). Ding, Klein, and Levi (2013a) used a phase combination paradigm to investigate binocular combination in six adult amblyopes (one with anisometropia, one with strabismus, and four with both anisometropia and strabismus). Two sine-gratings of equal but opposite phase (±45 deg) were shown to each eye. Normal participants would fuse the two gratings and perceive a sinusoid with a combined phase of 0 (Ding et al., 2013b). In amblyopic participants, the same gratings would be fused to give a resultant grating with a phase shifted closer to the non-amblyopic eye. When the contrast ratio increased, i.e. higher contrast in the amblyopic eye than the non-amblyopic eye, the perceived phase of the binocularly combined out-of-phase gratings shifted towards the amblyopic eye's actual phase. This result demonstrated that amblyopic binocular contrast vision could be balanced to permit normal binocular combination, similar to Baker et al. (2007).

Balanced binocular vision so that the perceived phase is 0, was achieved by adjusting contrasts in either amblyopic or non-amblyopic eyes. This allows the assessment of the effect that the non-amblyopic has on the amblyopic eye, and vice versa. If only the amblyopic eye contrast is changed, a larger inter-ocular contrast ratio (amblyopic/non-amblyopic) is required, compared to if only the non-amblyopic eye contrast is changed. This suggests the role of inter-ocular enhancement of the non-amblyopic eye's grating by the amblyopic eye, as well as inter-ocular inhibition (suppression) of the non-amblyopic eye on the amblyopic eye's perception. Therefore, binocular combination in amblyopes, or those with abnormal binocular vision, is weighted towards the non-amblyopic eye. Inter-ocular suppression is imposed on the amblyopic by the non-amblyopic eye, and the amblyopic eye also enhances the dominant eye input.

1.3.2.2 Combination of second-order stimuli

For normal observers, perceived phase and modulation depth of binocularly combined LM gratings varies non-linearly with changes in inter-ocular contrast

ratio, irrespective of the amount of phase difference between the two eyes (Zhou, Liu, Zhou and Hess, 2014). On the other hand, variation with equivalent CM gratings and inter-ocular modulation (i.e. contrast modulation) ratios shows a linear relationship with no phase disparity difference. Increasing phase difference, however, saw a reduction in perceived modulation depth (Zhou, Georgeson and Hess, 2014). As uncorrelated or anti-correlated noise carriers did not affect CM performance, these two results together suggest that binocular LM and CM processing are served by different mechanisms. Furthermore, changing carrier visibility of CM gratings does not have a large effect on CM modulation sensitivity functions of non-amblyopic and amblyopic eyes (Gao et al., 2014). Gao et al. (2014) consequently suggested that amblyopic deficits are extra-striate in nature, as second-order information is still extracted regardless of changes to first-order carrier.

If some extra CM stimulus processing stage occurs in extra-striate cortex it may be expected that disruption to binocularity, whether induced in normals or occurring in amblyopic visual systems, would make it more difficult for binocularly incompatible images to be combined, and therefore suppression might be more likely to occur. As LM stimuli are thought to be processed by earlier, simpler, monocular mechanisms, disruption to binocularity may have less of an effect on the binocular combination of images. Experiments reported in this thesis will be able to test this prediction made by such up-to-date models of binocular combination. To date, these models address binocular combination (or depth of suppression) in amblyopia only in the central visual field. The following section reviews more historical clinical and experimental measures of suppression depth and extent, and can therefore give some idea of binocular combination across the visual field.

1.4 Clinical and experimental measurements of suppression

1.4.1 Clinical Methods

Clinical methods of measuring suppression are generally gross, detecting rather than accurately quantifying foveal suppression. Additionally, there is little agreement among results obtained across different suppression tests. Bagolini (1967) compared assessment of retinal correspondence, suppression and diplopia in a sample of 165 esotropic patients, with deviations ranging from less than 10 to above 40 prism dioptres using the Bagolini striated lens and Worth 4-dot tests. Results are shown in Figure 1.15.

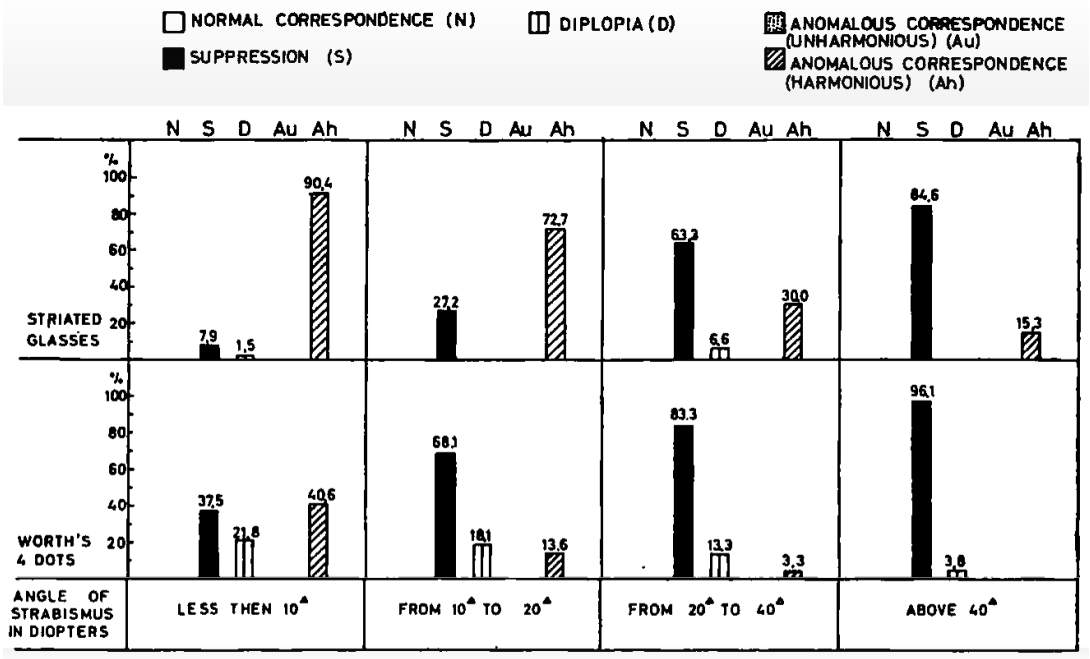

Figure 1.15: Histograms showing the number of participants with normal correspondence, suppression, diplopia, or anomalous retinal correspondence (harmonious or unharmonious), assessed with striated lenses and the Worth 4-dot test. Participants are grouped according to the angle of strabismus. From Bagolini (1967)

As the size of the deviations increased a larger proportion of participants demonstrated suppression with both tests. These results suggest that participants with larger angle deviations are more likely to suppress than to have abnormal retinal correspondence (ARC). This is defined as the fusion of the same object imaged on non-corresponding retinal areas, in some cases with no

manifest deviation and measurable, though reduced, stereopsis (Burian, 1947). However, different proportions of diagnoses are found for the same group of strabismics for each test. Both of these clinical tests only detect suppression in the central visual field.

A Sbisa (or Bagolini filter) bar can be used to estimate depth of suppression (Godts, Trau and Tassignon, 2006). The bar consists of red filters of increasing density, and can be used in conjunction with Bagolini striated lenses (Knowles and Griffiths, 2003), as opposed to viewing a fixation light alone. Through Bagolini lenses, a suppressor would only perceive one arm of a cross. Filter density is increased in the non-suppressing eye until both arms of a cross are perceived. A neutral density filter bar may also be used in place of the Sbisa bar (Henson and Williams, 1980).

In an attempt to quantify suppression across a wider region of the visual field, Lang (1971) described a method of measuring inter-ocular suppression scotomata with binocularly viewed Amsler charts combined with polarised projection. An Amsler grid (20 deg square frame with a grid of black lines) is presented to the amblyopic eye and a square frame only is presented to the non-amblyopic eye. Although no data were presented in Lang's (1971) study, examples of 'hazy' parts of the grid to illustrate central (associated with anisometropic amblyopia), and a paracentral extending to fixation point scotomata (associated with strabismic amblyopia) are provided. Lang's test could potentially have enabled the measurement of extent of inter-ocular suppression. However, this test does not appear to be widely used in clinical practice, perhaps because information on binocular scotoma extent is of limited use to practitioners.

To investigate the depth and extent of suppression, different methods must be combined. Recently some researchers and clinicians have begun treating amblyopia by intentionally reducing suppression (Hess, Mansouri and Thompson, 2010b; a; Black et al., 2011; To et al., 2011; Knox et al., 2012; Hess et al., 2014). Thus an effective, efficient measure of suppression depth and extent could not

only give a prognosis of potential treatment effectiveness, but would also enable effective monitoring of treatment. A review of experimental methods that assess suppression more thoroughly will be described in the following section.

1.4.2 Experimental methods

If a new method of mapping suppression depth and extent across the visual field is to be developed, previous methods need to be carefully assessed. The following sections review, in detail, various techniques that have been used to measure suppression across the visual field. A table summarising the results for ease of comparison, follows these sections (see Table 1.2). There are generally two types of scotomata found in strabismic amblyopia: 1) a central scotoma – centred on the deviating eye fovea, and 2) fixation point scotoma – centred on the corresponding retinal point (of the deviating eye) to which the fixating eye fovea is imaged (Joosse, Simonsz and Jong, 2000). Anisometropic amblyopes show a central scotoma, although there are fewer studies that have investigated anisometropic compared with strabismic suppression.

1.4.2.1 Extent of suppression

In addition to his numerous major contributions to ophthalmology, Albrecht von Graefe (1856) was the first to investigate inter-ocular suppression across the visual field when he investigated visual perception in strabismics using kinetic perimetry. Travers (1938) adapted this method, with apparatus shown in Figure 1.16A. A strabismic participant views a Bjerrum screen, without correction for the angle of deviation. The centre of the Bjerrum screen was aligned with the non-strabismic eye fovea, and a white fixation light with the fovea of the strabismic eye, by means of an alternate cover test. During this cover test, the participant was instructed to fixate on either the centre of the screen or the fixation light, depending upon which eye was covered. The position of the fixation light on the Bjerrum screen was moved until no movement was detected with the alternate cover test, and then fixed in this position. The distance between the fixation light and the centre of the Bjerrum screen gave the size of

the manifest deviation at the 1 m testing distance. A red lens was then placed over the non-strabismic eye. A 1 deg white test stimulus was then moved across the visual field and the perceived colour was noted at different positions. If the test stimulus was red, the strabismic eye was suppressing at that visual field location, if pink, the test stimulus was fused and perceived simultaneously with both eyes, and one red and one white test stimulus seen at the same time, indicated that diplopia was present. Outside of the non-strabismic eye monocular visual field, the test stimulus would only be perceived by the strabismic eye, and would therefore appear white. Generally, Travers found that the test stimulus appeared red over varying areas when close to the fixation light, demonstrating central suppression of the strabismic eye.

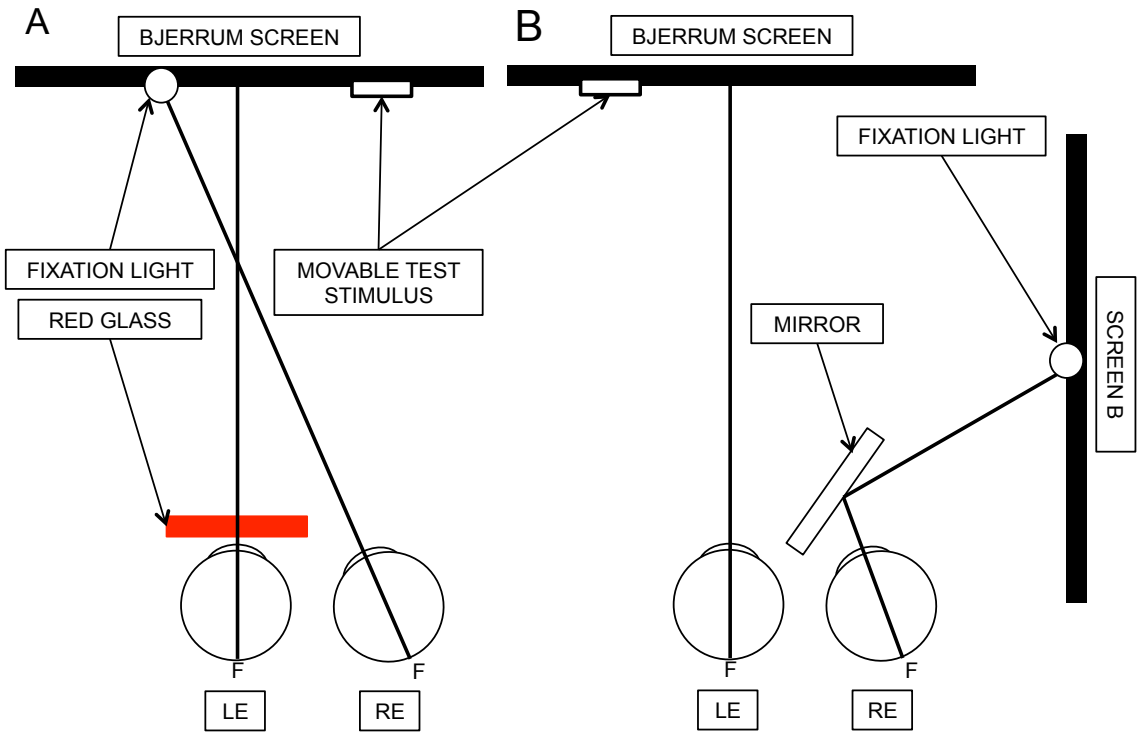

Figure 1.16: A) Experimental set-up for Travers' Modified von Graefe Red Lens Test B) Experimental set-up for Travers' Mirror-Screen Test. In both cases, the patient has a right esotropia (see text for details). 'F' represents the foveal point for each eye. Redrawn from Travers (1938).

Travers (1938) went on to describe another kinetic perimetry test where a mirror was used to separate the visual fields of each eye. Here a black screen with a

static fixation light is presented to the strabismic eye through a mirror (right eye – Figure 1.16B). A white test stimulus (0.25 deg) is moved across a Bjerrum screen viewed by the non-strabismic (left) eye. Suppression of the strabismic eye is present when the observer (right esotropic amblyope, with visual acuities: R – 6/60, L – 6/6) does not perceive the fixation light. The position on the visual field of the test stimulus at which this occurs is noted using the Bjerrum screen scale. The same procedure is then carried out with the strabismic eye viewing the Bjerrum screen, and the non-strabismic eye viewing the fixation light. Results for each of these conditions are shown in Figure 1.17. The same 7 deg central suppression scotoma was measured in each case, i.e. the fixation light disappeared when the test stimulus was presented to the fovea of the non-amblyopic eye, and the test stimulus disappeared when it was moved over the fovea of the amblyopic eye.

Increasing the luminance of the fixation light when viewed by the non-amblyopic eye made the scotoma larger. Furthermore, if a larger test stimulus was presented to the amblyopic eye, the scotoma would be smaller. This result suggests that scotoma size is dependent on stimulus strength. The Mirror-Screen Test provides more natural viewing conditions to that used in the red lens test and may therefore be a more accurate measure of suppression.

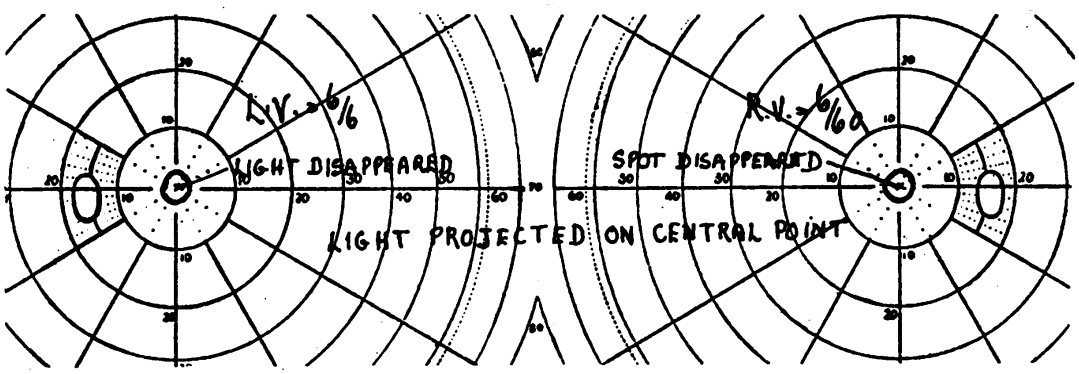

Figure 1.17: Suppression scotomata for a participant with a 10 deg right esotropia as measured with the Mirror-Screen Test. From Travers (1938)

Being particularly aware of the effect of artificial laboratory conditions on measures of suppression, Jampolsky (1955) used Risley prisms to dissociate

the eyes and estimate the horizontal and vertical extents of suppression. Vertical prism power was increased in front of the deviating eye (without strabismus angle correction) while the non-strabismic eye was fixating, until vertical diplopia was perceived. This was repeated horizontally. Jampolsky found an “egg-shaped” hemi-retinal suppression scotoma in the binocular visual field between the central point and fixation point scotoma. This study showed asymmetry of suppression linked to the angle of deviation, i.e. information from the deviating nasal retina in esotropia and the temporal retina in exotropia is suppressed under binocular viewing conditions.

Although aware of the need for more natural viewing conditions to measure suppression, the dissociation of the two eyes with prism is less than natural, and induced motor responses to the introduction of prisms may confound results. With this in mind, Jampolsky (1955) used a haploscope to present similar stimuli to each eye, and found similar results to prism scotometry. A small stimulus is used for the non-amblyopic eye to fixate, and larger stimuli are presented at various points across the visual field of the deviating eye. In agreement with Travers (1938), increasing the intensity of the stimulus presented to the amblyopic eye at the fixation point did not break suppression. Using similar prism dissociation methods, Pratt-Johnson and Tillson (1983) and Irvine (1948) found similar patterns of scotomata with strabismics to those found by Travers and Jampolsky. Irvine also demonstrated central point suppression scotomata in anisometropic amblyopes with amblyopic eye.

Campos (1982) carried out kinetic perimetry (similar to von Graefe’s method) to assess binocular perimetry in five small angle (6-16 prism dioptre) and six large angle (>20 prism dioptre) unilateral comitant exotropes. Small angle exotropes showed no suppression, and large angle exotropes showed suppression of the deviated eye. Participants fixated a black test spot (0.5 deg diameter) on a white tangent screen (5 cd/m^2). A white stimulus (0.5 deg diameter, 115 cd/m^2) was moved about the 30 deg central circular binocular visual field. Both eyes viewed the tangent screen through orthogonally orientated Bagolini lenses (to check for binocular vision status), and the fixing eye additionally viewed through red filters

of increasing density. For the five small angle exotropes, binocular single vision was noted across the visual field. For the large angle exotropes, central suppression was measured for all deviating eyes. Introducing a red filter in front of the fixing eye reduced the suppression scotoma size or resulted in diplopia. This result suggests that larger degrees of dissociation reveal smaller suppression scotomata, or that larger scotomata are found with stimuli that are more similar to habitual viewing.

Campos (1982) also compared the above method with 'participation perimetry' (of Harms, 1937). Participation perimetry involves red-green anaglyph lenses (red presented before the deviating eye; green before the fixing eye). Participants indicated if a white test stimulus appeared green (suppression of the amblyopic eye), red (suppression of the non-amblyopic eye) or perceived lustre (the normal binocular fusion response). A similar method ('exclusion participants') used a red instead of white test stimulus.

All 13 participants (small angle esotropic strabismus ranging from 6-16 prism dioptres) showed single vision with both eyes tested for all but the peripheral visual field, where diplopia occurred. For the same participants, the von Graefe technique showed central areas (30 deg) of anomalous binocular vision, i.e. ARC. Participation perimetry gave varied results, 11 of 13 participants had diplopia, as well as fixation point or central scotomata. Exclusion perimetry showed five participants having no scotoma, and eight having either fixation point (n=1), central (n=3) or both types of scotomata (n=4). The presence of suppression is therefore conditional on the method used to detect it. Both types of Harm's perimetry are perhaps more dissociating than von Graefe's technique (the red and white stimuli can at least be fused to make pink), and therefore may quantify suppression inaccurately.

Mehdorn (1989) used phase-difference haploscopy to present different images to each eye, a method first described by Aulhorn (1966). Two projectors with 90 deg out-of-phase rotating segmented disks in front of each projected images onto a screen (Figure 1.18). Corresponding to each rotating segmented disk, is

another in front of each eye, allowing separate images to be presented to each, with no cross-talk.. A pattern of black letters on a white background (subtending 18 deg horizontally by 12 deg vertically) was viewed by both eyes. The stimuli were two horizontally disparate vertically orientated bars (20' by 4', 3.2 cd/m^2) viewed dichoptically for 2-4 s. Horizontal disparity of these bars was adjusted to produce crossed or uncrossed disparities and therefore an illusion of depth in front of or behind the fusion pattern of black letters. Binocular rivalry perimetry was performed by modifying the same apparatus by rotating one of the horizontal bars by 90 deg to form a cross. The perception of only one of the arms of the cross indicated suppression.

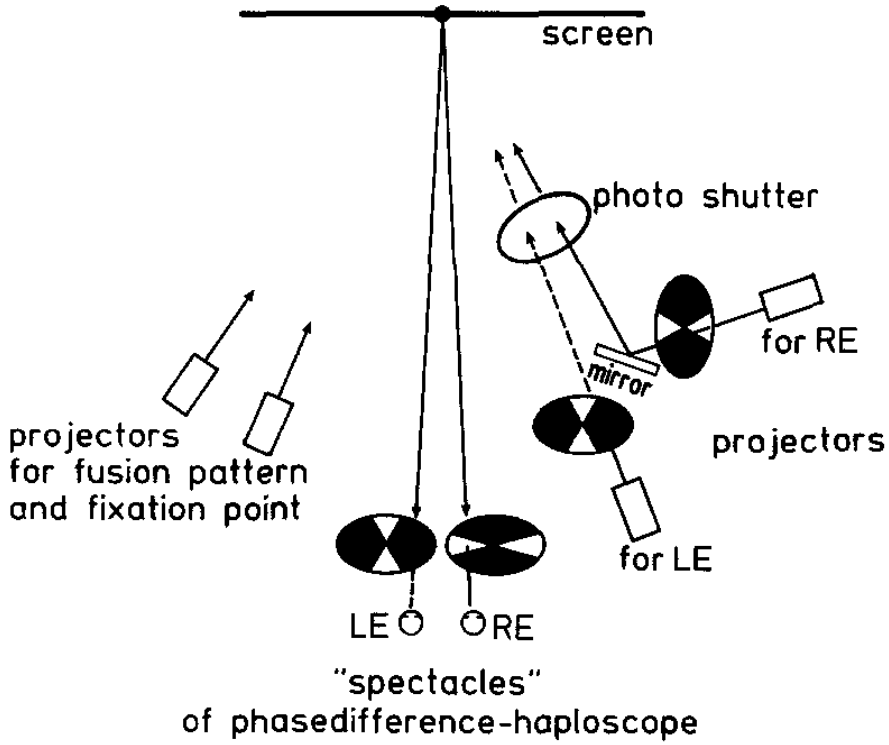

Figure 1.18: Experimental apparatus for phase difference haploscopy, for dichoptic presentation of stimuli. From Mehdorn (1989)

A fixation light was moved across the fusion pattern in order to measure different areas of the visual field, whilst the horizontal bars remained in the centre of the letter pattern. A lack of stereopsis measured suggested that suppression was present. The results of the stereo-perimetry test were compared with prism scotometry and the Bagolini striated lens test. Eight

participants with microstrabismus (i.e. 6 prism dioptres or less), stereoacuity worse than 120 arc secs, and suppression with Bagolini striated glasses took part in the study. Three binocularly normal participants and two with central monocular scotomata due to macular retino-choroidal scars served as controls.

One participant with a circumscribed macular lesion showed a 1 deg scotoma with striated glasses, and a 1.5 deg horizontal and 1 deg vertical scotoma with stereo-perimetry technique, demonstrating good agreement between tests. With the Bagolini test, six of eight microstrabismics showed central suppression ranging between 1-2 deg. Five out of these six participants also showed a comparable scotoma with the prism-scotometry, though it was usually elliptical and wider horizontally as described by Jampolsky (1955). Generally it was found that the more dissociative method (rivalry perimetry) produced slightly smaller extents of suppression. This opposes findings of Campos (1982), though participants in that study had larger deviations (6-16 prism dioptres). The difference between these two studies suggests that microstrabismics and strabismics have different patterns of suppression, although it should be noted that different methods of suppression measurement were used in each study.

Sireteanu, Fronius, and Singer (1981) also used a similar stereo-perimetry paradigm to test binocularity at local areas across the visual field, although dynamic opposed to static stereopsis was used. At different locations across the visual field, two squares (side length 2.5 deg, contrast ~67%) presented independently to each eye (using polarising filters) were moved away from each other at the same speed. Normal fusion would give the observer the illusion of only one square moving directly toward them. If this illusion was not perceived, e.g. the square moved to one side, suppression of one eye's square is implied.

Strabismics that had undergone corrective surgery (n=4) showed large asymmetric areas across the visual field measured (approximately 25 deg vertical by 35 deg horizontal) with no motion-in-depth perceived. Anisometropes (n=2) showed symmetric central point areas of suppression. Microstrabismics (4 prisms dioptres or less, n=5) that had had no treatment showed central point

areas of lack of suppression measured. The larger area of the visual field suppressed found with the motion-in-depth paradigm (20-30 deg compared to approximately 2 deg in Mehdorn's study) suggests that extent of suppression is larger for this type of stimulus. The difference between the two studies could be due to the different neural processing mechanisms proposed for motion-in-depth versus static stereo-perimetry (e.g. Poggio and Talbot, 1981). To date, a systematic assessment of suppression extents and depths along different visual processing pathways is open for investigation, but could be investigated with carefully chosen visual stimuli. The experiments detailed in this thesis are a small start towards addressing this gap in knowledge.

1.4.2.2 Modern estimates of depth and extent of suppression

Recent advances in technology becoming more available have allowed development of new methods of measuring suppression. Methods of measuring inter-ocular suppression just described mainly concern extent, rather than depth, although depth is generally graded using different densities of red filters or neutral density filters to break suppression (Godts, Trau and Tassignon, 2006; Knowles and Griffiths, 2003; Henson and Williams, 1980; see Section 1.4.1). A more naturalistic estimation of suppression depth and extent would be obtained if images viewed by the two eyes could be made as similar as possible under normal viewing conditions. Suppression across the visual field including both central and fixation point scotomata ideally would be investigated (Campos, 1982; Jampolsky, 1955; Mehdorn, 1989; Schor, 1977).

Joosse et al. (1999) achieved stimulus similarity by combining two dichoptically viewed Friedmann visual field analysers (through a stereoscope) with visually complex pictures of an Antarctic landscape scene with penguins. The scenes were perforated at the same locations of the original test stimuli of the field analyser. Depth of suppression across the binocular visual field could be measured by detection threshold measurement at the different points in the binocular visual field. Results for a monocular condition, where the amblyopic eye was tested whilst the other occluded, were subtracted from the dichoptic condition to give 'net' suppression. Participants were exotropes, with angles of

deviation ranging from 3 to 25 prism dioptres. Of the 15 strabismic participants, four were amblyopic.

Table 1.1: Characteristics of suppression for participants as measured with Joosse et al.'s (1999) method. T - temporal, A - above midline, U - under midline.

			Scotoma (binocular viewing conditions)		
Patient	**Preferred Eye**	**Eye**	**Depth (dB)**	**Type**	**Foveal projection in deg (1/2 objective angle)**
1	R	L	5	Total supp.	11 T
2	L	R	4	Total supp.	4.5 T
3	L	R	5	Total supp.	3.5 T
4	L	R	4	Fixation point	10/2 T/A
5	L	R	4	Total supp.	7.5 T
6	L	R	4	Total supp.	1.5 T
7	R	R	3	Total supp.	4 T
8	L	R	10	Total supp.	12.5 T
9	L	R	4	Total supp.	10 T
10	L	R	6	Nasal hemisup.	8.5 T
11	L	L	16	Total supp.	4 T
12	L	-	-	-	4 T
13	R	L	14	Total supp.	6.5 T
14	R	L	14	Nasal hemisup.	3.5 T
15	L	R	6	Fixation point	5/1 T/U

Table 1.1 shows the results of the study. The majority of the participants showed 'total' suppression, referring to general suppression across the whole visual field measured (for the stimuli used). Using similar methods but with small angle esotropes, Joosse et al. (1997) found no suppression scotomata in nine of 14 participants, with angles of squint ranging from 1 to 8 deg. In the five participants with suppression there was a central point scotoma around the fovea of the deviating eye ranging from 4 to 14 dB, from 2.5 to 15 deg in diameter. Those participants that showed these scotomata also showed a central suppression scotoma with the Bagolini striated lens test. The combined results of these two studies suggest that larger angle squints show larger areas of suppression. As the upper limit of suppression depth in Joosse et al.'s (1999) study is higher, it suggests that larger angle strabismic participants have deeper

inter-ocular suppression.

Joosse et al. (1999) found deeper suppression in the nasal hemifield (corresponding to temporal retina) with two exotropes. Sireteanu and Fronius (1981) found similar asymmetry in strabismic esotropes. Initially, grating acuity of each eye was measured in two anisometric amblyopes and nine strabismics across the horizontal meridian (40 deg either side of fixation). Separately, the detection threshold of a green test square viewed by the amblyopic eye was measured by reducing the luminance with neutral density filters until the square was no longer perceived. This was first performed monocularly with the amblyopic eye viewing through the green lens of anaglyph red-green glasses. Then the non-amblyopic eye was uncovered and viewed a red square dichoptically and the detection threshold measured again by reducing the luminance (with ND filters) of the amblyopic eye. A comparison between monocular and dichoptic thresholds gave a measure of inter-ocular suppression.

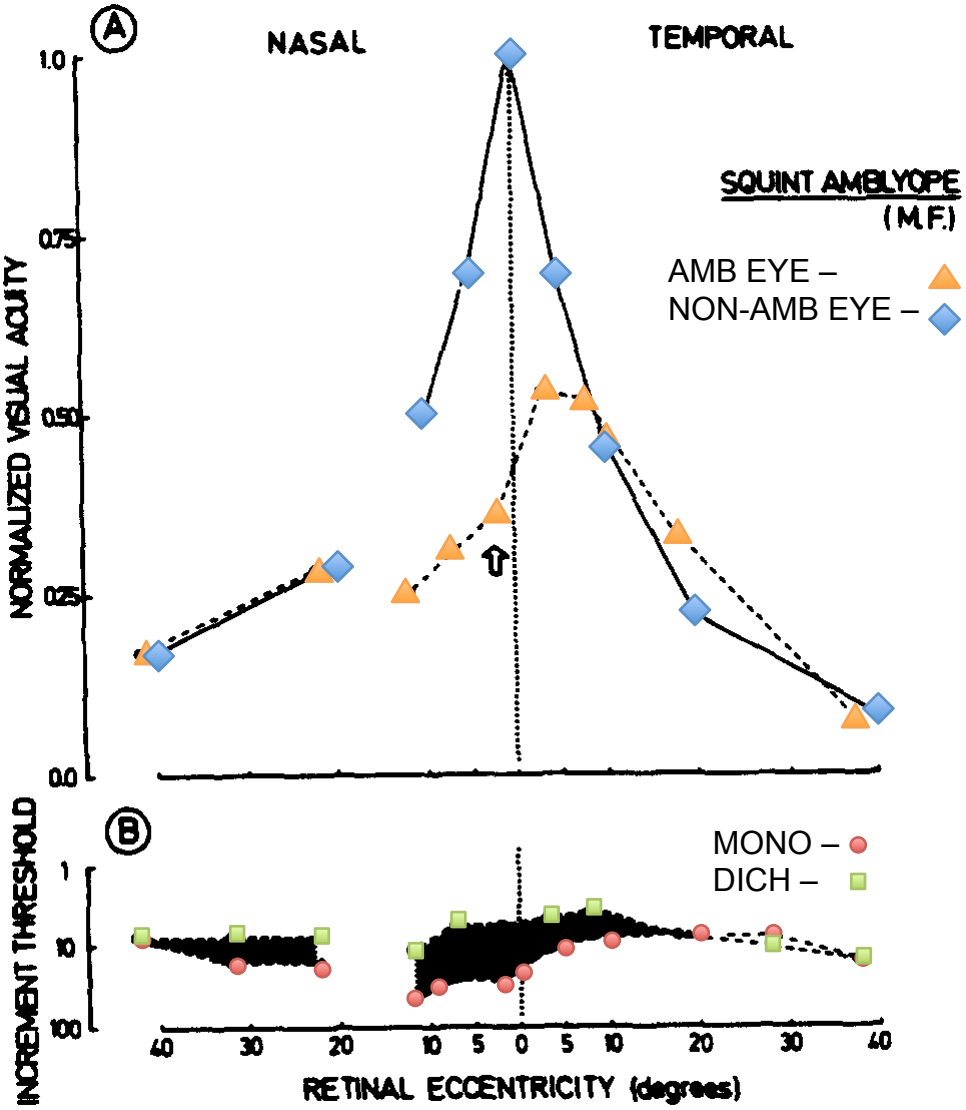

Figure 1.19: A) Visual acuity across different eccentricities lying on the horizontal meridian for one strabismic participant. Solid line represents the non-amblyopic eye acuity, and the dotted line represents the amblyopic eye grating acuity. The arrow denotes the point of eccentric fixation. B) Inter-ocular suppression for the same participant compared with the monocular detection thresholds of the non-amblyopic eye. Vertical height of black area gives depth of suppression. Adapted from Sireteanu and Fronius (1981)

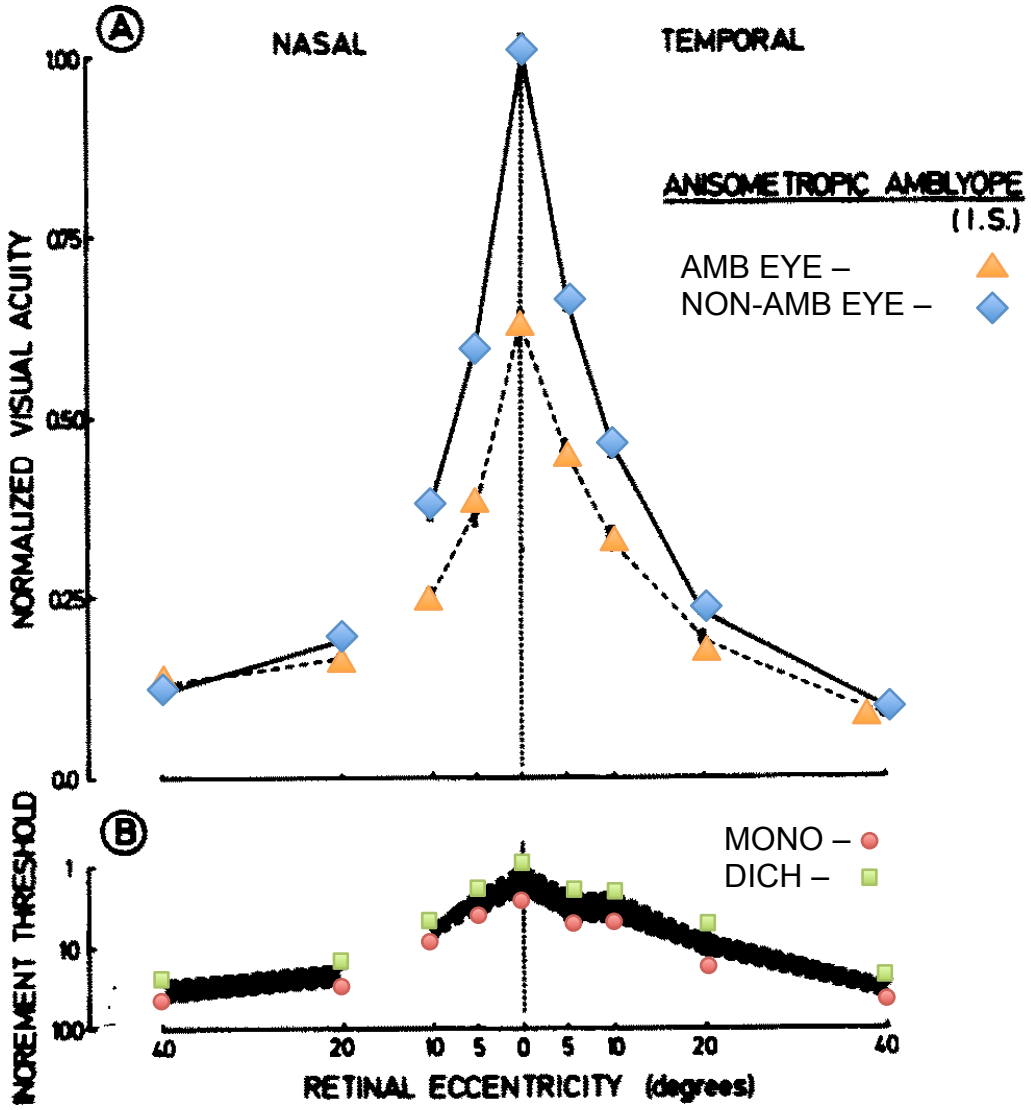

Figure 1.20: Results for an anisometropic amblyope shown in the same fashion as Figure 1.17

Figures 1.19 and 1.20 show results for a strabismic and an anisometropic amblyope, respectively. Figure 1.19A depicts the difference in monocular grating acuities for the amblyopic and non-amblyopic eye of a strabismic amblyope. Figure 1.19B shows the level of inter-ocular suppression (shaded area) for the same participant. The deficit in acuity across the visual field varies similarly with depth of inter-ocular suppression across the visual field. In other words, a larger inter-ocular acuity difference (i.e. amblyopia) shows deeper inter-ocular suppression at corresponding areas along the horizontal midline. This opposes Holopigian et al.'s (1988) finding (discussed in Section 1.1). Similar results were

seen for the other strabismic participants. Figure 1.20A shows that for an anisometropic amblyope, inter-ocular acuity difference and the level of inter-ocular suppression were more equal and symmetric across the visual field than for strabismic amblyopes. Both types of amblyope, therefore, showed good correspondence between acuity loss and depth of inter-ocular suppression across the visual field. Furthermore, taken with Joosse et al.'s (1999) finding with exotropes, location of suppression scotomata are dependant on direction of strabismus.

The retinotopic correspondence between inter-ocular suppression and reduced visual acuity led Sireteanu and Fronius (1981) to infer a causal relationship between the two. Visual acuity is worse and peak contrast sensitivity occurs at lower spatial frequencies in younger visual systems (e.g. Banks and Salapatek, 1978). The spatial range over which fusion occurs would be large as sensitivity to lower spatial frequencies develops before sensitivity to higher spatial frequencies (e.g. Norcia, Tyler and Hamer, 1990). As visual acuity develops, Panum's area gets smaller and consequently the visual system's ability to fuse smaller disparities increases (e.g. Held, Birch and Gwiazda, 1980). With strabismic individuals, ocular misalignment during the visual developmental period results in a lack of fusion. If images are not fused, binocular rivalry may occur. Due to inherent ocular imbalance (e.g. Yang, Blake and McDonald, 2010; Zhang et al., 2011), the non-dominant eye would be suppressed more, and over time amblyopia could develop with its associated functional spatial deficits. In anisometropia, uncorrected refractive imbalance causes symmetrical inter-ocular grating acuity loss across the whole visual field and suppression was measured at an equal depth across the visual field. However, data for the anisometropic amblyope shown in Figure 1.19 reveal better visual acuity with their amblyopic eye and shallower suppression compared with the strabismic participant (Figure 1.20). In order to compare differences across the visual field, some standardisation should be implemented, for example, equating anisometropic and strabismic amblyopes based on their visual acuity.

A novel, portable method of measuring inter-ocular suppression depth and extent was recently published by Babu et al. (2013), which aligns images presented to the two eyes enabling both fixation and corresponding point scotomata to be measured. Suppression is quantified across the central circular 20 deg visual field using stimuli comprising five concentric adjacent rings (1 deg radius) of alternating polarity, each split into eight sectors (total 40 sectors) against a mean luminance background. A central black fixation spot was present in both eyes. Stimuli were presented using head-mounted displays, one for each eye (Figure 1.21). Stimuli were initially aligned using software prior to testing to present each (half) stimulus on corresponding retinal points.

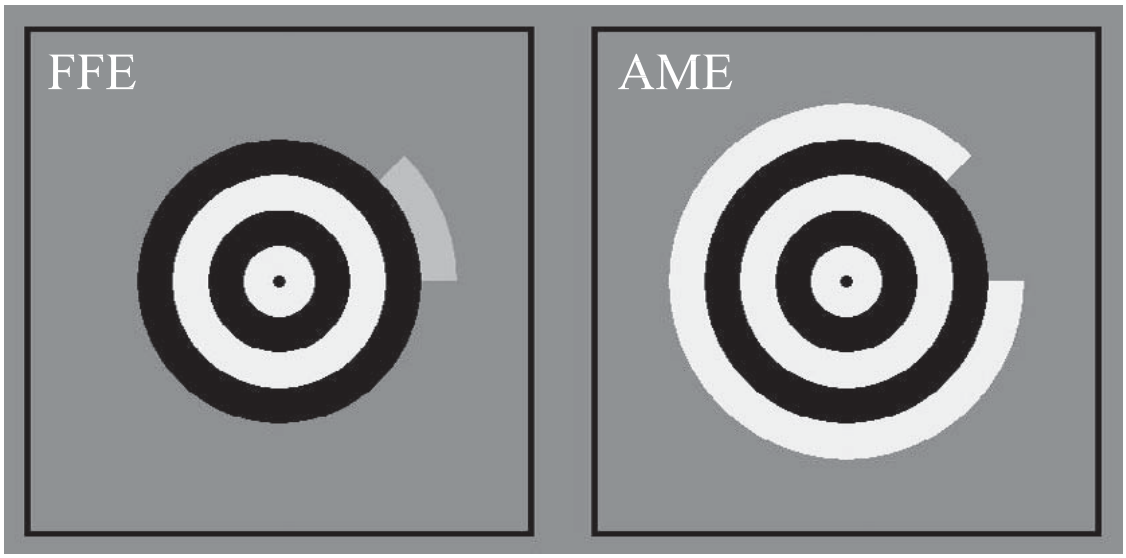

Figure 1.21: Stimuli presented to each eye dichoptically (FFE – fixating eye. AME – amblyopic eye). Taken from Babu et al. (2013)

Amblyopic eye ring contrast compared to the background mean luminance was fixed at 80% for both dark and light rings. One sector at a time (e.g. Figure 1.21) was adjusted in brightness by the non-amblyopic eye to perceptually match the corresponding ring presented to the amblyopic eye using a method of adjustment. Luminance is adjusted in the non-amblyopic eye to match the amblyopic eye luminance perception. The procedure was repeated for each of the 40 sectors three times, with decreases in step size (10, 5 and 1% contrast) with each attempt. Participants were normal healthy adults (n = 10), strabismics (microesotropia = 4, esotropia = 5, exotropia = 1), or anisometropes (n = 4). All strabismics and anisometropes were amblyopes.

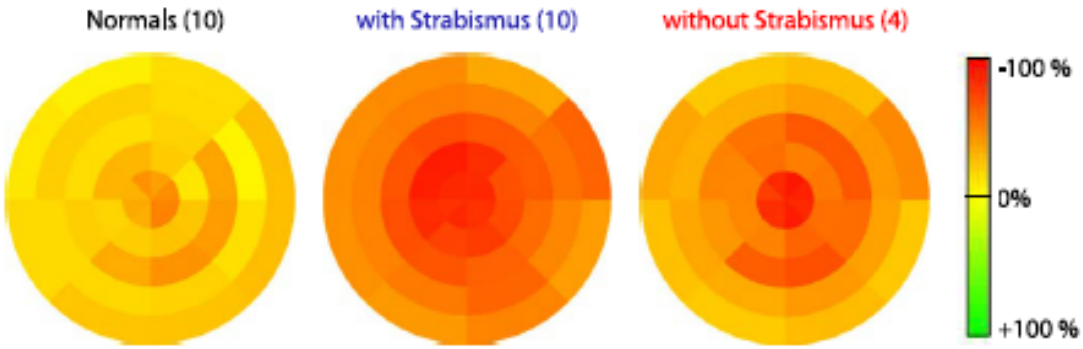

Figure 1.22: Suppression maps averaged of each group of participants (normals, strabismics, and anisometropes). Each sector is represented by a colour. The colour-bar on the right shows that yellow represents no suppression (i.e. an inter-ocular match), green facilitation (signal strength in the non-amblyopic eye is increased to match the amblyopic eye) and red for suppression (signal strength is decreased in the non-amblyopic eye to match the amblyopic eye). Taken from Babu et al. (2013)

Data averaged across each group showed significant central suppression for the amblyopic participants (Figure 1.22). Average visual acuity loss was similar between anisometropes and strabismics. Contrary to previous studies, strabismics only show a central point scotoma, without deeper measureable suppression at the fixation point. This may have been due to the averaging across all participants where individual suppression maps may have shown some asymmetry and different positioning of the corresponding points. Also in contrast to previous studies showing large central areas of suppression (Sireteanu and Fronius, 1981; Sireteanu et al., 1981), in the Babu et al study, anisometropes show a smaller, central (within 3 deg) scotoma that reduces to near normal with increasing eccentricity. This result may be due to the presence of a centrally fused fixation spot, or the introduction of rivalry and lustre, combined with the method of adjustment used. Also, fixation was not monitored throughout the procedure potentially contributing another source of inaccuracy. Moreover, as pointed out by Ding et al. (2013b) (see Section 1.3.2.1), in order to measure the influence of the non-amblyopic eye on the amblyopic eye during binocular viewing (i.e. inter-ocular suppression), the non-amblyopic eye contrast should remain fixed and the amblyopic eye varied. Therefore Babu et al. may be measuring the effect of the amblyopic eye on the non-amblyopic eye, and not suppression.

Table 1.2. Suppression characteristics of reviewed studies. Participant types are highlighted: Strabismics – red, microstrabismics – pink, anisometropes – green.

STUDY	PARTICIPANTS (number)	METHODOLOGY	ANGLE CORRECTION	DISTRIBUTION OF SUPPRESSION
(von Graefe, 1856)	Strabismic amblyopes (clinical observations)	Kinetic perimetry (red lens dissociation)	No	Central point
(Harms, 1937)	Strabismic amblyopes (13)	Red-green dissociation	No	Central point
(Travers, 1938)	Strabismic amblyopes (3)	Mirror-Screen Test	Yes	Fixation point to central point Less dense at scotoma periphery
(Irvine, 1948)	Strabismic amblyopes (25) Anisometropic amblyopes (15)	Prism dissociation	Yes	Strabismics – fixation to central point Anisometropes – central point
(Jampolsky, 1955)	Strabismic amblyopes (clinical observations)	Prism dissociation Haploscope with similar stimuli	Yes	Hemiretinal suppression between central and fixation point (both methods)
(Herzau, 1980)	Alternating strabismic (28) Strabismic amblyopes (21)	Haploscope with monocularly presented grid	Yes	Fixation to central point
(Sireteanu, Fronius and Singer, 1981)	Microstrabismics (5) Strabismic amblyopes (4) Anisometrope amblyopes (2)	Stereo-perimetry	Yes	Microstrabismics – asymmetric central point Strabismics – variable Anisometropes – symmetric central point
(Sireteanu and Fronius, 1981)	As above	Monocular vs. binocular detection thresholds	Yes	Strabismics and microstrabismics – asymmetric central point Anisometropes – central point
(Campos, 1982)	Strabismic amblyopes (6)	Red-green dissociation	No	Central point
(Hallden, 1982)	Microstrabismics (2) Strabismics amblyopes (3) All with ARC	Prism dissociation	No	Central point
(Pratt-Johnson and Tillson, 1983)	Strabismic amblyopes (17)	Prism dissociation	Yes	Hemiretinal suppression between central and fixation point
(Mehdorn, 1989)	Microstrabismics (8)	Stereo-perimetry (a), prism dissociation (b), Bagolini perimetry (c), rivalry perimetry (d)	No	(a) no scotoma (i.e. lack of stereopsis), (b) and (c) variable scotomata, (d) generally larger central point than other methods
(Gottlob, Charlier and Reinecke, 1992)	Strabismic (including mixed) amblyopes (17) Anisometropic amblyopes (3)	Red-green dissociation	No	Central point (all participants)
(Joosse et al., 1997)	Strabismic (11) Strabismics amblyopes (4)	Dichoptic visual field analysers (stereoscope)	Yes	Central point scotoma in five of 14 participants
(Joosse et al., 1999)	Alternating strabismics (14)	As above	Yes	Total suppression of deviating eye (all participants)
(Babu et al., 2013)	Strabismic amblyopes (6) Microstrabismics (4) Anisometropic amblyopes (4)	Interocular contrast matching	Yes	Central point scotoma for all participant groups

Table 1.2 shows the main conclusions of previously conducted studies that investigate inter-ocular suppression across the visual field. Generally, studies that do not correct the angle of squint to measure suppression do not find a fixation point scotoma, with the exception of Babu et al. (2013). This refers to the point on the amblyopic eye that receives the same image and the non-amblyopic eye fovea during habitual viewing, when the squint angle is not corrected. When images are directed onto corresponding points, for microstrabismics whose angle of deviation is less than 6 prism dioptres, there is generally only a fixation point scotoma. For strabismics with deviations greater than 6 prism dioptres, suppression extends from the central to the fixation point. Anisometropes generally only show central point scotomata.

Upon review of the extant literature, different depths and extents of suppression are found with different methods of measurement. These could be due to the stimuli used (motion-, luminance-, contrast-, or stereoscopically-defined), the level of dissociation, the aetiology of amblyopia, or most likely a combination. Furthermore, in order to measure suppression more accurately, the participant would ideally be presented with similar visual stimuli to each eye, as this will allow both fixation and corresponding point scotomata to be quantified.

Additionally, in order to test the potential values any new method of suppression measurement (e.g. with novel second-order spatial stimuli), it would be ideal to be able to specify the degree of amblyopia (i.e. inter-ocular acuity difference), anisometropia and angle of strabismus. As this is not possible, different levels of inter-ocular suppression can be created in normal vision. Ideally, these simulations would have some relevance to visual perception in the clinical condition. If perception in amblyopia is successfully mimicked, the suppression mapping tool and experimental paradigms can be modified to be more effective, before applying it to the clinical condition. This is the strategy taken in this thesis, and the subject of modelling visual perception in amblyopic is discussed in the following section.

1.5 Models of amblyopia

Stimuli and procedures for measuring inter-ocular suppression have varied greatly throughout history. After a period of relative dormancy, research into inter-ocular suppression has recently become very active, in part due to the availability of new portable technology, and in part due to changes in beliefs about recoverability of binocularity in amblyopia. The generation of a new robust method for measuring inter-ocular suppression in amblyopia initially requires refining on participants with controlled amounts of inter-ocular suppression. Therefore simulating the inter-ocular imbalance in amblyopia with dioptric blur and neutral density (ND) filters in normal vision will be reviewed in the following section. Monitoring changes in suppression depth and extent in a known, induced level of inter-ocular suppression will give an idea of the reliability of the new method of quantifying suppression. Furthermore, any potentially valuable effects of inter-ocular suppression on the perception of first- and second-order spatial stimuli can also be examined.

1.5.1 Blur

Barbeito et al. (1987) found that monocularly reducing luminance (with neutral density filters) affected the optotype acuity of anisometropic amblyopic eyes and monocularly blurred (+1.25 D) normal eyes in a similar way. Seven strabismic and seven anisometropic amblyopes were compared to six binocularly normal participants. Monocular visual acuity was measured using Landolt C optotype charts, where participants identified the location of a gap in a ring from one of four possible positions.

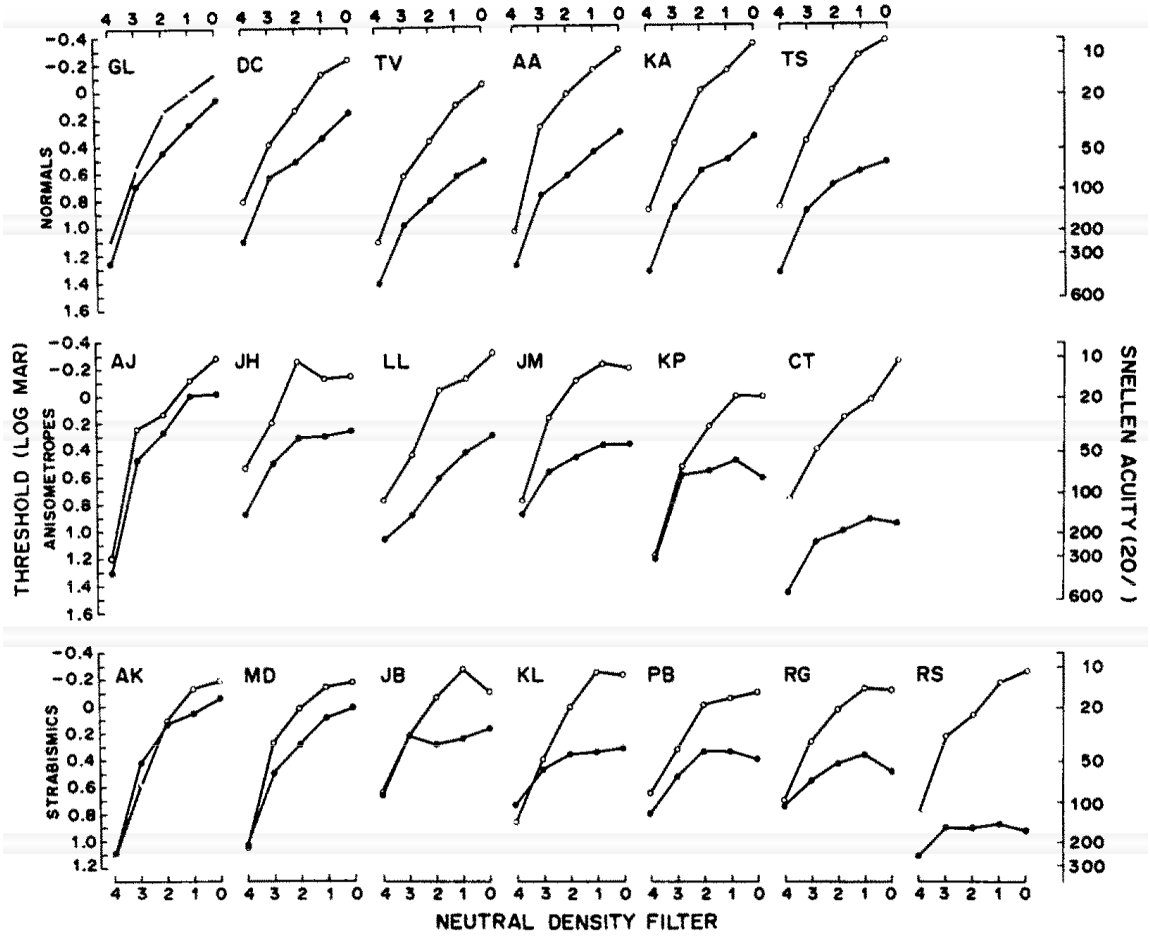

Figure 1.23: The effect of neutral density filters on the visual acuity of the blurred – filled circles, and non-blurred eye – unfilled circles (top row). The middle row shows data for the anisometropic amblyopic participants' amblyopic (filled circles) and non- amblyopic (unfilled circles) eyes, and the bottom row the same curves for the strabismic amblyopic participants. Taken from Barbeito et al. (1987)

Figure 1.23 shows acuity thresholds for the blurred normal, anisometropic and strabismic participants as indicated to the left of each row. For each participant, the top curve is either the non-blurred eye (top row) or the non-amblyopic eye. As neutral density filter is increased, the acuity of all eyes generally reduces. For blurred eyes or anisometropes' amblyopic eyes this occurs at all levels of neutral density filter. However, increasing neutral density filter for strabismics reduced the acuity of the amblyopic eye to a lesser degree than with anisometropic amblyopic eyes. The blurred eye's acuity is therefore similar to the anisometropic amblyopic eye when reducing luminance with neutral density

filters, but not strabismic amblyopic eyes.

More recently, Song et al. (2014) compared flanked (by other letters) and unflanked letter optotype acuity of blurred normals, normal eccentric viewing, anisometropic and strabismic amblyopes (see Section 1.3.1.1). Results are shown in Figure 1.24, where flanked acuity ('Threshold spacing S') is plotted against unflanked acuity ('Acuity A'). Threshold spacing is calculated as flanked acuity multiplied by a fixed spacing factor (1.1) between the flankers and the targets. Blurred normals had similar ratios of flanked to unflanked acuity to pure anisometropic amblyopes, suggesting blur as a good model for optotype acuity in anisometropic amblyopes (Figure 1.24A). These results were not repeated with strabismic amblyopes (Figure 1.24B), who showed a larger crowding effect, i.e. flanked to unflanked thresholds were larger than anisometropes and blurred normals. Moreover, a study by Formankiewicz and Waugh (2013) investigated the effect of blur and eccentric viewing on crowding of high contrast optotypes. The results of Song et al.'s (2014) anisometropes and blurred normals are similar to the blurred normals used in the Formankiewicz and Waugh (2013) study.

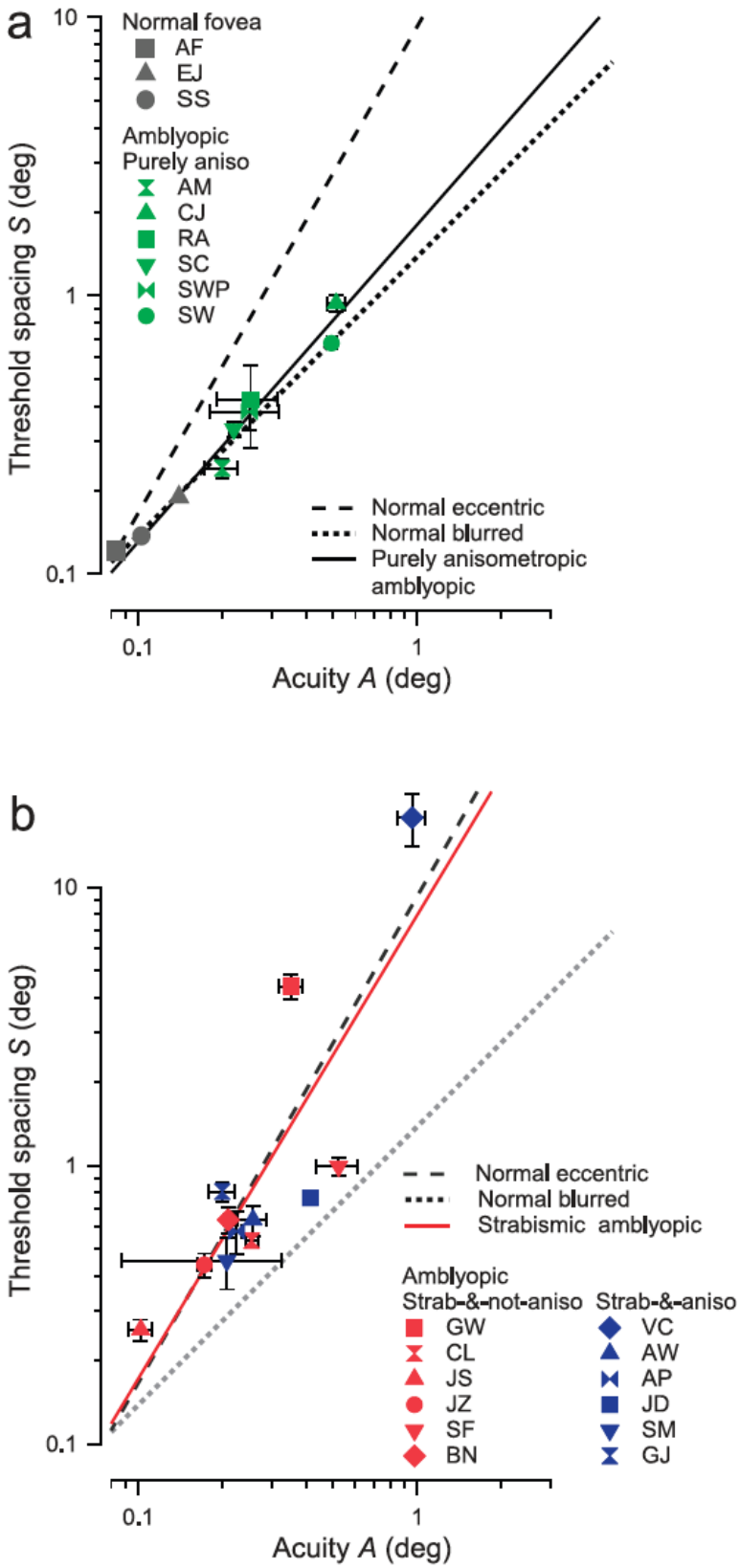

Figure 1.24: Results of Song et al.'s (2014) study presenting Threshold spacing vs. Acuity (see text). Dotted lines represent blurred normal data, A) anisometropes (green), and B) strabismics (red) including strabismic-anisometropic amblyopes (blue). Taken from Song et al. (2014).

Many animal studies have used optically induced anisometropia to study the effect on perception and neurophysiology (e.g. Smith, Harwerth and Crawford, 1985; Smith, Harwerth, Duncan and Crawford, 1986; Wensveen, Smith and Harwerth, 2001). Kiorpes et al. (1998) is another example. Three monkeys were reared with optically induced anisometropia (see Section 1.3.1.1 for experimental details). Optically inducing anisometropia in monkeys caused similar changes in the contrast sensitivity function compared with anisometropic amblyopic humans.

In humans, however, we seek only to mimic anisometropic amblyopia, not induce it. With dioptric blur, similar to anisometropic amblyopia, high spatial frequencies are attenuated when viewing monocularly. In order to gain insight into habitual viewing of an amblyope, vision during binocular viewing must be assessed in order to account for inter-ocular suppression. Pianta and Kalloniatis (1998) artificially induced anisometropic suppression in normal participants and compared this with anisometropic amblyopic participants in a reaction time paradigm. Temporal summation was measured using stimuli as seen in Figure 1.25 below.

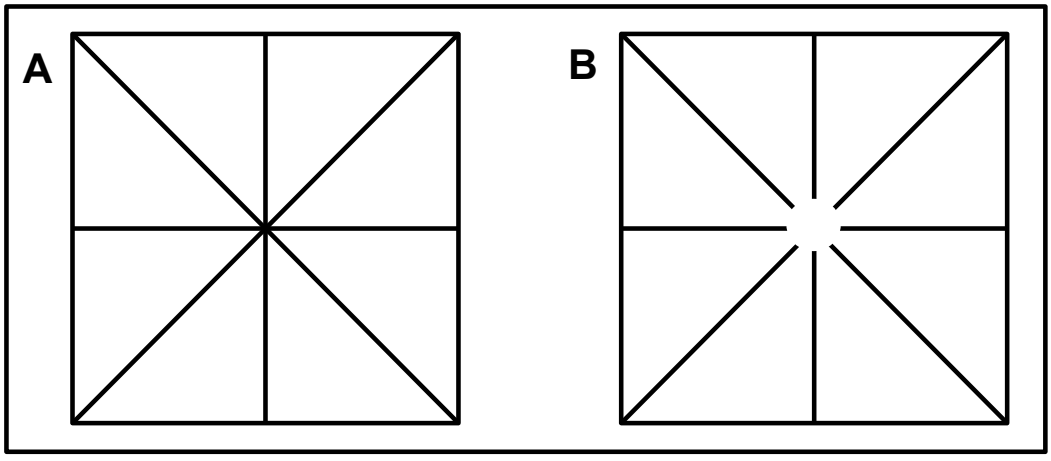

Figure 1.25: Synoptophore targets used by Pianta and Kalloniatis (1998).

Figures 1.25A and 1.25B were presented dichoptically. The missing central region of Figure 1.25B was 1 deg in diameter, otherwise the stimuli were the same with a line width of 0.55 deg. The stimulus was a 0.65 deg diameter disk

presented in the centre of the target in Figure 1.25A. Reaction time to the onset of the disk was measured. The luminance of the disk was subsequently reduced in 0.1 log Td steps after each response whilst continually measuring reaction times. Different levels of anisometropia were induced for these measurements with dioptric blur. Three conditions were tested: monocular (viewing target A only), suppression (suppressing eye viewed target A, and non-suppressing eye viewing target B), and dominance (non-suppressing eye viewed target A, and suppressing eye viewing target B).

Figure 1.26 shows criterion reaction time thresholds against the illuminance of the stimulus for anisometropic amblyopes (left column), and data for normal participants are plotted in the right column. For these normal participants, there is approximately a 0.6 log unit general luminance increase in threshold at all durations with +2 D and greater anisometropic blur. All amblyopic participants show similar characteristics comparing amblyopic and non-amblyopic eyes. All curves are shape invariant, and anisometropic amblyopic performance can be simulated by “scaling up” normal vision with blur.

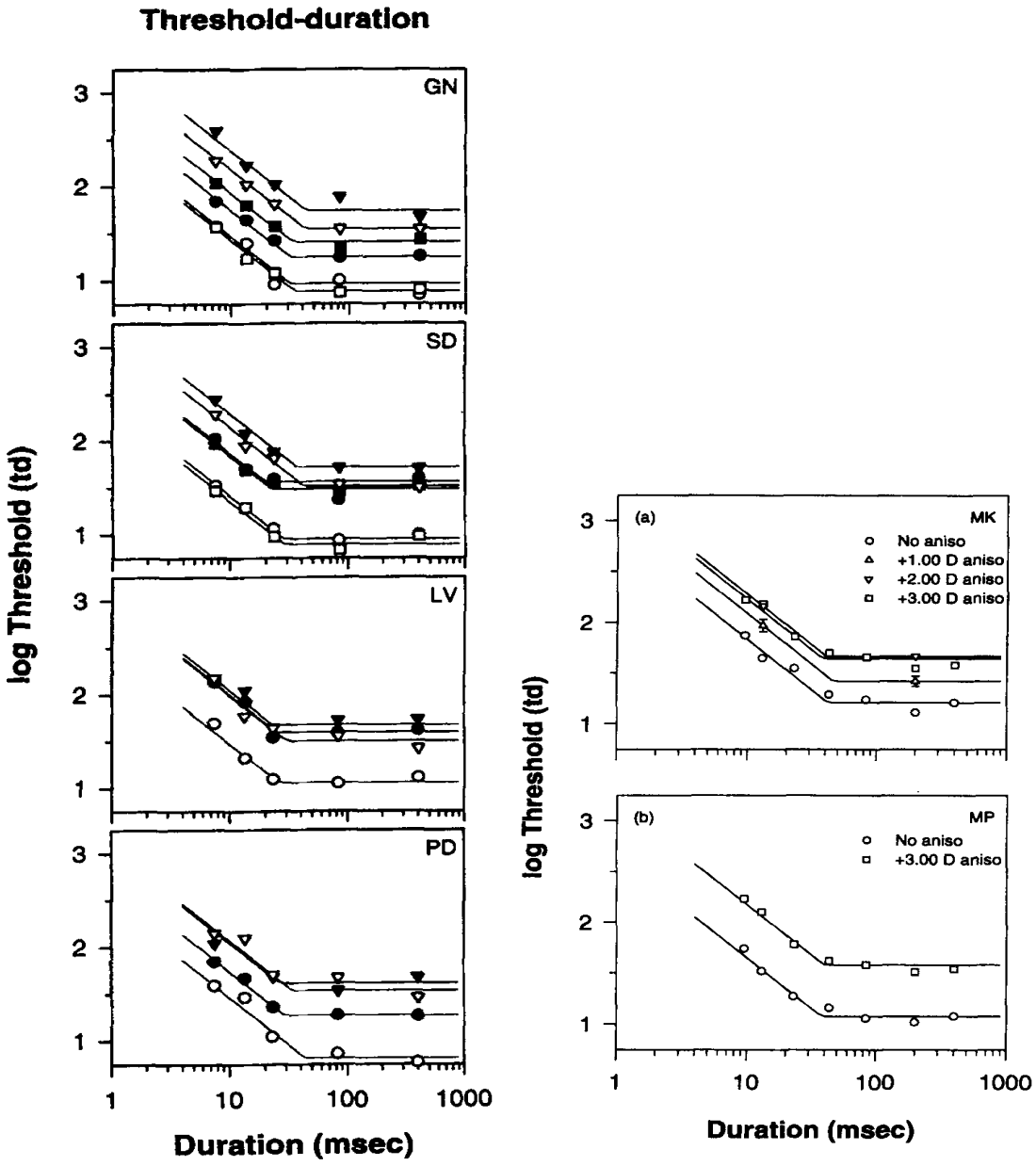

Figure 1.26: Left column shows data for amblyopic participant criterion reaction time against luminance of stimulus. Circles, triangles and squares denoting dominance, suppression and monocular conditions respectively. Open symbols represent the non-amblyopic eye, and filled symbols the amblyopic eye. Right column shows results for binocularly normal participants with the legend denoting the level of blur used. Standard errors of means are smaller than symbols where not indicated. From Pianta and Kalloniatis (1998)

Some evidence for the simulation of anisometropic amblyopia with dioptric blur is present, though fewer conclusions have been drawn with respect to the inter-ocular viewing with monocular blur. However, we know that monocular blur causes monocular deficits similar to that of the amblyopic eye when viewing monocularly. We can therefore accept guardedly that images presented to each eye will be different enough to cause inter-ocular suppression, similar to long-term inter-ocular suppression throughout visual immaturity that leads to anisometropic amblyopia developing.

1.5.2 Neutral density filters

Baker et al. (2007) compared binocular summation in strabismic amblyopes and a normal participant viewing binocularly with a monocular 1.5 ND filter. With compared to without the monocular ND filter, the control participant had a reduced binocular summation ratio (given by binocular/best monocular sensitivity). Adjusting the contrast to the filter eye stimulus (by a factor non-filter/filter eye monocular sensitivities) and reassessing binocular summation ratios showed close to normal values, above $\sqrt{2}$. Similar results were found for strabismic amblyopes with the contrast adjustment, showing that binocular summation is present in amblyopic participants and is demonstrated when the contrast deficit of the amblyopic eye is accounted for. Furthermore, monocular ND filters during binocular viewing in a normal mimicked binocular summation in strabismic amblyopes.

Determining suprathreshold sensitivity is more comparable to real world spatial viewing, as opposed to the above studies where threshold vision is assessed. Baker, Meese and Hess (2008) investigated monocular, dichoptic and binocular contrast discrimination for 10 pedestal contrasts from 0 to 32% in 5 dB steps in strabismic amblyopes, and also compared the resulting dipper functions to a normal participant with a 1.5 ND monocular attenuation. Contrast increments were added to 3 c/deg sinusoidal gratings. The normal participant's left and right monocular functions were of a similar shape to previously determined contrast

discrimination (dipper) functions (see Section 1.3.1.2). Facilitation was greater binocularly, however, when the 1.5 ND filter was added in front of the left eye only, binocular advantage was almost absent. This result is similar to that obtained from strabismic amblyopes, therefore suggesting ND filters in normal foveal viewing as a good model for strabismic amblyopic binocular contrast discrimination.

Previous studies have used ND filters (i.e. luminance attenuation) in front of non-amblyopic eyes during binocular viewing to equate vision between amblyopic and non-amblyopic eyes. For example, an early study by Pugh (1954) employed ND filters to measure foveal suppression in a number of unilateral amblyopes (n=150, VA ranging from hand movements to 6/12, from 10 to 55 years, either anisometropic, strabismic or both). To one eye, a ring comprising eight dots arranged in a circle was presented and to the other eye, a corresponding ring had two vertical and two horizontal dots coinciding with four of the dots on the ring, and one in the centre. Participants were asked to count the dots of sizes equivalent to 1/60 to 6/6 Snellen letters. Initially this was carried out with the non-amblyopic eye completely occluded, and then binocularly. For the latter tests amblyopic eye acuity was markedly reduced compared with monocular viewing, as expected (due to inter-ocular suppression). This reduction (i.e. suppression) was quantified by the addition of ND filters to the non-amblyopic eye until acuity similar to amblyopic eye monocular acuity was achieved. Of amblyopes with normal retinal correspondence 20% showed a return to monocular amblyopic eye acuity when the non-amblyopic eye luminance was reduced with up to 2.95 ND, the rest requiring a reduction in luminance with 3-4 ND to equate with monocular amblyopic eye acuity. Pugh's results suggest a range of neutral density filters that can neutralise different levels of amblyopia. The mechanism of this amblyopic eye vision improvement may be that ND filters are mimicking amblyopic eye vision in the non-amblyopic eye, and so rebalancing vision.

The above study investigated the behaviour of amblyopic visual systems at the highest spatial frequencies resolvable (i.e. acuity limit), and how the amblyopic

deficit can be measured by attenuating non-amblyopic eye input with ND filters. Levi and Harwerth (1977) measured contrast sensitivity with sinusoidal gratings across a range of spatial frequencies in anisometropic and strabismic amblyopes. Amblyopic participants were adults with amblyopic eye visual acuities of 6/15 to 6/60. Data showed reduced sensitivity for all spatial frequencies for the amblyopic relative to the non-amblyopic eye. With the addition of a 1 ND filter, sensitivity was reduced at all but the lowest spatial frequencies in the non-amblyopic eye, and there was little effect on the sensitivity of the amblyopic eye. Inclusion of an ND filter in front of the non-amblyopic eye did not reduce contrast sensitivity to a similar level in the amblyopic eye (6/60), although perhaps a denser filter, such as those used in Pugh's study, would have. Levi and Harwerth (1977), however, determined only monocular contrast sensitivity functions and therefore binocular interaction was not assessed.

Leonards and Sireteanu (1993) measured the time course of binocular rivalry in normal and amblyopic participants, with low spatial frequency sinusoidal orthogonally presented gratings (0.5 c/deg, 6 deg diameter). Neutral density filters were used to attenuate the luminance of the grating presented to the non-dominant or non-amblyopic eye. Adding ND filters to normal participants gave constant suppression of one of the stimuli, and the incidence of constant suppression increased with increasing filter density. The converse was true for amblyopes, with no filter there was constant suppression of the grating presented to the amblyopic eye. As ND filter density was increased, rivalry occurred. Different densities of filter caused this across participants. Superimposition of the gratings, similar to normals, occurred for durations of 150 ms and below. Two conclusions may be drawn from the study: amblyopic participants can experience binocular rivalry, in agreement with Schor (1977); and monocular ND filters during binocular viewing mimics the constant suppression seen in amblyopia.

With a dichoptic global motion coherence paradigm, Zhang et al. (2011) measured sensory eye dominance in the normal population. Addition of ND

filters (1, 2, and 3 ND) showed increasingly strong inter-ocular suppression as measured by a shift in the 'balance point' to lower contrasts. These results are similar to previously mentioned studies with amblyopes, suggesting monocular ND filters during binocular viewing as a model for amblyopia. Although, here the deficit of more complex visual stimuli is shown to be modelled well with ND filters. Hess, Mansouri, Thompson and Gheorghiu (2009) also show this by measuring residual stereo function in amblyopes with a motion in depth paradigm, also thought to be subject to extrastriate processing. Addition of ND filters in front of the non-amblyopic eye balanced inter-ocular performance.

Evidence provided in these studies builds a strong case for the use of neutral density filters to model central vision in strabismic amblyopia. The attenuation of all frequencies of light equally seems to mimic what is occurring during binocular viewing. In order to simulate an amblyopic eye and subsequently to measure inter-ocular suppression, it is important to have an idea of the binocular perception with this simulation, namely its similarity to the amblyopia it is attempting to model. Using neutral density filters to measure the inter-ocular suppression of spatial stimuli is therefore in line with the aims of this thesis.

The above studies also give evidence for the simulation of inter-ocular suppression in amblyopia with ND filters for a range of visual functions thought to be processed in the striate and extrastriate cortex, along different processing pathways. Contrast-modulated stimuli in the present experiment are thought to be subject to processing by binocular neurones, possibly located in the extrastriate cortex. Using ND filter suppression and blur to model amblyopes will provide an idea of the contrast-modulated processing deficit in amblyopia. Furthermore, the effect of luminance attenuation, and low pass filtering and contrast reduction, with ND filters and blur, respectively, can be determined.

1.6 Specific Aims

Upon review of extant literature, several gaps and uncertainties in knowledge have been identified, namely how depth and extent of suppression across the visual field is associated with both induced and inherent binocular disturbance, and how far along spatial processing pathways suppression progresses. In this thesis, an accurate and easy to use method of measuring both depth and extent of expression will be developed, allowing assessment of suppression scotomata in participants with different types of binocular vision disturbance. Secondly, suppression of complex spatial stimuli (second-order) will be compared with simpler spatial stimuli (first-order) to assess the progression of deficits along different processing pathways.

Normal binocular vision involves equal contribution from each eye to a binocular percept. If one eye receives an image that is sufficiently different to the other eye's image, suppression of one image occurs. This difference will be induced by either monocular blur, monocular adaptation to an ND filter, or will be present due to pathological binocular disturbance, i.e. amblyopia. In these cases, to avoid diplopia the eye with the degraded image is suppressed. In order to measure the depth of this suppression, the suppressed eye's image will be increased in signal strength (either luminance- or contrast-modulation) until images to each eye are perceived with equal intensity. As this inter-ocular difference in signal strength is rebalancing the experimentally induced or innate binocular disturbance that led to suppression, it is considered to be a direct measure of depth of suppression in the following experiments detailed in this thesis.

To refine methods and evaluate equipment for the novel suppression mapping procedure, controlled levels of image degradation will be imposed on normal participants with monocular dioptric blur or neutral density filters during binocular viewing.

The current study is divided into three experiments:

1) Quantifying the effects of monocular dioptric blur on inter-ocular suppression of luminance-modulated and contrast-modulated noise stimuli
2) Quantifying the effects of monocular neutral density filters on inter-ocular suppression of luminance-modulated and contrast-modulated noise stimuli
3) Quantifying the inter-ocular suppression of amblyopic participants and those with binocular disruption with luminance-modulated and contrast-modulated noise stimuli.

These experiments have been formulated in order to answer the following questions:

1) How does inter-ocular blur induced suppression in normal vision vary across the visual field?

Maps of suppression across the visual field will be measured using different types of stimuli on blurred normal participants, in order to simulate anisometropic amblyopia. Results will also help us to understand adaptation to unilateral blur in other conditions, e.g. monovision contact lens wear.

2) How does inter-ocular luminance difference induced suppression in normal vision vary across the visual field?

Contrast detection and discrimination in strabismic and anisometropic amblyopia has been simulated in previous studies with normal participants using monocular neutral density filters, and therefore will be used with binocularly normal participants to measure suppression across the visual field. The results will help understand binocular vision in patients with amblyopia and other conditions producing delayed uniocular responses, e.g. in cataract or in optic neuritis.

3) How do suppression maps differ when measured with stimuli probing different pathways and depths of processing in visual cortex?

Maps for different stimuli will be compared, furthering our understanding of visual processing and binocular suppression at different levels of neural processing.

4) How do suppression maps for amblyopic participants differ using different visual stimuli, and how does amblyopic suppression relate to inter-ocular suppression of blur and neutral density filters in normal vision?

Refined stimuli and protocols will generate suppression maps, which could ultimately be used to monitor amblyopia treatment.

CHAPTER 2

EXPERIMENT 1 – INVESTIGATION OF INTER-OCULAR BLUR SUPPRESSION USING LUMINANCE-MODULATED AND CONTRAST MODULATED NOISE STIMULI [1]

2.1 Introduction

Different levels of blur presented to the two eyes creates images that cannot be fused into a single percept. Diplopia and confusion ensue and the input of one eye is suppressed (Travers, 1938; Sireteanu and Fronius, 1981; Harrad, Sengpiel and Blakemore, 1996; Sengpiel and Blakemore, 1996). Inter-ocular blur suppression can also occur pathologically in response to unequal refractive error, i.e. anisometropia (von Noorden, 1985), as well as in response to organic causes of inter-ocular blur differences such as monocular cataract, leading to form-deprivation (Wiesel and Hubel, 1963a).

During visual development, disturbances of binocular vision such as those mentioned above may result in amblyopia (Wiesel and Hubel, 1963b; Hubel and Wiesel, 1965; von Noorden, 1974; Daw, 2006), which is characterised by deficits in many aspects of monocular spatial vision, as well as binocular motion integration and stereo-acuity (McKee et al., 2003). However, binocular function is not absent in amblyopia, as Baker et al. (2007) measured normal central binocular summation in amblyopes when contrast strength in threshold units was equated between the eyes.

Monocular blur effects on normal vision have been found to mimic some aspects of spatial perception in anisometropic amblyopia (Barbeito et al., 1987; Levi and Klein, 1990a, 1985; Formankiewicz and Waugh, 2013; Song, Levi and Pelli, 2014). For example, Levi and Klein (1982a, 1982b) found the same relative differences in Vernier and grating acuities in anisometropic amblyopia

[1] This chapter has been published as:
Chima, A.S., Formankiewicz, M.A., and Waugh, S.J., 2015. Investigation of interocular blur suppression using luminance- modulated and contrast-modulated noise stimuli. *Journal of vision*, 15(3), pp.1–22.

to those found in normal vision, but scaled to their level of visual acuity. Therefore, if normal vision could be made worse, for example by using optical blur, spatial perception similar to anisometropic amblyopes may occur. Additionally, Barbeito et al. (1987) found that reducing luminance levels (with neutral density filters) degraded optotype acuity of anisometropic amblyopic eyes and monocularly blurred normal eyes similarly. Formankiewicz and Waugh (2013) recently reported that the ratio of visual acuity to the extent of crowding remains constant in monocularly blurred normals and this result was confirmed in anisometropic amblyopes (Song et al., 2014). Interestingly, a close relationship between this ratio and stereopsis, a binocular measure related to inter-ocular suppression, was also noted. Song et al. (2014) further suggest that blur is a good model for purely anisometropic amblyopia, which is mainly size limited, as is normal central vision with added blur. Pianta and Kalloniatis (1998) compared binocular suppression characteristics of monocularly blurred normals and anisometropic amblyopes using a reaction time paradigm for the detection of a 0.65 deg dichoptically flashed test disc across different luminance levels. Similar reaction times were measured for the two groups, indicating similarity of inter-ocular suppression characteristics. Physiological evidence also shows that rearing animals with monocular blur under binocular viewing conditions, leads to anisometropic amblyopia (Maguire, Smith, Harwerth, and Crawford, 1982; Smith, Harwerth, and Crawford, 1985; Smith et al., 1997; Kiorpes et al., 1998).

Clinical and experimental methods of measuring inter-ocular suppression in amblyopia have been employed for over 150 years (for review, see: Joosse, Simonsz, and Jong, 2000; Chapter 1, Section 1.4.2.2). Clinical techniques are generally insensitive and largely only detect, rather than quantify, foveal suppression. Suppression studies of anisometropic amblyopia have shown a central circular loss in the visual field (Sireteanu, Fronius and Singer, 1981; Sireteanu and Fronius, 1981), which may also be expected with inter-ocular blur suppression. Ideally, to assess real differences in suppression depth *per se* across the visual field, stimuli should be scaled to account for the larger spatial summation areas in the periphery. The task could also be made more comparable to real world vision by employing supra-threshold contrast

matching, rather than threshold luminance detection during suppression (e.g. Joosse et al., 1997, 1999; Barrett, Panesar, Scally, and Pacey, 2012). Finally, stimuli would be binocularly viewed with only a small dichoptic element tested, to further simulate natural viewing conditions.

A new method of suppression mapping has satisfied some of these criteria (Babu et al., 2013). Suppression depth and extent was quantified using a method of adjustment and a supra-threshold inter-ocular contrast matching task. Strabismic and non-strabismic amblyopic participants decreased the signal strength in the non-amblyopic eye to match the surrounding ring seen by the amblyopic eye. Deeper suppression was measured centrally compared to peripherally.

All previous suppression studies have used visual targets that can be discriminated from their background by luminance differences. However linear receptive fields of V1 are not able to detect stimuli without systematic differences in mean luminance (Chubb and Sperling, 1988). One example of a visible stimulus not defined by changes in mean luminance is a contrast-modulated noise (CM) stimulus, constructed by multiplying a square-wave envelope by a dynamic noise carrier, rather than adding to it, as is the case for a comparable luminance-modulated noise (LM) stimulus. The dynamic noise carrier would be detected by a multitude of early striate, high spatial frequency, linear mechanisms. For the CM stimulus however, the envelope could not be extracted until after a subsequent non-linear rectification stage, by another lower spatial frequency linear filter (for review, see Baker and Mareschal, 2001; Baker, 1999; Chapter 1, Section 1.3.1.2). It is currently unclear where in the cortex the non-linear rectification step occurs, and whether the spatial mechanisms involved receive greater degrees of binocular input, than do the simple linear mechanisms of early cortex, that process LM stimuli (Allard and Faubert, 2006, 2007).

Those individuals who have disrupted binocularity, e.g. amblyopes, show a greater loss of sensitivity for CM, compared to LM stimuli, in both amblyopic and non-amblyopic eyes (Wong, Levi and McGraw, 2001, 2005; Simmers,

Ledgeway, Hess and McGraw, 2003; Mansouri, Allen and Hess, 2005). Mechanisms for CM stimulus processing then, may be more successfully driven by co-ordinated binocular input (Wong, Levi and McGraw, 2001, 2005; Ellemberg, Allen and Hess, 2004; Hairol and Waugh, 2010), than are LM stimulus mechanisms (e.g. Zhou and Baker, 1993).

We aim to measure inter-ocular blur suppression using LM and CM dynamic noise stimuli, in order to determine whether clinical mapping of suppression using them might be valuable, and to gain additional insight into the nature of CM stimulus processing. If they are more sensitive to inter-ocular blur suppression, they may also hold significance for earlier detection of suppression and more sensitive monitoring of treatment in clinical conditions of degraded binocularity, e.g. amblyopia.

The existence of dynamic visible noise making up LM and CM noise stimuli may in itself affect suppression measurements, as target detectability (e.g. Nordmann, Freeman, and Casanova, 1992; Rovamo and Kukkonen, 1996; Schofield and Georgeson, 1999, 2003) and discriminability (Legge, Kersten, and Burgess, 1987) are reduced. It is also known (at least anecdotally) that clinical suppression depth is “broken down” by the introduction of temporal transients to the stimulus of the suppressed eye (also see Scheiman and Wick, 2008).

In this study, experiments are designed to map inter-ocular blur suppression in participants with normal vision with increasing degrees of inter-ocular blur, using luminance (L), luminance-modulated noise (LM) and contrast-modulated noise (CM) stimuli. Inter-ocular blur may simulate suppression that occurs in anisometropic amblyopia. Additionally, it provides insight into basic mechanisms of blur suppression, also encountered in monovision contact lens wear, where vision is intentionally unbalanced encouraging suppression to enable clear viewing across a wide range of viewing distances. First, suppression measurements are compared for luminance (L), and luminance-modulated noise (LM) stimuli to experimentally assess the effects that noise *per se* has on suppression depth. Second, comparisons are made between

suppression maps for luminance-modulated noise (LM) and contrast-modulated noise (CM) stimuli. Depth and extent of suppression is measured across the central 24 deg of the binocular visual field. Deeper suppression measured for CM stimuli would provide evidence that these stimuli are processed by mechanisms optimally driven by co-ordinated binocular input, a potentially valuable finding both theoretically and clinically.

2.2 Methods

2.2.1 Participants

Four binocularly normal non-presbyopic participants (two male and two female) participated; one was the author (ASC) and the others (SE, SP and CP) were naïve to the purpose of the experiments. Each participant wore their optimal refractive correction (all spherical equivalent refractive errors ≤±1.00 D). All participants had 6/5 or better corrected visual acuity in each eye and stereoacuity of at least 30 arcsec, as measured with the Dutch Organization for Applied Scientific Research (TNO) stereo test (Lameris Ootech, Ede, The Netherlands). All participants were right eye dominant with the sighting dominance test (Fink, 1938). Table 2.6 (see Appendix, Section 2.6.2) shows clinical details of all participants. Informed consent was obtained from all participants and the Anglia Ruskin University Research Ethics Committee approved the conduct of the research project, thus ensuring that the research complied with the tenets of the Declaration of Helsinki.

2.2.2 Equipment

Stimuli were generated with an Apple MacBook Pro (MacBook Pro; Apple Computer, Cupertino, CA) running Matlab (The MathWorks, Natick, MA) with Psychophysics Toolbox (Brainard, 1997; Pelli, 1997; Kleiner, Brainard and Pelli, 2007). They were then presented on eMagin DualPro head-mounted OLED displays (Dual Pro Z800; eMagin Corp., Hopewell Junction, NY) via Matrox DualHead2Go adapter (Matrox Graphics Inc., Quebec, Canada). These eMagin displays have been shown to have an 8-bit luminance capability with a linear

response profile (Black et al., 2011). However, luminance profiles obtained for each of our screens after one hour “warming-up” showed poor linearity. We linearised and equalised the luminances of each screen by recording outputs with a ColorCAL II Colorimeter (Cambridge Research Systems, UK) and gamma-corrected look-up tables. Cooper et al. (2013) measured two similar Sony OLED displays and found minimal or no adjacent pixel spatial interactions with wide contrast ratios, although this may vary across manufacturers.

One screen for each eye allowed for the dichoptic presentation of stimuli. Each screen had a resolution of 800x600 pixels, refresh rate of 60 Hz, and mean luminance 45 cd/m^2. The effective viewing distance was found to be 80 cm, and thus any blurring lens was added to the power of a lens with this focal length, i.e. +1.25 D, accounting for the amount of accommodation required for the viewing distance.

2.2.3 Stimuli

Schematics of the L, LM and CM stimuli are provided in Figure 2.1 (A-F). Luminance (L) stimuli are similar to, but not the same as, those used in a recent study of amblyopic suppression mapping (Babu et al., 2013). Images presented to the left eye (Figure 2.1A – left) were fused with those presented to the right eye (Figure 2.1A - right) to give one fused cyclopean image.

For L (Figure 2.1A, B) and LM (Figure 2.1C, D) conditions, stimuli consisted of eight concentric rings. The central ring (a circle) had a radius of 0.75 deg. Each subsequent ring from the centre was doubled in area, resulting in the outermost ring having a radius of 12 deg. The area of subsequent rings was doubled to account for larger spatial summation areas in the periphery relative to the central visual field. Figure 2.2A shows a schematic depiction of a fused L stimulus, where sectors are delineated by black lines showing 64 sectors in total. Sector orientation is defined by the blue dashed lines (not perceived by participants during experiments).

Figure 2.1 (following page): Examples of L (A), LM (C), and CM (E) stimuli. B, D, and F show luminance profiles (excluding blind-spot markers) taken one pixel above the horizontal midline, where the red line is mean luminance. Left and right columns show each eye respectively. For CM stimuli (E-F). Average luminance of the stimuli remains constant about the mean luminance, though the contrast of the high and low CM rings and the adjustable sector change. Thus the difference between each ring is the modulation of contrast, rather than modulation of luminance. A, C, and E show green and red blind-spot markers for right and left eyes, respectively. All horizontal axes show horizontal pixel numbers. Ordinate axis vary as in E and F.

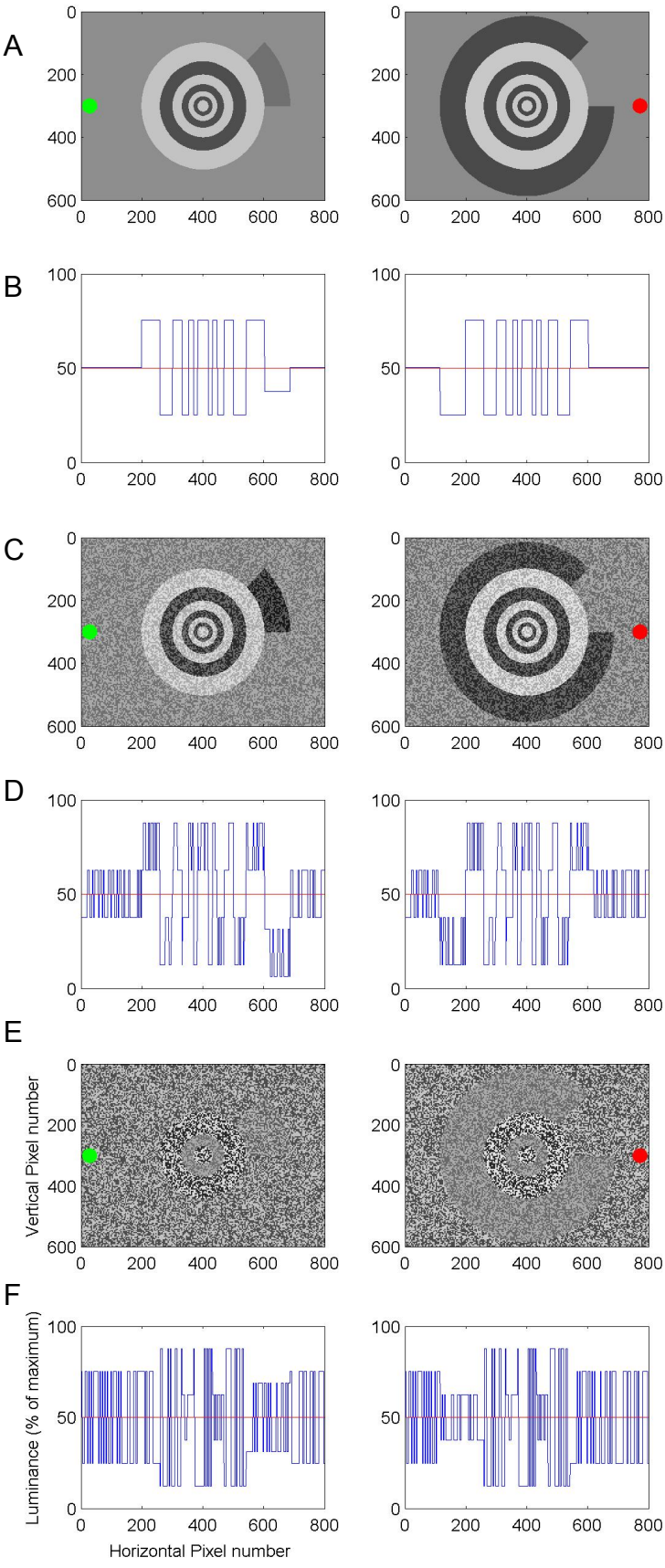
A
B
C
D
E
F
Vertical Pixel number
Luminance (% of maximum)
Horizontal Pixel number

Figure 2.2 (following pages)**:** A) Schematic representation of L stimuli. Black lines delineate sectors. Blue dashed lines show orientations (see Analysis section for explanation). B) Schematic representation of L stimuli, showing numbering of sector eccentricities for statistical analysis in one of four orientations. C) Illustration of how L and LM stimuli adjacent sectors were averaged to give the same number and area of sectors as CM stimuli. Blue dashed radial lines and black tangential lines delineate two sectors whose depth of suppression values were averaged, and sectors are numbered in red. No lines appear on actual stimulus.

A

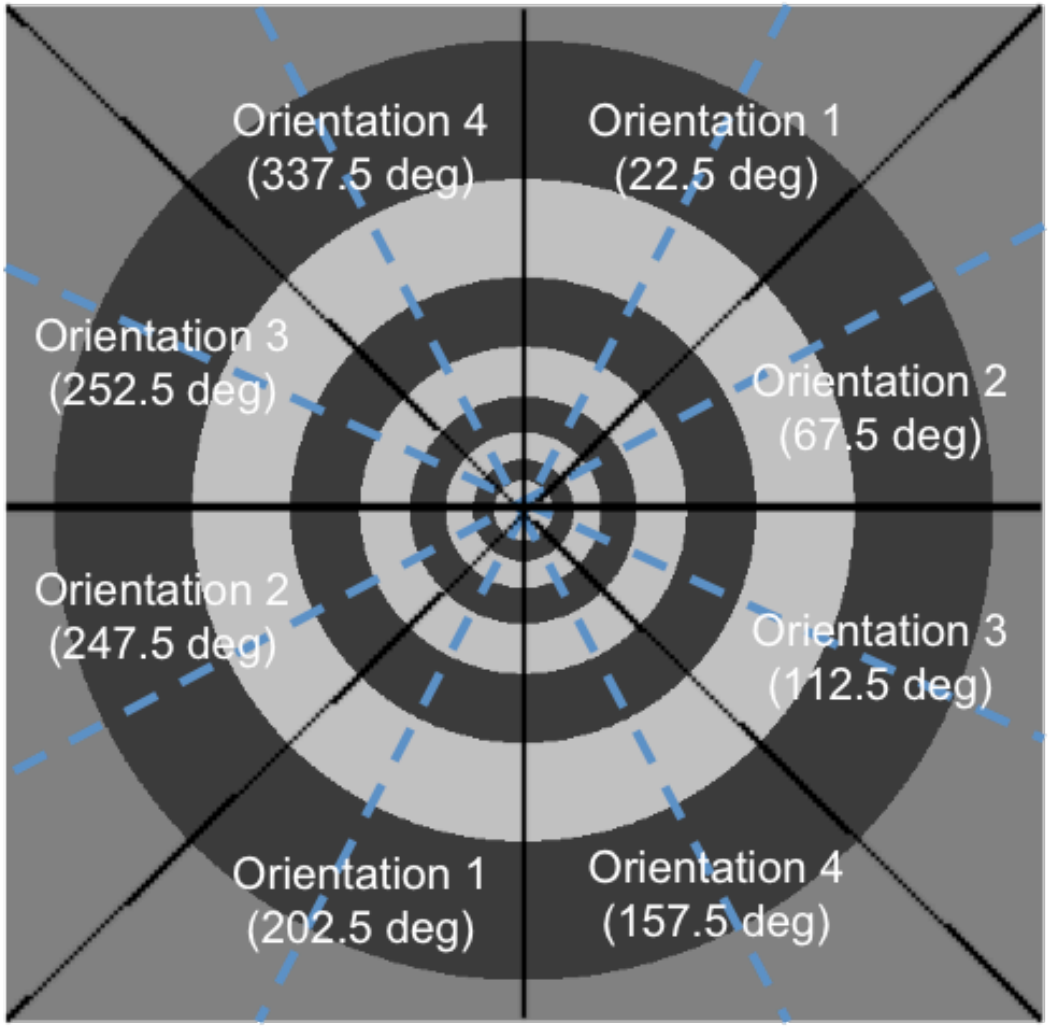
Orientation 4
(337.5 deg)
Orientation 1
(22.5 deg)
Orientation 3
(252.5 deg)
Orientation 2
(67.5 deg)
Orientation 2
(247.5 deg)
Orientation 3
(112.5 deg)
Orientation 1
(202.5 deg)
Orientation 4
(157.5 deg)

B

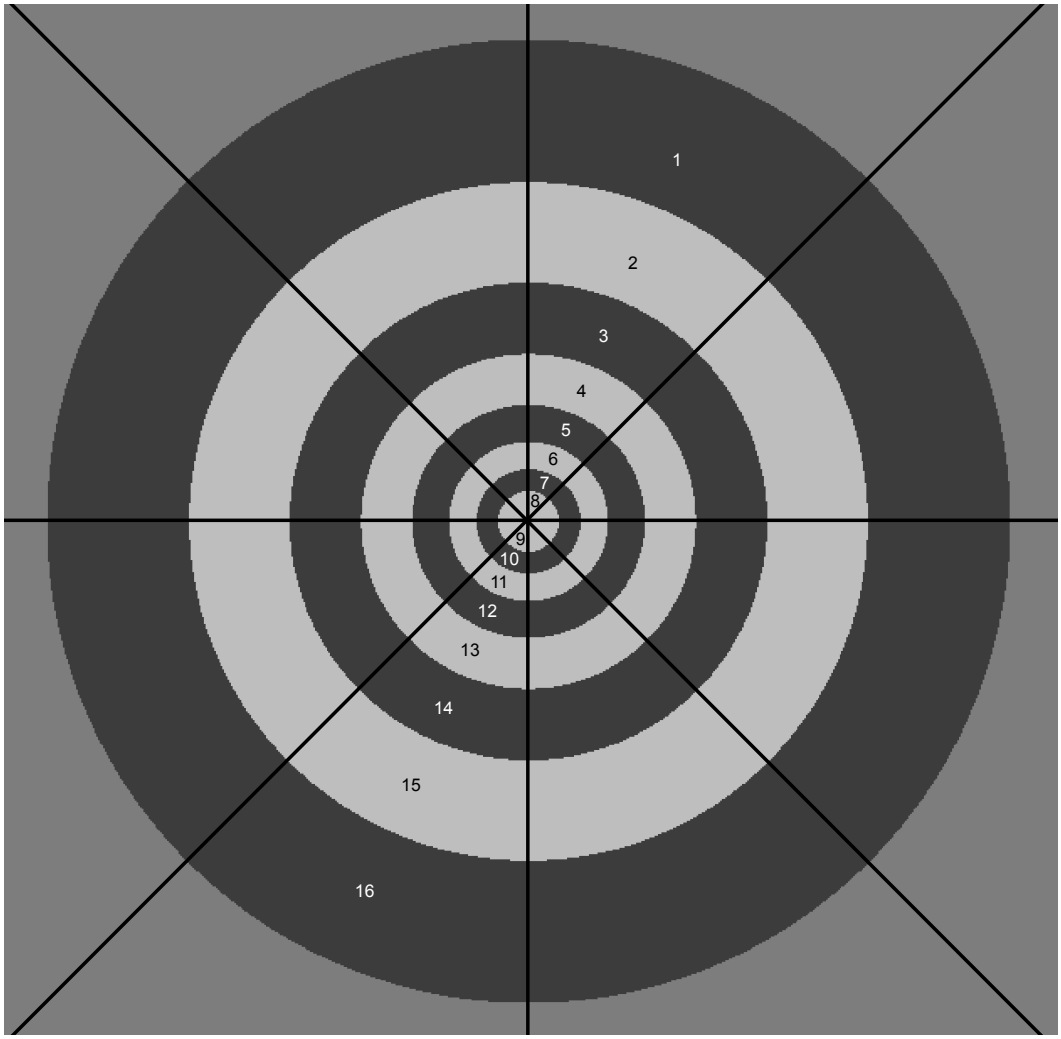

C

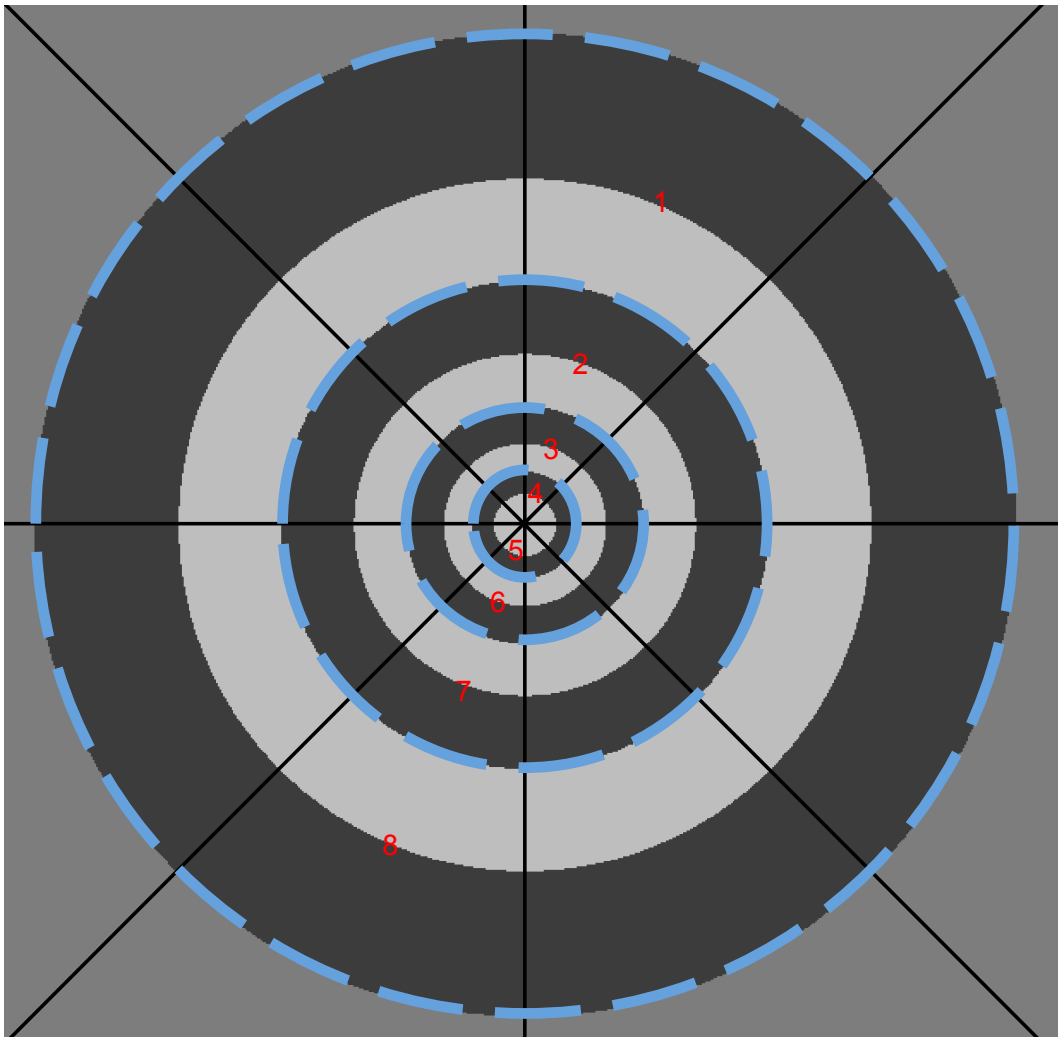

For the CM condition (Figure 2.1E, F) four rings were created covering the same 24 deg visual angle, making the sectors double the size of L and LM stimuli, to account for larger spatial summation areas found foveally and peripherally for CM relative to LM stimuli (Sukumar and Waugh, 2007). Although different spatial summation areas have not always been found for foveally viewed stimuli, e.g. Schofield and Georgeson (1999), and spatial summation slopes (exponents of power functions fit to the data) are similar for LM and CM spatial stimuli (Wong and Levi, 2005; Sukumar and Waugh, 2007), Sukumar and Waugh were able to quantify critical summation areas out to 10 deg eccentricity, finding CM areas to be consistently larger. In the current study, we conduct a control experiment to show that this choice of differently sized sectors for different stimulus types does not affect experimental outcomes. The rate of fall-off with eccentricity in spatial summation is similar for LM and CM stimuli (Smith and Ledgeway, 1998; Sukumar and Waugh, 2007), thus the same scaling with eccentricity (i.e. sector area doubling) was used for all L, LM and CM stimuli. Each ring for all stimulus types (L, LM and CM) was divisible into eight sectors (as shown in Figure 2.2A, black lines) so that any localised suppression scotomata, or orientation effects, could be revealed.

The following equation (Schofield and Georgeson, 1999) describes how L, LM and CM stimuli were constructed:

$$I\,(x,y) = I_0\,[1 + nN(x,y) + lL(x,y) + mnM(x,y)N(x,y)] \qquad \text{Eq. (1)}$$

where *I(x,y)* is the luminance at position *(x,y)* and I_0 is mean luminance; *n* is noise contrast (set to 0 for L stimuli). Noise was different for LM (*n* = 0.25) and CM (*n* = 0.50) to give the largest adjustable modulation range available to each of LM and CM stimuli. The effect of different LM and CM noise amplitudes is assessed in a control experiment (see Results section). *N(x, y)* is the value of binary noise at position *(x, y),* either -1 (dark) or 1 (bright). The Weber contrast of the rings, *l,* was set to 0.50 and -0.50 for light and dark rings (Figures 2.1A and C), respectively, in relation to the mean L background. For each adjustable sector, *l* changed according to the participant response. The background provides the baseline from which modulation measures are taken. As LM and

CM stimuli are varied in luminance- or contrast-modulated noise respectively, the rings and adjustable sector are quantified in terms of their 'modulation', i.e. *l* for L and LM stimuli, or *m* for CM stimuli. Thus for L stimuli, *n* = 0, *m* = 0 and *l* is adjusted; for LM stimuli n = 0.25, *m* = 0 and *l* is adjusted; and for CM stimuli n = 0.50, *l* = 0 and *m* is adjusted.

For LM and CM stimuli, the noise check size was 4x4 pixels with an angular subtense of 10 arcmin at 80 cm (equivalent viewing distance), clearly resolvable for all of our participants at all eccentricities tested (previous luminance resolution thresholds reported in the literature for a 12 deg eccentricity range from 2.5-6.3 arcmin; e.g. Ludvigh, 1941; Millodot, Johnson, Lamont, and Leibowitz, 1975; Rovamo, Virsu, and Näsänen, 1978; Anderson and Thibos, 1999a; b). The smallest sector has a radius of 0.75 deg. Kukkonen, Rovamo, and Näsänen (1995) found that for binary noise to be effectively spectrally flat (or white), a minimum of four noise checks per cycle of grating should be present. If one cycle of a grating is considered equivalent to two rings, this criterion is satisfied. Schofield and Georgeson (2003) found that noise type and amplitude had no effect on CM modulation sensitivity functions. For LM modulation functions, sensitivity was reduced where noise spectral energy was strongest. Therefore, spectrally broad-band binary noise is sensible to use in the present study. Dioptric blur degrades energy more at high spatial frequencies, however as the noise is broad-band, energy existing at lower frequencies still supports both LM and CM stimuli. The effect of blur on specific stimulus detectability is examined in a control experiment.

Ten different spatial frames of stimuli were drawn after each participant response using randomly generated noise, which was always correlated between the eyes. These spatial frames were presented in a random order every two temporal frames, to create dynamic noise. Head-mounted displays were running at 60Hz with screens that were refreshed simultaneously; so each frame was presented for 33.33 ms. Smith and Ledgeway (1997) demonstrated the importance of using dynamic noise when investigating contrast-defined motion perception.

2.2.4 Procedure

Participants were instructed to look in the centre of the binocularly viewed central ring (0.75 deg radius). Brightly coloured blind-spot markers (1 deg diameter discs) were also presented 15 deg temporally on each screen along the horizontal midline (see Figure 2.1). If accurate fixation was not maintained, these markers became highly visible, no response was made, and participants were instructed to re-fixate before making a valid response. Furthermore, alignment calibration was performed during preliminary experiments to ensure binocular fusion. Two squares of 1 deg side length with centres vertically displaced by 1 deg were presented dichoptically (i.e. one square to each eye). If squares were horizontally offset, participants moved the squares using the keyboard until they were perceived as one above the other. Alignment in pixels was recorded and the main experiment stimuli were moved accordingly. Binocular fusion was achieved in all participants in these experiments without adjustment (as they were binocularly normal).

Before testing began, participants were given a practice session with each type of stimulus until comfortable with the task, i.e. the standard deviation of staircases had stabilised to within 15% of the mean (see Appendix, Figure 2.15). In brief, a matching task allowed for measurement of the point of subjective equality (PSE) using a one-up, one-down staircase and a 2AFC (two-alternative forced-choice) psychophysical paradigm. The participant had to decide whether the stimulus strength of the sector to be judged in the fused stimulus was stronger or weaker than the surrounding ring. After each response, the stimulus was changed with a square-wave temporal profile. The variable sector was always presented to the blurred (non-dominant) eye, with the surrounding ring presented to the non-blurred (dominant) eye.

In more detail, the target was presented binocularly, excluding the sector to be adjusted (a sector to be adjusted is shown in the outer ring in Figures 2.1A, C, and E), which was presented dichoptically. In the left (non-dominant) eye the ring that the sector was a part of was set to mean modulation whilst the adjustable sector varied in modulation according to the participant response. In

the right (dominant) eye, the sector corresponding to that being adjusted was set to mean modulation, whilst the surrounding ring was either a fixed increment (0.50) or decrement (-0.50) modulation. Both of these fixed deviations from the mean modulation are collectively known as the 'baseline modulation', which is 0.50.

One sector at a time was assessed, in L, LM or CM modulation, until the PSE was reached. This occurred when the adjusted sector (presented to the blurred eye) was perceived as having the same characteristics as the surrounding ring (presented to the non-blurred eye). Staircases were initiated randomly from either halfway between a true average and maximum modulation; or halfway between a true average and minimum modulation. Step size was initially 0.10 (of a maximum 1.0 modulation range), reducing to a 0.05 step size after the first two staircase reversals. The PSE for each sector was calculated from the mean of the last four of six reversals. An audio cue signified a modulation change after each participant response. There was no time limit placed on judgements made. Participants were encouraged to take enough time as they felt necessary to make an accurate response. After the PSE was obtained for each sector, a longer audio cue of a lower pitch signified that a new sector was to be adjusted. No feedback was given, and the order of sector presentation was systematic and counterbalanced carefully parcelling out the effects of practice, adaptation and fatigue. Systematic presentation order reduced overall variability of responses and also alerted participants to the location of the patch.

Suppression mapping was performed for five levels of blur (no blur, +0.50D, +1.00D, +2.00D, and +4.00D) placed before the non-dominant (left) eye. The 'no blur' condition was used to provide a baseline measurement of suppression as participants did not all have a perfectly balanced inter-ocular match, possibly due to sensory eye dominance. Some participants reported binocular rivalry for very differently presented luminances to the two eyes during pilot experiments, particularly for the most central sectors. In this case, participants were instructed to continue responding in the direction of adjustment until perception without rivalry was perceived, i.e. the modulation difference between adjustable sector and corresponding mean luminance became more similar. No rivalry was

reported close to a perceived inter-ocular match, which is reflected in the small staircase standard deviations. Therefore rivalry served as a cue to grossly bracket the inter-ocular matching task in some (usually no and low blur) conditions, which was followed by adjustments relying on inter-ocular suppression.

2.2.5 Analysis

Mean points of subjective equality (PSE) were obtained from four runs for each of the five levels of blur (including the 'no blur' condition) across the three types of stimuli (L, LM and CM), except for participant SE, who completed either two or three runs. Each participant therefore completed between 1600-3200 staircases (800-1600 for participant SE). Point of Subjective Equality (PSE) modulation values are normalised across stimulus type using the following equation:

$$S_{norm} = \frac{(M_{match} - M_{baseline})}{M_{baseline}} \quad \text{Eq. (2)}$$

where S_{norm} is the normalised depth of suppression, M_{match} is the PSE modulation and $M_{baseline}$ is the baseline modulation. Depth of suppression (S) is expressed as -1 to 1, where 1 is the maximum level of suppression (signal strength needed to be doubled for the sector in the blurred eye to match perception of the surrounding ring), 0 is an inter-ocular match (signal strength is perceived as the same in each eye), and -1 is maximum binocular facilitation (signal strength in the blurred eye was reduced to minimum to match perception of the surrounding ring).

Pilot experiments showed that with high levels of blur, suppression was sometimes too deep to measure. Here, the staircase reached the maximum measurable normalised suppression value (see Appendix, Section 2.6.4). If this occurred, the S_{norm} was set to the maximum value for analysis. After practice, in experiments, this occurred for participant CP, using CM stimuli for the +4D blur condition, and SE using LM stimuli for the +4D blur condition. This is

reflected by the lack of standard error bars for CP and SE's set of data for those conditions.

2.3 Results

Mean depth of suppression averaged across all four observers is plotted using colour-coded maps of the measured visual field for each monocular blur level in Figure 2.3. Each sector of the stimulus is represented by a colour. Red denotes inter-ocular suppression, i.e. the stimulus strength was increased in the blurred eye to obtain a binocular perceptual match. Green sectors show facilitation, i.e. the stimulus strength was decreased in the blurred eye to obtain a binocular perceptual match. Yellow sectors depict a perceived inter-ocular match that occurred for equal stimulus strengths to each eye. The colour bar to the right of Figure 2.3 shows the scale where a normalised value of 1 is given to the deepest level of suppression (red), 0 to an inter-ocular match (yellow), and -1 to the highest level of binocular facilitation (green).

All data in these experiments has been subjected to repeated measures Analysis of Variance (ANOVA) with the conservative Greenhouse-Geisser correction for violation of sphericity and independence of errors. In subsequent sections we specifically address experimental hypotheses of 1) the effect of noise on suppression and 2) the effect of different types of stimulus (LM vs CM) with similar dynamic noise on suppression.

The data set contributing to Figure 2.3 were analysed with factors of stimulus type (3 levels), blur (5 levels), sector orientation (4 levels) and sector eccentricity (8 levels – L and LM adjacent sectors were averaged as in Figure 2.2C to cover the same area as CM sectors). Results are shown in Table 2.1. Values for two sectors of L and LM stimuli were averaged to compare to CM sector values due to differences in sector sizes. There is an overall effect of stimulus type [$F(1.47, 4.42) = 16.56$, $p = 0.010$] such that CM stimuli were more deeply suppressed than L or LM stimuli. There is also an overall effect of blur [$F(1.82, 5.46) = 43.78$, $p<0.0005$] such that any level of blur led to statistically deeper suppression than the no blur condition. Overall, there was no significant

effect of sector eccentricity [F (7.00,3.73) = 1.64, p = 0.29] or orientation [F (1.70, 5.11) = 0.19, p = 0.80], and no higher order interactions.

An *a priori* hypothesis was that increasing blur may lead to differential eccentricity effects on suppression; hence the overall analysis conducted above. To visualise eccentricity effects more clearly, in Figures 2.4, 2.5 and 2.6, data have been collapsed across orientation, to view graphs of depth of suppression across eccentricity for L, LM and CM stimuli, respectively.

Table 2.1: ANOVA results for all data, with factors stimulus type (3), blur (5), sector orientation (4), eccentricity (8).

Source	Degrees of Freedom	F	Sig.
Stimulus Type	1.472	16.561	0.010
Blur	1.818	43.782	<0.0005
Orientation	1.702	0.193	0.798
Eccentricity	1.244	1.639	0.286
Stimulus Type * Blur	1.345	2.036	0.236
Stimulus Type * Orientation	1.949	0.907	0.451
Blur * Orientation	2.175	0.212	0.831

Figure 2.3 (next page): Colour-coded suppression maps averaged across four participants, for each level of blur (no blur, +0.50 D, +1.00 D, +2.00 D, and +4.00 D), for each stimulus type (L, LM, and CM). Each sector is represented by a colour denoting the depth of suppression on a scale where green is facilitation (normalised value of -1), yellow is an inter-ocular match (normalised value of 0), and red is deep suppression (normalised value of 1), as illustrated in the colour bar to the right of the Figure, where maximum and minimum values are given.

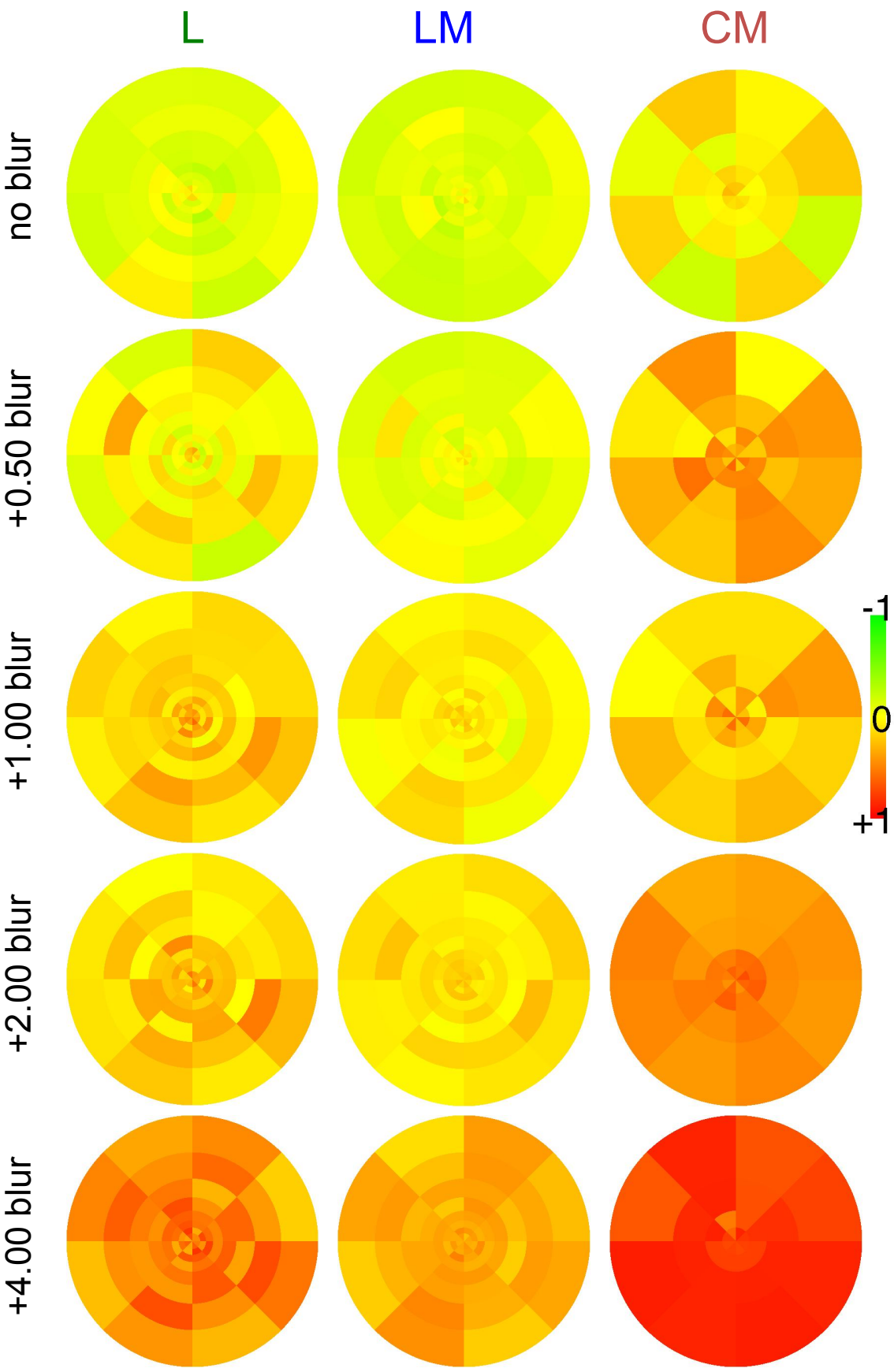
L
LM
CM
no blur
+0.50 blur
+1.00 blur
+2.00 blur
+4.00 blur
-1
0
+1

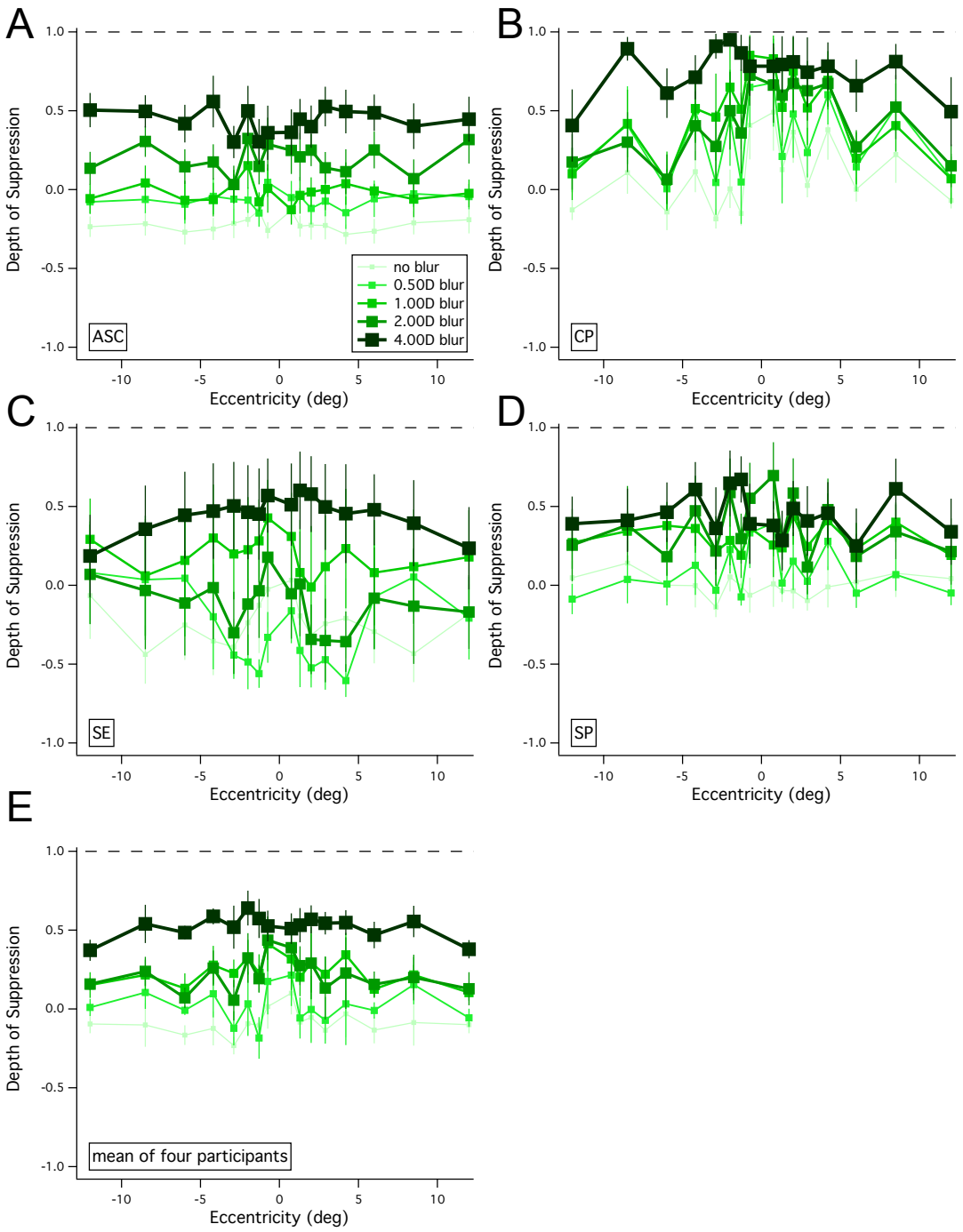

Figure 2.4: Average of all orientations (blue lines - Figure 2.2A) was taken for each level of blur for L stimuli, for participants A) ASC, B) CP, C) SE, and D) SP, where error bars represent standard error. The mean across all participants is shown in E), where the error bars represent standard deviation across participants. Legend in A applies to A-E. Dashed line represents ceiling of suppression value.

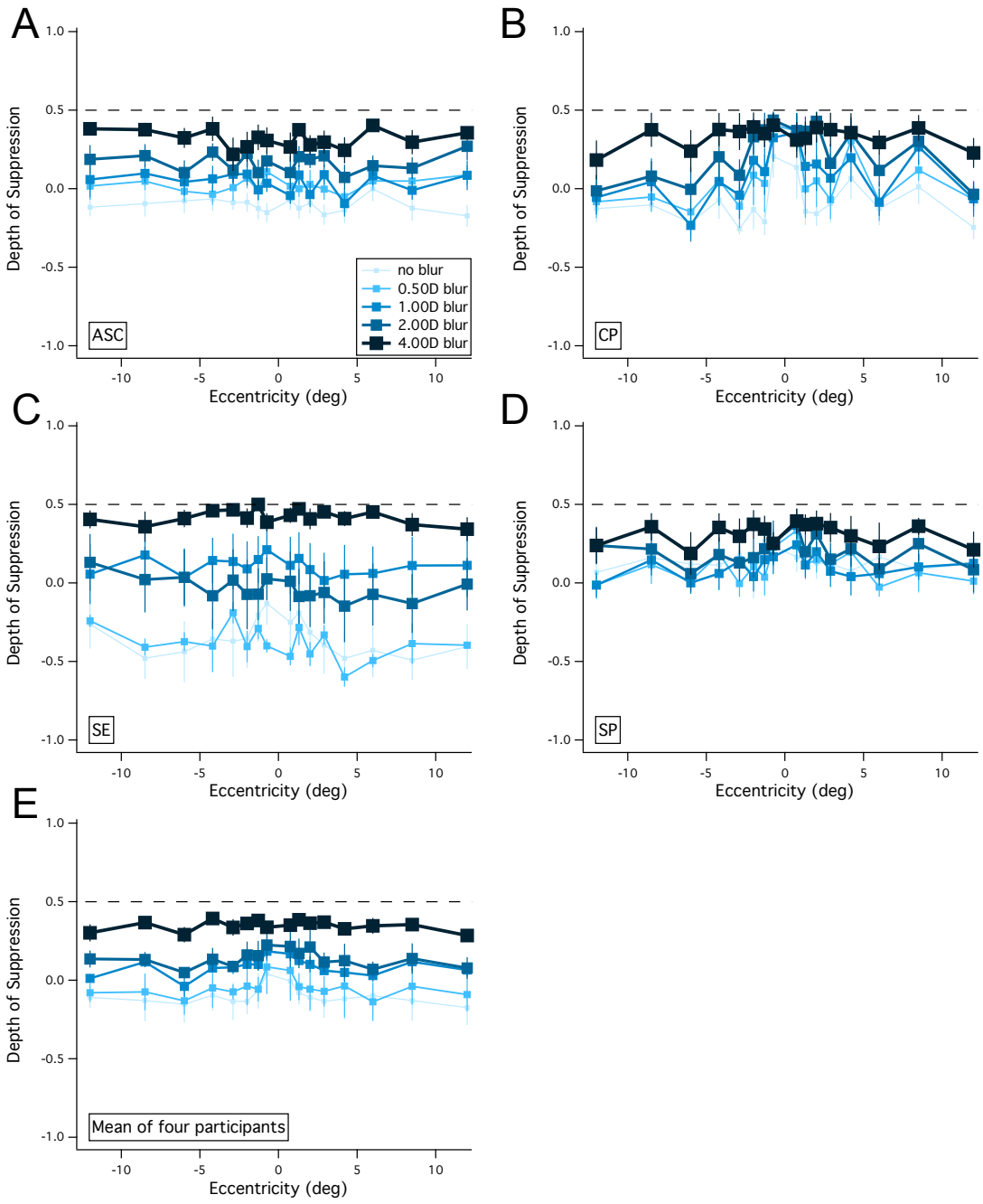

Figure 2.5: LM stimuli, details as previous Figure

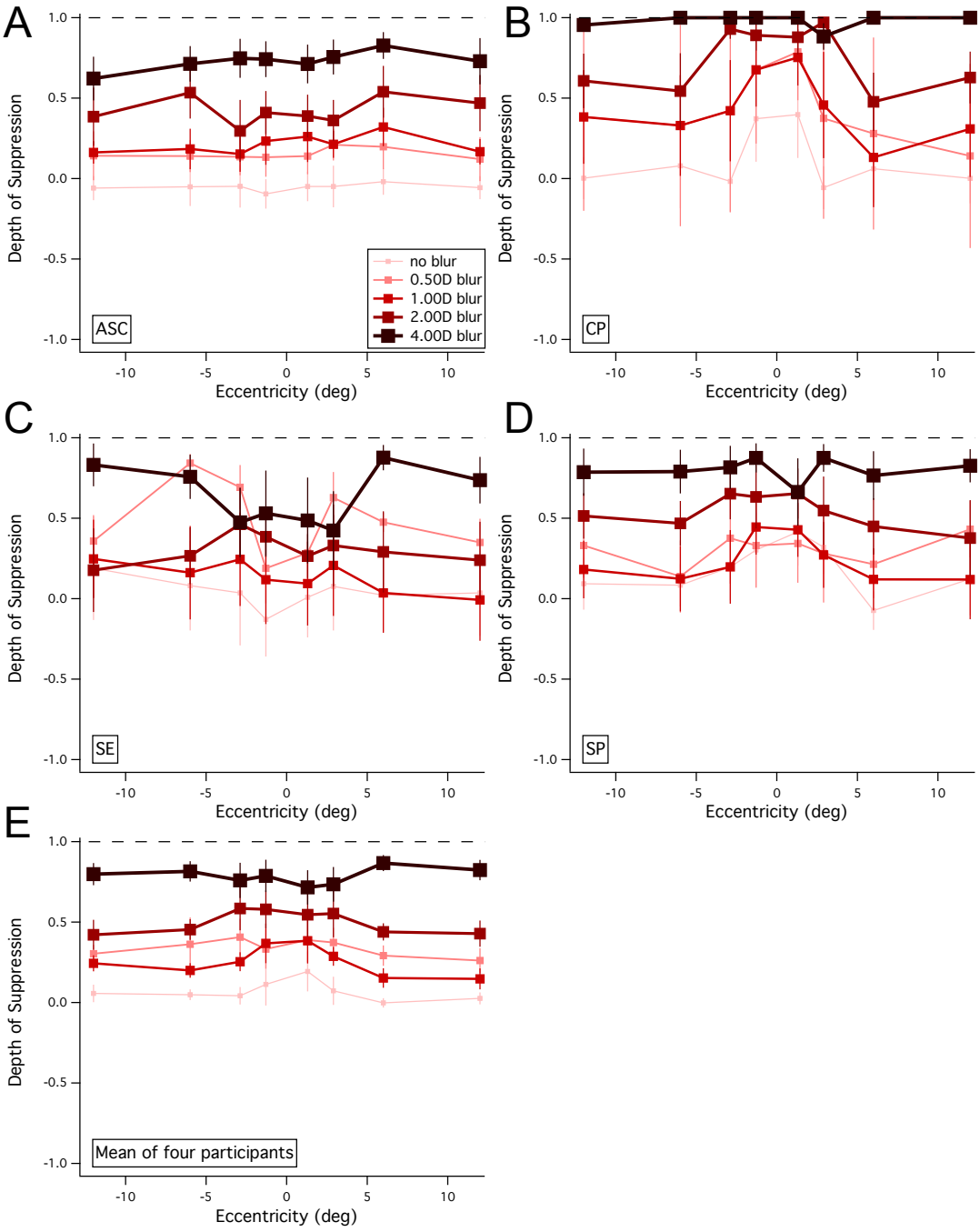

Figure 2.6: CM stimuli, details as previous Figure

2.3.1 Suppression of luminance (L) versus luminance-modulated noise (LM) stimuli

In order to investigate the effects of noise itself on inter-ocular blur suppression, the results for L and LM stimuli only, were statistically compared. The repeated-measures ANOVA was performed with factors of stimulus type (2 levels), blur (5 levels), sector orientation (4 levels) and sector eccentricity (16 levels – as depicted in Figure 2.2B). Outcomes are shown in Table 2.2. There was a significant main effect of blur [$F(1.37, 4.11) = 15.59$, $p = 0.014$], but no main effects of stimulus type [$F(1, 3) = 2.09$, $p = 0.24$], eccentricity [$F(1.33, 4.00) = 1.83$, $p = 0.26$], or orientation [$F(1.53, 4.60) = 0.85$, $p = 0.45$]. There were also no significant higher order interactions. Thus no localised regions of blur suppression occurred within the central 24 deg. Suppression values of some LM sectors with +4D blur were above the measurable range for participant SE, which artificially reduces the variance for this level of blur. When the ANOVA was carried out without the +4D data, statistical significance outcomes were unchanged.

Table 2.2: ANOVA results for L and LM data, with factors stimulus type (2), blur (5), sector orientation (4), eccentricity (8). Non-significant higher order interactions are not shown.

Source	Degrees of Freedom	F	Sig.
Stimulus Type	1	2.088	0.244
Blur	1.373	15.59	0.014
Orientation	1.533	0.853	0.454
Eccentricity	1.332	1.833	0.259
Stimulus Type * Blur	1.693	1.743	0.261
Stimulus Type * Orientation	1.471	0.543	0.565
Blur * Orientation	2.217	0.938	0.447

To obtain *relative* depth of suppression values, depth of suppression averaged across eccentricity and orientation for each level of blur, for each participant, was subtracted from their respective no-blur values. Mean relative depth of suppression data are plotted against level of blur in Figure 2.7 and fit with linear functions, to provide an estimate of *rate* of increase in depth of suppression with increasing level of blur.

Slope values for each participant, and averaged across participants are provided in Table 2.3. Absolute slope values are different for each participant, but they are always steeper for L, than LM stimuli, and this difference in rate is statistically significant [F (1, 3) = 50.67, p = 0.006]. Thus, noise reduces the effect of blur on measured depth of suppression. This difference is on average 0.045 ± 0.026 relative depth of suppression units per dioptre.

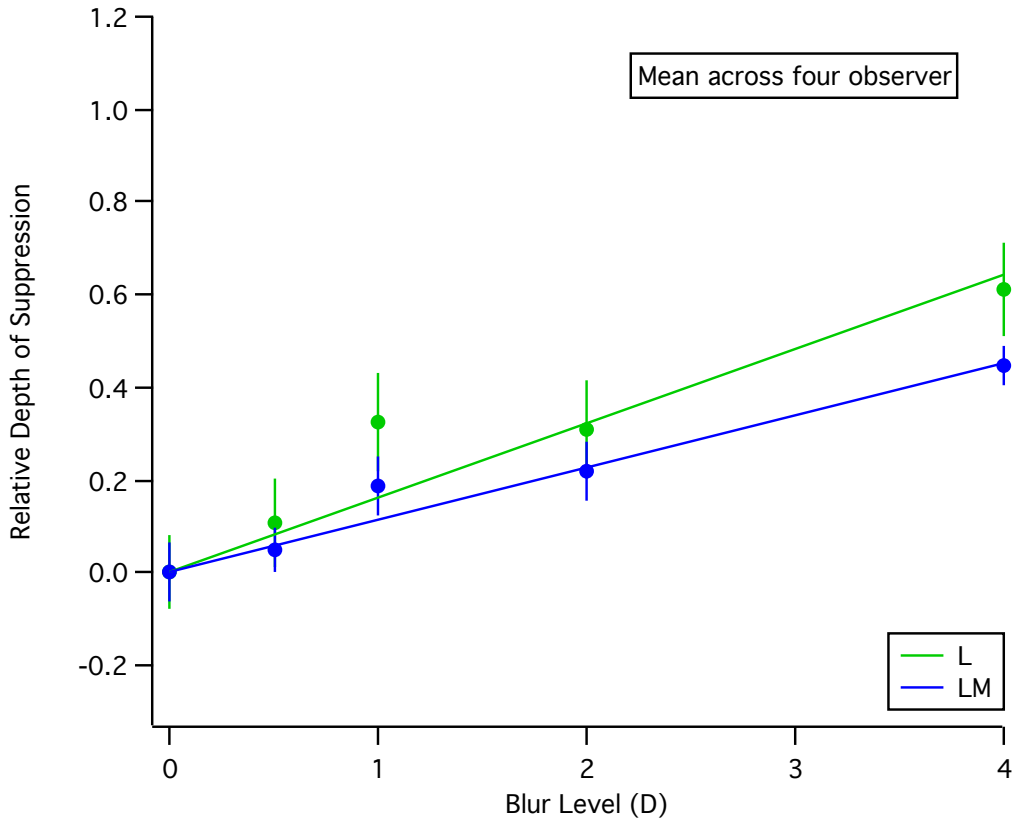

Figure 2.7: Average across four participants of all sectors in the L and LM stimuli for each level of blur (dioptres). Data averaged across four participants are shown and fit with linear functions. Continuous with previous colour coding, L is represented by green, and LM by blue. Error bars show standard deviation.

Table 2.3: Values for L and LM slopes and the difference between them for each participant, with the mean (± standard error) for each participant and the mean across all participants (± standard deviation) in bold

Participant	Slope ± 1SE for L Stimuli	Slope ± 1SE for LM Stimuli	L – LM Slopes (± 1SE)
ASC	0.16 ± 0.015	0.10 ± 0.012	0.06 ± 0.0096
CP	0.14 ± 0.033	0.099 ± 0.017	0.041 ± 0.019
SE	0.17 ± 0.068	0.14 ± 0.0038	0.030 ± 0.0039
SP	0.099 ± 0.017	0.052 ± 0.012	0.047 ± 0.010
Mean (±1 SD)	**0.15 ± 0.042**	**0.11 ± 0.049**	**0.045 ± 0.026**

2.3.2 Suppression of luminance- (LM) versus contrast-modulated (CM) stimuli

To compare inter-ocular blur suppression for different types of spatial stimuli that use the same dynamic noise, results obtained for LM and CM stimuli were statistically compared. Sectors for luminance-modulated noise (LM) stimuli were averaged to match sector sizes for CM stimuli (illustrated in Figure 2.2C) to allow for statistical comparison across stimulus type (2 levels), blur (5 levels), sector orientation (4 levels) and eccentricity (8 levels). Outcomes of the ANOVA are shown in Table 2.4.

There is a significant effect of stimulus type [$F(1,3) = 37.59$, $p = 0.009$], so that CM stimuli are suppressed more deeply than LM stimuli. There is also a significant effect of blur on depth of suppression [$F(1.83,5.50) = 48.05$, $p <$

0.0005]. As with the L versus LM comparison, comparing LM and CM stimuli showed no significant effects of eccentricity [$F(1.29,3.86) = 1.47$, $p = 0.31$] or orientation [$F(1.52,4.57) = 0.056$, $p = 0.91$] on measured depth of suppression and there were no significant higher order interactions. Results averaged across orientation are plotted across eccentricity for different blur levels in Figures 2.5 and 2.6, for LM and CM stimuli, respectively. With increasing inter-ocular blur, depth of suppression increases approximately evenly across the visual field for both types of stimuli, however, suppression is deeper for CM stimuli. For participants SE (with LM stimuli) and CP (with CM stimuli), there were several sectors that required maximum modulation to be perceptually near a match for the highest level of blur, artificially reducing the variance of the data. Re-analysis without the +4D blur data reveals that the significant effects of stimulus type [$F(1,3) = 18.98$, $p = 0.022$] and blur [$F(1.88,5.64) = 18.00$, $p < 0.004$], still hold true.

Table 2.4: ANOVA results for LM and CM data, with factors stimulus type (2), blur (5), sector orientation (4), eccentricity (8).

Source	Degrees of Freedom	F	Sig.
Stimulus Type	1	30.555	0.031
Blur	1.343	30.456	0.015
Orientation	1.101	1.544	0.338
Eccentricity	1.476	0.395	0.65
Stimulus Type * Blur	1.033	1.027	0.418
Stimulus Type * Orientation	1.315	0.623	0.539
Blur * Orientation	1.948	1.817	0.276

Figure 2.8 (following pages): A) Mean taken across each sector in the LM and CM stimuli for each level of blur (dioptres). Data averaged across four participants are shown and fit with linear functions. LM is represented by blue and CM by red. Blue within red circles denote overlying points. Error bars show standard deviation. B) Box and whisker plots for L (green), LM (blue), and CM (red) stimulus types for each blur level. Box tops and bottoms show 75^{th} and 25^{th} percentiles, respectively, while the centre line shows the median. Whiskers show maximum and minimum extreme values.

A

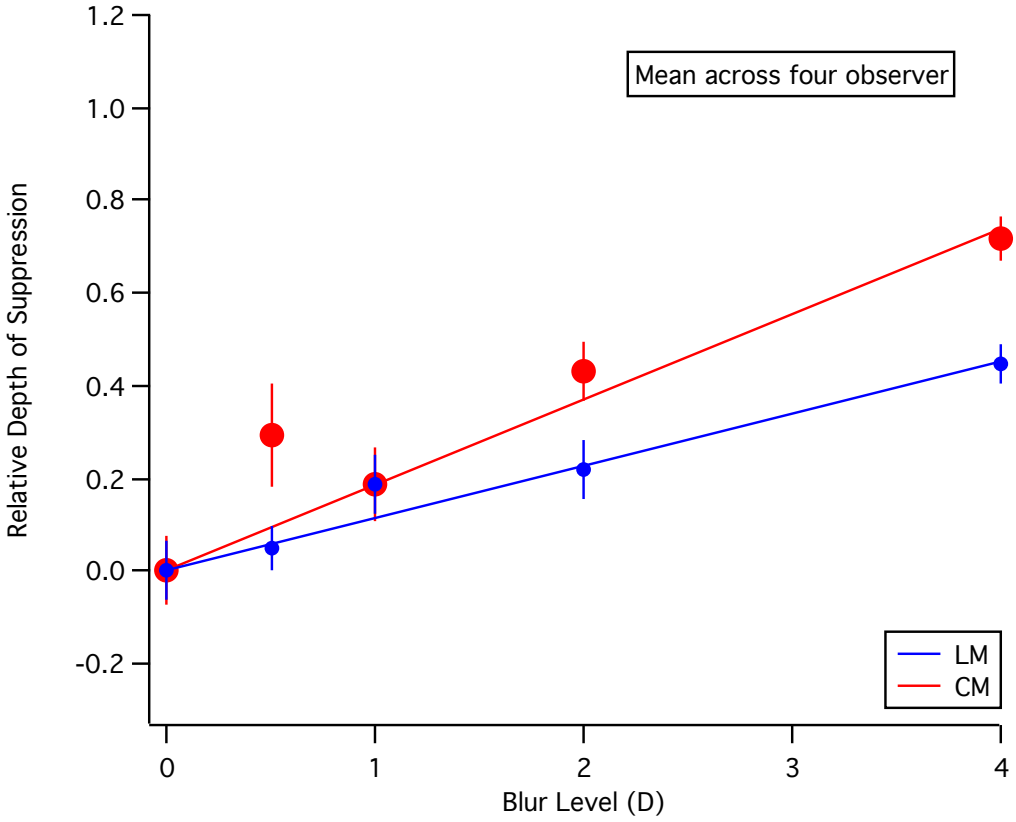
Mean across four observer
Relative Depth of Suppression
1.2
1.0
0.8
0.6
0.4
0.2
0.0
-0.2
0
1
2
3
4
Blur Level (D)
LM
CM

B

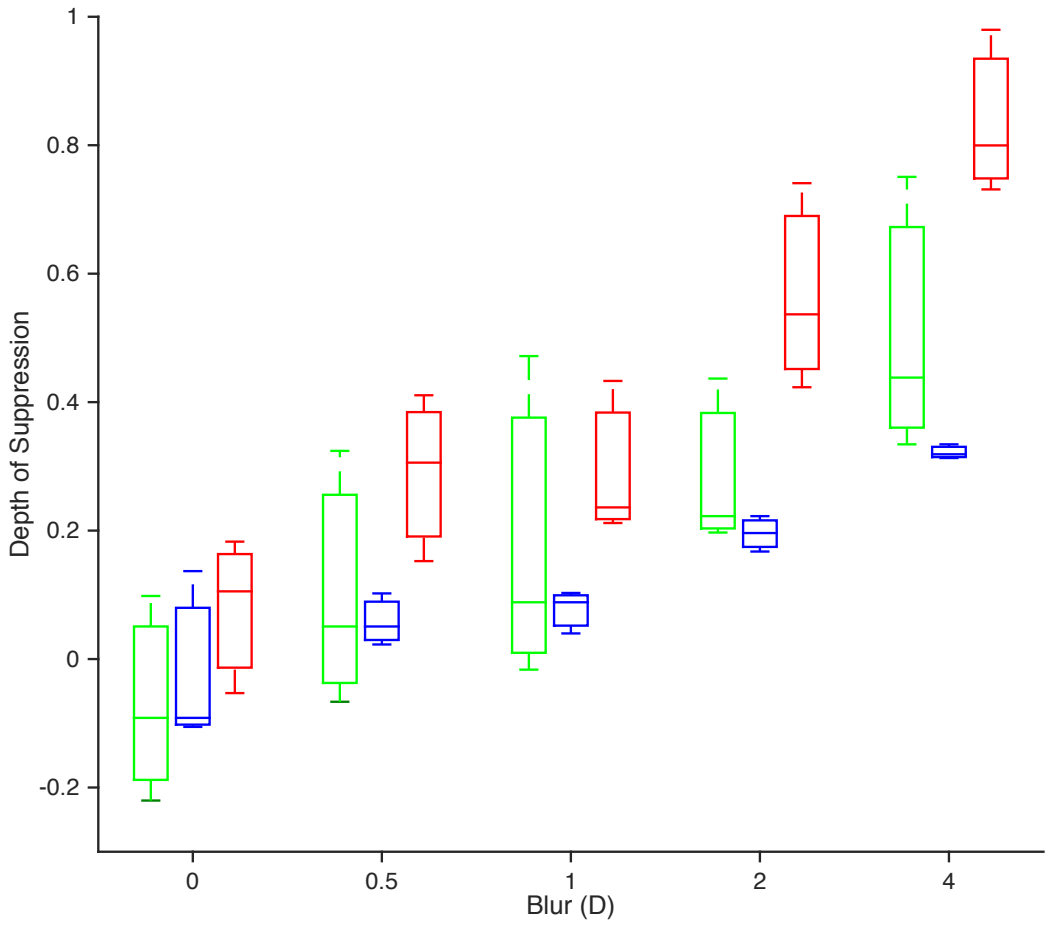

To more clearly view the rate of change of suppression with increasing inter-ocular blur, data are collapsed across all orientations and eccentricities for each participant and normalised by each participant's no-blur depth of suppression measure to calculate a relative depth of suppression. The averaged data obtained across the four observers for each level of blur is shown in Figure 2.8A. The results of linear fits are provided in Table 2.5. Again, although absolute slope values are different for each participant, slopes are consistently higher for CM stimuli [$F(1,3) = 84.69$, $p = 0.003$]. The difference between LM and CM slopes is on average 0.087 ± 0.006 relative depth of suppression units per dioptre. Differences between participants for all stimulus types are illustrated in Figure 2.8B.

Table 2.5: Values for LM and CM slopes and the difference between them for each participant, with the mean (± standard error) for each participant and the mean across all participants (± standard deviation) in bold.

Participant	Slope ± 1SE for LM Stimuli	Slope ± 1SE for CM Stimuli	CM – LM Slopes (± 1SE)
ASC	0.10 ± 0.012	0.19 ± 0.017	0.09 ± 0.010
CP	0.10 ± 0.017	0.20 ± 0.035	0.10 ± 0.019
SE	0.14 ± 0.0038	0.23 ± 0.0082	0.09 ± 0.0045
SP	0.052 ± 0.012	0.19 ± 0.017	0.14 ± 0.010
Mean (±1SD)	**0.11 ± 0.049**	**0.19 ± 0.0050**	**0.087 ± 0.0060**

In these experiments, in order to attain equivalent modulation amplitude ranges, different amplitudes of noise were used (see stimulus details section). In addition, to more fairly compare suppression depths measured for LM and CM stimuli, different sector sizes were used to account for previously reported different summation areas for detecting the two types of stimuli (Sukumar and Waugh, 2007). Could these differences have accounted for our measured

differences in suppression depth? Was the effect of dioptric blur different on visibility strength of supra-threshold LM and CM stimuli, accounting for increased suppression measured for CM stimuli? Control experiments were performed to determine whether our key result, that CM stimuli are more deeply suppressed with inter-ocular blur than LM stimuli, was due to these other potential confounding factors.

2.3.3 Control Experiment 1: LM versus CM sector size

Mean results for *relative* depth of suppression (relative to the 'no blur' condition) for two participants (ASC and SP) for whom the size of LM sectors was doubled to match CM sector size and the size of CM sectors was halved to match LM sector size are shown in Figure 2.9. Each point represents the average of sectors of two full orientations. For both sizes of LM sectors, slope values were similar: 0.081 ± 0.008 for smaller, and 0.088 ± 0.019 for larger sectors. Thus, the difference in measured suppression depth between LM and CM stimuli in the main experiment was not due to the difference in sector size. When CM sectors were made smaller (to match LM sector sizes in the main experiment), *even higher* slope values were found (0.23 ± 0.026 versus 0.18 ± 0.010) showing that reducing sector size could have the effect of increasing measured suppression depth.

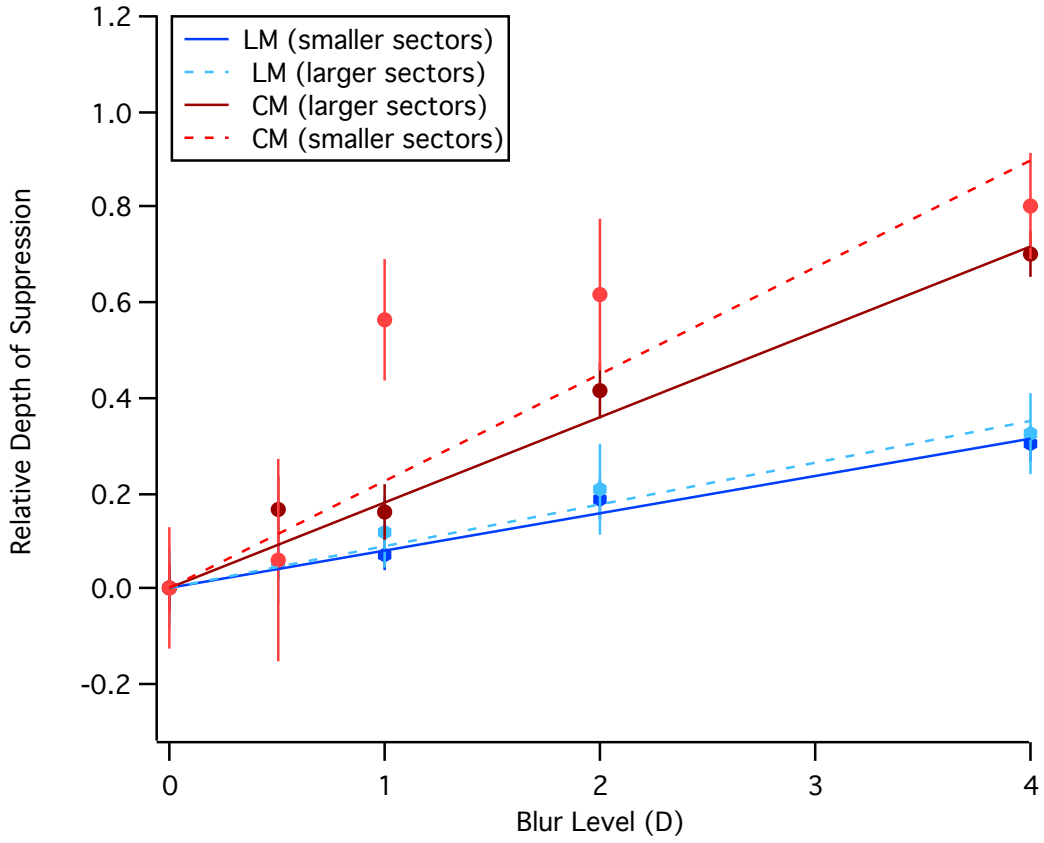

Figure 2.9: Depth of suppression for different levels of blur (dioptres) for the smaller sector LM stimuli (used in main experiment) are fit with a solid blue line, and the dashed blue line LM is fit to data for larger LM stimuli (control experiment) with doubled area sectors. Solid red lines denote larger CM sectors (as used in main experiment) and dashed red line denotes smaller LM sectors (control experiment). Error bars show standard error.

2.3.4 Control Experiment 2: Visibility of LM versus CM stimuli

Sensitivity to detecting CM stimuli is much lower than that for detecting LM stimuli (Schofield and Georgeson, 1999). Could differences in strength of stimulus visibility (i.e. difference in modulation between the rings and background) between the LM and CM stimuli have resulted in different depths of suppression measures? Monocular detection thresholds for individual LM and CM sectors were measured for two participants (ASC and SP) for similar configuration stimuli to Figures 2.11C and E, with same noise contrasts as were used in the main experiment. A 3-up, 1-down staircase with a 2AFC procedure was used in which participants monocularly viewed the concentric ring stimuli and in each trial indicated whether a near-detection sector was in one of two positions in the central ring. The sector was either to the right of the vertical midline in the superior half of the ring, or directly opposite in the inferior half of the ring. An average of four measurements from each participant revealed that stimuli for the main experiments were 4.6x detection threshold for LM stimuli, and 3.7x detection threshold for CM stimuli (see Figure 2.11B). Visibility of the LM stimulus was then reduced to 2x and 3.5x visibility, and depth of suppression mapped across two full orientations for a +2.00 D inter-ocular blur condition. Suppression depth did not change significantly with the reduction in LM stimulus visibility, as shown in Figure 2.10. Thus, it is unlikely that our main result can be explained on the basis of differing stimulus visibility levels.

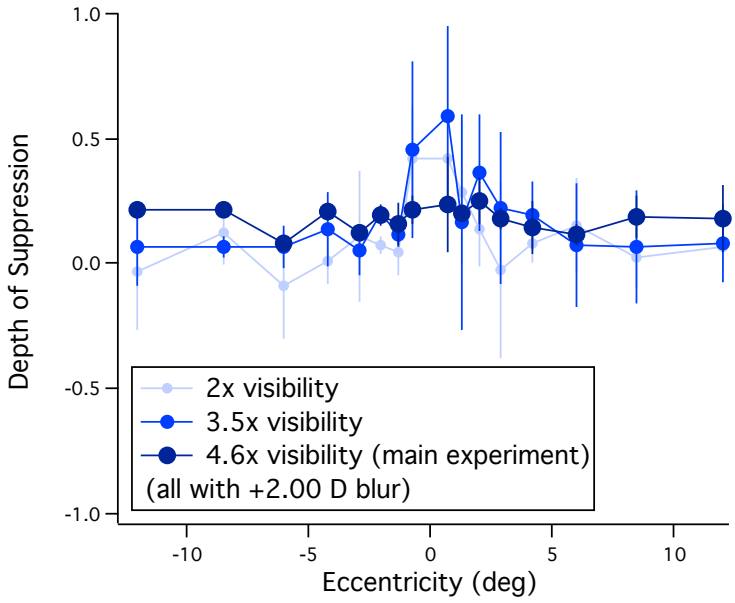

Figure 2.10: Depth of suppression measured with different visibilities of LM stimuli with +2.00 D inter-ocular blur. As with 2.5 and 2.6, the average across orientations was taken to give depth of suppression for each eccentricity. The ceiling varied for each visibility, and therefore maximum level is not shown. Error bars show standard deviation.

2.3.5 Control Experiment 3: Discriminability of LM versus CM stimuli

Given that the main experimental task was a suprathreshold matching task, it is possible that blur had differential effects on discriminability, rather than detectability of LM and CM stimuli, leading to a difference in measured suppression. To test this, two participants performed a contrast discrimination task for LM and CM stimuli for a 'no blur' and +2D binocular blur condition. A method of constant stimuli was used to obtain a measure of discriminability from the psychometric function slope:

$$f(x) = 100 * (0.5 - 0.5 * \mathrm{erf}\,(\frac{x - x_0}{\beta * \sqrt{2}})) \qquad \text{(Eq. 2)}$$

where x_0 is the offset of the error function (*erf*) along the abscissa and represents the stimulus matching point. Slope parameter β represents discriminability. A 2AFC task was employed where participants decided whether

a peripheral or central sector was of higher or lower modulation, than the surrounding ring.

Without blur, slopes were similar for LM (0.20±0.05) and CM (0.25±0.11) stimuli; with blur similarly, for LM (0.19±0.02) and CM (0.22±0.03). Thus differences in measured depth of suppression between LM and CM stimuli found in the main experiment, are not likely due to increased difficulty in detecting modulation change, for CM versus LM stimuli.

2.3.6 Control Experiment 4: The effects of noise amplitude and blur on stimulus visibility

Is the finding of deeper inter-ocular blur suppression for CM stimuli dependent on the amplitude of noise used? In the main experiment, to ensure an equal range of measurable suppression depth, different noise amplitudes were required: 0.5 for CM and 0.25 for LM. A control experiment measured the effect of noise amplitude on relative depth of suppression of LM and CM stimuli with inter-ocular blur. Two full orientations of stimuli at each noise amplitude were measured, and the average taken across all measured sectors (see Figure 2.11A). For LM stimuli, relative depth of suppression decreased as noise amplitude increased. The converse is true for CM stimuli. When noise amplitude is increased, relative suppression increases.

Stimulus detectability also varied with different noise amplitude (see Figure 2.11B). Detection thresholds were obtained in the same way as in Control Experiment 2. At low noise amplitudes, LM stimuli were more visible than CM stimuli, approaching similar visibility at 0.5 noise amplitude. As stated above in the main experimental condition (amplitudes of 0.5 for CM and 0.25 for LM), LM stimuli were slightly more visible (4.6x threshold) than CM stimuli (3.7x threshold). These visibility levels were quite robust to the effects of increasing levels of blur (see Figure 2.11C). Thus neither the increased inter-ocular suppression measured with increasing levels of blur, nor the significant differential effects of inter-ocular suppression measured for LM and CM stimuli, can be explained by differential stimulus visibilities.

Figure 2.11 (following page): Results from control experiments with participants ASC and CP. A) Relative depth of suppression taken as the difference between mean suppression values across all measured sectors for no blur and +2.00 D blur conditions, for different noise amplitudes. Red markers indicate data for CM stimuli (noise amplitudes 0.25, 0.375, 0.50 and 0.625), blue markers for LM stimuli (noise amplitudes 0, 0.125, 0.25, 0.375, and 0.50). Error bars show ±1 SE. Open blue square shows datum for LM stimuli with noise amplitude = 0.50. B) Mean visibility estimates (plotted as multiples above detection threshold) for LM and CM. § and * denote noise amplitudes used in the main experiment (CM noise amplitude=0.50 and LM noise amplitude=0.25). Visibility estimate for L stimuli (noise amplitude = 0) is also shown in green. C) Detection thresholds (left axis) for stimuli from the main experiment taken as the average of two central and two peripheral for LM stimuli, or one central and one peripheral CM sector covering the same area of the visual field. Data are plotted for each of four blur levels. Purple diamonds depict the ratio of CM:LM visibility (right axis), where 1 is equal visibility, and LM is more visible if less than 1. All error bars show ± 1 SE.

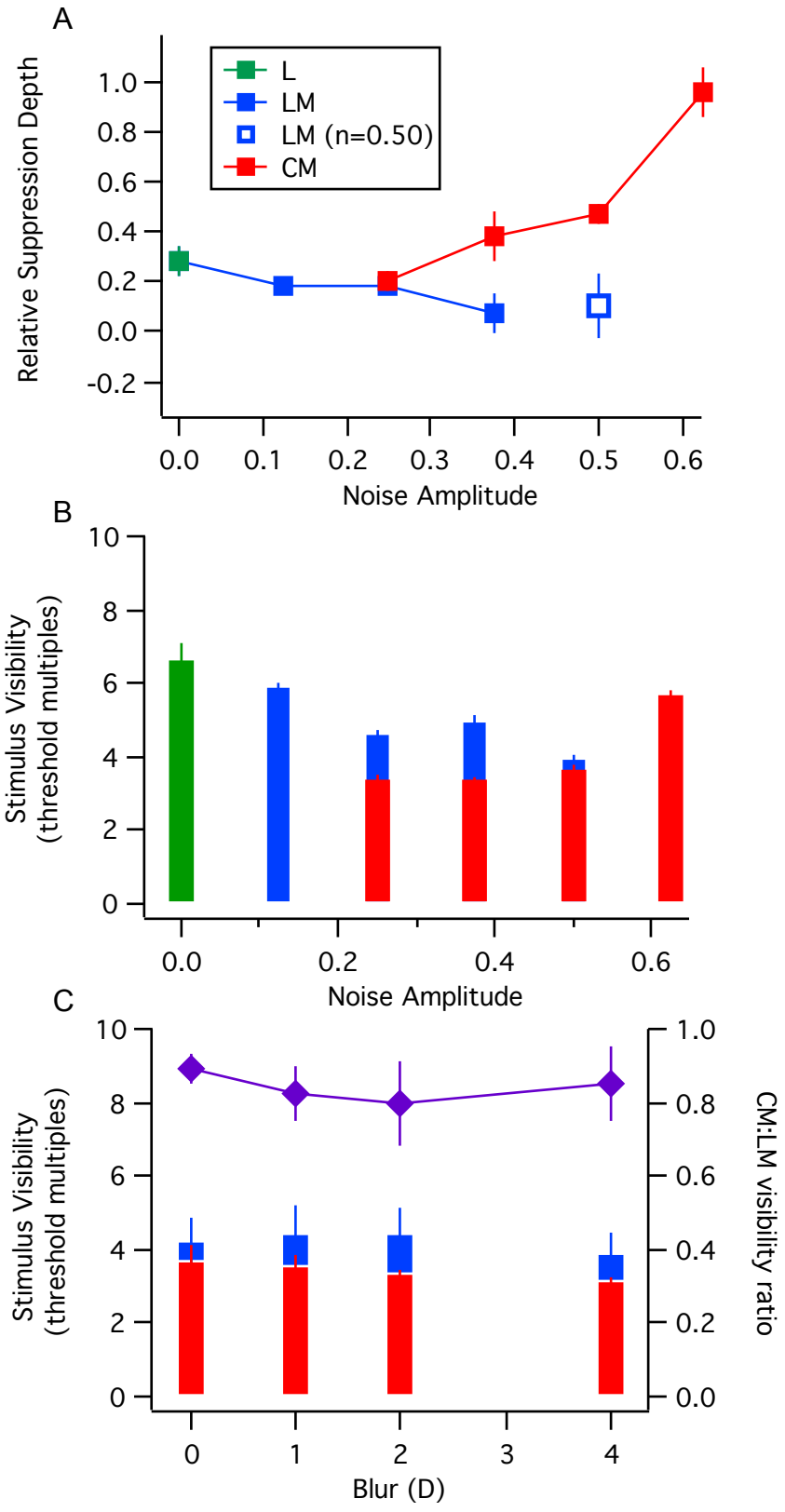
A
Relative Suppression Depth
L
LM
LM (n=0.50)
CM
1.0
0.8
0.6
0.4
0.2
0.0
-0.2
0.0
0.1
0.2
0.3
0.4
0.5
0.6
Noise Amplitude
B
Stimulus Visibility
(threshold multiples)
10
8
6
4
2
0
0.0
0.2
0.4
0.6
Noise Amplitude
C
Stimulus Visibility
(threshold multiples)
CM:LM visibility ratio
10
8
6
4
2
0
1.0
0.8
0.6
0.4
0.2
0.0
0
1
2
3
4
Blur (D)

2.3.6 Control Experiment 5: The effects of inter-ocular blur on stimulus visibility

Although we have shown so far that the effects of blur on overall stimulus visibility cannot explain measured differences in inter-ocular depth of suppression found for LM and CM stimuli, they do not directly simulate experimental conditions in which a blurred stimulus and sector is combined with a non-blurred stimulus. Adding dioptric blur only to one image introduces differential stimulus magnification, which varies depending on what part of the lens the image enters (for a +5.25 D, comprising the working distance and 4 D blur, by a maximum of 8.7% centrally, to 9.1% at 12 deg). Effective dioptric power also varies slightly across the lens (by 0.15D at 12 deg, or 2.85%) (Jalie, 2003). Despite these differences, our participants were able to align images successfully and make perceptual matches of the blurred sector to the surrounding ring for both LM and CM stimuli.

An ideal control would be to enable this to occur under monocular viewing conditions so that one could examine visibility and blur effects on the supra-threshold matching task itself for both LM and CM stimuli, and compare the results to those performed dichoptically, such as was done to measure inter-ocular suppression depth.

In the Appendix (Section 2.6.1) we show how we achieved monocular and dichoptic experimental set-ups, using matching CRT monitors and combinations of optical components. We assessed perceptual matches monocularly and dichoptically, with and without +2D imposed blur. The results shown in Figure 2.12 suggest that 1) carefully calibrated CRT monitors arranged dichoptically produce deeper suppression for CM than LM stimuli, in a manner similar to that measured with the virtual reality goggles, and 2) when arranged in monocular fashion, with blurred and non-blurred rings combined, a larger increase in modulation was required to perceptually match a blurred LM sector with the surrounding ring, than was required to match a blurred CM sector with the surrounding ring, the opposite result to what is found for inter-ocular suppression measurements.

Therefore, deeper inter-ocular suppression of CM compared to LM stimuli cannot be explained by differences in target visibility with blur, noise level chosen, discriminability or spatial summation properties.

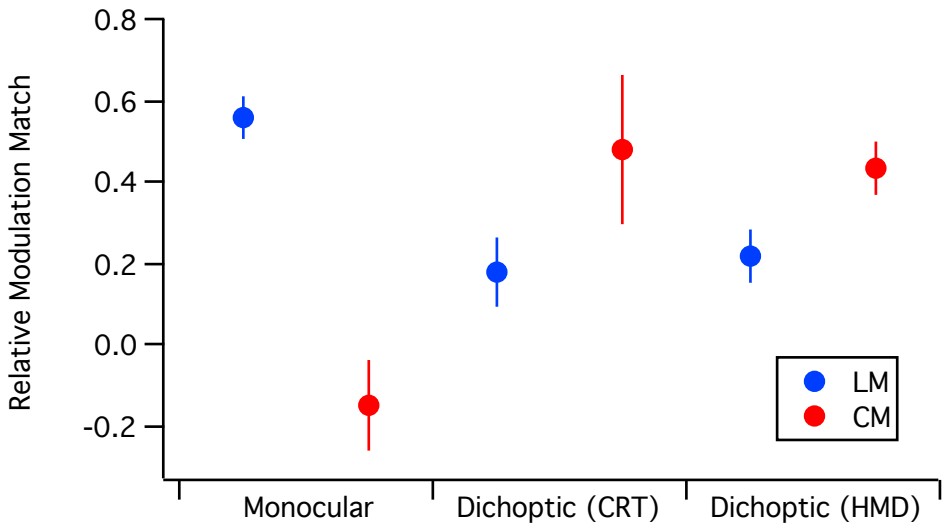

Figure 2.12: Relative modulation match for monocular, dichoptic with CRT screens and dichoptic with HMDs from the main experiment, averaged across all sectors measured, calculated as the difference between +2D blurred and non-blurred PSE. Error bars show standard error.

2.4 Discussion

In this study, inter-ocular blur suppression of luminance (L), luminance-modulated noise (LM) and contrast-modulated noise (CM) stimuli during binocular viewing was measured in binocularly normal participants across the central 24 deg visual field. For the 'no blur' condition, some participants showed mild suppression or facilitation, rather than a perfect inter-ocular match, suggesting that sensory eye dominance is being quantified. Li et al. (2010), using a dichoptic motion coherence paradigm to assess sensory eye dominance in a binocularly normal population, found a large minority (39%) with inter-ocular imbalance.

2.4.1 Depth and extent of blur suppression

Our results show no localised inter-ocular blur suppression regions within the central circular 24 deg of the visual field measured. Simpson (1991) when measuring suppression at fixation, found a greater inter-ocular blur difference (1.75D) was required to cause suppression of a larger stimulus (triangles subtending 0.57 deg) than a 0.75D blur difference required to suppress a smaller one (triangles subtending 0.28 deg). This result suggests that increasing inter-ocular blur difference leads to increases in the extent of suppression. The present study however, using sector sizes of 0.75 deg or larger, found no systematic change in the extent of suppression across the visual field with greater levels of inter-ocular blur, though increasing depth of suppression was measured.

Previous studies have shown that increasing monocular blur progressively reduces stereopsis (e.g. Sireteanu, Fronius and Singer, 1981; Goodwin and Romano, 1985; Lovasik and Szymkiw, 1985). Stereopsis is also below normal levels in monovision correction for presbyopia (e.g. Back, Grant and Hine, 1992; Jain, Arora and Azar, 1996; Du Toit, Ferreira and Nel, 1998). This worsening of stereopsis in both cases may be caused by inter-ocular suppression of the blurred image, corroborating our results.

Differences in measured depth of suppression between the present study and those mentioned above may also be due to different suppression mapping techniques. Mehdorn (1989) found varying scotoma sizes for each of four different binocular visual field mapping techniques in small angle strabismics. Techniques that incorporated more binocularity generally showed less suppression than those that gave more disparate inputs to each eye. As the more binocular tests are more similar to natural viewing conditions, Mehdorn reasoned that anomalous retinal correspondence rather than suppression is present in the everyday viewing in microstrabismics. Bagolini (1967) also found suppression rather than anomalous retinal correspondence in strabismic participants with larger compared to smaller angles with his striated lens test, which provided more natural viewing conditions. The present study provides a large area of binocular stimulus whilst only one dichoptic sector at a time is presented, in an attempt to simulate viewing conditions more similar to real world viewing, perhaps providing a more realistic measure of suppression (Joosse et al., 1997, 1999; Kilwinger et al., 2002; Schor, 1977).

Binocular rivalry alternations were reported centrally by some participants in the present study with no and 0.50D blur. Binocular lustre, for which uniform light and dark fields combine to produce a lustrous, metallic appearance (Helmholtz, 1925), may also be in part responsible for deeper central suppression measured with luminance (L) stimuli, rather than fusion and binocular brightness averaging (Levelt, 1965). This should only have contributed to responses at largest modulation differences (Anstis, 2000). As these differences reduced near the point of subjective equality, binocular brightness averaging occurred, therefore having minimal effect on measurement of depth of suppression.

2.4.2 Blur as a model of anisometropic amblyopia

Although previous studies have found optical blur to be a good model for monocular spatial vision in anisometropic amblyopia (Barbeito et al., 1987; Levi

and Klein, 1982a, 1982b; Pianta and Kalloniatis, 1998; Song et al., 2014), not all aspects of amblyopic perception are mimicked well by short-term application of blur. For example, Hess, Pointer, Simmers and Bex (2003), showed that anisometropic amblyopes perceive sharp edges as sharp, as opposed to blurred, with an inter-ocular blur discrimination task, unlike normal participants blurred monocularly.

Babu et al. (2013), using luminance only mapping stimuli, found deeper suppression centrally than peripherally in anisometropic amblyopes within the central 20 deg diameter visual field. Our results averaged across four normal observers for inter-ocular blur suppression show no localised suppression. Thus, monocular dioptric blur in binocularly normal adults might not be an accurate model for inter-ocular suppression in anisometropic amblyopia. However other small differences in target and experimental paradigm also exist between Babu et al's study and our own, which might influence the measured outcomes. For example, Babu used a central black fixation dot only to monitor fixation, which may also have influenced central suppression assessment, and a method of adjustment to determine the perceptual matches, which is more prone to effects of visual adaptation. Only by using our stimuli and experimental paradigm on anisometropic amblyopes will it become clearer how well our inter-ocular blur suppression results relate to suppression patterns found in anisometropic amblyopia.

2.4.3 Addition of noise

The addition of noise to luminance (L) stimuli reduces the effectiveness of inter-ocular blur suppression. Adding noise reduces stimulus visibility (see Figure 2.11B), which therefore might be expected to be more easily suppressed. Rather, our results show empirically that the presence of dynamic noise breaks suppression down, a finding known anecdotally to clinicians, perhaps through mechanisms of flash suppression (e.g. Wolfe, 1986; Tsuchiya and Koch, 2005; Yang and Blake, 2012).

2.4.4 Suppression of luminance-modulated noise (LM) and contrast-modulated noise (CM) stimuli

The present study is the first to compare inter-ocular blur suppression across the visual field for LM and CM stimuli. Deeper suppression is measured for CM, than for LM stimuli, with increasing levels of blur.

It is thought that separate additional processing is required for detecting CM, than LM spatial stimuli (Mareschal and Baker, 1998; Schofield and Georgeson, 1999; Baker and Mareschal, 2001; Ellemberg, Allen, and Hess, 2006; Allard and Faubert, 2007). Larsson, Landy, and Heeger (2006) found striate and extra-striate fMRI responses to be similar in magnitude for luminance stimuli, however a larger extra-striate than striate response was evoked by contrast-modulated noise stimuli, implying additional extra-striate processing present for contrast-modulated stimuli. Similarly, monkey V2 cells respond to contours not defined by a change in luminance (Leventhal, Wang, Schmolesky and Zhou, 1998; Von der Heydt, Peterhans and Baumgartner, 1984; Peterhans and Von der Heydt, 1989), and more recently specifically with contrast-modulated stimuli (Li et al., 2014) as found previously in cat (Mareschal and Baker, 1998).

It has also been suggested that CM stimuli engage more binocularly-driven units in their processing than do LM stimuli (Wong et al., 2005; Hairol and Waugh, 2010). The current results showing deeper inter-ocular blur suppression for CM stimuli, support this notion. Other differences in our LM and CM stimulus characteristics (sector size, stimulus strength), the effects of blur on stimulus visibility and on stimulus discriminability were investigated and could not account for measurements of deeper suppression using CM stimuli.

2.4.5 The effect of blur on LM and CM stimuli

The low-pass filtering effect of blur may have affected LM and CM stimuli differently. Control experiments were performed where a blurred sector was monocularly matched to a non-blurred surrounding ring. Relative modulation matches (differences between blurred sector and non-blurred surrounding ring

modulation) were higher for LM than CM stimuli for the monocular task, different from the findings of the main experiment. The dichoptic control again showed deeper suppression for CM, compared to LM stimuli, mirroring results of the main experiments. Thus, suppression measures cannot be explained by the effect of blur on the monocular perception of the stimuli, and are specific to inter-ocular blur suppression. This agrees with clinical findings in which inter-ocular blur suppression occurs in successful monovision contact lens wear, as blurred images at distance or at near are not perceived (Simpson, 1992; Collins and Goode, 1994; Kirschen, Hung and Nakano, 1999; Yang, Blake and McDonald, 2010); rather suppression acts to negate perception of the blurred image.

Adding blur only marginally reduces the ability to extract second-order contrast-modulation information (the envelope), demonstrated by a small decrease in stimulus visibility. Monocular effects of blur on stimuli, i.e. low-pass filtering and contrast reduction, therefore cannot explain the increase in blurred eye signal required to overcome inter-ocular suppression to obtain an inter-ocular match. The first stage of linear processing in current filter-rectify-filter models (Zhou and Baker, 1993; Baker and Mareschal, 2001) of second-order stimulus processing is little affected by blurring stimuli in the present study due to the broadband nature of the noise and the energy remaining after the effects of blur.

Recent literature suggests that because stereopsis (Wilcox and Hess, 1996) and binocular phase combination (Zhou, Georgeson and Hess, 2014; Zhou et al., 2014) for CM stimuli are unaffected by inter-ocular carrier correlation, extraction of CM envelope information occurs before binocular combination. More interestingly here, binocular combination for LM and CM stimuli appears to be different. The results of the current study suggest that extraction of the CM envelope occurs by units more sensitive to binocular disruption.

2.5 Conclusion

Inter-ocular blur suppression operates broadly across the central 24 deg visual field, rather than in localised areas. Suppression of CM stimuli is deeper than for LM stimuli and is more affected by increasing differences in inter-ocular blur. This result suggests that CM stimuli may be processed by later, more binocular processing mechanisms, than those required for the processing of LM stimuli. Similar to the binocularly normal participants with inter-ocular blur differences in this study, unilateral amblyopes have disrupted binocularity, and may show deeper suppression for CM than LM (or L) stimuli. The appropriate use of L, LM and CM stimuli may therefore prove to be valuable in clinical mapping of inter-ocular suppression in normal and anomalous spatial vision.

2.6 Appendix

2.6.1 The effect of blur on modulation matching

The effect of blur on perception of CM relative to LM stimuli may have caused the different results for LM and CM stimuli. Therefore, a monocular control experiment was devised to see if similar results to the main experiment were obtained. If results are similar, differences in LM and CM results in the main experiment cannot be due to inter-ocular blur suppression, as this would not be present in the monocular condition. The task was to monocularly match a dioptrically blurred sector to a non-blurred surround, whereas the entire left eye stimulus was blurred in the main experiment, including the variable sector, which was matched to a non-blurred surrounding ring. Figure 2.13 shows the experimental set-up.

On one CRT display, only a sector surrounded by mean luminance was presented, which was 25 cd/m^2 through a 5 cm square beam-splitter, which reduced luminance by 50%, and had similar reflectance. Another CRT of the same model displayed the rest of the stimulus (horizontally inverted due to use of beamsplitter) with the corresponding sector as mean luminance. This arrangement was the same for all stimulus types. Stimuli covered the same central 24 deg of the visual field at 40 cm. Luminance LUTs were defined in a similar way to the HMDs used in the main experiment, and luminances were selected from linearised LUTs (with luminances equated across both screens) to draw the stimuli. A beamsplitter was used to physically combine the image of each screen (image paths shown by dashed lines in Figure 2.13), to the left eye only which was fully corrected with +2.5 D working distance lens to control accommodation. A +1.75 D lens at 7 cm blurred (+2 D effective blur) the left screen image only, i.e. a sector on a noiseless mean luminance background. The right screen area corresponding to the sector was also noiseless mean luminance.

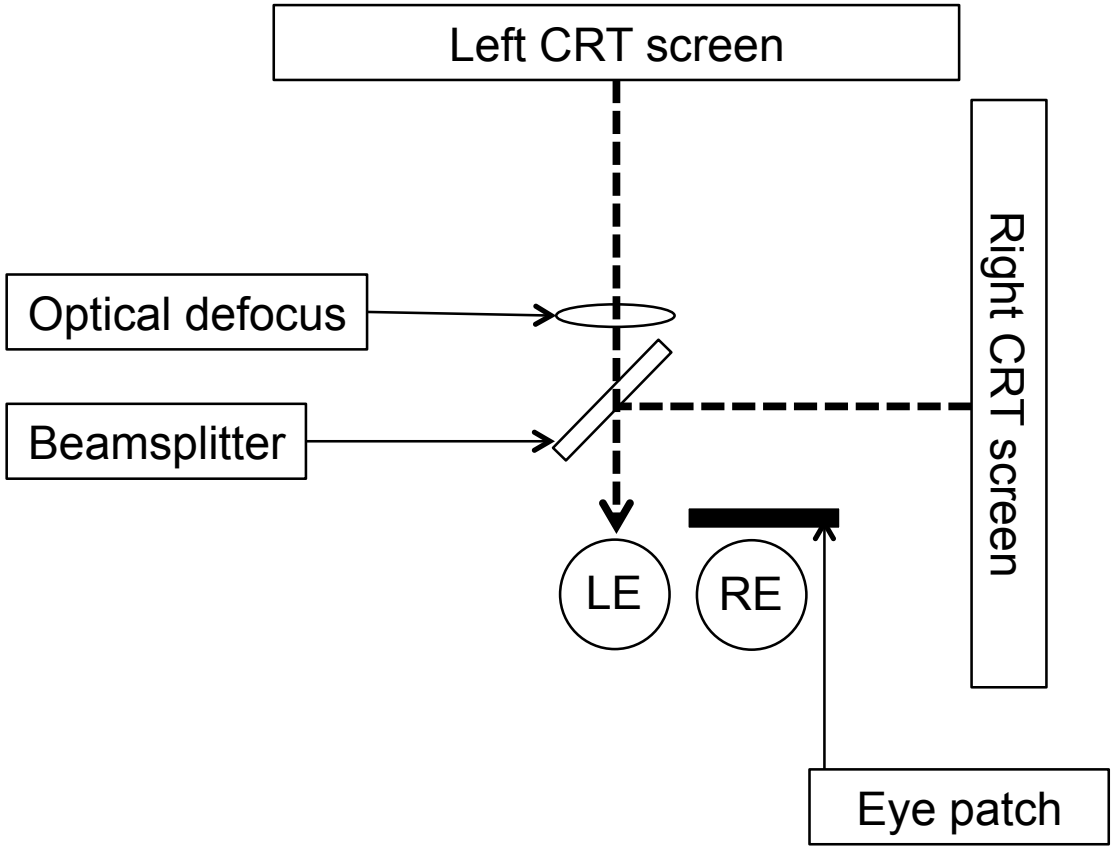

Figure 2.13: Control experiment set-up. Stimuli from left and right screens are combined to give a similar percept to the main experiments, with the exception of blur affecting only the adjustable sector presented on the left screen. The rest of the stimulus is presented on the right screen. Dashed lines shows image projection paths, where they are physically combined at the beamsplitter. An eye patch covered the right eye.

Participants (ASC, SW, and SP) matched sector to surrounding ring modulation. For LM stimuli two central and two peripheral sectors were adjusted and for CM one central and one peripheral sector were chosen (covering the same area of the visual field as the two central and two peripheral LM sectors, respectively). A similar modulation matching task was performed with two CRT screens dichoptically (Figure 2.14) to investigate whether inter-ocular modulation matches would differ from the monocular task (Figure 2.13), and also to compare with the main experiment. Experimental set up was similar to the monocular task, though a mirror was used and not a beamsplitter (Figure 2.14).

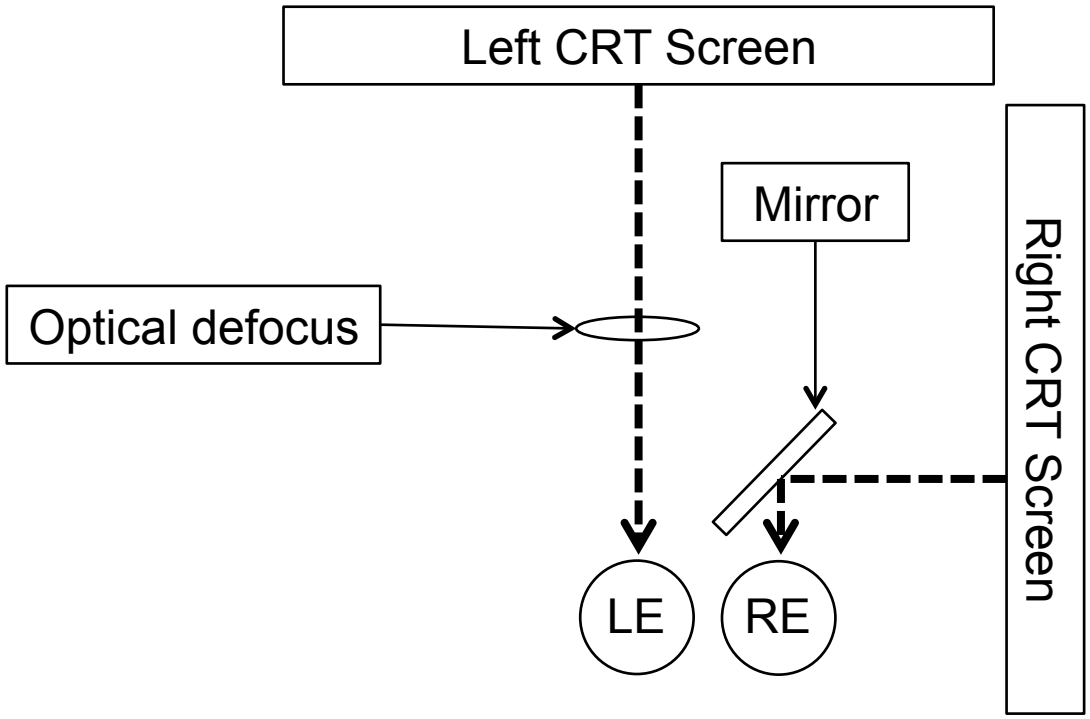

Figure 2.14: Experimental set-up for dichoptic equivalent of monocular modulation matching task. Stimuli from each screen (dashed lines) are binocularly fused to give a cyclopean percept with the use of an angled mirror, which also prohibited cross talk. This experiment is analogous to the main experiment with HMDs.

Each of six conditions (monocular or dichoptic, LM or CM, with or without blur) was repeated four times by ASC and SP, and 1-2 times by SW. Modulation matches between central and peripheral sectors were similar for all conditions, and therefore the mean of all sectors for each condition was taken to provide a single PSE value of the sector relative to the surrounding ring. The relative modulation match was then calculated as the difference between with and without blur for each condition, and data plotted in Figure 2.12.

2.6.2 Clinical attributes of participants

Table 2.6: Clinical measurements of participants used in the present study. OMB – ocularmotor balance, W4d – Worth 4-dot suppression test, NMD – no movement detected on cover/uncover or alternating cover test. Monocular fixation was measures with visuoscopy (reticule filter of a direct ophthalmoscope).

Participant	Age/Sex	Refraction	Visual Acuity	OMB	Monocular Fixation	Stereo-acuity	W4d	Sbisa
ASC	27 M	-0.50/-0.50x60	6/3.8	NMD	central, steady	15"	no supp	no supp
		-0.75/-0.50x130	6/3.8		central, steady			
CP	22 F	∞/-0.50x110	6/4.8	NMD	central, steady	30"	no supp	no supp
		∞	6/4.8		central, steady			
SE	19 F	+0.25 DS	6/4.8	NMD	central, steady	30"	no supp	no supp
		+0.50 DS	6/4.8		central, steady			
SP	31 M	-0.75/-0.75x152	6/4.8	NMD	central, steady	30"	no supp	no supp
		-0.25/-0.75x29	6/4.8		central, steady			

2.6.3 Staircase standard deviation

Prior to formal data collection, practice runs were performed for each participant until the standard deviation of the staircase was within 15% of the Point of Subjective Equality (PSE). Figure 2.15 shows how for participant SP, this occurred after four runs.

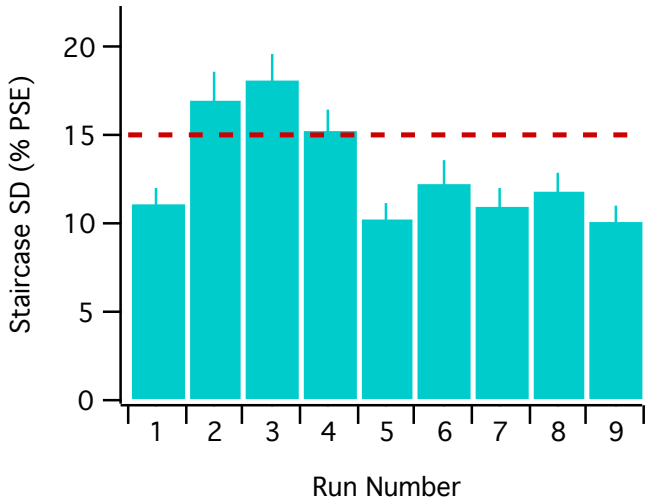

Figure 2.15: Stabilisation of staircase standard deviation to below 15% of the PSE for participant SP, taken as the mean of all staircases in each run. Dotted red line indicates 15% SD, error bars show +1 standard error.

2.6.4 High blur levels

Suppression measured in individual experimental runs for some participants was outside the measurable range. This resulted in the same, maximum, suppression values being assigned to all sectors, thus producing a suppression map with no variation (Figure 2.16) and also with a staircase standard deviation of 0. Therefore a maximum blur level of 4 D was selected from the pilot experiment results to ensure that relative differences suppression in localised areas could be revealed. An 8 D blur suppression map also appeared as in Figure 2.16.

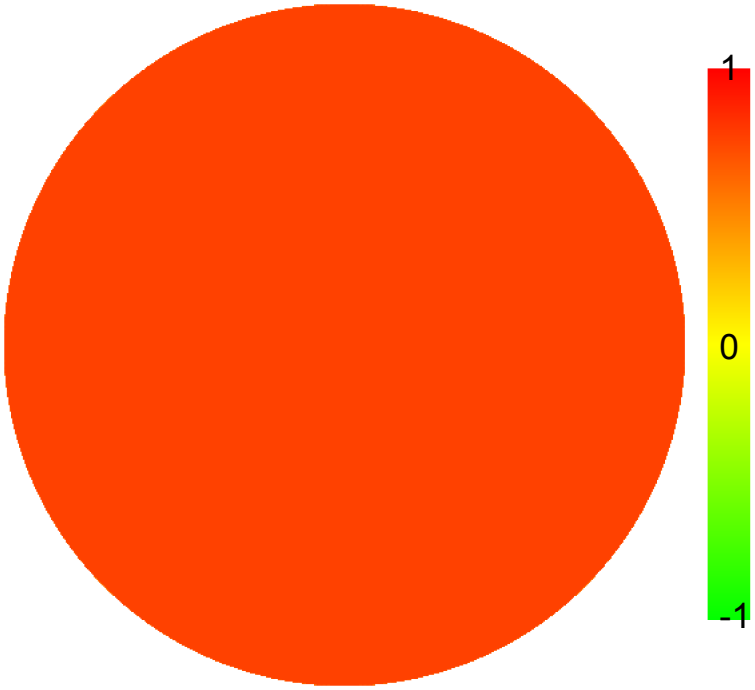

Figure 2.16: An example of a suppression map where all values are above the measurable range of suppression, and therefore localised areas of suppression cannot be assessed.

CHAPTER 3

EXPERIMENT 2 – INVESTIGATION OF INTER-OCULAR LUMINANCE DIFFERENCE ON SUPPRESSION OF LUMINANCE-MODULATED AND CONTRAST-MODULATED NOISE STIMULI

3.1 Introduction

Inter-ocular suppression is a binocular condition that occurs when mismatched images are presented to each eye. To prevent confusion (superimposition) or diplopia (simultaneous perception), one image is cortically suppressed (Sengpiel, Blakemore, Kind and Harrad, 1994). Inter-ocular suppression can result from a number of binocular abnormalities, e.g. unequal inter-ocular refractive error, strabismus, or organic causes such as monocular cataract. Constant inter-ocular suppression also occurs in amblyopia, possibly in response to these uncorrected binocular abnormalities (Travers, 1938; Sireteanu and Fronius, 1981; Harrad, Sengpiel and Blakemore, 1996; Sengpiel and Blakemore, 1996).

Li et al. (2011) recently showed that the degree of amblyopia (as measured by inter-ocular acuity difference) was positively correlated with suppression depth measured in the central visual field. Suppression was measured as the amount of contrast attenuation required in the non-amblyopic eye to provide similar performance in both eyes with a dichoptic global motion coherence task. No differences in suppression depth existed between anisometropic or strabismic amblyopes with similar inter-ocular acuity differences. However, evidence in the literature suggests that anisometropic amblyopes generally show suppression scotomata centred around the fovea of the amblyopic eye, whilst suppression extends from this central point to the point corresponding to the non-amblyopic eye fovea in strabismics (Irvine, 1948; Sireteanu, Fronius and Singer, 1981). Further studies have also shown similar asymmetric suppression patterns across the visual field of strabismic amblyopes (Travers, 1938; Jampolsky, 1955; Herzau, 1980; Campos, 1982; Pratt-Johnson and Tillson, 1983).

The present study will evaluate a new method of suppression mapping in order to accurately quantify suppression across the visual field. Amblyopic suppression will be simulated in normal vision by creating an inter-ocular difference in luminance to disrupt binocularity. A companion study (Chapter 2, Experiment 1) demonstrated that progressively disturbing binocularity by increasing monocular blur increased depth of inter-ocular suppression. Systematic differences in inter-ocular blur were used to simulate anisometropic amblyopia, for which differences in refractive error between the two eyes results in inter-ocular suppression in order to reduce confusion. In the present Experiment, in place of inter-ocular blur differences, inter-ocular differences in retinal illuminance are introduced to investigate the properties of the resultant inter-ocular suppression. It may follow that the progressive attenuation of monocular luminance will also lead to increasingly deeper suppression, as suppression in amblyopes is quantified clinically by reducing retinal illuminance of the non-amblyopic eye (with ND or progressively denser red filters) until a stimulus is perceived by the non-amblyopic eye (Mallett, 1988; von Noorden and Campos, 2002; Rowe, 2012).

Attenuating retinal illuminance in one eye, in normal vision during binocular viewing of stimuli, leads to reduced binocular performance in stereoacuity (Lovasik and Szymkiw, 1985), binocular contrast detection (Pardhan, Gilchrist, Douthwaite and Yap, 1990; Baker et al., 2007), binocular contrast discrimination (Baker, Meese and Hess, 2008), predominance of one eye's input during binocular rivalry (de Belsunce and Sireteanu, 1991; Leonards and Sireteanu, 1993), reduced binocular visual evoked potential amplitude (Pardhan et al., 1990; Heravian-Shandiz, Douthwaite and Jenkins, 1991), change in habitual sensory eye dominance (Zhang, Bobier, Thompson and Hess, 2011), and imbalanced binocular phase combination (Zhou, Jia, Huang and Hess, 2013).

The above deficits can be measured in unilateral amblyopes, who in addition show no improvement in binocular over monocular sensitivity during habitual viewing, i.e. binocular summation (e.g. Levi, Harwerth and Manny, 1979; Levi, Harwerth and Smith, 1980; Sireteanu et al., 1981; McKee et al., 2003). Li et al. (2013) used a dichoptic global motion coherence task to assess suppression in anisometropic amblyopes by reducing image contrast to the non-amblyopic eye

until performance was the same for the two eyes. Suppression in normal participants was matched to anisometropic amblyopes measured with the Bagolini striated lens test, by increasing monocular ND filters (on average 1.7 ND, range 0.3-2.1 ND) in front of one eye during binocular viewing until the filter eye was suppressed. Using this filter density in normals, dichoptic global motion coherence task performance was similar to that measured in amblyopes. Similar suprathreshold dichoptic global motion stimuli have also been used to measure suppression depth in amblyopes (Mansouri et al., 2008; Black et al., 2011; Hess et al., 2010a; Li et al., 2011, 2013a; 2013b). Zhang et al. (2011) used the dichoptic global motion task to investigate sensory eye dominance in normal participants. Adapting those participants monocularly to various retinal illuminances, deeper suppression was measured with increasing filter density, much like different depths measured with amblyopic suppression of varying degrees. Liu et al. (2002) showed that shifts in ocular dominance as determined by fMRI (functional Magnetic Resonance Imaging) on participants with normal binocular vision, but who wore monocular neutral density filters (2 ND), mimicked those found in naturally occurring anisometropic and strabismic amblyopia more closely than did the wearing of monocular blur to reduce VA to 6/60. This result suggests that ND filters applied to normal vision may be a better model than blur in mimicking binocular vision amblyopia.

Neutral density filters have also been found to have different effects on visual acuity for anisometropic and strabismic amblyopes. For example, Barbeito, Bedell, Flom and Simpson (1987) found that increasing ND filters in both eyes could lead to equalising amblyopic and non-amblyopic eye monocular acuities in strabismic amblyopia. This was not the case for blurred normal or anisometropic amblyopic eyes, for which inter-ocular differences in acuity remained even at the darkest luminance level. Reducing luminance also degraded contrast thresholds to the detection of sinusoidal gratings for strabismic, but not anisometropic, amblyopes (Hess, Campbell, and Zimmern, 1980). Other studies have found that non-amblyopic eye luminance attenuation improved visual acuity of the amblyopic eye during binocular viewing (Pugh, 1954; von Noorden and Leffler, 1966). Moreover, monocular retinal illuminance attenuation of normals during binocular viewing simulates amblyopic visual behaviour with respect to constant

suppression of one rivalrous image in binocular rivalry (Leonards and Sireteanu, 1993), lack of binocular summation of sinusoidal gratings at threshold (Baker et al., 2007) and worsened contrast discrimination above threshold (Baker, Meese and Hess, 2008) measured only with strabismic amblyopes, and binocular phase combination (Zhou et al., 2013) in strabismic and anisometropic amblyopia. Monocular retinal illuminance attenuation is therefore considered to be a good model for amblyopia, although the above studies do not agree on whether anisometropic or strabismic amblyopia is better simulated. Possibly, monocular retinal illuminance attenuation mimics anisometropic amblyopia with some tasks, and strabismic amblyopic with others, but a more direct comparison is warranted.

Traditional clinical measures of suppression generally aim to detect and grossly estimate depth of foveal suppression. Although the recently developed dichoptic global motion coherence paradigm provides a more sensitive method of quantifying suppression depth, it specifically engages the motion processing pathway and primarily tests the central visual field. In order to quantify suppression of spatial stimuli across the visual field, stimuli should ideally account for larger spatial summation areas in the periphery and be more comparable to habitual viewing with a supra-threshold task (Joosse et al., 1997, 1999). To further emulate habitual viewing, stimuli should be as similar as possible. As some difference in stimuli between the two eyes is required to measure suppression, only the part of the visual field being assessed should be dichoptic. Babu et al. (2013) satisfied some of these criteria, and measured both depth and extent of suppression with a method of adjustment and a supra-threshold inter-ocular contrast matching task, carried out at different locations across the central circular 20 deg visual field. They found that with a group of 10 strabismic and four anisometropic amblyopes, suppression was deepest foveally whilst reducing with retinal eccentricity. They also reported that suppression was generally deeper with greater difference in inter-ocular visual acuity.

The use of visual stimuli, thought to undergo more complex processing than standard luminance stimuli to measure depth of suppression, may reveal the nature of binocularity processing and the extent of inter-ocular suppression at

different stages along the visual pathway. Contrast-modulated noise (CM) stimuli are thought to be processed in areas receiving predominantly binocular input, compared to early neural areas able to process luminance (L), or luminance-modulated noise (LM) stimuli (Wong, Levi and McGraw, 2001, 2005; Hairol and Waugh, 2010; also see Chapter 1, Section, 1.3.1.2). Evidence supporting this supposition comes from the finding that there are greater deficits found in both amblyopic and non-amblyopic eyes (i.e. in binocularly disrupted visual systems) for CM, than for LM, grating detection (Wong et al., 2001, 2005), Gaussian patch detection (Mansouri et al., 2005), and global motion coherence thresholds (Simmers et al., 2003). The linear (simple) receptive fields of V1 cells are not able to detect CM stimuli due to the lack of change in mean luminance across the stimulus (Chubb and Sperling, 1988). Li et al. (2014) recently found neural correlates of CM boundary perception in monkey V2, where most cells are non-linear and receive input from both eyes. Thus, comparing depth and extent of suppression of LM and CM stimuli will allow us to assess in greater detail how disruption of binocularity affects visual processing along the visual pathway.

In this study, experiments are designed to map inter-ocular suppression in binocularly normal participants using luminance (L), luminance-modulated noise (LM) and contrast-modulated noise (CM) stimuli for differential inter-ocular mean luminances. First, suppression measurements for L and LM stimuli are compared to measure the effects that dynamic noise *per se* has on suppression depth created by inter-ocular retinal illuminance differences. Suppression is known to be reduced by introducing temporal transients (e.g. Scheiman and Wick, 2008), and therefore less suppression of LM compared with L stimuli is expected. Comparisons are then made between suppression maps measured for LM and CM stimuli. Depth and extent of suppression is investigated across the central 24 deg of the binocular visual field for all stimulus types. Deeper suppression measured for CM than for LM stimuli, would provide additional evidence that they are processed by non-linear mechanisms receiving binocular input.

3.2 Methods

3.2.1 Participants

Four binocularly normal non-presbyopic participants (three male and one female, aged 18-32 years) took part in the experiment, of which one was the author (ASC) and the others (CP, SM, and SP) were naïve to the nature and purpose of the experiments. Participant SM had no previous experience with psychophysical experiments, whilst CP and SP were well practiced in a similar task, contributing to the results of a previous experiment (Chapter 2, Experiment 1). All participants had 6/5 or better corrected visual acuity in each eye and stereoacuity of at least 30 arcsec, as measured with the Dutch Organization for Applied Scientific Research (TNO) stereo test (Lameris Ootech, Ede, The Netherlands). All participants were right eye dominant determined with the sighting dominance test (Fink, 1938). Clinical details for each participant are show in the Appendix (see Section 2.6.2). Informed consent was obtained from all participants and the Anglia Ruskin University Research Ethics Committee approved the conduct of the research project, ensuring that the research complied with the tenets of the Declaration of Helsinki.

3.2.2 Equipment

Equipment was similar to that described in Experiment 1 (see Chapter 2, Section 2.2.2). In brief, an Apple MacBook Pro (MacBook Pro; Apple Computer, Cupertino, CA) running Matlab (The MathWorks, Natick, MA) with Psychophysics Toolbox (Brainard, 1997, pelli, 1997) was used to generate stimuli. They were then presented on eMagin DualPro head-mounted OLED displays (Dual Pro Z800; eMagin Corp., Hopewell Junction, NY) via a Matrox DualHead2Go adapter (Matrox Graphics Inc., Quebec, Canada). One screen for each eye allowed for dichoptic presentation of stimuli. Each screen had a resolution of 800x600 pixels, refresh rate of 60 Hz, and mean luminance 45 cd/m^2.

Although these eMagin displays have demonstrated 8-bit luminance capability

with a linear response profile (Black et al., 2011), luminance profiles obtained for each of our screens after one hour “warming-up” showed poor linearity. We linearised and equalised the luminances of each screen by recording outputs with a ColorCAL II Colorimeter (Cambridge Research Systems, UK) and gamma-corrected look-up tables. Cooper et al. (2013) measured two similar Sony OLED displays and found minimal or no adjacent pixel spatial interactions with wide contrast ratios, although this may vary across manufacturers.

Neutral density filters (Kodak Wratten 2 No.96, Rochester, NY) were used to give an inter-ocular difference in retinal illuminance. These particular filters reduce luminance energies of all visible wavelengths equally, although stimuli used in the present study were constructed from a series of grey levels only. Luminance attenuation was checked using a ColorCAL II Colorimeter (Cambridge Research Systems, UK), confirming that the three filter strengths used were indeed, 1.5, 2, and 3 ND, attenuating luminance by 32x, 100x, and 1000x, respectively. The results of pilot experiments showed that a 1.5 ND filter was the least dense filter that showed some measurable suppression. Filters were cut and mounted in photographic slide frames, and temporarily fixed to the left goggle screen of the eMagin head mounted displays (all participants’ non-dominant eye was the left eye), such that the whole of the left display was attenuated. The right and left eye displays were positioned very close to the eyes, so that the nose effectively blocked any luminance from one eye from reaching the other.

3.2.3 Stimuli

Schematics of the L, LM and CM stimuli are provided in Figure 3.1 (A-F). Stimuli consist of four concentric rings of alternating polarity, such that the high modulation rings (e.g. the central ring) differ from the background mean modulation by the same magnitude as the low modulation rings (e.g. the outermost ring). Images presented to the left eye (Figure 3.1 – left) were fused with those presented to the right eye (Figure 3.1 – right) by the brain to give one fused cyclopean image subtending 24 deg of the central circular visual field.

Although larger foveal and peripheral spatial summation areas have been found for CM compared to LM stimuli (Sukumar and Waugh, 2007), a previous control experiment (see Chapter 2, Section 2.3.3) found that equalising sector sizes showed no significant difference in suppression depth. Therefore, sector sizes were the same for L (Figure 3.1A, B), LM (Figure 3.1C, D), and CM (Figure 3.1E, F) stimuli, with each of the four concentric rings split into eight sectors (a total of 32 sectors), denoted by blue lines in Figure 3.2 (participants perceived no blue lines during experiments). The stimuli were split into these sectors to reveal any local areas, or asymmetry of suppression. The central ring (a circle) had a radius of 1.3 deg. Each subsequent ring from the centre was doubled in area to account for larger spatial summation areas in the peripheral relative to the central visual field.

Figure 3.1 (following page): Examples of L (A), LM (C), and CM (E) stimuli. B, D, and F show luminance profiles (excluding blind-spot markers) taken one pixel above the horizontal midline, where the red line is mean luminance. Left and right columns show each eye respectively. For CM stimuli (E-F). Average luminance of the stimuli remains constant about the mean luminance, though the contrast of the high and low CM rings and the adjustable sector change. Thus the difference between each ring is the modulation of contrast, rather than modulation of luminance. A, C, and E show green and red blind-spot markers for right and left eyes, respectively. All horizontal axes show horizontal pixel numbers (as in F). Ordinate axes of A and C are the same as E, and B and C the same as F.

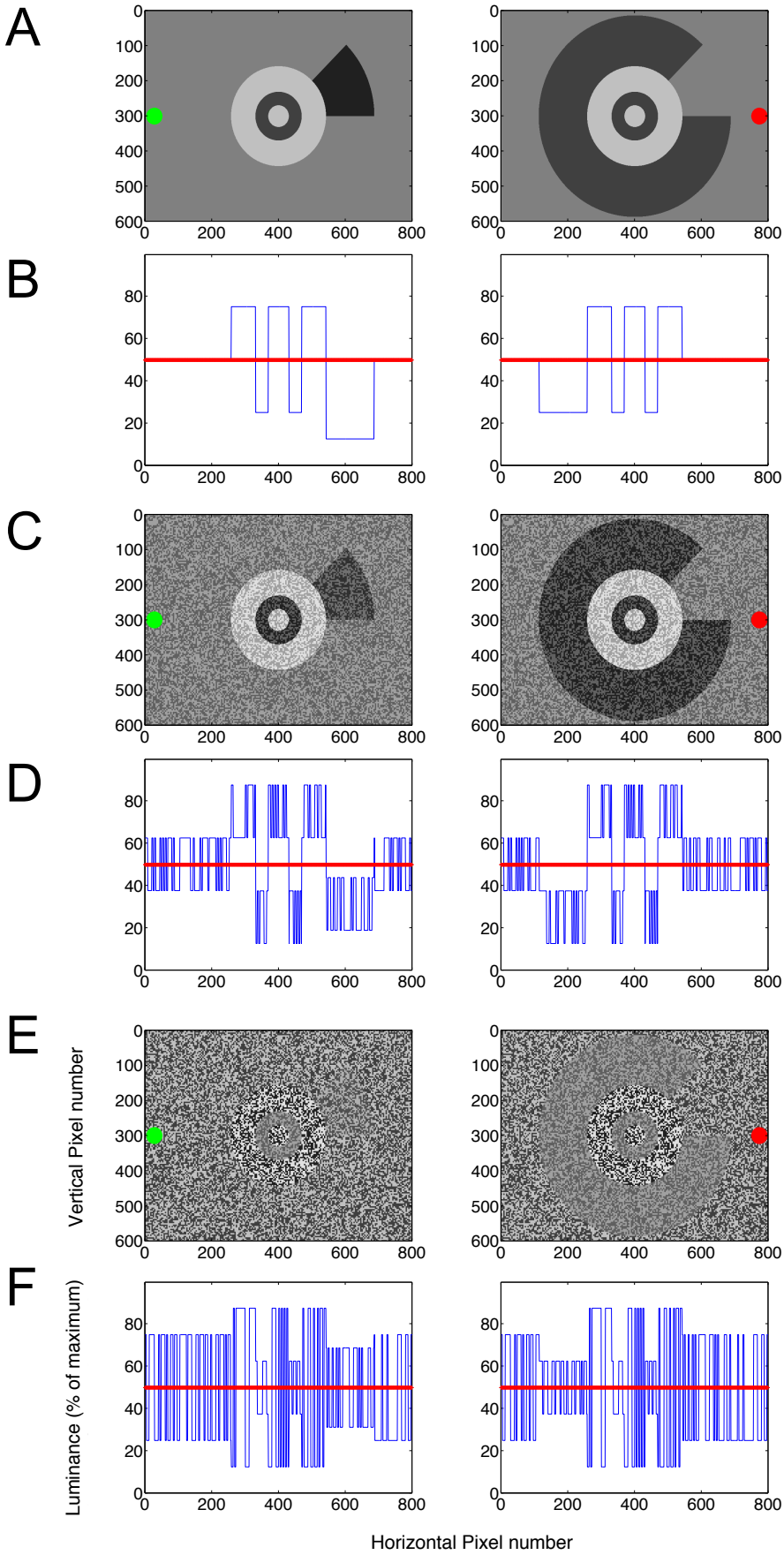
A
B
C
D
E
F
Vertical Pixel number
Luminance (% of maximum)
Horizontal Pixel number

Figure 3.2 (following pages): A) Schematic representation of L stimuli. Black lines delineate sectors. Blue lines show orientations (see Analysis section for explanation). These lines do not appear on actual stimulus. B) Order of sector presentation.

A

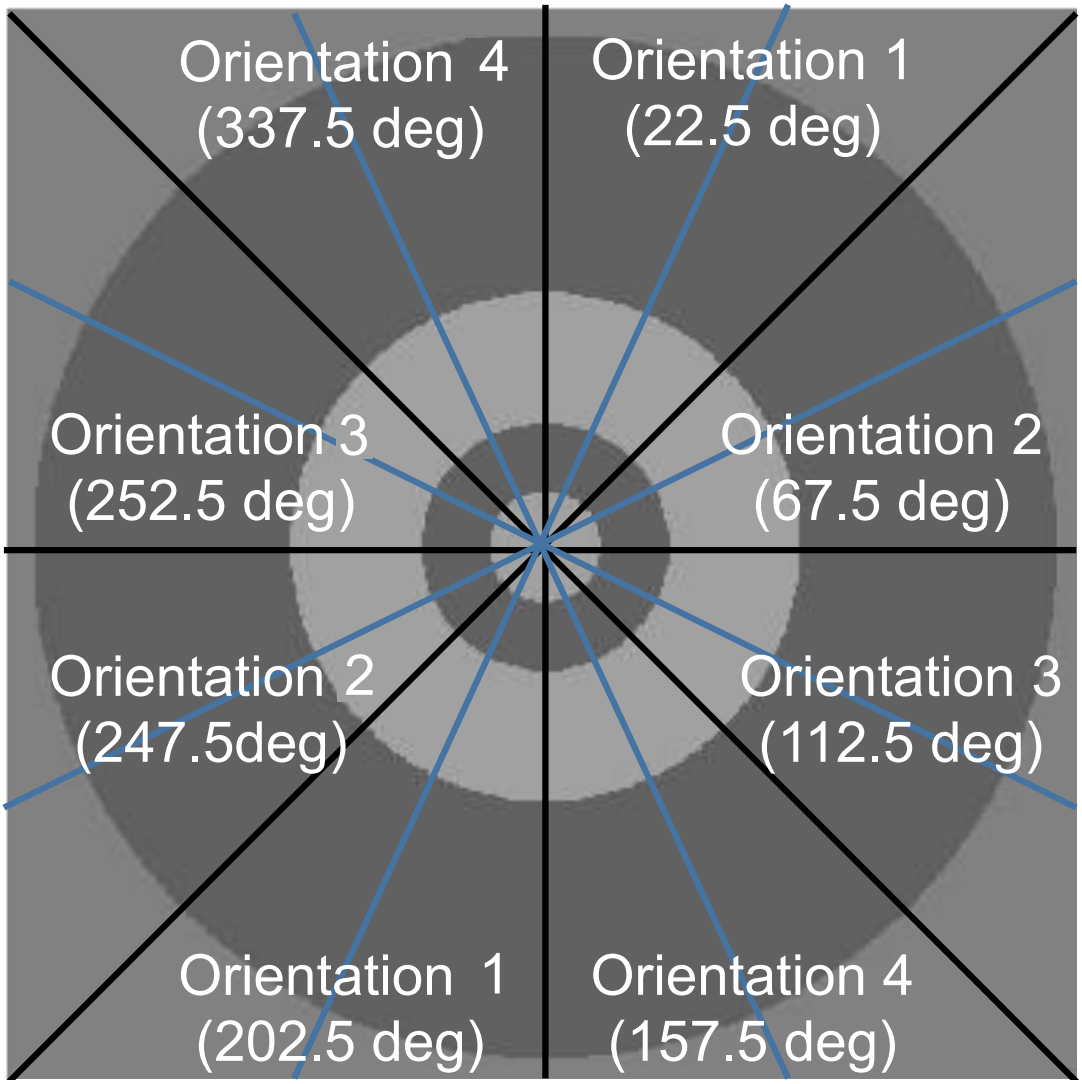
Orientation 4
(337.5 deg)
Orientation 1
(22.5 deg)
Orientation 3
(252.5 deg)
Orientation 2
(67.5 deg)
Orientation 2
(247.5deg)
Orientation 3
(112.5 deg)
Orientation 1
(202.5 deg)
Orientation 4
(157.5 deg)

B

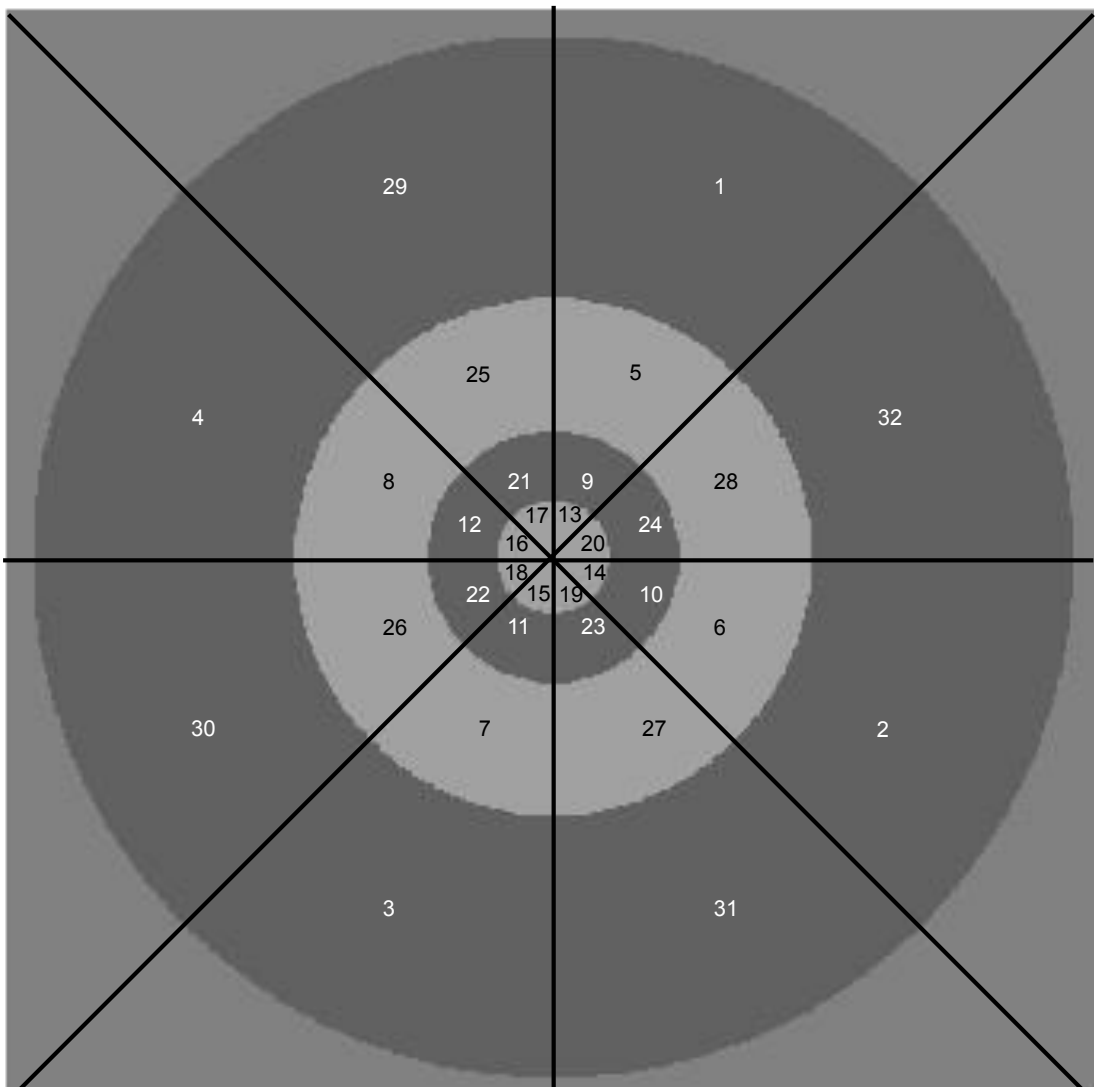
29
1
25
5
4
32
8
21
9
28
17
13
12
24
16
20
18
14
22
15
19
10
26
11
23
6
30
7
27
2
3
31

The background luminance provides the baseline from which modulation measures are taken. As LM and CM stimuli are varied in luminance- or contrast-modulated noise respectively, the rings and adjustable sector are quantified in terms of their 'modulation'. The following equation (Schofield and Georgeson, 1999) describes how L, LM and CM stimuli were constructed:

$$I\ (x,y) = \ I_0\ [1 + \ nN(x,y) + \ lL(x,y) + \ mnM(x,y)N(x,y)] \qquad \text{Eq. (1)}$$

where *I(x,y)* is the luminance at position *(x,y)*; I_0 is mean luminance; *n* is noise contrast; *N(x, y)* is the value of binary noise; *l* is the (luminance) modulation of L and LM rings; *m* is (contrast) modulation of CM rings. For L stimuli, *n* = 0, *m* = 0 and *l* is adjusted; for LM stimuli n = 0.25, *m* = 0 and *l* is adjusted; and for CM stimuli n = 0.50, *l* = 0 and *m* is adjusted. More details are provided in Chapter 2 (Section 2.2.3).

For noisy (LM and CM) stimuli, the noise check size was 4x4 pixels with an angular subtense of 10 arcmin at 80 cm (equivalent viewing distance), clearly resolvable for all of our participants at all eccentricities tested (Ludvigh, 1941; Millodot et al., 1975; Rovamo, Virsu and Näsänen, 1978; Anderson and Thibos, 1999a; b). Schofield and Georgeson (2003) found that noise type and amplitude had no effect on CM modulation sensitivity functions, though for LM functions, sensitivity was reduced where noise spectral energy was strongest. Therefore, spectrally broad-band binary noise is sensible to use in the present study.

Ten different spatial frames of stimuli were compiled after each participant response using randomly generated binocularly correlated noise, with no noise for L stimuli. Presenting the 10 spatial frames in a random order every two temporal frames created dynamic noise stimuli, with each frame presented for 33.3 ms. Smith and Ledgeway (1997) demonstrated the importance of using dynamic noise when investigating contrast-defined motion perception, when local stochastic biases in static noise produced luminance artefacts in second-order stimuli.

3.2.4 Procedure

Experiments were performed in a dark room with the participant viewing a video binocularly in the head-mounted displays for at least 20 mins with the same density filter to be used in the experimental run. MacMillan, Gray and Heron (2007) adapted normal observers to an inter-ocular retinal illuminance difference, the maximum inter-ocular difference being 0.9 ND. Every 15 mins during adaptation (to ambient room lighting), participants performed a binocular brightness match to a 150 cd/m^2 test field presented to the non-filter eye. A 600 cd/m^2 test field was presented to the other eye, and both fields were perceived simultaneously (adjacently, i.e. not fused) and luminance was adjusted until a match between both test fields was perceived. Adaptation (taken as the change in test field matches) reached asymptote at approximately 45 mins, though changes in adaptation were small after 20 mins.

Any minimal effect of continuing adaptation in the present study would be spread over the conditions as the mean was taken of multiple counter-balanced runs (see below). If the run required no filter, a shorter adaptation period took place, and the run was still carried out in a dark room. Participant pupil size was not controlled, and therefore the effect of ND filter may have varied slightly between participants. However, this is likely to have been similar for each participant across the three types of stimuli.

After the adaptation period, suppression was measured using an inter-ocular modulation matching task, the same as in a previous study (see Chapter 2, Section 2.2.4 for more details). Before testing began, participants were given a practice session with each type of stimulus until comfortable with the task, i.e. standard deviation of staircase was stable (within 15% of the mean). Throughout testing, participants were advised to maintained fixation on the centre of the stimulus. If gaze wandered, brightly coloured blind spot markers would become visible and the participant re-fixated before responding.

An inter-ocular modulation matching task allowed for measurement of the point of

subjective equality (PSE) in 32 different areas across the central circular 24 deg of the visual field. Participants decided in a 2AFC paradigm whether a modulation increase or decrease of a particular sector presented to the left (non-dominant) eye (e.g. Figure 3.1, left column), was required to match the surrounding ring presented to the right (dominant) eye (e.g. Figure 3.1 right column). The variable sector was always presented to the left eye, which also viewed through any ND filter (0 ND, 1.5 ND, 2 ND, or 3 ND).

For each sector, a (1-down 1-up) staircase was initiated randomly from either halfway between a physical modulation match and maximum adjustable modulation; or halfway between a modulation match and minimum adjustable modulation. An audio cue signalled once six reversals were complete, after which the staircase was terminated and a new sector was adjusted. In each experimental run, 32 staircases were completed, i.e. one for each sector. The order of sector presentation was systematic to distribute the effects of practice, adaptation, and fatigue. Within each experimental run, odd-numbered sectors were presented from the outside ring inwards clockwise, then even-numbered sectors from the inside ring outwards anti-clockwise (see Figure 3.2B). Table 3.1 shows the order of experimental runs across ND and stimulus type conditions. When the 12 conditions had been completed (as in Table 3.1), they were run in reverse order across ND and stimulus type (i.e. from 12 - 1). This entire process was repeated, giving a total of four experimental runs of each condition.

Table 3.1: Order of experimental runs.

Stimulus type	**No ND**	**1.5 ND**	**2 ND**	**3 ND**
L	1	6	7	12
LM	2	5	8	11
CM	3	4	9	10

Suppression mapping was therefore performed for four levels of ND (0, 1.5, 2, and 3 ND) placed before the non-dominant (left) eye. The 0 ND condition was used to find a baseline measurement of suppression, as participants did not all

have a completely balanced inter-ocular match, possibly due to sensory eye dominance.

3.2.5 Analysis

For each sector in each condition, the mean point of subjective equality (PSE) was estimated as the mean of four experimental runs for each ND level (0, 1.5, 2, and 3 ND) across each stimulus type (L, LM, and CM). Point of subjective equality (PSE) modulation values are normalised across stimulus type using the following equation:

$$S_{norm} = \frac{(M_{match} - M_{baseline})}{M_{baseline}} \quad \text{Eq. (2)}$$

where S_{norm} is the normalised depth of suppression, M_{match} is the PSE modulation and $M_{baseline}$ is the baseline modulation. Depth of suppression is expressed as -1 to 1, where 1 is the maximum level of suppression (signal strength needed to be doubled for the sector in the filter eye to match perception of the surrounding ring), 0 is an inter-ocular match (signal strength is perceived as the same in each eye), and -1 is maximum binocular facilitation (signal strength in the filter eye was reduced to minimum to match perception of the surrounding ring).

Preliminary experiments showed that with higher levels of ND, suppression was too deep to measure in two participants with 3 ND for CM stimuli, and for one of two participants with L and LM stimuli. If the staircase reached the maximum measurable normalised suppression value, the S_{norm} was set to the maximum value for analysis. In the main experiment, as this occurred for all participants with 3 ND and CM stimuli, and two of four participants with 3 ND L and LM stimuli, statistical analyses were conducted with and without 3 ND suppression values (as the variance was artificially reduced with 3 ND). Maximum suppression values were also exceeded for mainly central sectors with L and LM stimuli with this filter.

All data were subjected to a repeated measures design Analysis of Variance (ANOVA) with factors of stimulus type (three levels – L, LM, and CM), ND strength (four levels – 0, 1.5, 2, and 3 ND), sector orientation (four levels – blue lines in Figure 3.2), and sector eccentricity (eight levels – along orientation from the peripheral sector to the centre and out to the opposite periphery). All ANOVAs were performed with conservative Greenhouse-Geisser correction for violation of sphericity and independence of errors.

3.3 Results

Suppression depth for all sectors measured for all stimulus types and inter-ocular luminance levels across the central circular 24 deg of visual field, are averaged and presented as colour maps in Figure 3.3. Each sector measured is represented by a colour. Without any filter (0 or no ND), no suppression is measured for L and LM stimuli, with very mild suppression measured for CM stimuli. There looks to be no systematic variation with sector eccentricity or orientation.

With increasing ND, from 1.5 ND to 2 ND to 3 ND, suppression deepens for all stimulus types, with sectors changing from mild facilitation (light green) or inter-ocular match (yellow), to orange (mild suppression) and red (deep suppression). Suppression appears deeper for L, than for LM stimuli; and also for CM than LM stimuli. No systematic variation in suppression is noticeable across orientation although suppression appears deepest for all stimulus types in the central region. Additionally for L and LM stimuli, particularly with 1.5 and 2 ND filters, suppression appears to be deeper for alternate rings, giving “bull’s eye” suppression maps, an effect not seen with CM stimuli.

For the 3 ND condition, this differential suppression pattern is reduced for L and LM stimuli, leaving only central suppression, possibly due to the suppression depth being above the measurable range (as noted in Section 3.2.5: Analysis). Suppression depth was set to the maximum measurable value when ceiling was reached. The results of the full ANOVA are provided in Table 3.2.

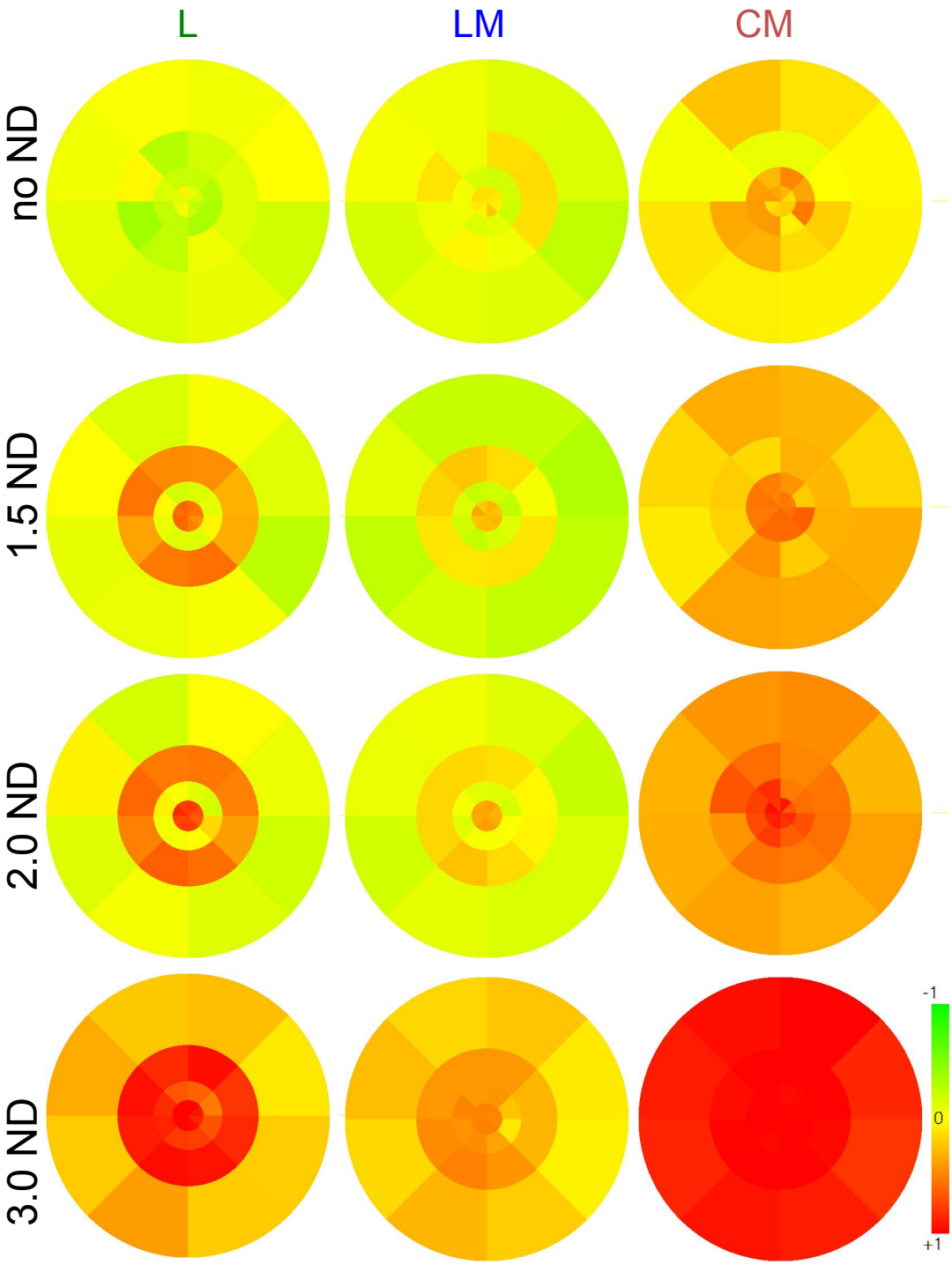

Figure 3.3: Colour-coded suppression maps averaged across four participants, for each level of ND (0 ND, 1.5 ND, 2 ND, and 3 ND), for each stimulus type (L, LM, and CM). Each sector is represented by a colour denoting the depth of suppression on a scale where green is facilitation (normalised value of -1), yellow is an inter-ocular match (normalised

Table 3.2: Results of the repeated measures ANOVA with factors stimulus type (3) x ND strength (4), sector orientation (4), and sector eccentricity (8). Significant main effects and interactions are highlighted in red, and those nearing-significance in amber. Non-significant higher order interactions are not shown.

Source (number of levels)	Degrees of Freedom	F	Sig.
Stimulus type (3)	1.17	38.71	0.005
ND strength (4)	1.51	47.27	0.001
Orientation (4)	2.34	4.11	0.062
Eccentricity (8)	1.55	8.12	0.033
Stimulus Type* ND strength	2.70	9.66	0.005
Stimulus Type* Orientation	2.09	0.11	0.907
Stimulus type * Eccentricity	1.90	11.58	0.010
Orientation * Eccentricity	2.39	0.69	0.557
ND strength * Orientation	1.98	1.40	0.318
ND strength * Eccentricity	2.04	4.89	0.054

There are significant main effects of ND strength, stimulus type and eccentricity. Overall, the stronger the ND filter (i.e. the greater the inter-ocular luminance difference), the deeper the suppression measured; deepest suppression is measured for CM, shallower for L, and least deep for LM stimuli; and overall suppression is deeper centrally than peripherally. These main effects are displayed in Figure 3.4. However there are several key significant statistical interactions that indicate that the effects of eccentricity depend on the stimulus type used to measure it, and on the level of ND examined.

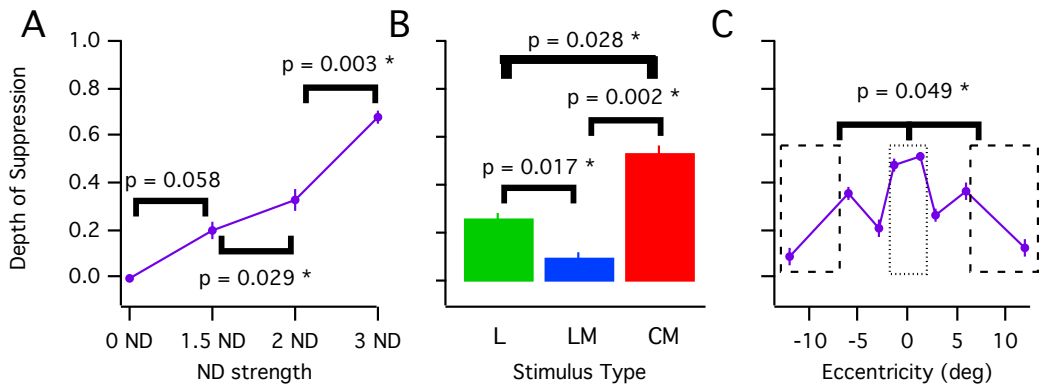

Figure 3.4: A) Suppression depth averaged across all sectors, stimulus types, and participants for each ND level. B) Suppression depth averaged across all sectors, ND strengths, and participants for each stimulus type. C) Suppression depth averaged across all orientations, participants, and stimulus types for each eccentricity. All ordinate axes show the same scale of depth of suppression, and all error bars show ±1 standard error. Significance (p-values) from tests of simple effects are shown in each Figure, where statistically significant comparisons are marked with an asterisk

As in these experiments ND filters are used to potentially mimic suppression effects across the visual field in amblyopia (which have been known to vary across the visual field), specific interactions with eccentricity are now examined in more detail. Data are collapsed across orientation (as there were no significant differences in suppression across orientation) for individual participants in Figures 3.5, 3.6 and 3.7 for L, LM and CM stimulus types, respectively.

Figure 3.8 shows these data averaged across each stimulus type for four different levels of inter-ocular luminance difference created by the ND filters across the eight eccentricities (i.e. also averaged across orientation). On viewing Figure 3.8, it can be seen that overall the depth of suppression increases, i.e. the curves for each ND move progressively higher on the ordinate, as the inter-ocular luminance difference increases, for all stimulus types.

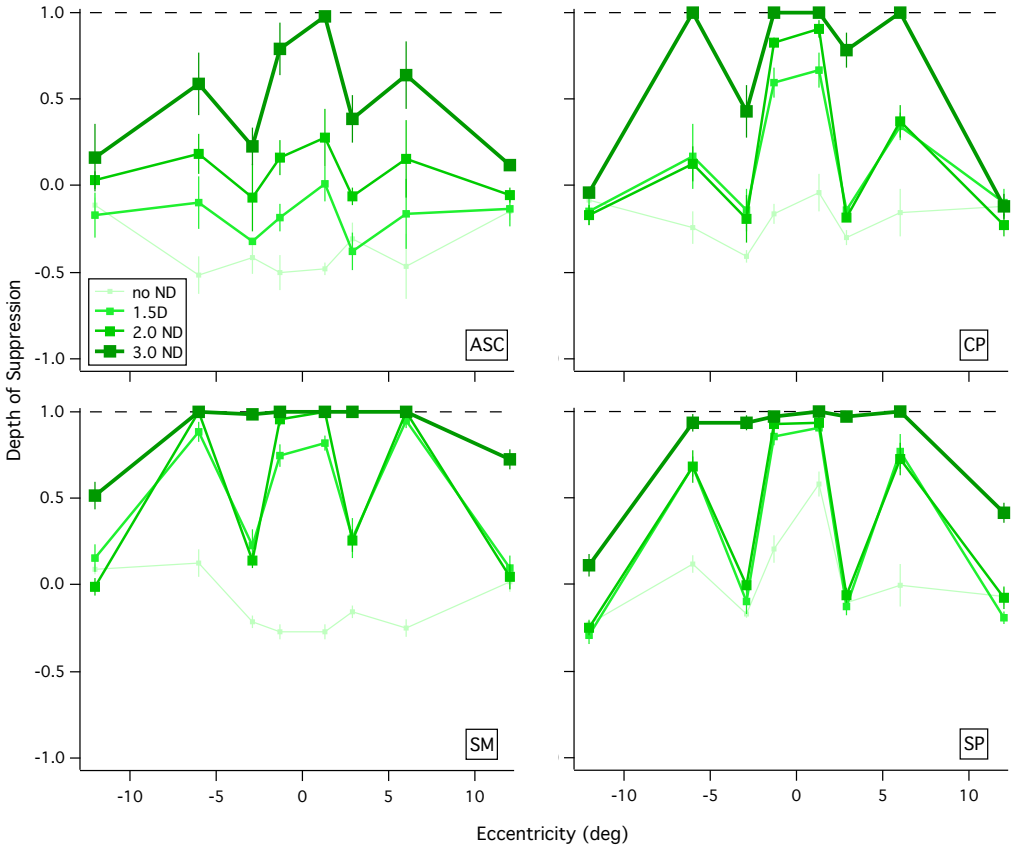

Figure 3.5: Averages of depth of suppression of each sector eccentricity across all orientations (blue lines – Figure 3.2) were taken for each ND filter strength, for L stimuli. Legend in top left panel applies to all panels, which show data for individual participants. Dashed lines show the maximum adjustable suppression level. Error bars represent ±1 standard error.

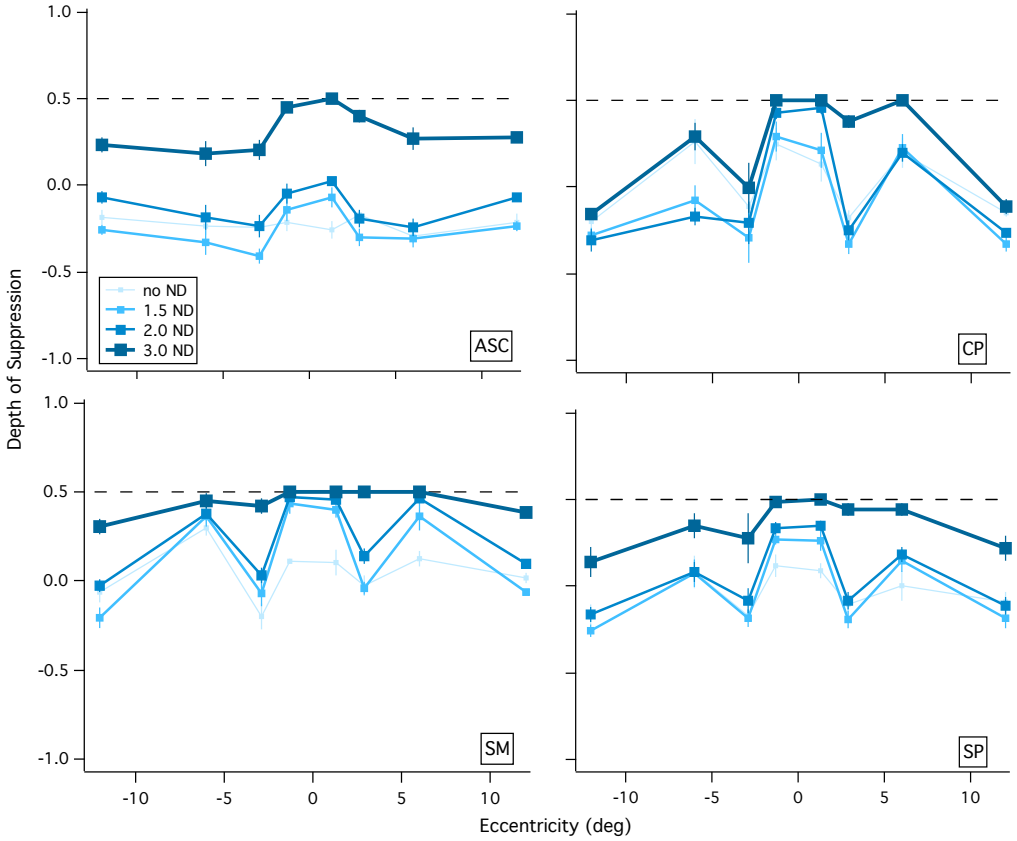

Figure 3.6: Suppression of LM stimuli. Figure details are the same as previous Figure.

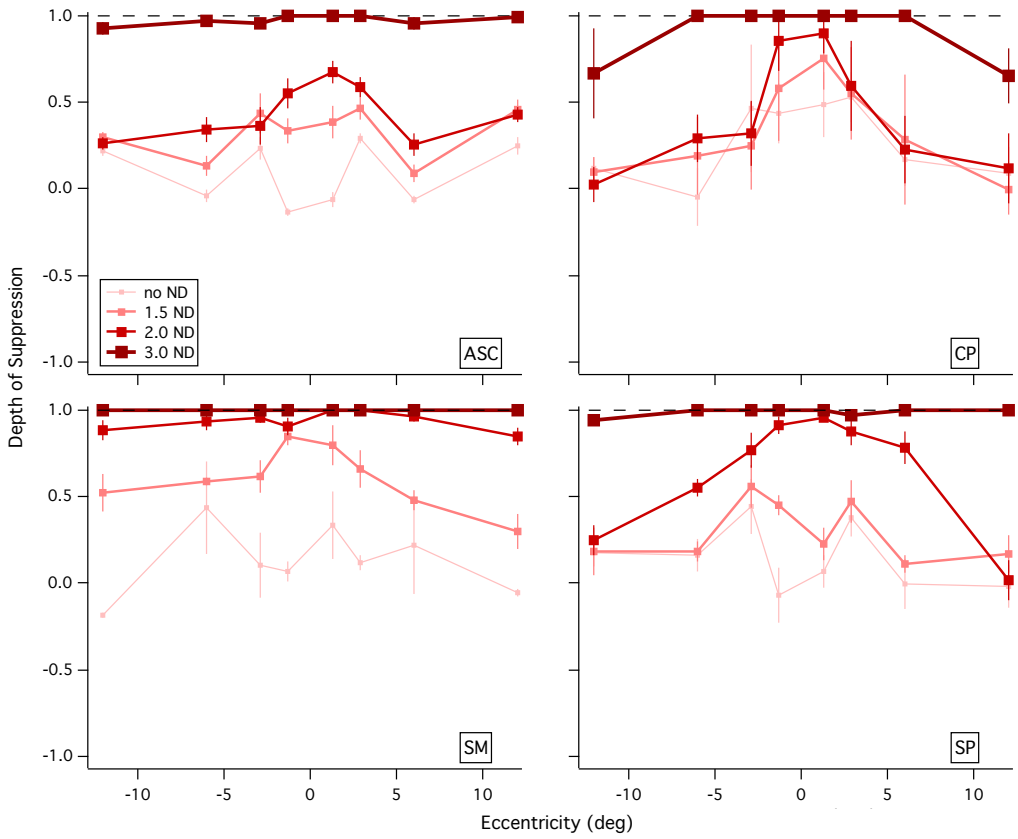

Figure 3.7: Suppression of CM stimuli. Figure details are the same as previous Figure.

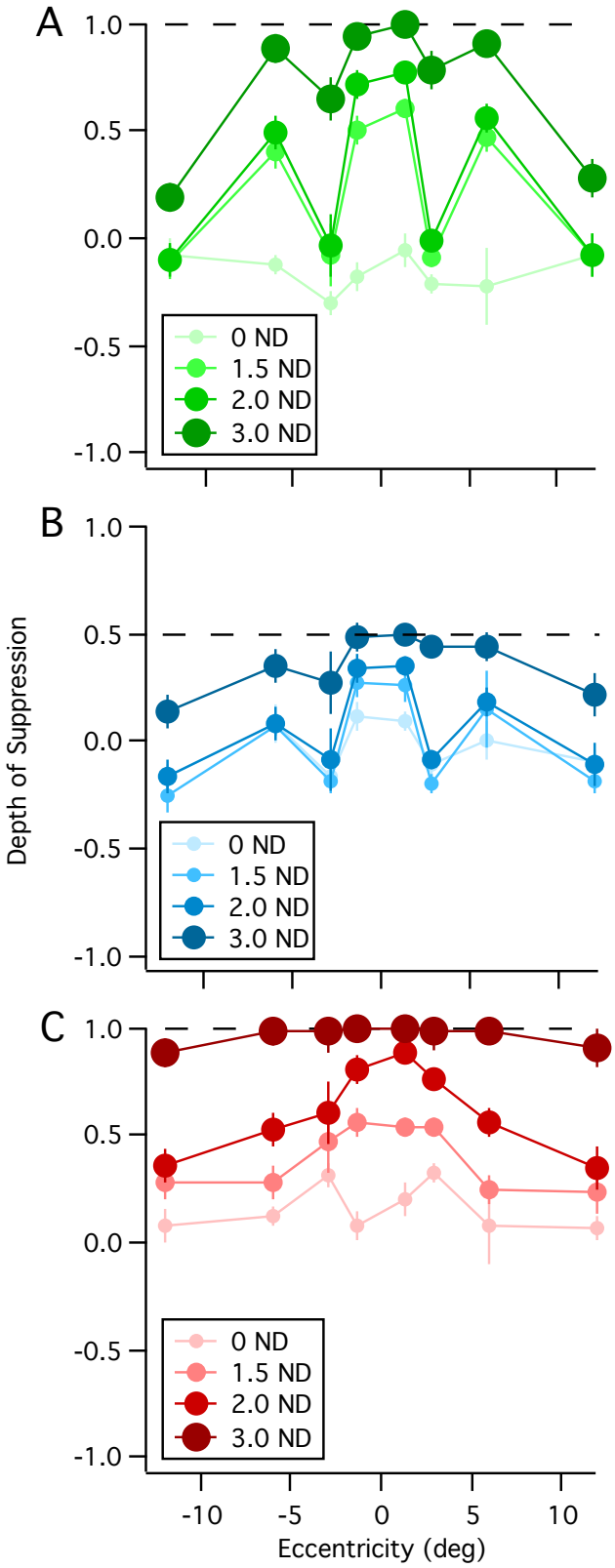

Figure 3.8: Depth of suppression averaged across all participants and orientations for each ND level, and for each stimulus type. Dashed lines show the maximum adjustable suppression level. Error bars show ±1 standard error

On average, without any inter-ocular luminance difference (the 0 ND condition), there is no significant effect of eccentricity on the pattern of suppression [$F(1, 3) = 0.027$, $p = 0.881$]. For the 1.5 ND and 2 ND conditions, patterns of suppression do appear across eccentricity, however for the 3 ND condition, this pattern flattens. As mentioned above though, on examining the data for the 3 ND condition, suppression for a significant number of eccentricities reached maximum. For this condition then, due to a ceiling effect, the variance was artificially minimised (as indicated by a lack of error bar associated with these data points). This can be seen for L stimuli in Figure 3.5 (where the maximum achievable suppression measure is 1.0 for participants CP, SM and SP, and LM stimuli in Figure 3.6 (where the maximum measureable value is 0.5) for all participants, particularly for the increment (i.e. lighter) sectors. It is also clear for data obtained using CM stimuli in Figure 3.7 (where the achievable suppression measure is 1.0) for all participants.

Due to restrained variance in the 3 ND condition, leading to a potentially severe violation of the sphericity of variance, the ANOVA was conducted on a reduced data set excluding the 3 ND data. The results of this analysis are provided in Table 3.3. Despite exclusion of the 3 ND inter-ocular luminance condition, the main outcomes of this statistical analysis are very similar to those revealed in Table 3.2.

Table 3.3: Outcomes of ANOVA, with factors stimulus type (3) x ND strength (3), sector orientation (4), and sector eccentricity (8). Significant interactions are highlighted in red, and those nearing significance in amber. Non-significant higher order interactions are not shown.

Source (number of levels)	Degrees of Freedom	F	Sig.
Stimulus type (3)	1.19	29.97	0.007
ND strength (3)	1.10	13.53	0.029
Orientation (4)	2.22	3.10	0.110
Eccentricity (8)	1.61	5.76	0.056
Stimulus Type* ND strength	2.41	7.67	0.014
Stimulus Type* Orientation	2.31	0.29	0.786
Stimulus type * Eccentricity	1.74	7.96	0.028
Orientation * Eccentricity	2.53	0.50	0.663
ND strength * Orientation	1.38	0.93	0.425
ND strength * Eccentricity	2.53	15.52	0.002

3.3.1 How does inter-ocular luminance suppression change across eccentricity?

As noted in the ANOVA results tables, there is a significant effect of eccentricity on inter-ocular luminance suppression that depends on the stimulus type used to measure it. As there is no significant effect of eccentricity on the 0 ND condition and the effect of eccentricity is constrained (though significant) for the 3 ND condition [$F(1, 3) = 191.41$, $p = 0.0008$], eccentricity effects for the 1.5 and 2 ND conditions are examined statistically. The main results are illustrated in Figure 3.9.

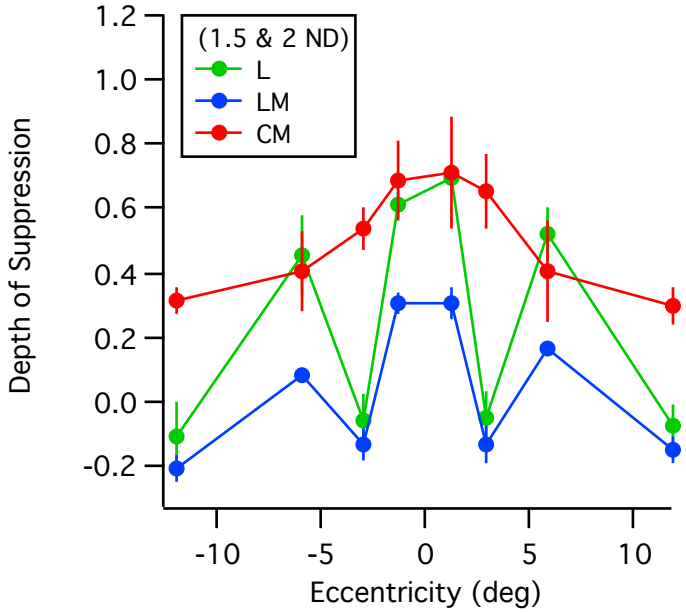

Figure 3.9: Suppression depth averaged across participants, orientations, and 1.5 and 2 ND, for each eccentricity. Separate curves show different stimulus types. Error bars show ±1 standard error between ND levels.

There is a significant effect of ND filter on the level of suppression, being significantly deeper for 2 ND than 1.5 ND [$F(1, 3) = 24.92$, $p = 0.015$], however there is no significant interaction between eccentricity and ND filter for these two filters, so that the pattern across eccentricity remains the same (see Figure 3.8). Figure 3.9 shows that suppression varies with eccentricity for stimulus type with 1.5 ND and 2 ND combined, such that the CM pattern of suppression is significantly different from the L and LM pattern [$F(1, 3) = 37.03$, $p = 0.009$].

For suppression measured with CM stimuli, the effect of eccentricity is significant [$F(1, 3) = 42.22$, $p = 0.007$] with a pattern of central suppression evident (see Figure 3.9). The pattern of suppression for L and LM stimuli is more complicated for L [$F(1.56 ,4.67) = 11.32$, $p = 0.018$] and LM [$F(1.58, 4.75) = 9.92$, $p = 0.027$]. Two patterns are evident, a zig-zag pattern and a deeper central than peripheral pattern. Examination of these data reveal correspondence between deeper suppression and incremental (lighter) sectors, and shallower suppression with decremental (darker) sectors. Planned

comparisons revealed that suppression measured for incremental and decremental sectors is statistically significant [F(1, 3) = 14.54, p = 0.032].

In order to test whether there is a specific central suppression effect for L and LM stimuli, the effects of eccentricity were examined on increment only sectors across eccentricity and decrement only sectors across eccentricity. The power of this analysis is decreased severely for both increment only and decrement only sectors, due to the reduced eccentricity range testable for both (see Stimulus in Figure 3.1). Incremental sectors were most central (foveal – 0-1.3 deg eccentricity) and also at 3-6 deg. Decremental sectors missed foveal testing, but incorporated sectors at 1.3-3 deg and 6-12 deg eccentricity. Even with these restricted ranges, it was possible to achieve statistically significant effects of eccentricity for increment-only L and LM sectors [F(1, 3) = 12.02, p = 0.040]. A significant eccentricity effect was also found for decrement-only L sectors when data for the 3 ND were examined [F(1.70,5.11) = 10.36, p = 0.017]. Data for 3 ND for decremental L stimuli are valid to use, as unlike for incremental stimuli, the ceiling value was not reached. These results can be visualised in Figure 3.10 below.

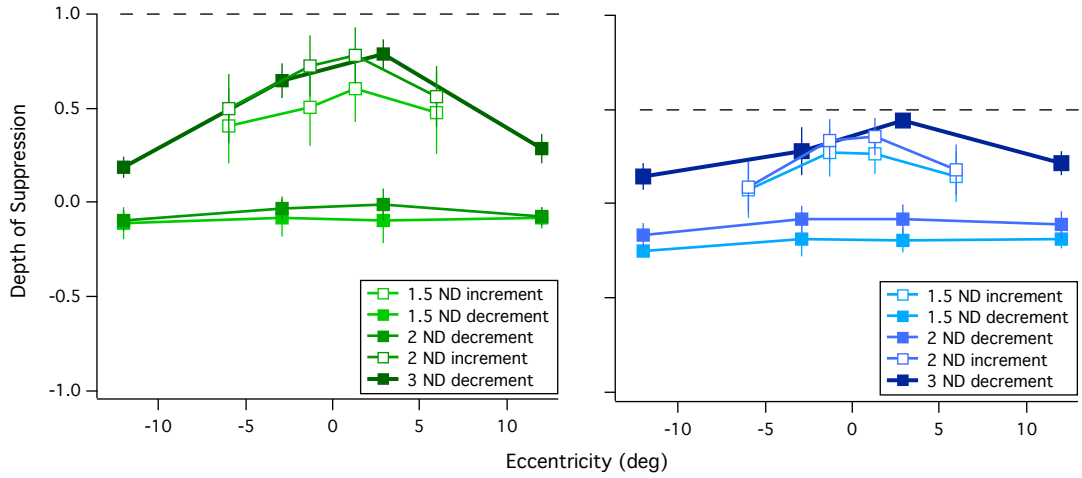

Figure 3.10: Depth of suppression data from main experiment L (green) and LM (blue) stimuli replotted as separate modulation increments (open squares) and decrements (filled squares) for 1.5 ND (lighter), 2 ND (darker), and 3 ND decrements only (darkest). Data are averaged across four participants. Dashed lines show the maximum adjustable suppression level. Error bars show ± 1 standard deviation between participants.

3.3.2 A more detailed investigation of eccentricity on suppression of incremental and decremental modulation stimuli

Due to the design of the target stimulus in the main experiments, it is difficult to disentangle true eccentricity effects of inter-ocular luminance suppression, from the effects of differential suppression on incremental versus decremental modulation stimuli. These differences were found only for luminance (L) and luminance-modulated noise (LM) stimuli.

The present control experiment tested the same eight eccentricities with the same (as the main experiment) and reversed polarity stimuli, to reveal any underlying differences in suppression between the central and peripheral visual fields. The same methods as the main experiment were used to measure suppression across two (only) orientations of L, LM, and CM stimuli for two participants (ASC and SP). In the “reversed” configuration, sectors previously created as modulation increments were created as decrements, and sectors previously created as decremental sectors were created as increments. Four runs were performed (for each of the two orientations) for each stimulus type with 2 ND filter for each participant. Increment data from this control experiment and increment data from the main experiment together, provided measurements of suppression at all eccentricities measured, and the same was done for decrements (Figure 3.11).

Figure 3.11 confirms that, on average (dashed lines), suppression is deeper centrally than peripherally for both L and LM stimuli. The data in Figure 3.11 also confirm that suppression is deeper for L than LM stimuli, for both increments and decrements. In addition, the differential increment-decrement suppression seen in noiseless stimuli is reduced, when noise was added. Suppression across the visual field with L or LM increments is similar, with less obvious central suppression than is found for L and LM decrements. Modulation decrement suppression occurs very centrally for this ND condition, i.e. within 2.6 deg of the visual field (0 – 1.3 deg eccentricity).

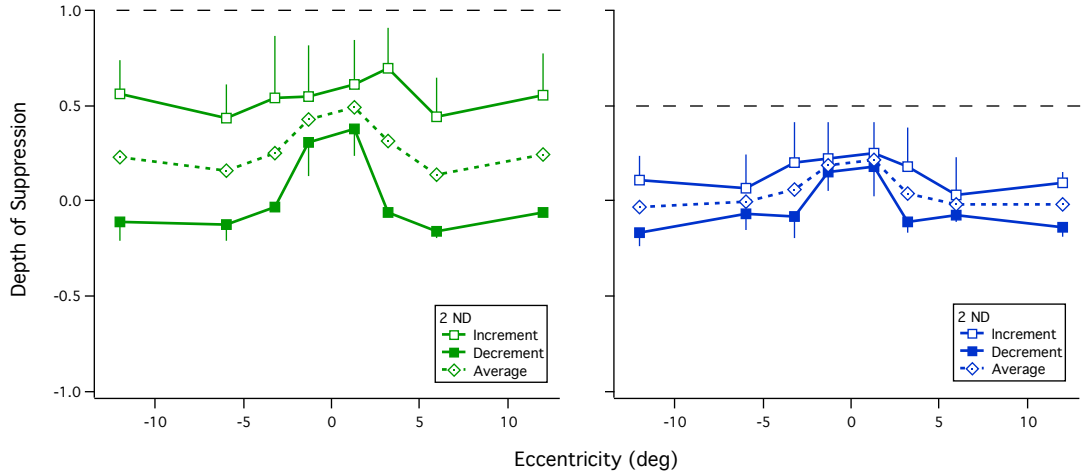

Figure 3.11: Depth of suppression with a 2 ND filter for L (green) and LM (blue) stimuli, for increments (open squares), decrements (filled squares), and the arithmetic mean of increments and decrements (dotted diamonds). Dashed black line shows maximum suppression level. Error bars show +1 standard error for increments and -1 standard error for decrements.

As with the main experiment, no differential CM polarity suppression was found, with similar levels of suppression measured for CM incremental and decremental noise modulations. A comparison of suppression results for the LM and CM stimuli in this control experiment (Figure 3.12) shows that whereas suppression for incremental LM stimuli broadly peaked at the centre, it was only measured centrally for LM decremental stimuli. Suppression of CM increments and decrements is similar at all eccentricities, however central CM suppression was deeper than in the periphery (Figure 3.12 right), and spread over a larger central area (0 to 3.0 deg) than LM decremental central suppression (0 to 1.3 deg), also found in the main experiment. Taking the averages of increment and decrement measurements, suppression is again measured to be deeper for CM versus LM stimuli. These findings are illustrated in Figure 3.12.

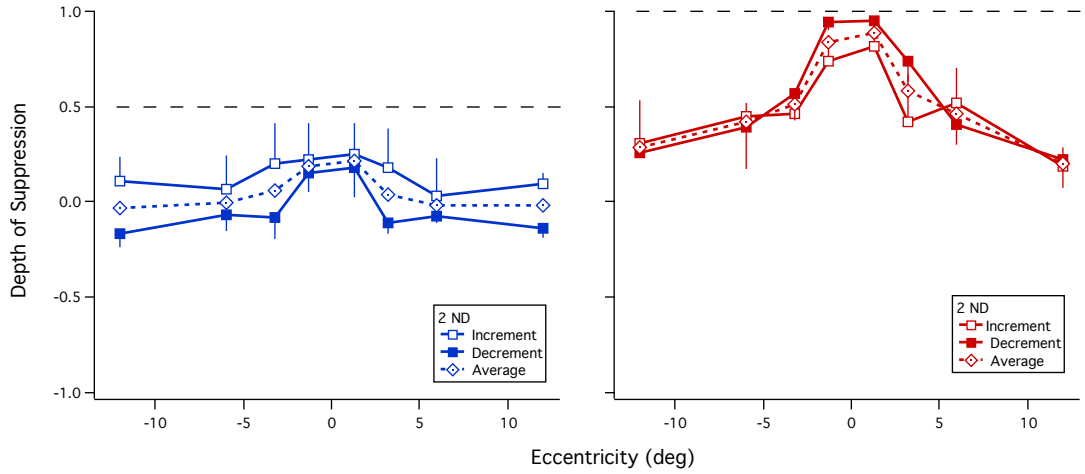

Figure 3.12: Depth of suppression with a 2 ND filter for LM (blue) and CM (red) stimuli. Details are the same as those in Figure 3.11.

3.3.3 The effect of noise on ND filter suppression depth

As indicated above, measured suppression for LM stimuli is less deep overall than for L stimuli, although the effects of eccentricity for these two types of stimuli is similar. Noise was added to luminance stimuli primarily to enable comparison with second-order CM stimuli, which require a noise carrier to modulate. Hence it is important to know what effect noise *per se* has on suppression measurements. It is also important clinically to understand what effect the addition of temporal and spatial noise has on suppression measurement to enable best selection of suppression test to use on compromised normal, or abnormal binocular vision.

The effects of noise on suppression measurement are assessed by comparing suppression measurement outcomes for L versus LM stimuli. This was conducted within the main ANOVA, as there was a significant effect of stimulus type on suppression measurement, and specifically suppression was found to be significantly deeper for L than LM stimuli [$F(1, 3) = 23.11$, $p = 0.017$]. There was also a significant interaction between the inter-ocular luminance difference imposed (depth of ND filter) and stimulus type on measured suppression. This is indicated in Figure 3.13.

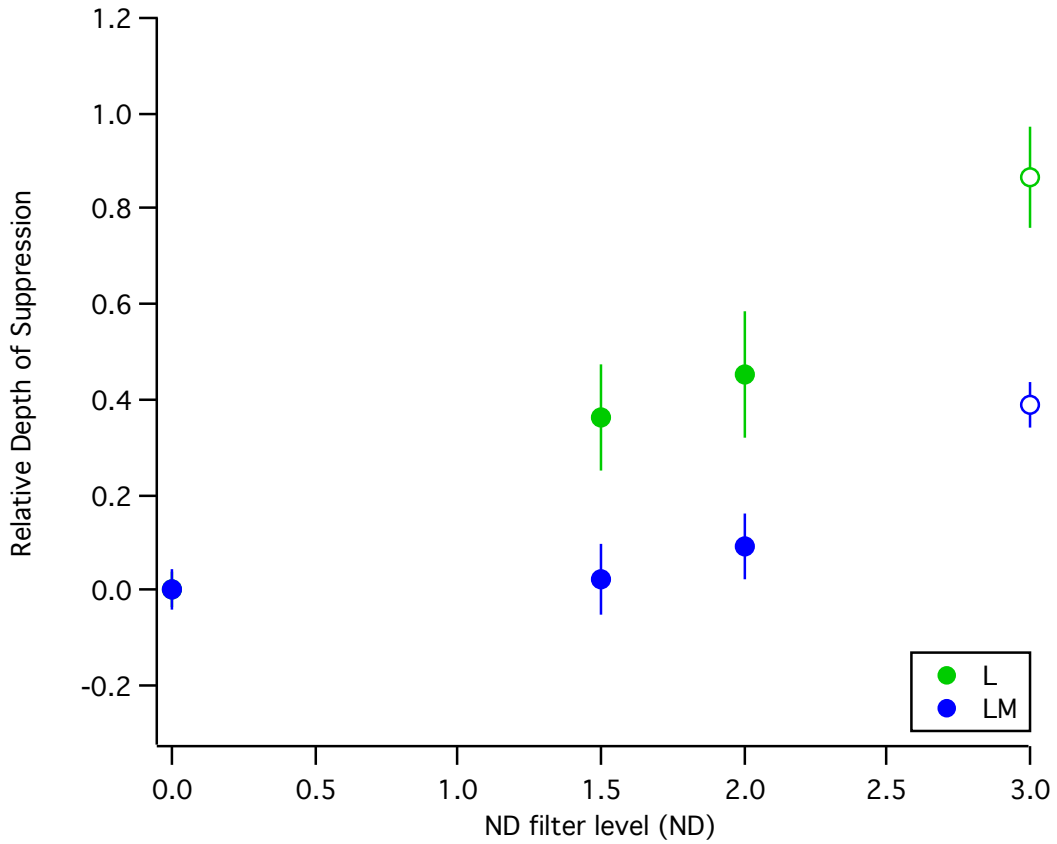

Figure 3.13: Suppression depth average across all sectors for L (green) and LM (blue) stimuli. Data for 3 ND are shown as open circles, but are not included in linear function fits (see text). Error bars show ±1 standard error.

This significant interaction indicates that the effect of ND filter on measured suppression is different when using L versus LM stimuli, i.e. L slope value is greater than LM slope value when linear functions were fit to the data. This means that suppression depth increased at a greater rate per ND unit for L (0.23±0.012) compared with LM (0.04±0.026), for the 0 to 2 ND range. As shown in Figure 3.11, suppression is deeper for L increments than decrements, and also for LM increments than decrements to a lesser degree. Separate slope values for increment and decrement data were always greater for L than LM stimuli. Inter-individual differences can be seen in box and whisker plots in Figure 3.14B.

3.3.4 Suppression of luminance- versus contrast-modulated noise stimuli

Suppression is deeper for CM than LM stimuli at the same ND level at all eccentricities measured (Figure 3.9). There is also a significant interaction between suppression measured for LM versus CM stimuli across ND level, i.e. the slope showing the effect of monocular ND filter on suppression is steeper for CM than LM stimuli (Figure 3.14A).

To estimate the rate of suppression depth increase with increasing inter-ocular luminance difference, suppression was averaged across the visual field for all LM and CM sectors, and plotted against filter strength (Figure 3.14A). Greater CM (0.21±0.06) than LM (0.04±0.03) slope values indicate that suppression increases at a greater rate for CM than LM stimuli with increasing ND strength (for the 0 to 2 ND range).

Figure 3.14 (following pages): A) Suppression depth average across all increment (open symbols) and decrement (closed symbols) sectors for LM (blue) and CM (red) stimuli. Data for 3 ND are shown as crossed squares, but are not included in linear function fits (see text). Error bars show ±1 standard error. B) Box and whisker plots for L (green), LM (blue), and CM (red) stimulus types for each ND level. Box tops and bottoms show 75^{th} and 25^{th} percentiles, respectively, while the centre line shows the median. Whiskers show maximum and minimum extreme values.

A

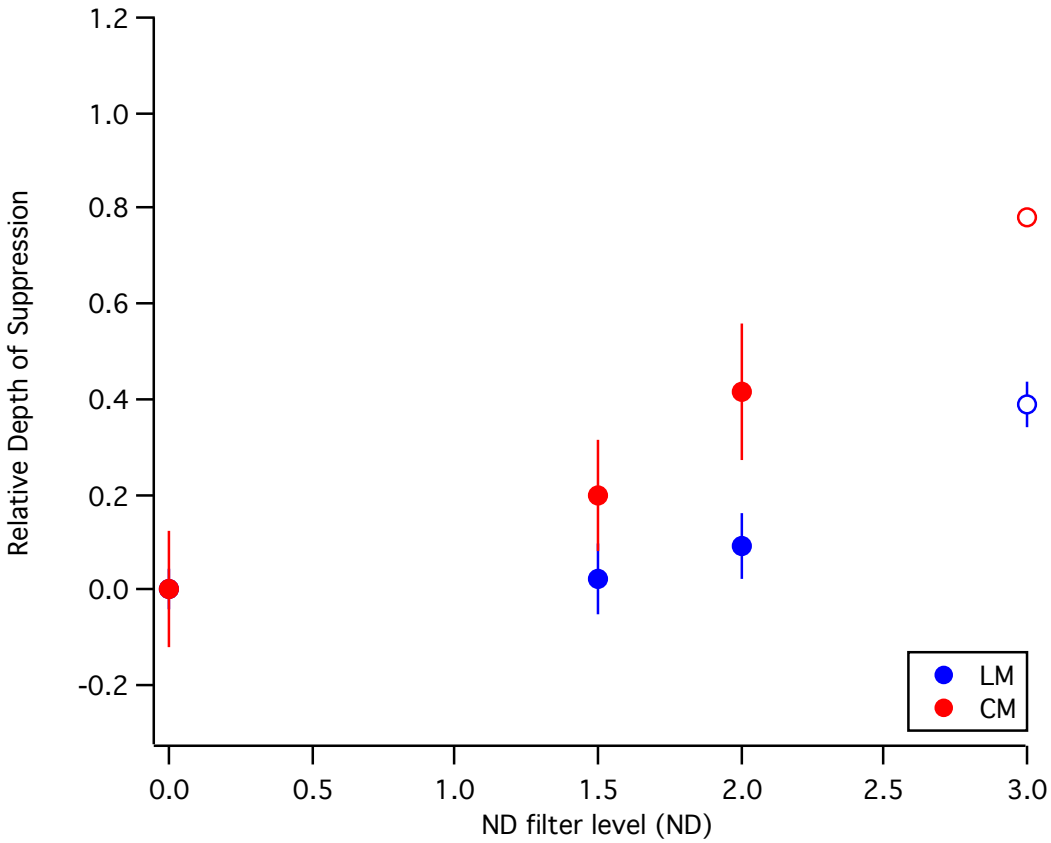
Relative Depth of Suppression
1.2
1.0
0.8
0.6
0.4
0.2
0.0
-0.2
0.0
0.5
1.0
1.5
2.0
2.5
3.0
ND filter level (ND)
LM
CM

B

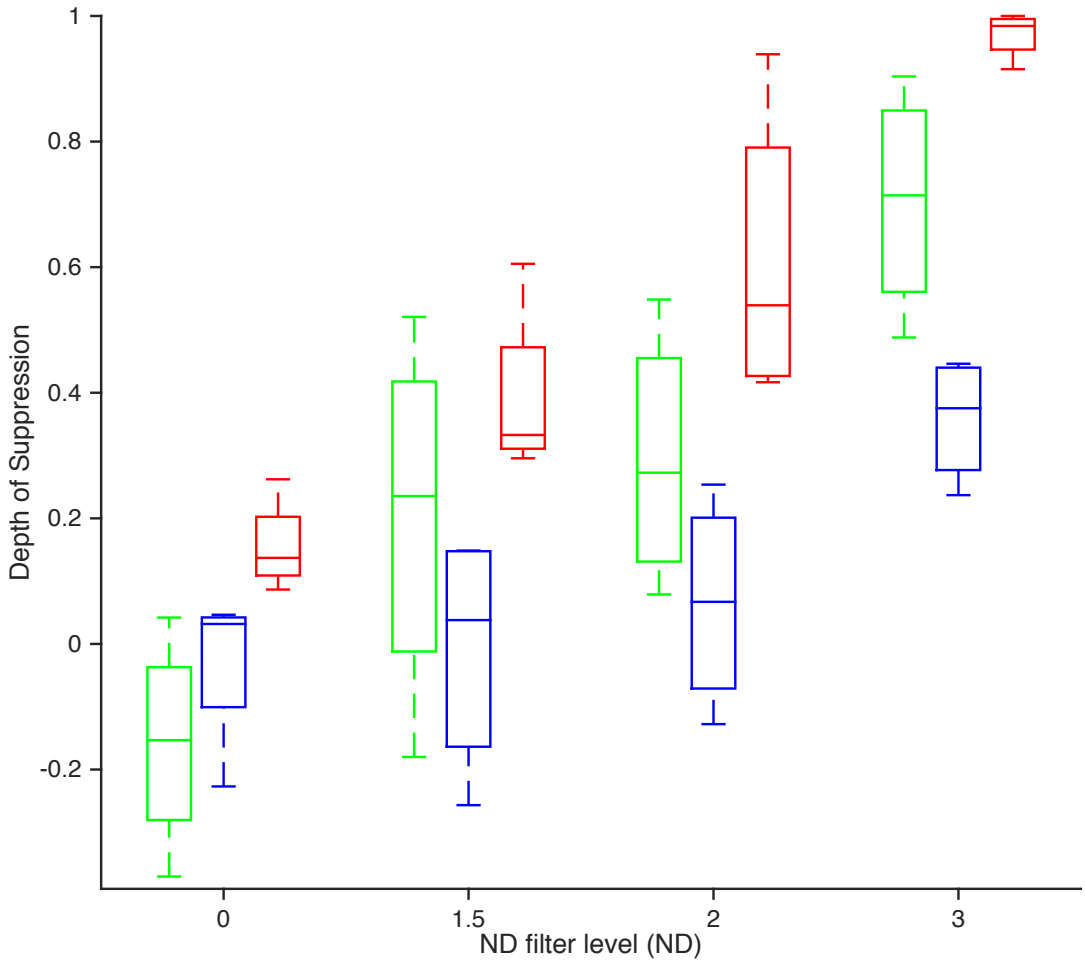
1
0.8
0.6
0.4
0.2
0
-0.2
Depth of Suppression
0
1.5
2
3
ND filter level (ND)

Suppression was deeper for the four central CM eccentricities (0 to 3 deg) when compared with the remaining peripheral sectors [F(1, 3) = 10.71, p = 0.047]. Suppression was deeper for the central two eccentricities (0 to 1.3 deg) compared to all other peripheral sectors for LM stimuli [F(1, 3) = 15.21, p = 0.030] (Figure 3.15). This may have been due to differential polarity suppression only affecting LM stimuli, however, a smaller area of central LM than CM suppression can be seen in Figure 3.12, where the differential polarity effect is controlled. Therefore, suppression is deepest in the central visual field for both LM and CM stimuli, though across a larger extent for CM than LM stimuli. This is illustrated below in Figure 3.15.

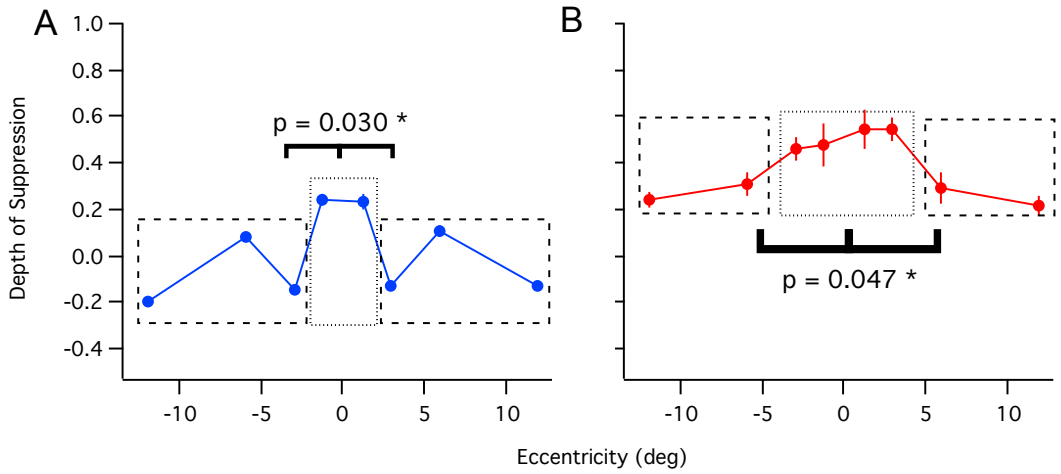

Figure 3.15: Suppression across eccentricity for averaged across all ND levels for LM (blue) and CM (red) stimuli, showing significant differences (with p-values) between central sectors (dotted box) and peripheral sectors (dashed box). Note the greater extent of CM than LM central suppression.

3.3.5 The effect of stimulus polarity and ND filter strength on stimulus visibility

Differences in suppression may be due to different visibilities between stimulus types, and also within stimulus type differential increment and decrement visibility. Therefore, detection thresholds are measured for all stimulus types. An average of four measurements was taken for L, LM, and CM modulation increment and decrement stimuli to estimate thresholds, averaged across participants ASC and SP. A 3-down, 1-up staircase with a 2AFC procedure was

used in which participants monocularly viewed the concentric ring stimuli and in each trial indicated whether a near-detection sector was in one of two positions in the central ring. The sector was either to the right of the vertical midline in the superior half of the ring, or directly opposite in the inferior half of the ring. Sectors were more visible for L than for LM stimuli, but similar for incremental or decremental stimuli (Figure 3.16).

This pattern of stimulus visibility results is very unlike that found for suppression, thus differences in detectability of the targets did not cause the differences in suppression depth measured. Detection thresholds of CM increments and decrements were also similar, with decrement sensitivity slightly worse than increments (Figure 3.16). Furthermore, LM and CM results were similar, suggesting that the deeper CM than LM suppression measured is not due to variability in stimulus detectability.

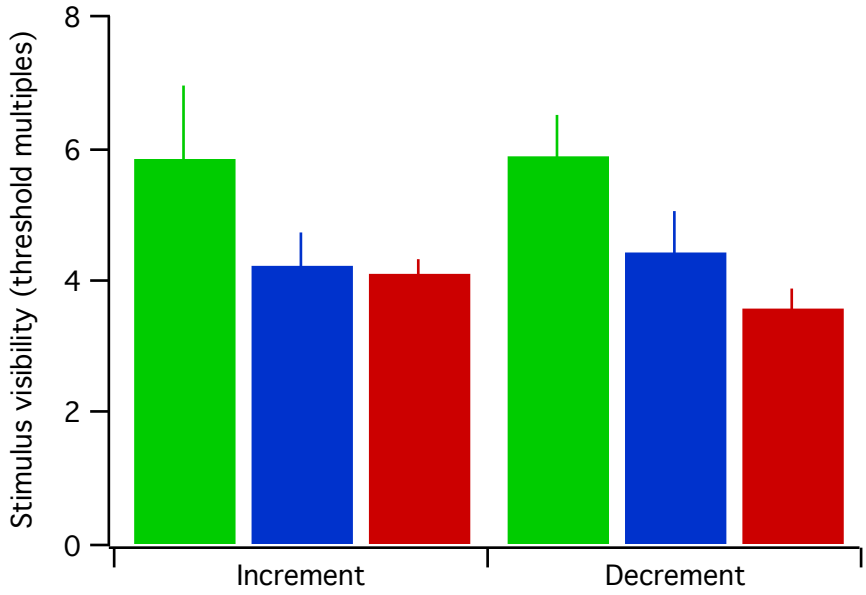

Figure 3.16: Stimulus visibility (i.e. multiples above detection thresholds with 0 ND) for the central sectors that were either modulation (luminance) increments or decrements. L (noiseless) sectors are shown in green, LM sectors are shown in blue, and CM sectors in red. Error bars show standard deviation.

For all stimulus types, detection thresholds were also measured with each ND level, with the same detection threshold method. Only incremental central sectors

were used, and participants ASC and SP took part in this control. Participants were dark adapted to the filter (if worn) as described in the Methods section. The eye without the filter was then occluded for measurements. Results are shown in Figure 3.17 below.

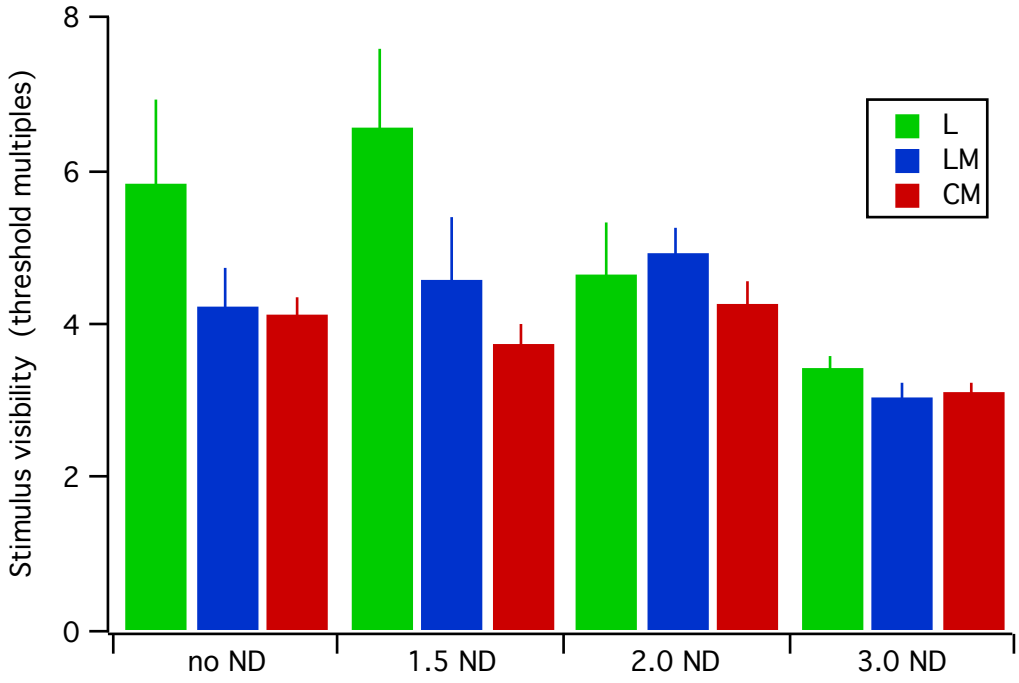

Figure 3.17: Stimulus visibility (multiples of detections thresholds) for central modulation increment sectors of stimuli used in the main experiment for each stimulus type (L – green, LM – blue, CM – red) and each level of ND. Error bars show standard deviation.

Visibility of L stimuli was greater than LM stimuli except for the 2 ND filter condition where thresholds are similar, possibly due to this level of ND removing the effect of dynamic noise on detection. All stimulus types generally show an initial improvement in visibility, until 3 ND where visibility for all stimulus types is reduced to a similar level. This initial improvement has also been noted in a previous study (Snowden, Hess and Waugh, 1995). Changes in stimulus visibility do not vary systematically with suppression measured with different ND filter levels, and therefore depth of suppression is unlikely due to differences in

stimulus visibility caused by adaptation to different ND strengths across stimulus types.

3.3.6 The effect of noise amplitude on suppression depth

Differences in CM and LM suppression depth could be attributable to different noise amplitudes used, 0.50 and 0.25, respectively, which were chosen to increase the measureable modulation range for LM stimuli for measurement of suppression. Therefore, in another control experiment noise amplitude (*n* in Equation 1) was equated for LM and CM stimuli at 0.375. At this noise amplitude for the 0 ND condition, stimuli were equally visible (dotted line – Figure 3.18). LM and CM stimuli were also of similar visibility with noise amplitudes used in the main experiment (LM, *n*=0.25; CM, *n*=0.50). For LM stimuli, increasing noise amplitude (from 0.25 to 0.375) decreased visibility (3.9x±0.2 to 3.2x±0.2) but gave similar suppression depths to the main experiment (of 0.10±0.10 and 0.08±0.02, for 0.25 and 0.375 noise amplitudes, respectively), as measured by the average across all sectors for 0 and 2 ND, and subtracting the difference (blue bars – Figure 3.18). For CM stimuli, visibility was slightly reduced when *reducing* noise amplitude from 0.50 to 0.375 (3.7x±0.5 to 3.4x±0.3). Concurrently, suppression was reduced from 0.42±0.07 to 0.26±0.09 (red bars – Figure 3.18. Thus, despite equating noise amplitude and visibility for both stimulus types, suppression was found to be deeper for CM compared with LM stimuli (0.26±0.09 and 0.08±0.02, respectively). The difference in suppression depth then, between LM and CM stimuli, was not due to stimulus visibility differences.

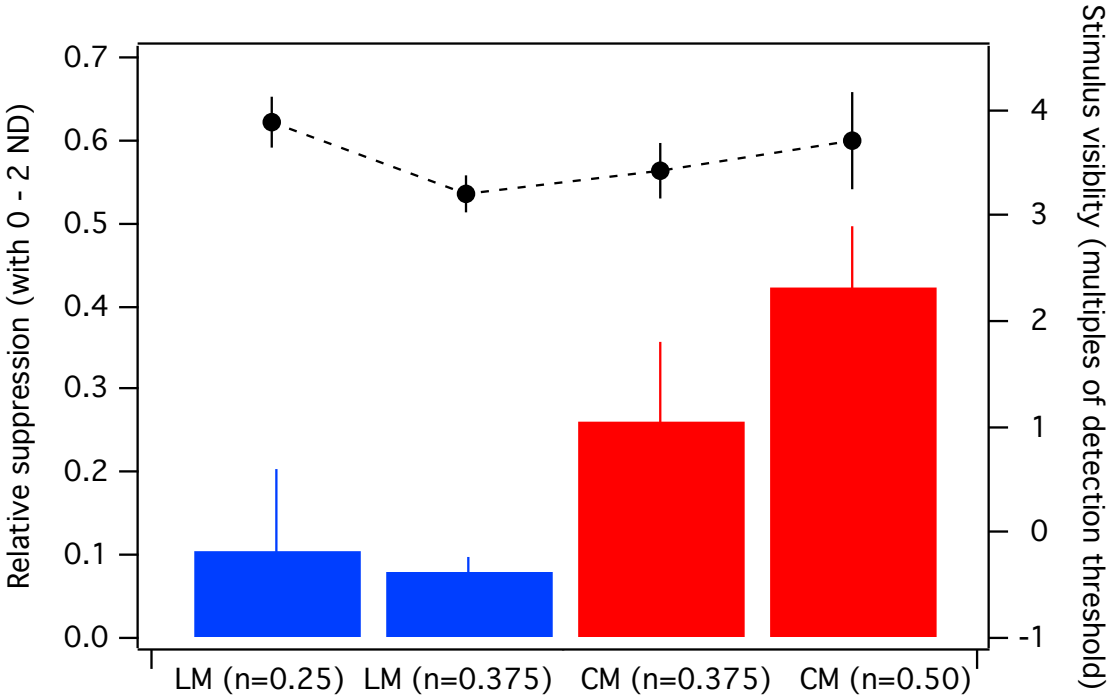

Figure 3.18: Relative suppression (left ordinate axis) calculated as the difference between no filter and 2 ND conditions, when all sectors were averaged. Coloured bars show LM (blue) and CM (red) with different noise amplitudes. The black line shows stimulus visibility defined as multiples of detection threshold (right ordinate axis). Error bars represent standard error.

3.4 Discussion

In this study, suppression deepened when inter-ocular retinal illuminance difference was increased for luminance (L), luminance-modulated noise (LM) and contrast-modulated noise (CM) stimuli. This result suggests that a larger inter-ocular differences in retinal illuminance (with monocular ND filters) creates a greater inter-ocular imbalance in adaptation between the two eyes, and the greater this difference the deeper the measured suppression. Using moving luminance dots to quantify suppression in the central circular 11.1 deg with a dichoptic global motion coherence paradigm, Zhang et al. (2011) also found increased suppression with increasing inter-ocular retinal illuminance differences. The present study differs in that localised suppression was measured in discrete areas within the central circular 24 deg visual field. Results showed deeper central suppression for all L, LM and CM stimulus types, although the depth varied across stimuli, as well as across the visual field.

Adding noise (LM) to luminance-defined (L) stimuli reduced measured suppression, and suppression of contrast-modulated noise (CM) was deeper than for LM stimuli using similar dynamic noise, for the same levels of luminance adaptation. These differences in suppression were not due to stimulus visibility differences, adaptation to attenuated retinal illuminance causing variations in stimulus visibility, or different noise amplitudes. Suppression was deeper centrally for all stimulus types, and was spread over a larger area for CM stimuli. For L and LM stimuli only, suppression was deeper with modulation increments than decrements, although this difference was smaller for LM than L stimuli. Suppression of L and LM increments occurred across the visual field, with marginally deeper central suppression (Figure 3.11). For L and LM decrements, suppression occurred only in the central visual field, and this finding is discussed in the following section.

3.4.1 Differential suppression measures using increment and decrement modulation rings

Differential increment/decrement suppression could have been caused by differences in absolute luminance reduction. The absolute luminance reduction with a 2 ND filter is approximately three times greater with L and LM increments (67.5 to 0.675 cd/m^2, reduction of 66.8 cd/m^2) than decrements (22.5 to 0.225 cd/m^2, reduction of 22.8 cd/m^2). However, difference between increments and decrements are proportionally the same with and without ND filters. As the present study involves making inter-ocular luminance- or contrast-modulation matches, considering absolute luminance values may not explain all of the results. Indeed, it has been shown that the same contrast but different mean luminances (as in the present study) presented to each eye shows similar binocular percepts compared to stimuli with the same contrasts and mean luminances presented to each eye (Teller and Galanter, 1967).

Local adaptation to decrements more than increments, may also contribute to the different increment/decrement suppression measured with L and LM stimuli. Kingdom and Whittle (1996) found that monocular contrast discrimination of gratings improved at higher pedestal contrasts (>50%) of low spatial frequencies (0.125 – 0.5 c/deg). Grating phase was changed such that fixation was centred on either light or dark bars. The main results were replicated with dark bars only, suggesting that these decrements were used in determining contrast discrimination thresholds. Results were explained by local adaptation to the decrement bars of the gratings. Other models of contrast perception also incorporate local light adaptation (Peli, 1990; McIlhagga and Peterson, 2006) which are consistent with single cell responses of monkey and cat V1 neurons (Geisler and Albrecht, 1997). As CM stimuli have no change in mean luminance, local luminance adaptation and therefore differential increment/decrement suppression did not occur.

3.4.2 Depth and extent of suppression

Central suppression was found for all stimulus types in the present study. To

disentangle differential effects of increment and decrement stimuli on suppression mapping, the experiment was repeated and averaged with reversed stimulus polarity. These averaged data showed deeper central circular (1.3 deg radius) suppression for all stimulus type decrement sectors that reduced peripherally (Figure 3.11 and 3.12). For L and LM increments, suppression was approximately equal across the visual field, deepening slightly only in the centre. Suppression occurred across the visual field similarly for CM increments and decrements, and was markedly deeper centrally, spreading over the central 6 deg.

Legge and Kersten (1987) found monocular contrast discrimination to be the same centrally and peripherally, once local contrast sensitivity was accounted for. Local contrast sensitivity *per se* was not accounted for in the present study, though sector area was increased with eccentricity as spatial summation occurs over larger areas in the periphery. Therefore, differences between central and peripheral suppression is unlikely to be caused by difference in discriminability. Indeed, previous psychophysical studies have shown that peripheral performance is similar to foveal performance when size is scaled in the periphery for various visual tasks (e.g. Rovamo, Virsu and Näsänen, 1978; Levi, Klein and Aitsebaomo, 1985; Yap, Levi and Klein, 1987; Levi, Klein and Yap, 1987; Pointer and Hess, 1989).

Suppression was deeper centrally for all stimulus types. Cone density drops off steeply and asymptotes at approximately 1.4 deg eccentricity from the fovea, coinciding with an increase in density of rod cells where peak rod density is at approximately 14 deg eccentricity (e.g. Curcio, Sloan, Kalina and Hendrickson, 1990), outside of the outer ring eccentricity of the present stimuli. Outside of the central cone-dominated area, sensitivity to lower luminance becomes more dependent on rod sensitivity as ND filters reduced luminance to mesopic levels. This suggests that the reason for central 1.3 deg suppression with L and LM stimuli could be due to the reduced sensitivity of cone photoreceptors (within the central 1.4 deg) at the mesopic levels achieved with the ND filters used in the present experiment.

Purpura, Kaplan and Shapley's (1988) data from single cell recording of macaque retinal ganglion cells suggest that the magnocellular pathway conveys information to the cortex via the lateral geniculate nucleus (LGN), in scotopic and mesopic conditions. A greater density of rod (relative to cone) cells in the periphery feed the magnocellular pathway (Lee, Smith, Pokorny and Kremers, 1997), which is more sensitive at lower luminance levels than the predominantly cone-fed parvocellular pathway. A lack of peripheral suppression with L and LM stimuli (Figure 3.11) may therefore be due to the greater sensitivity of rods at mesopic ranges imposed by ND filter introduction. The cone-dominated fovea is relatively less sensitive at these lower luminance levels, therefore introducing a local inter-ocular luminance difference that cannot be fused and is subsequently suppressed.

A cortical origin of inter-ocular suppression in amblyopia has been indicated in a number of electrophysiological, anatomical and imaging studies with monkeys (e.g. Wong, Burkhalter and Tychsen, 2005; Sengpiel, Jirmann, Vorobyov and Eysel, 2006) and humans (e.g. Conner, Odom, Schwartz and Mendola, 2007; Farivar, Thompson, Mansouri and Hess, 2011). Specifically, layer 4 of the primary visual cortex is implied due to this being the first hierarchical stage where monocular information is combined (Hubel and Wiesel, 1977). Sengpiel et al. (2006) suggest that strabismic suppression is deeper centrally due to lack of binocular convergence of small foveal receptive fields, in agreement with Sireteanu and Fronius (1981). Differences in responses from receptive fields in mesopic compared to scotopic illumination (Ransom-Hogg and Spillmann, 1980; Peichl and Wässle, 1983) could be responsible for left and right input disparities resulting in suppression. Peripheral receptive field size is similar between the two eyes as they are mainly rod-mediated. Although luminance in the present study spread across mesopic and photopic ranges (i.e. not scotopic), the binocular convergence of different receptive field sizes may have led to central suppression measured.

Perception during inter-ocular suppression of different mean luminances presented to each eye may also involve inhibitory LGN interactions (Zhang et al.,

2011). Cortico-geniculate connections providing feedback to the LGN may inhibit responses of the suppressed eye. Models of binocular brightness averaging describe weighting coefficients of each eye's inputs, which in turn informs inter-ocular inhibition (i.e. suppression) exerted on one eye to the other (Ding et al., 2013b; Meese et al., 2006). Greater weighting may be given to the magnocellular pathway in the periphery, and conversely to the parvocellular pathway (of which activation is reduced with ND filters) in the central visual field, explaining central suppression that reduces with eccentricity. Correlates of inter-ocular suppression in rivalry have been found in human LGN (Wunderlich, Schneider, and Kastner, 2005), presumably through feedback from visual cortex, as there are no single LGN cells activated by both eyes.

3.4.3 Modelling amblyopia with ND filters

Previous workers have shown that monocular ND filters during foveal binocular viewing simulate some aspects of strabismic amblyopic vision well. Maehara et al. (2011) measured inter-ocular suppression in 10 mild amblyopes of which six were purely strabismic. Two reference squares (3.5 deg side length) of fixed luminance were presented diagonally adjacent to one another to one eye whilst to the other eye two more diagonally adjacent squares. The dichoptic percept was of four squares, two above and two below. One eye's two squares were adjusted in luminance to match the fixed squares in either the amblyopic or non-amblyopic eye. Five of six strabismic amblyopes increased stimulus luminance of amblyopic eyes to match the non-amblyopic eye reference squares. Although only carried out in the central visual field, this is similar to the inter-ocular L stimuli modulation matching task of the present study, and indeed the normal participants with ND filters in front of one eye showed similar results in the central visual field.

Other studies with strabismic amblyopes have shown central suppression areas (Harms, 1937; Campos, 1982; Hallden, 1982; Gottlob, Charlier and Reinecke, 1992) without squint angle correction, and both central suppression and in the area corresponding to the non-amblyopic eye fovea when squint angle was

corrected (Travers, 1938; Irvine, 1948; Jampolsky, 1955; Herzau, 1980; Pratt-Johnson and Tillson, 1983). Central suppression of the filter eye was found in the present study, which increased in depth with increasing ND filter for all stimulus types (Figures 3.7B). Suppression corresponding to the non-amblyopic eye fovea could not be investigated in this study due to lack of participant ocular misalignment (but this is addressed in Chapter 4, Experiment 3).

Suppression of the area corresponding to the non-amblyopic eye fovea of strabismics may occur as a result of long-term suppression (Sireteanu and Fronius, 1981). Babu et al. (2013) recently showed only deeper centrally localised suppression in both anisometropic and strabismic amblyopes, like the results found in the current study using ND filters on binocularly normal participants. Noiseless luminance stimuli similar to the present study were used, but with a central black fixation dot, to measure suppression across the central circular 20 deg, using a method of adjustment, perhaps causing differences with previous reports of suppression asymmetry in strabismic amblyopes.

Ding and Levi (2014) found that under certain conditions, i.e. with stimuli of a certain spatial frequency and contrast, vision between two eyes of amblyopes can be equalised with ND filters (i.e. by reducing luminance) in front of the non-amblyopic eye. Although only two amblyopes were used, and only one of those was purely strabismic (the other aniso-strabismic), balancing vision in amblyopia was achieved by reducing luminance to the non-amblyopic eye. This finding agrees with other studies using ND filters to simulate strabismic amblyopia (Baker et al., 2008; Baker et al., 2007; Barbeito et al., 1987; de Belsunce and Sireteanu, 1991; Kilwinger et al., 2002; Leonards and Sireteanu, 1993; Li et al., 2013; Zhang et al., 2011; Zhou et al., 2013), suggesting that monocular ND filters during binocular viewing in normal observers are a good model for the habitual binocular viewing of a strabismic amblyope.

3.4.4 Addition of noise to first-order stimuli

Suppression is shallower for first-order (luminance-defined) stimuli with noise

(LM) compared to those without noise (L), as can be seen in Figure 3.9. Minimal suppression of L and LM stimuli was measured in the periphery with 2 ND filter strength. Visibility was reduced with the addition of noise: L stimuli 5.8x above detection threshold, LM with 0.25 noise amplitude 3.9x and 0.375 noise amplitude 3.2x. A less visible stimulus, i.e. noisy (LM), may be expected to show deeper suppression than noiseless (L) stimuli. This was not the case, so the addition of dynamic noise reduced suppression, perhaps in a similar way to continuous flash suppression (Wolfe, 1986; Tsuchiya and Koch, 2005; Yang and Blake, 2012). Suppression deepened marginally when increasing ND strength from 0-2 ND for LM stimuli. However, Figure 3.8 shows that with 3 ND, LM suppression would be markedly deeper than with lower ND strengths. Thus a greater inter-ocular retinal illuminance difference was required before LM suppression was measured, compared with L stimuli, also suggesting that dynamic noise breaks down suppression.

3.4.5 LM versus CM suppression

The present study is the first to measure suppression for both luminance- (LM) and contrast-modulated (CM) noise stimuli in normal participants with inter-ocular luminance difference across the visual field. Suppression was deeper for CM than LM stimuli. No differences in suppression were observed between CM decremental and incremental stimuli. A similar pattern of suppression is found with LM decremental and CM incremental and decremental stimuli, specifically deeper central than peripheral suppression, though spread over a greater area for CM stimuli.

The filtered eye adapts to lower luminances induced by the ND filter (MacMillan, Gray and Heron, 2007). There is no change in mean luminance across CM stimuli and ND filters retain stimulus contrast, and thus local retinal adaptation to an ND filter is unlikely to account for deeper suppression measured with these stimuli (providing CM increments and decrements adapt similarly).

Deeper CM than LM suppression may therefore have been caused by

differences in cortical processing mechanisms for the two stimulus types. Specifically, that disrupted binocularity interferes with processing of CM stimuli thought to be served by predominantly binocular mechanisms. Zhou, Liu, Zhou and Hess (2014) investigated suprathreshold binocular combination of CM compared with LM sinusoids. The perceived phase of dichoptically combined vertically offset horizontal gratings was measured at different inter-ocular grating contrast ratios of normal participants. Equalising inter-ocular modulation between the eyes results in perceived phase shifting towards zero, indicating balanced binocular combination. Performance with CM stimuli was similar irrespective of noise carriers being binocularly correlated, un-correlated or anti-correlated, a finding replicated by Zhou, Georgeson and Hess (2014). This lack of requirement for carrier correlation suggests that CM envelope extraction occurs after binocular combination. Previous work at detection threshold showed similar results (Georgeson and Schofield, 2011; Schofield and Georgeson, 2011). In Zhou et al.'s (2014) study, combined LM phase varied non-linearly with inter-ocular modulation difference, though for CM stimuli, performance was linear, further suggesting different mechanisms for processing of each stimulus type.

The above studies contribute to the idea that CM stimulus extraction is served by mechanisms receiving binocular input differently from LM stimuli (Mareschal and Baker, 1998; Schofield and Georgeson, 1999, 2003; Baker and Mareschal, 2001; Wong, Levi and McGraw, 2001; Allard and Faubert, 2007; Hairol and Waugh, 2010), and that this is disrupted when each eye is adapted to different luminances, to a greater degree for CM stimuli with increasing luminance difference in the present study. Stimulus visibility was similar for LM and CM stimuli; therefore deeper CM suppression was not due to reduced detectability. Noise amplitude was greater for CM stimuli in the main experiment, however even when it was equated to LM stimuli, suppression was still deeper for CM compared with LM. Differences in suppression depth could also not be accounted for by difference in stimulus strengths or visibility, which was similar in the main experiment and when noise amplitudes were equated.

Evidence for additional extrastriate processing for CM compared with LM stimuli has been found using fMRI (Larsson et al., 2006). Furthermore, Mareschal and

Baker (1998) provide neurophysiological evidence in cats that suggests V2 as a locus for the extra processing required for CM stimuli, which has recently been confirmed in monkeys (Li et al., 2014). Monkey V2 cells also respond to second-order contours not defined by changes in luminance (Leventhal et al., 1998; Peterhans and Von der Heydt, 1989; Von der Heydt et al., 1984). If part of contrast-modulated stimulus processing occurs in the extrastriate cortex, with its preponderance for binocular input, deeper CM stimulus suppression may reflect more binocular processing and a larger response (i.e. inter-ocular suppression) to image dissimilarity, such as is created in the present study with adaptation to ND filters. A larger area of central CM than LM suppression found in the present study lends further support to the idea that CM envelope extraction involves cortical areas with larger receptive fields (e.g. V2) than earlier striate areas, found in previous physiological studies (Gattass, Gross and Sandell, 1981; Foster, Gaska, Nagler and Pollen, 1985; Kennedy, Martin, Orban and Whitteridge, 1985; Gattass, Sousa and Gross, 1988). Cortical representation of the fovea is also larger in V2 than V1 (Schira, Tyler, Breakspear and Spehar, 2009), suggesting that deeper suppression is required to remove this larger area from perception, i.e. to prevent diplopia.

3.5 Conclusion

Suppression in response to inter-ocular luminance adaptation differences is deepest centrally, and deeper for CM stimuli than LM stimuli. This may be due to the processing by mechanisms receiving binocular input of CM compared with LM stimuli, and that binocularity is disrupted with inter-ocular adaptation differences (caused by monocular ND filters). As strabismic amblyopic suppression may be similar to disrupted binocularity (using monocular ND filters) in normal vision, CM stimuli may be more sensitive at detecting mild suppression during clinical measurement of amblyopic suppression. Suppression of CM stimuli is also more robust to local retinal luminance adaptation. Suppression measures using luminance-based images are dependent on local retinal adaptation and clinicians should be wary of determining geographical measures that might be dependent on the luminance differences, rather than suppression differences.

3.6 Appendix

3.6.1 Clinical measurements of participants

Table 3.4: Clinical measurements of participants used in the present study. OMB – ocular-motor balance, W4d – Worth 4-dot suppression test, NMD – no movement detected on cover/uncover or alternating cover test. Monocular fixation was measures with visuoscopy (reticule filter of a direct ophthalmoscope).

Participant	Age/Sex	Refraction	Visual Acuity	OMB	Monocular Fixation	Stereoacuity	W4d	Sbisa
ASC	27 M	-0.50/-0.50x60	6/3.8	NMD	central, steady	15"	no supp	no supp
		-0.75/-0.50x130	6/3.8		central, steady			
CP	22 F	∞/-0.50x110	6/4.8	NMD	central, steady	30"	no supp	no supp
		∞	6/4.8		central, steady			
SM	19 M	∞	6/4.8	NMD	central, steady	30"	no supp	no supp
		∞	6/4.8		central, steady			
SP	31 M	-0.75/-0.75x152	6/4.8	NMD	central, steady	30"	no supp	no supp
		-0.25/-0.75x29	6/4.8		central, steady			

3.6.2 Selection of ND levels

As CM stimuli may be most affected by inter-ocular luminance adaptation imbalance, the minimum strength of ND filter to cause suppression with these CM stimuli was investigated. Pilot experiments with one participant (ASC) with different ND levels showed similar suppression depths between 0, 0.5, and 1 ND (Figure 3.19). Data are averaged across all sectors for each ND level (two runs for each level). Therefore, 1.5 ND was selected as the lowest level to be used in this experiment, as this showed some measurable suppression compared to with no filter.

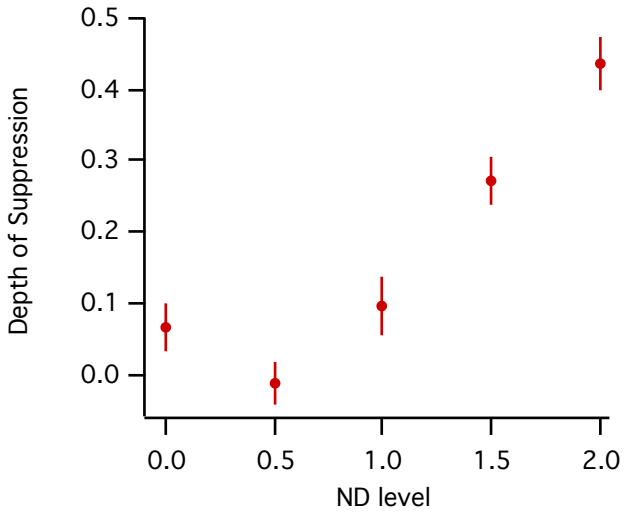

Figure 3.19: Depth of CM stimulus suppression with varying ND levels. Data are averaged across all sectors for each ND level.

CHAPTER 4

EXPERIMENT 3 – INTER-OCULAR SUPPRESSION OF LUMINANCE- AND CONTRAST-MODULATED NOISE STIMULI IN BINOCULARLY ABNORMAL PARTICIPANTS

4.1 Introduction

Inter-ocular suppression is a binocular condition occurring when binocularity is disrupted, e.g. strabismus, anisometropia, or pathologies affecting one eye's input more than the other (von Noorden, 1985). If images are sufficiently different and cannot be fused into a single percept, one image is cortically suppressed (Sengpiel, Blakemore, Kind and Harrad, 1994; Harrad, Sengpiel and Blakemore, 1996; Sengpiel and Blakemore, 1996; Sengpiel, Jirmann, Vorobyov and Eysel, 2006; Farivar, Thompson, Mansouri and Hess, 2011). Inter-ocular suppression is also associated with amblyopia, and indeed long-term suppression has been suggested as a factor in amblyopia development (Sireteanu and Fronius, 1981). The present study employs a new method with novel stimuli to measure suppression across the visual field of those with abnormal binocular vision.

Early and recent attempts at treating amblyopia have aimed to break down suppression in children and adults, and a concurrent reduction in inter-ocular acuity difference was seen with suppression reduction (Cohen, 1981; Wick, Wingard, Cotter and Scheiman, 1992; Hess, Mansouri and Thompson, 2010b; a; Black, Thompson, Maehara and Hess, 2011; To et al., 2011; Black et al., 2012; Knox, Simmers, Gray and Cleary, 2012; Mansouri, Singh, Globa and Pearson, 2014). A positive correlation between suppression depth and magnitude of inter-ocular acuity difference has also been found in other studies in both adults and children (Sireteanu and Fronius, 1981; Agrawal et al., 2006; Li et al., 2011; 2013; Narasimhan, Harrison and Giaschi, 2012). One previous study found a negative correlation between depth of suppression and amblyopia. This study used a contrast increment task to assess suppression depth (Holopigian, Blake and Greenwald, 1988), although the majority of their

participants were alternating strabismics with little or no inter-ocular acuity difference. Strong suppression in non-amblyopic (Goodman et al., 2011) compared with amblyopic strabismics has been found more recently, perhaps suggesting different mechanisms of strabismic suppression with and without amblyopia. Bi et al. (2011) also found a positive correlation between amblyopia and suppression in monkeys with induced squint. Suppression was quantified as the ratio of peak amplitude response to binocular over monocular stimuli of single cells in the cortex of the monkeys. Therefore, depth of suppression is positively correlated with higher degrees of amblyopia.

Greater degrees of amblyopia, and therefore suppression, suggest a larger disruption to binocularity. The present study is concerned with measuring suppression in participants with binocular disruption, namely strabismus and microstrabismus. Strabismics experience constant inter-ocular suppression during normal binocular viewing, where visual sensitivity of the suppressed eye is reduced compared to when it is monocularly viewing (Mehdorn, 1989; see Chapter 1, Section 1.1). Measured suppression in strabismic amblyopia is deepest when similar stimuli are presented to each eye (Schor, 1977; Kilwinger, Spekreijse and Simonsz, 2002).

Baker et al. (2007) dichoptically presented similar gratings to corresponding retinal points in strabismics in order to measure binocular summation, the binocular over monocular advantage greater than that predicted by increased probability of having two eyes rather than one. They showed that binocular combination of amblyopic and non-amblyopic input could lead to binocular summation in strabismic amblyopes, if amblyopic and non-amblyopic eye stimulus visibility was equated, differing from previously held views that the architecture for binocular vision is lost in amblyopes (Hubel and Wiesel, 1965). Recent models of normal binocular combination, therefore, include suppressive and excitatory mechanisms (Meese et al., 2006; Ding et al., 2013b). Ding et al. (2013a) measured the perceived phase of dichoptically combined horizontal sinusoidal gratings with equal but opposite phases (± 45 deg) presented to each eye. Amblyopic participants perceived the phase of the combined grating as balanced toward the grating phase seen by the non-amblyopic eye. Inter-ocular

suppression was quantified as the non-amblyopic to amblyopic eye inter-ocular contrast ratio that elicited a perceived phase of zero. When amblyopic eye contrast was adjusted, suppression was being measured, and when the non-amblyopic eye was adjusted, inter-ocular enhancement was being measured. Other studies also found similar interocular asymmetries in amblyopes with similar inter-ocular phase discrimination paradigms (Huang et al., 2009; Zhou, Jia, Huang and Hess, 2013).

Previous studies have compared various techniques of suppression measurement across the visual field (Herzau, 1980; Campos, 1982; Mehdorn, 1989) that varied in terms of dissociation between the eyes, i.e. how much the stimuli to each eye varied. All studies found that the more dissociating the method, e.g. von Graefe's Red Lens Test (see Chapter 1, Section 1.4.2.1 for review), the smaller the measured suppression scotoma, compared to tests that involve a higher degree of association between the eyes, e.g. Bagolini Striated Lens Test (see Chapter 1, Section 1.4.2.1). Similarly, Jampolsky (1955) found suppression in strabismic amblyopes when the same images were presented dichoptically, to corresponding retinal points. However, replacing the amblyopic eye stimulus with one of similar size but a different shape enabled simultaneous perception of the two images. Deepest suppression therefore occurs when the same stimuli are presented to each eye (Kilwinger et al., 2002). As one eye's stimulus needs to be adjusted in some way to provide a measure of suppression, every effort to provide as similar stimuli to each eye as possible must be taken, with only the area being measured presented dichoptically.

In the strabismic amblyopic eye during binocular viewing, a central as well as a fixation point scotoma (corresponding to the non-amblyopic eye fovea) has previously been revealed (Travers, 1938; Irvine, 1948; Jampolsky, 1955; Sireteanu, Fronius and Singer, 1981; see Chapter 1, Section 1.4.4.2 for discussion). Pratt-Johnson and Tillson (1983) found complete suppression of the amblyopic eye in the binocular visual field. Previous studies have demonstrated only a central suppression point in microstrabismics (Sireteanu, Fronius and Singer, 1981; Campos, 1982; Mehdorn, 1989; Babu et al., 2013).

Current opinions are divided on how amblyopia, anisometropia, and strabismus interact with suppression, showing further need for an accurate method of measuring suppression, specifically over the binocular visual field. Accurately mapping suppression across the visual field allows specific localised areas of suppression to be targeted to provide a more effective treatment, and efficacy of current amblyopia treatments aimed at localised suppression could then be assessed. Some amblyopes regress after monocular therapy initiated during childhood (Bhola et al., 2006). Promoting and maintaining binocular single vision by breaking down suppression may stop this regression, as both eyes will continue to be stimulated. With the method of suppression mapping developed in this experiment, the state of suppression in these cases can be revealed.

Recently, Babu et al. (2013) used a method of mapping suppression across the visual field that presents as similar images as possible to each eye. Stimuli were large (20 deg central circular visual field) binocular rings with a dichoptic element in one part of the visual field. Contrast of an adjustable sector was reduced in the non-amblyopic eye to match a surrounding ring seen by the amblyopic eye. Although amblyopic eye to non-amblyopic eye enhancement may have been measured (rather than suppression *per se*), the inter-ocular matching task provided suprathreshold stimuli more similar to real world viewing. Deeper central than peripheral suppression was found for both strabismic and anisometropic amblyopes.

In the present study, the addition of dynamic noise to luminance-defined (L) stimuli will lead to the creation of luminance-modulated noise (LM) stimuli. Dynamic noise is known to reduce detectability (Nordmann, Freeman and Casanova, 1992; Rovamo and Kukkonen, 1996; Schofield and Georgeson, 1999, 2003) and discriminability (Legge, Kersten and Burgess, 1987), and therefore suppression of LM may be deeper than L stimuli. However, the clinical belief is that temporal transients (caused by dynamic noise) will “break” suppression (e.g. Scheiman and Wick, 2008). The effect of noise on suppression in both normal and abnormal binocular visual systems is therefore worthy of investigation.

All previous studies of suppression in amblyopia have used stimuli defined by changes in luminance to measure suppression. Contrast-modulated noise (CM) stimuli have no systematic changes in luminance, and therefore cannot be detected by the simple V1 linear receptive fields (Chubb and Sperling, 1988). These stimuli are constructed by multiplying (instead of adding) a binary dynamic noise carrier to a square-wave stimulus. Both the noise and the square-wave envelope are detected by early simple linear V1 filters. The CM envelope is extracted by a lower spatial frequency linear filter, after an interim non-linear rectification stage (for reviews see Zhou and Baker, 1993; Mareschal and Baker, 1998). The cortical location of the non-linear rectification stage is currently unclear, in addition to whether or not these mechanisms receive more binocular input than the simple linear mechanisms serving luminance-modulated stimuli (Allard and Faubert, 2006, 2007).

In addition to the effect of noise on suppression of luminance-defined (LM versus L) stimuli, suppression of both LM and CM stimuli is compared in the present study across the central circular 24 deg visual field of participants with abnormal binocular vision. Contrast-modulated noise (CM) stimuli may be subject to different stages of processing by mechanisms receiving binocular input compared to those processing LM stimuli (Wong et al., 2001, 2005; Hairol and Waugh, 2010). The disruption to binocularity present in amblyopes (e.g. McKee et al., 2003) may consequently cause reduced sensitivity to CM stimuli. This view gains further support from the reduction in both non-amblyopic and amblyopic eye sensitivity for CM compared with LM stimuli (Wong, Levi and McGraw, 2001, 2005; Simmers, Ledgeway, Hess and McGraw, 2003; Mansouri, Allen and Hess, 2005). Therefore, using CM stimuli may provide a more sensitive method of measuring amblyopic suppression than LM stimuli. This has implications for the earlier detection of suppression, as well as the initiation of and effectiveness of treatment. In addition, the amblyopia deficit can be assessed with CM stimuli thought to be subject to more complex processing, giving an idea of the deficit at different stages of visual processing.

4.2 Methods

4.2.1 Participants

Sight tests were performed on each of nine female participants prior to suppression mapping. This involved recording available relevant history, subjective refraction, best corrected visual acuity, strabismus (as detected with cover/uncover test, quantified with an alternating cover test, and neutralised with prisms), monocular fixation with Haidinger Brush (Macular Integrity Tester; Bernell, Mishawaka, IN) and visuoscopy (Professional Direct Ophthalmoscope reticule filter, Keeler, Windsor, UK) and stereoacuity with the Dutch Organization for Applied Scientific Research (TNO) stereo test (Lameris Ootech, Ede, The Netherlands). The Worth 4-Dot test (Lunea Ophthalmologie, Prunay Le Gillon, France) detected the presence or absence of suppression in the central visual field. It was performed at 3m, where the four dots subtended approximately 0.76 deg visual angle, similar to the 0.75 deg central sector radius for L and LM stimuli (used in the current experiments and described below). A red filter (Sbisa or Bagolini) bar (Richmond Products, Albuquerque, NM) was used to measure suppression depth (e.g. Henson and Williams, 1980; Mallett, 1988; Knowles and Griffiths, 2003; Godts, Trau and Tassignon, 2006). This involved binocular viewing (with appropriate prism correction) of a white fixation light. Red filters were increased in density in front of the non-suppressing eye so that the fixation light appeared red, and the patient reported when the light changed back to white. The level of filter when this occurred was recorded as the depth of suppression.

Microstrabismus is described as a condition with unequal inter-ocular visual acuities, suppression scotoma, harmonious abnormal retinal correspondence (hARC), and non-foveal (eccentric) monocular fixation (Helveston and von Noorden, 1967). Here one eye's fovea is associated with an extra-foveal retinal point in the other eye to give single clear vision in spite of ocular deviation (Bagolini, 1967). Eccentric monocular fixation was detected with visuoscopy and with Haidinger's brush, and comparable results were found.

There were nine participants, clinical details of whom are presented in Table 4.1. Four participants are classified as strabismic with deviations above 6 prism dioptres, and five participants are microstrabismics with deviations of 6 prism dioptres and below (e.g. Mehdorn, 1989; Kilwinger, Spekreijse and Simonsz, 2002; Millodot, 2014), and the aforementioned characteristics. Participants were recruited through advertising at Anglia Ruskin University, and consist of staff and students of the university. Informed consent was obtained from all participants and the Anglia Ruskin University Research Ethics Committee approved the conduct of the research project thus ensuring that the research complied with the tenets of the Declaration of Helsinki. No participants were purely anisometropic as eccentric fixation was found in all.

4.2.2 Equipment

Equipment was the same as that described in Experiment 1 and 2 (see Chapter 1 and 2, Sections 2.2.2 and 3.2.2, respectively). An Apple MacBook Pro (MacBook Pro; Apple Computer, Cupertino, CA) running Matlab (The MathWorks, Natick, MA) with Psychophysics Toolbox (Brainard, 1997; Pelli, 1997) was used to generate stimuli, which were then presented on eMagin DualPro head-mounted OLED displays (Dual Pro Z800; eMagin Corp., Hopewell Junction, NY) via Matrox DualHead2Go adapter (Matrox Graphics Inc., Quebec, Canada). One screen for each eye allowed for dichoptic presentation of stimuli. Each screen had a resolution of 800x600 pixels, refresh rate of 60 Hz, and mean luminance 45 cd/m^2.

Table 4.1: Clinical attributes of participants. F – female, M – male, fully accom. – fully accommodative strabismus, DS – sphere dioptres, NMD – no movement detected, L – left eye, R – right eye, XOT – exotropia, HYP – hypertropia, SOT – esotropia, int. alt. – intermittent alternating, strab. – strabismus, micro. – microstrabismus, aniso. – anisometropia, sup. – superior, inf. – inferior, temp. – temporal, nas. – nasal . All deviations are reported in prism dioptres. Monocular fixation was measured with the Haidinger Brush where magnitude of deviation is given. Measurements with location only were performed with visuoscopy. All acuities were measured with a logMAR chart (5 letters per line). Stereoacuity was measured with the TNO Stereotest. Suppression was detected with the Worth 4-Dot test (W4d), and quantified with a Sbisa red filter bar.

Participant	Age/ Sex	Type	Refraction	Acuity	Cover test (prism dioptres)	Monocular Fixation	Stereo-acuity	Suppression	History
AH	18/F	Strab. (Int. alt.), aniso.	R -3.25 DS L -1.50 DS	6/9.5+2 6/6+2	20 int. RXOT, 2 RHYP	R 1.83 deg sup L 1.00 deg sup. temp.	>480"	Sbisa: changed dominance with filter eye W4d: int. R sup., int. fusion	Surgery at 7 years Patching from 5 years
CMa	32/F	Strab.	R +3.00/-2.25x11 L +2.25/-2.00x65	6/4.8-1 6/15	26 LSOT	R steady central L 0.52 deg nasal	>480"	Sbisa: 11 (R) W4d: L sup.	Patching from 3 years
CMc	30/F	Strab.	R +5.50/-1.00x102 L +6.00/-1.00x100	6/6+3 6/19+2	7 LXOT	R steady central L unsteady variable	480"	Sbisa: 15 (R) W4d: L sup.	Surgery at 4 years, patching from 4 years
JB	59/F	(Surgery corrected) Strab., Aniso.	R +4.25/-0.50x80 L +1.00/-1.00x100	6/15 6/6+2	NMD	R sup. nas. 0.86 deg L central steady	>480"	Sbisa: 12 (L) W4d: R sup.	Patching at 5 years Surgery at 5 years
AW	20/F	Microstrab.	R +6.50/-2.75x164 L +6.25/-3.25x3	6/4-2 6/5-1	6 LSOT	R central steady L 0.30 deg nasal	>480"	Sbisa: normal W4d: normal	Patching when child (patient unsure when)
AR	20/F	Microstrab., aniso.	R +2.25/-0.50x5 L +5.00/-0.75x22	6/4.8-1 6/6-1	NMD	R central, steady L temp., steady	120"	Sbisa: 13 (R) W4d: normal	None
DM	19/F	Microstrab.	R +2.25/-1.75x162 L +3.00/-2.25x7	6/4.8+3 6/6-1	NMD	R central, steady L inf. temp. 0.58 deg	120"	Sbisa: normal W4d: normal	Patching at 4 years
IR	20/F	Microstrab., aniso.	R -3.25/-2.00x35 L -0.75/-0.50x175	6/7.5 6/6	NMD	R 0.58 deg sup. temp. L central steady	120"	Sbisa: 2 (L) W4d: normal	Refractive correction since childhood
NS	19/F	Microstrab. (with refractive correction)	R +8.50/-2.25x5 L +8.25/-2.50x3	6/7.5-1 6/3.8	NMD (20 RSOT s. Rx)	R inf. nasal L central steady	240"	Sbisa: 6 (L) W4d: normal	Refractive correction since 4 years

4.2.3 Stimuli

Stimuli employed in the current experiment were similar to those used in Experiment 1. Refer to this Experiment for a detailed description of the stimuli (Chapter 2, Section 2.2.3). For noisy (LM and CM) stimuli, the noise check size was 4x4 pixels with an angular subtense of 10 arcmin at 80 cm (equivalent viewing distance), resolvable for all of our participants at all eccentricities tested. Sireteanu and Fronius (1981) measured grating acuity across the visual field of a range of amblyopes. On average, at 10 deg eccentricity the acuity was approximately 4 arcmin. The worst central visual acuity in the present study was 6/19, better than the average central amblyopic eye acuity of 6/38 for squint amblyopes in Sireteanu and Fronius's study. Therefore, noise was resolvable by all participants in the present study. Figure 4.1 below shows a schematic of a fused binocular percept of a noiseless (L) stimuli. Black lines delimit sectors, whilst dashed blue lines label the four orientations (neither of these sets of lines were perceived during the main experiment).

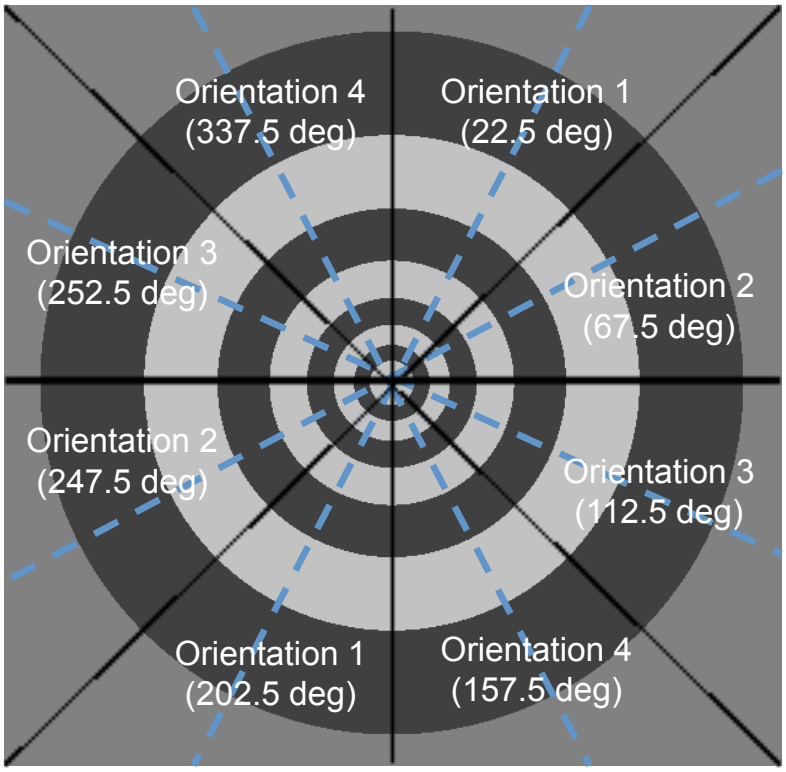

Figure 4.1: Schematic representation of L stimuli. Black lines delineate sectors. Blue dashed lines show orientations. No lines appear on actual stimulus.

4.2.4 Procedure

The present experiments use the same methodology as Experiment 1 (see Chapter 2, Section 2.2.4). Suppression mapping was carried out four to six times for each stimulus type: luminance (L), luminance-modulated noise (LM), and contrast-modulated noise (CM). Practice runs, if required, were carried out until participants were familiar with the task, i.e. staircase standard deviation was within 15% of the mean (on average standard deviation for all participants was 7.7%±4.3 of the mean).

Binocular alignment was carried out to ensure that the same images were presented to corresponding points in each eye. Two squares of 1 deg side length with centres vertically displaced by 1 deg were presented dichoptically (i.e. one square to each eye). If squares were horizontally offset, participants moved the squares using the keyboard in steps of 1 pixel (~2.5 arcmin) until they were perceived as one above the other. Alignment in pixels was recorded and the main experimental stimuli were moved accordingly. This was carried out at the beginning of each session, although magnitude did not change remarkably between sessions. Larger angle strabismus was corrected with prisms (incorporated into refractive correction) to grossly align images to each eye, and then the above alignment calibration was carried out.

Stimulus baseline modulation was determined initially for each participant. The ‘baseline’ refers to the modulation of the ring presented to the non-amblyopic eye to which the adjustable sector was matched, i.e. excursions from the mean modulation (either incremental or decremental). The lower the baseline, the higher the inter-ocular modulation difference that could be measured (due to display contrast limitations). A lower baseline modulation, therefore, allows deeper suppression to be measured, as some levels of suppression in previous experiments were above the adjustable modulation range (see Chapters 2 and 3). Baseline was reduced accordingly in those patients who had deeper suppression, whilst ensuring that stimuli were detectable. Baseline values were 0.25, 0.375, or 0.5.

Once baseline modulation had been determined, the procedure was similar to that employed in previous experiments (see Chapter 2, 3). The point of subjective equality (PSE) was measured for each location of the tested visual field. Participants increased or decreased sector modulation until it matched perceptually to the surrounding ring presented to the non-amblyopic eye. Staircases (1-down, 1-up) were initiated randomly from either halfway between a physical modulation match and maximum adjustable modulation or halfway between a modulation match and minimum adjustable modulation. An audio cue signified once each response was made, and a longer audio cue sounded when six reversals were complete, after which the staircase was terminated and a new sector was adjusted. Step size was initially 0.1 (of a maximum 1.0 modulation), reducing to 0.05 after two reversals. In each experimental run, 64 (L or LM) or 32 (CM) staircases were completed, i.e. one for each sector. Sector presentation order was systematic to distribute the effects of practice, adaptation, and fatigue. This involved working clockwise from the outside ring for at least two runs, and anti-clockwise from the inside ring for at least two runs. The average was taken of equal numbers of anti-clockwise and clockwise runs. Each run was carried out on a different day for each participant.

4.2.5 Analysis

For each sector, the mean point of subjective equality (PSE) was estimated as the mean of four to six experimental runs for each participant across each stimulus type (L, LM, and CM). Point of subjective equality (PSE) modulation values are normalised across stimulus type using the following equation:

$$S_{norm} = \frac{(M_{match} - M_{baseline})}{M_{baseline}} \quad \text{Eq. (2)}$$

where S_{norm} is the normalised depth of suppression, M_{match} is the PSE modulation of the sector and $M_{baseline}$ is the baseline modulation, i.e. the surrounding ring. Suppression was plotted in colour-coded maps. Baseline modulation was decreased to provide a larger range of measurable suppression. For example, a baseline of 0.25 would give a maximum

measureable suppression depth of 3.0 from Equation 2 ((1.0 – 0.25)/0.25). Comparing this with a baseline of 0.5, from Equation 2 ((1.0 – 0.5)/0.5) the deepest suppression measureable is 1.0. Experiments 1 and 2 had a maximum value of 1.0 (L and CM) or 0.5 (LM). Suppression depth was not measured above 2.0 for L and CM or 1.67 for LM. These LM stimuli differed due to restrictions imposed by noise on maximum M_{match} values. Colour-coded suppression maps therefore have a range of -1 (green – facilitation) to 2.0 (red – maximum suppression), with 0 (yellow) representing a physical match between the sector and surrounding ring modulation. Preliminary experiments ensured that baseline modulation was adjusted individually to maintain the suprathreshold aspect of the task, i.e. sectors were visible in order to make an inter-ocular modulation match (although detection thresholds were not formally measured).

Visual performance of amblyopes has been shown to be different for anisometropic and strabismic amblyopes (Levi and Klein, 1982a, b; McKee et al., 2003; Song et al., 2014; see Chapter 1, Section 1.3.1.1). Mixed amblyopes, however, have shown behaviour akin to strabismic amblyopes in terms of binocular performance (e.g. McKee et al. 2003). Therefore, despite participant JB having no manifest deviation and anisometropia, she is included in the strabismic category as she had strabismus surgery when she was a child. For two strabismics (AH and CMa) entire maps were rotated clockwise by one sector, in order to superimpose the clearly defined hemifield suppression when averaged with other participants (see coloured suppression maps in Appendix: Figures 4.13 and 4.14).

4.3 Results

Data from the nine binocularly abnormal participants (four with strabismus and five with micro-strabismus) were analysed along with those from four binocularly normal participants who contributed to Experiment 1, with the aim of addressing five principal questions. They are: 1) Is there a difference in measured magnitude of suppression between normal and binocularly abnormal participants? 2) Is there a specific eccentricity effect for suppression in strabismic participants, and does it differ between strabismic and microstrabismic participants? 3) Does the addition of luminance noise affect the measured magnitude of suppression in strabismic and microstrabismic participants? 4) Is there a modulation polarity effect on measured depth of suppression in strabismic and microstrabismic participants and 5) Do contrast-modulated noise (CM) stimuli provide a more sensitive test for suppression than do luminance-modulated noise (LM) stimuli in participants with abnormal binocular vision, i.e. in those with strabismus and microstrabismus?

A mixed design repeated measures Analysis of Variance (ANOVA) was performed with a between-subjects factor of participant group (with three levels of normal, microstrabismus, and strabismus), and within-subjects factors of stimulus type (three levels: L, LM, or CM), orientation (four levels: see Figure 4.1), and eccentricity (eight levels: from periphery to centre to opposite periphery). In this main statistical analysis, for L and LM stimuli, adjacent sectors were averaged to provide information about 32 sectors equivalent to those used for CM stimuli, across the visual field (as illustrated in Figure 2.2C). This enables statistical comparison across L, LM and CM stimulus types. Outcomes of this ANOVA are presented in Table 4.2.

Figure 4.2 shows data that contributed to this analysis in the form of averaged suppression maps for each participant group, and each stimulus type. For normal participants, the majority of sectors are either light green or yellow, showing mild facilitation or an inter-ocular match, respectively, for all stimulus types. For the microstrabismic group, suppression (as revealed by orange and red sectors) for L and LM stimuli is similar, with suppression present generally

in the central ring; whilst for CM stimuli suppression is more diffuse across the visual field, possibly with deeper suppression in one hemifield. For the strabismic group, suppression appears deeper for L than LM stimuli, with every second ring (from the centre) possibly showing deeper suppression. Suppression is also deeper in one hemifield than the other, along with central suppression. For CM stimuli, suppression occurs across the whole visual field, although it appears deeper centrally, and a consistent alternating pattern is absent.

Table 4.2: Results of repeated measures mixed design ANOVA with between-subjects factor participant group (3), and within-subjects factors stimulus type (3), orientation (4), and eccentricity (8). Significant results are highlighted in red, non-significant higher order interactions are not shown.

Source (number of levels)	Degrees of Freedom	F	Sig.
Participant group (3)	2	6.19	0.018
Stimulus type (3)	1.92	7.91	0.003
Orientation (4)	1.43	3.32	0.078
Eccentricity (8)	1.77	7.02	0.007
Stimulus type * Participant group	3.84	2.11	0.121
Orientation * Participant group	2.87	1.65	0.222
Eccentricity * Participant group	3.53	1.43	0.266
Stimulus type * Eccentricity	3.76	7.52	0.812

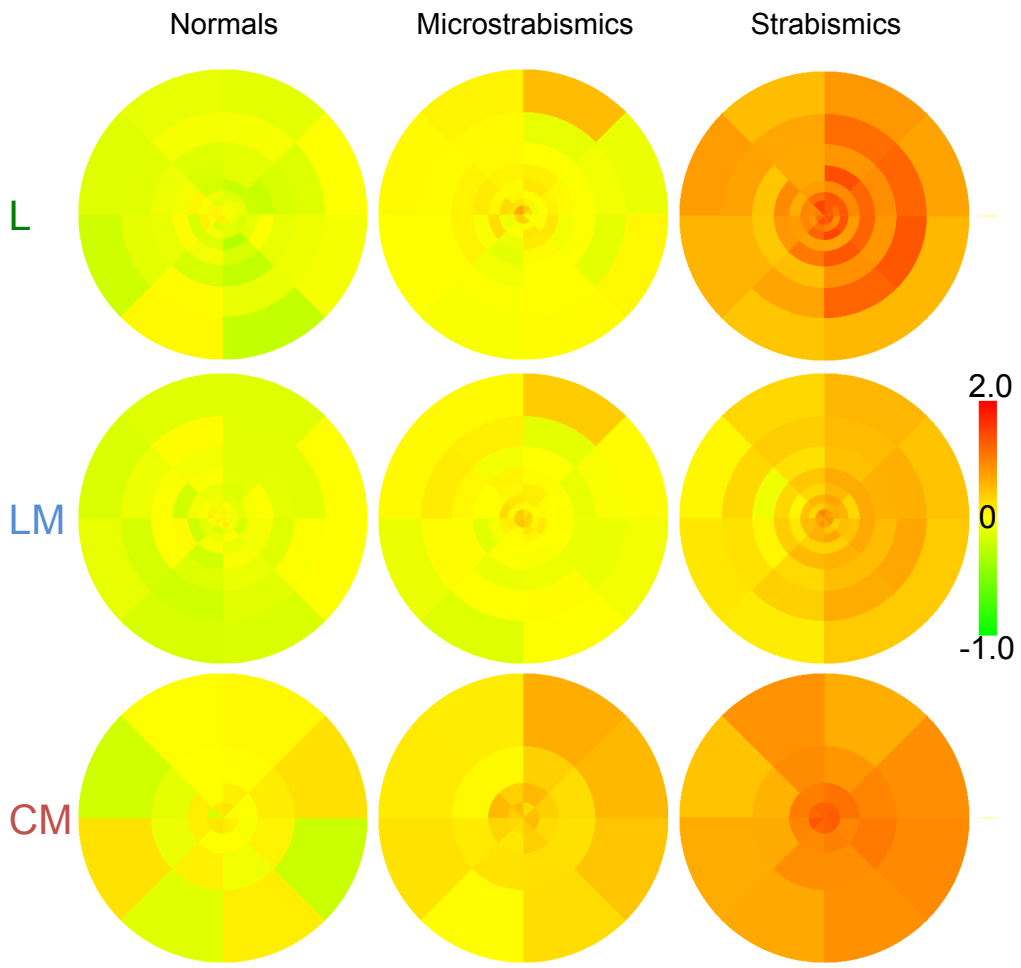

Figure 4.2: Coloured suppression maps averaged across participants within each group (normals, microstrabismics, strabismics) for different stimulus types (L, LM, CM). Colour bar on to the right of the Figure applied to all maps. A red sector shows deepest suppression, yellow no suppression, and a green sector showing facilitation.

Referring to Table 4.2, it can be seen that significant statistical differences were found between participant group, stimulus type and sector eccentricity. No statistically significant higher-order interactions were found suggesting that the effects of stimulus type and eccentricity are similar across all groups. However group sizes are small and there are good theoretical (*a priori*) reasons to investigate differences between groups, particularly for the significant main effects of stimulus type and eccentricity.

4.3.1 The effect of participant group on suppression depth

The main effect of group can be seen in Figure 4.2, where the colour maps change from green to yellow to orange-red for normal to microstrabismic to strabismic groups, respectively. This is more clearly shown in Figure 4.3, where the average of suppression measures across all sectors is compared between groups. Tests of simple effects on the significant main effect of participant group [$F(2, 10) = 6.19$, $p = 0.018$] revealed statistically deeper levels of suppression for strabismic, than microstrabismic [$p = 0.023$] and normal participants [$p = 0.007$]. The overall level of suppression in microstrabismic participants is much lower than in strabismic participants and not statistically significantly different from that measured in normal participants [$p = 0.412$].

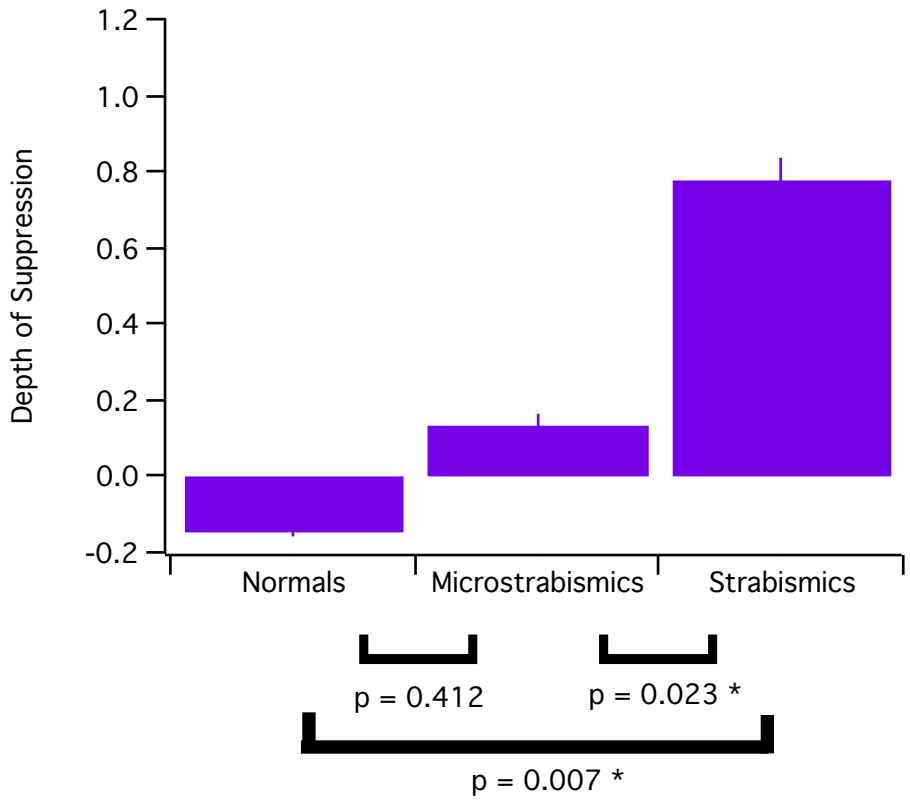

Figure 4.3: Suppression depth averaged across all sectors and all stimulus types for the three participant groups. P-values show that a significant (asterisk) difference between microstrabismics and strabismics only. Error bars show +1 standard error (-1 for normal participants).

4.3.2 The effect of eccentricity on suppression depth: Hemifield versus central patterns

The statistically significant overall main effect of eccentricity [F(1.77, 17.65) = 7.02, p = 0.007] is revealed in Figure 4.4. Simple contrasts comparing all sectors in one hemifield to those in the other hemifield revealed significantly deeper suppression in one hemifield compared to the other [F(1, 10) = 20.72, p = 0.001] (Figure 4.4A). Furthermore, comparing the two central sectors with the six other peripheral sectors revealed significantly deeper central suppression [F(1, 10) = 8.28, p = 0.016] (Figure 4.4B).

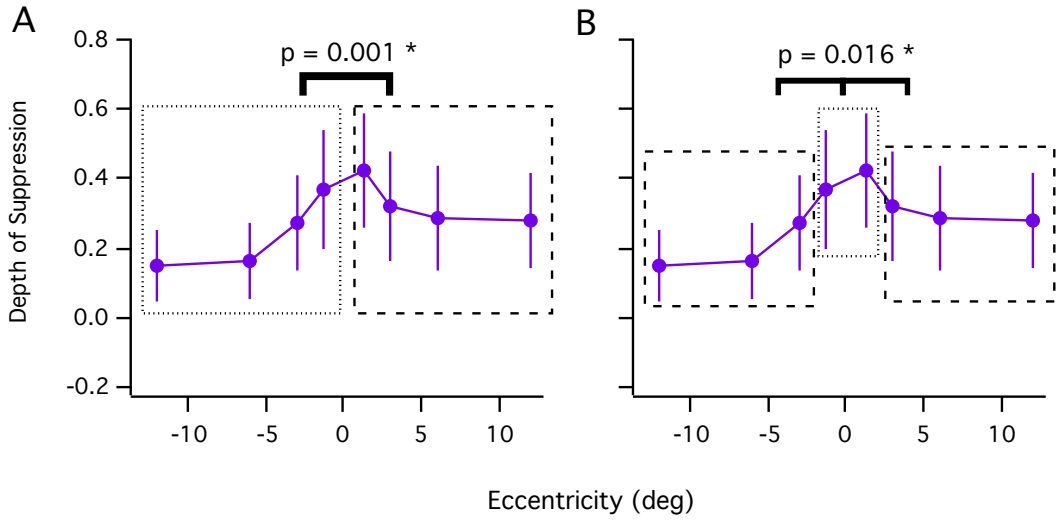

Figure 4.4: Both A and B show the same plots of suppression depth averaged across all participant groups and stimulus type for each eccentricity. A) Shows significant (asterisk) difference between one hemifield (dotted box) and the other (dashed box). B) Shows significant difference between central sectors (dotted box) and peripheral sectors (dashed box). Error bars show ±1 standard error.

Although no statistically significant interaction between group and eccentricity was revealed, previous research studies have described hemifield and central suppression patterns of suppression in strabismic participants and a central suppression pattern in anisometropic participants. Patterns of eccentricity dependence were therefore statistically investigated for the strabismic and microstrabismic groups in the current study using planned comparisons (there

were no significant effects of eccentricity found for the normal group). It is noteworthy though, that post-hoc comparisons with stringent family-wise error adjustment, resulted in very similar outcomes to those described below.

The effects of eccentricity (averaged across stimulus type) for each participant group are summarised in Figure 4.5. Planned comparisons for the microstrabismic group (Figure 4.5 – filled squares) showed a significant hemifield effect [$F(1,10) = 7.13$, $p = 0.023$] (Figure 4.5A), however central suppression as defined above, does not reach statistical significance [$F(1,10) = 2.33$, $p = 0.157$] (Figure 4.5B). This appears to result from a differential effect on the pattern of suppression for microstrabismics, depending on the stimulus type used to measure it (see Figure 4.5C). For L and LM stimuli, microstrabismic suppression is predominantly central (see section below looking more closely at the effect of noise on suppression for confirmation of this finding), whereas for CM stimuli a significant hemifield effect is found [$F(1,10) = 8.24$, $p = 0.017$].

Planned comparisons for the strabismic group (Figure 4.5 – filled diamonds) reveal both significantly deeper suppression in one hemifield compared to the other [$F(1, 10) = 23.06$, $p = 0.001$] (Figure 4.5A), and central suppression [$F(1,10) = 6.54$, $p = 0.028$] (Figure 4.5B). This pattern is consistent for all stimulus types (see Figure 4.5D).

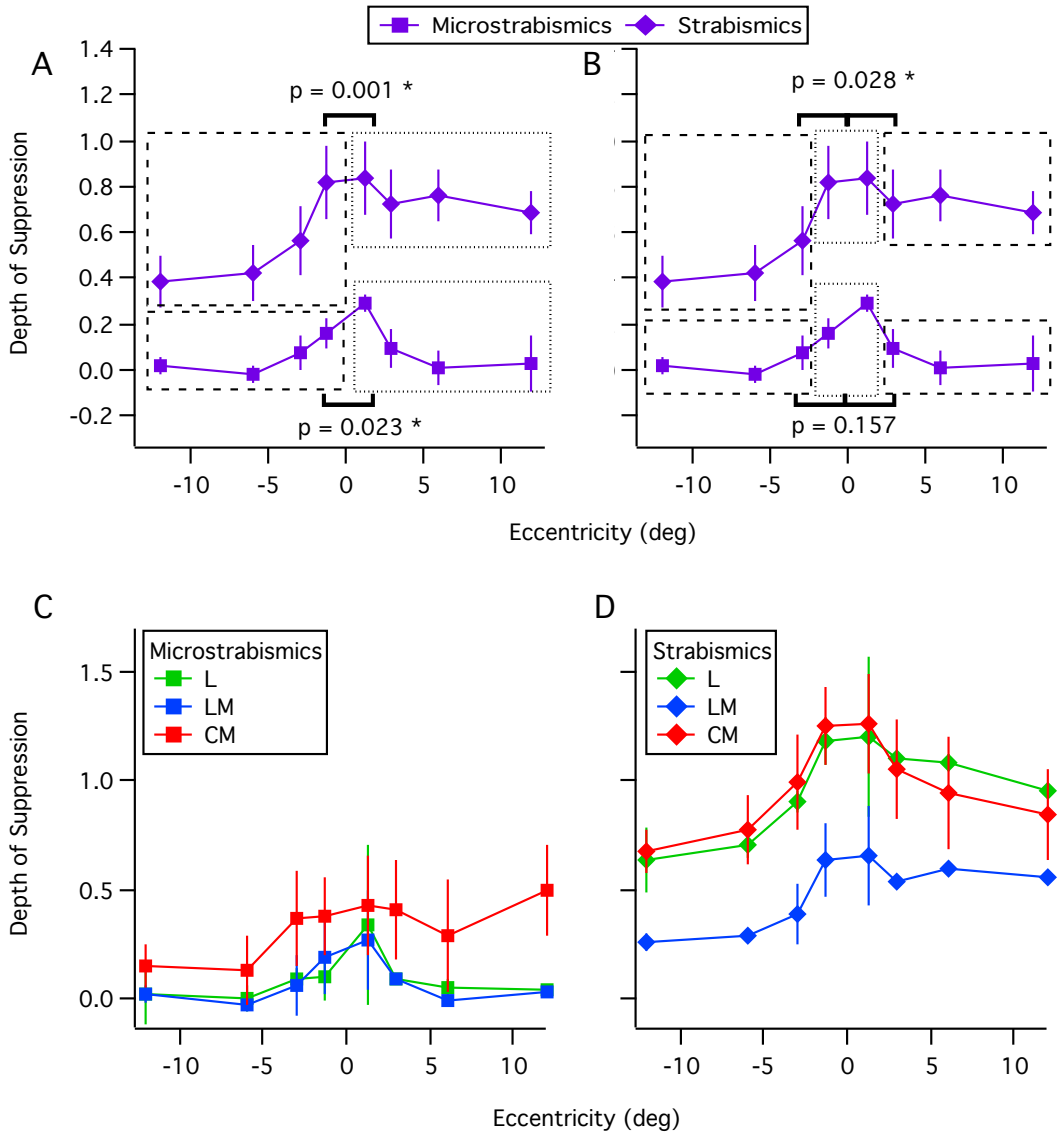

Figure 4.5: A) and B) show the same plots of suppression across eccentricity averaged across all stimulus types for microstrabismics (squares) and strabismics (diamonds). A) significant (p-values with asterisks) differences between one hemifield (dashed box) and the other (dotted box), B) p-values for central (dotted box) compared with peripheral (dashed box) sectors. C) and D) show data for individual stimulus types for microstrabismics and strabismics, respectively. Error bars show ±1 standard error.

4.3.3 The effect of stimulus type on measurement of suppression

Table 4.2 also reveals a main effect of stimulus type [$F(1.92, 3.84) = 7.91$, $p = 0.003$] on the magnitude of suppression. Suppression measured with CM stimuli is deeper than that measured with LM stimuli and reaches a highly

statistically significant difference [F(1, 10) = 19.68, p = 0.001]. Suppression is also deeper with L than LM stimuli, although this result just missed statistical significance [F(1, 10) = 4.73, p = 0.055]). Suppression depth measured for the different stimuli for the different participant groups is shown in Figure 4.6. Again, although the interaction between participant group and stimulus type was not statistically significant, there is theoretical reason to suggest that strabismic and microstrabismic participants are distinct clinical entities (Helveston and von Noorden, 1967; Lang, 1974).

For the microstrabismic group, suppression measured using L and LM stimuli was remarkably similar (given the deeper L than LM suppression found in Experiments 1 and 2 under conditions generating suppression in normal eyes), whereas suppression measured using CM stimuli was always deeper than that found when using LM stimuli [F(1, 10) = 5.32, p = 0.044]. For the strabismic group, suppression was reduced significantly when measured using LM compared to L stimuli [F(1, 10) = 11.82, p = 0.006]. This finding suggests that the addition of noise reduces suppression in these participants (a finding also reported in both Experiments 1 and 2, in which inter-ocular differences were created in binocularly normal participants). Again in strabismic participants, suppression measured with CM stimuli was significantly deeper than that measured with LM stimuli [F(1, 10) = 15.76, p = 0.003].

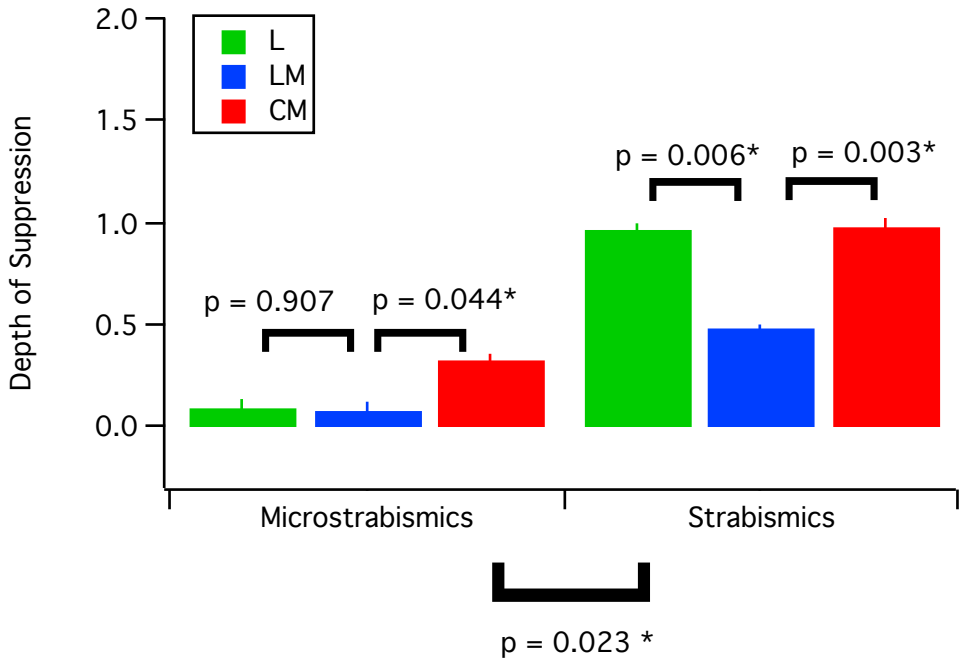

Figure 4.6: Suppression depth averaged across all stimulus type within microstrabismic and strabismic participant groups. P values describe whether or not differences were significant between stimulus types within groups, and also between groups (below abscissa). Error bars show ±1 standard error.

In the main statistical analysis reported in Table 4.2, 32 sectors for L and LM stimuli were created from the original 64 sectors, to enable direct comparison with results obtained for 32 sectors only with CM stimuli (see Figure 2.2C for example). In the following section, L and LM stimuli are examined across the full 64 sectors available (e.g. Figure 2.2B). This will give a more complete analysis of the effects of adding noise to luminance-based stimuli, particularly for the two binocularly abnormal groups. It will also allow an investigation of stimulus luminance polarity on measured suppression in the two binocularly abnormal groups. This factor was found to significantly affect suppression measurement in binocularly normal participants with artificially induced inter-ocular differences created using different neutral density (ND) filters placed before one eye.

4.3.4 The effect of noise on luminance suppression for different participant groups

Previous experiments that induced binocular imbalance in normals with either inter-ocular blur, or inter-ocular luminance differences (see Experiments 1 and 2 in Chapters 2 and 3, respectively), found that adding noise to luminance defined stimuli reduced measured suppression depth. Furthermore, deeper increment than decrement suppression for L stimuli in particular, was observed in normals with imposed inter-ocular luminance differences (see Chapter 3).

Similar to the main analysis conducted above, a mixed-design repeated measures ANOVA was performed across participant group (three levels: normal, microstrabismic, and strabismic), with within-subjects factors of stimulus type (two levels: L and LM), orientation (four levels: see Figure 4.1), and eccentricity (16 levels: see Figure 2.2B). Outcomes are reported in Table 4.3. As with the main analysis, when using L and LM stimuli only, there are significant main effects of group and eccentricity.

Table 4.3: Results of repeated measures mixed design ANOVA with between-subjects factors participant group (3), and within-subjects factors stimulus type (2), orientation (4), and eccentricity (16). Significant results are highlighted in red, near-significant results in orange, and non-significant higher order interactions are not shown.

Source (number of levels)	Degrees of Freedom	F	Sig.
Participant group (3)	2	6.099	0.019
Stimulus type (2)	1	4.731	0.055
Orientation (4)	1.901	2.917	0.081
Eccentricity (16)	2.925	4.707	0.009
Stimulus type * Participant group	2	3.855	0.057
Eccentricity * Participant group	5.85	1.311	0.284
Eccentricity * Stimulus type	2.93	0.576	0.632

Suppression was deeper for strabismics, than microstrabismics [F(2, 10) = 6.10, p = 0.019], much like that seen in Figure 4.6. The effect of adding noise to luminance stimuli (the main effect of stimulus type here) nears significance [F(1,10) = 4.73, p = 0.055], however the effect of stimulus type depends (or nearly so at p = 0.057) on the participant group analysed. The effect of adding noise reduces measured suppression for the strabismic group, but has little effect on measured suppression for the microstrabismic group. This interesting finding is revealed in Figure 4.7.

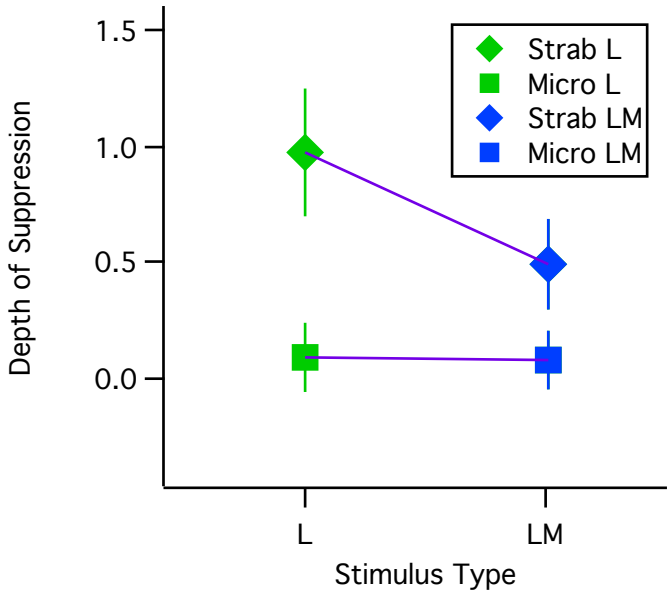

Figure 4.7: Suppression depth averaged across all sectors for each stimulus type, plotted for microstrabismics ("micro") and strabismics ("strab"). Error bars show ±1 standard deviation across all sectors.

4.3.5 Where do the significant eccentricity effects for luminance-defined (L and LM) stimuli come from?

When only luminance (L) and luminance-modulated noise (LM) stimuli are considered, a significant main effect of eccentricity [F(2.93, 5.85) = 4.71, p = 0.009] is found. These effects are revealed in Figure 4.8. Two eccentricity effects are revealed here: 1) a stimulus polarity effect, and 2) an eccentricity *per se* effect. These were investigated separately using planned comparisons.

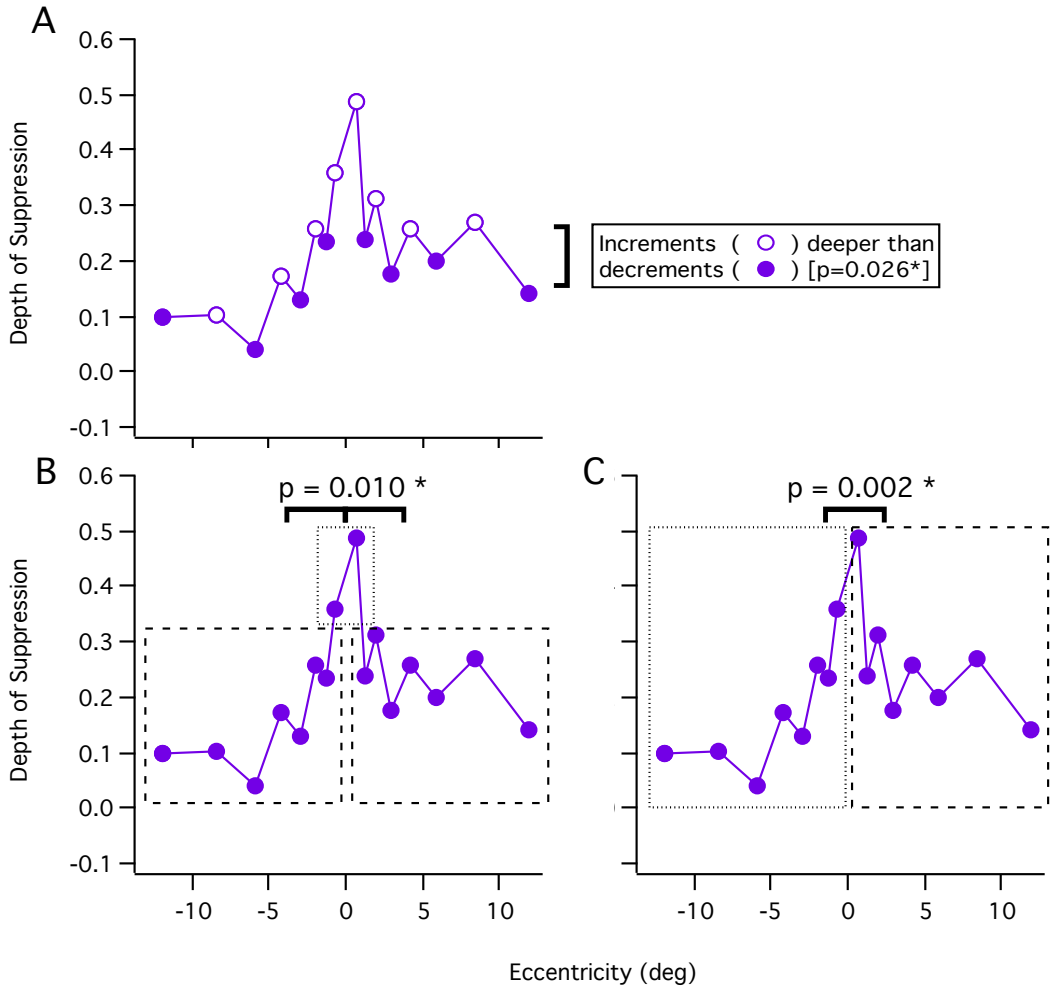

Figure 4.8: A), B) and C) all show the same depth of suppression for each eccentricity averaged across L and LM stimuli, and also averaged across all participant groups. A) Illustrates significantly deeper increment than decrement suppression, B) the significantly (asterisk) deeper central (dotted box) than peripheral (dashed box). B) shows hemifield effects difference. The legend gives significance value of deeper increment (open symbols) than decrement (filled symbol) sectors. Error bars are omitted for clear illustration of eccentricity effects.

Suppression measurements for luminance increment sectors and luminance decrement sectors (the stimulus polarity effect) were compared using planned comparisons and found to be significantly different [$F(1,10) = 6.83$, $p = 0.026$] such that luminance increments resulted in deeper suppression measurements than did luminance decrements. Although the previous results (see Chapter 3) warranted investigation of polarity, and thus planned comparisons were justified, post-hoc testing (using Tukey's pairwise comparisons) was also

carried out. Significant effects of luminance polarity on measured suppression values were revealed for the strabismic group only. No significant effect of stimulus polarity was found for the microstrabismic group.

Planned comparisons also reveal significant eccentricity *per se* effects. Overall, there is significantly deeper suppression in one hemifield than the other [$F(1,10) = 16.73$, $p = 0.002$], and deeper suppression of the central two sectors compared with all others [$F(1, 10) = 10.15$, $p = 0.010$]. No significant eccentricity effect is found for the normal group of participants. Microstrabismics showed deeper central suppression [$F(1, 10) = 5.56$, $p = 0.040$] but no hemifield suppression [$F(1, 10) = 2.16$, $p = 0.173$]. Strabismics showed both central [$F(1, 10) = 5.15$, 0.047] and hemifield [$F(1, 10) = 25.64$, $p<0.001$] suppression. These results are shown in Figure 4.9.

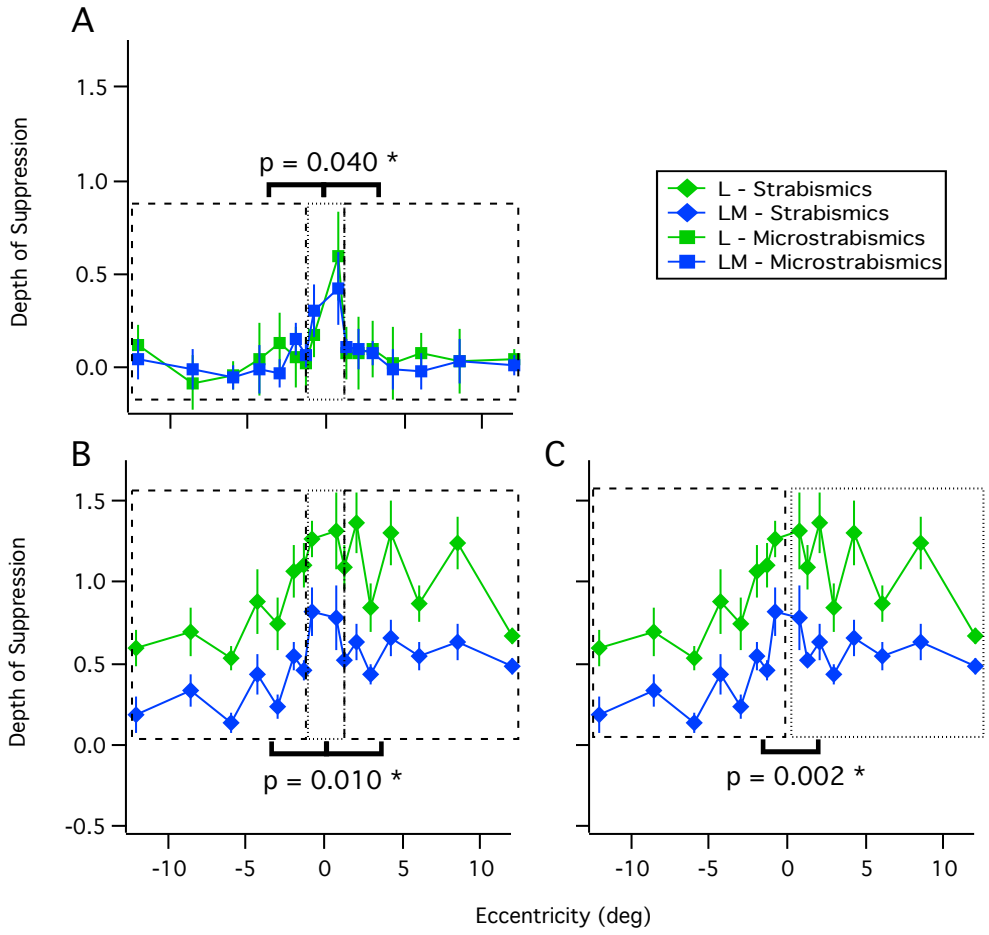

Figure 4.9: Suppression depth across eccentricity for L (green) and LM (blue) stimuli for A) microstrabismics showing significantly (asterisk) deeper central (dotted box) suppression compared with peripheral sectors (dashed box). Both B) and C) show central and hemifield (respectively) suppression for strabismics. Error bars show ±1 standard error.

4.3.6 LM versus CM stimulus suppression

Finally, do contrast-modulated noise (CM) stimuli provide a more sensitive test for suppression than luminance-modulated noise (LM) stimuli in participants with abnormal binocular vision? Our results so far indicate that suppression of CM stimuli is deeper for our strabismic and microstrabismic participants, than either L or LM stimuli (see Figure 4.6) suggesting that for mild anomalies of binocular vision, they would reveal greater levels of suppression.

An alternative way to indicate sensitivity would be to examine slopes of how depths of suppression measured vary for different levels of binocular anomaly. The steeper the slope, the more sensitive the stimuli used would be to changes in suppression depth with treatment or with disease progression.

Figure 4.10A shows data addressing the effects of added noise on luminance stimuli, whilst Figure 4.10B compares suppression measures for LM and CM stimuli directly (i.e. comparing two types of stimuli created from the same dynamic noise). In Figure 4.10A, the mean depth of suppression across all sectors for L and LM stimuli is plotted against inter-ocular visual acuity differences for microstrabismic and strabismic participants. There were significant positive correlations between depth of suppression and inter-ocular visual acuity difference for both L [r =0.877, p = 0.002] and LM [r = 0.787, p = 0.006] stimuli.

Linear functions fit to the data reveal that suppression depth increases with increasing inter-ocular visual acuity difference at a significantly greater rate [p =0.0001] when L, rather than LM stimuli are used (L slope value of 0.28 ± 0.06, compared to LM slope value of 0.15 ± 0.05). This result suggests that L stimuli are more sensitive to *changes* in binocularity and that LM stimuli may be more suitable for quantifying very deep suppression, i.e. for stronger levels of amblyopia or inter-ocular acuity differences such as in strabismus (see Figure 4.10A).

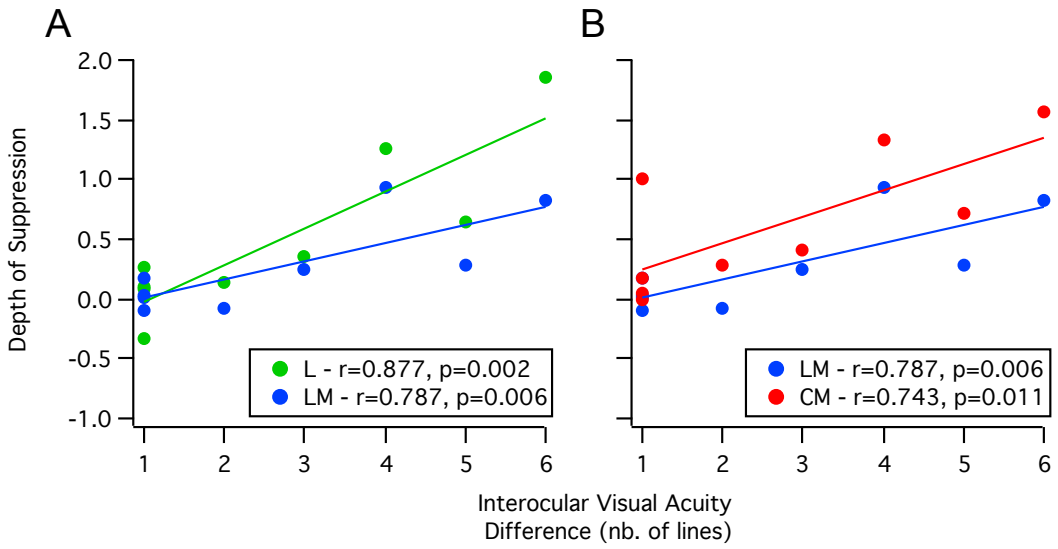

Figure 4.10: Suppression depth (averaged across all sectors for each participant) plotted against inter-ocular visual acuity difference for A) L and LM stimuli, and B) LM and CM stimuli. Legends show Pearson's correlation coefficient (r) with significance values.

Figure 4.10B compares suppression measures for LM and CM stimuli averaged across all sectors, plotted against individual inter-ocular acuity difference. These linear functions show that CM slopes are significantly greater [p = 0.037] than LM slopes (LM: 0.15 ± 0.05, CM: 0.23 ± 0.05) indicating that suppression measured for the two types of stimuli may change with binocularity changes at a greater rate for CM than LM stimuli. Suppression is also consistently deeper when measured with CM, than LM stimuli, suggesting that the use of CM stimuli may be more sensitive at detecting milder forms of suppression (for example in microstrabismics – see Figure 4.11). Again, suppression depth is significantly positively correlated with inter-ocular visual acuity difference for both LM [r = 0.787, p = 0.006] and CM stimuli [r = 0.743, p = 0.011].

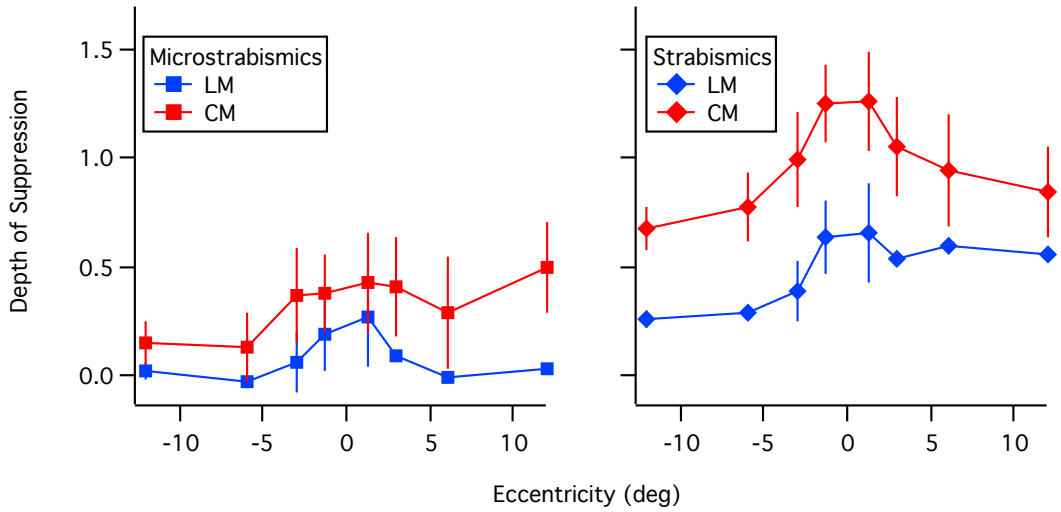

Figure 4.11: Suppression depth across eccentricity for LM (blue) and CM (red) stimuli for microstrabismics (left panel) and strabismics (right panel). Error bars show ±1 standard error.

4.3.7 Suppression depth and clinical findings

Figure 4.12 shows correlations between stereo-sensitivity and red filter suppression and depths of suppression measured using L (green), LM (blue) and CM (red) spatial stimuli. Suppression measures for all participants were averaged across all sectors for each participant for the aforementioned stimulus types. Linear regression tests revealed Pearson's *r* value and the significance level of the relationships between this new suppression measure and established clinical measures of stereo-sensitivity and red-filter suppression described in the methods section (see insets Figure 4.12).

For all stimulus types, there were significant positive correlations between the new depth of suppression measure and inter-ocular visual acuity differences calculated from fitted slopes of Figures 4.10A and B, illustrating that larger inter-ocular differences in acuity show deeper suppression.

Comparing depth of suppression measured in this experiment for the three stimulus types with the red filter method, using a spot of light as a stimulus, the following results were found: L [r = 0.618, p = 0.038] and LM [r = 0.709, p = 0.016] stimulus types showed a significant positive correlation, whilst CM stimuli

[r = 0.508, p = 0.082] did not. Negative correlations existed between clinically determined stereo-sensitivity and suppression depth measured using the new tool developed in these experiments, although this only reached significance for LM stimuli, as can be seen in Figure 4.12. Therefore, deeper suppression is negatively correlated with reduced stereo sensitivity, and red filter suppression measurement can estimate overall suppression depth, but not suppression extent. Correlations would be strengthened by adding data from more participants.

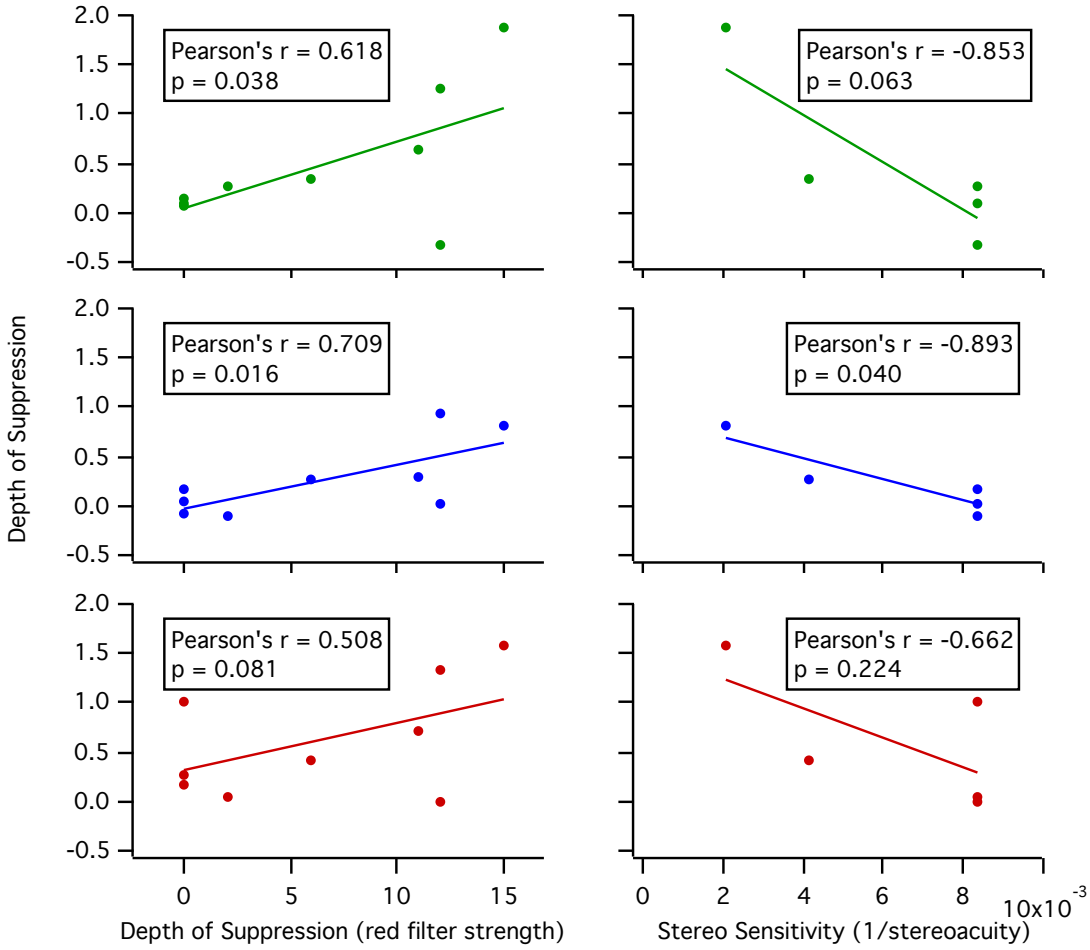

Figure 4.12: Correlations between depth of suppression (taken as average of all sectors) for L (green), LM (blue), and CM (red) stimuli with stereo-sensitivity taken as 1/ stereoacuity (left column) and red filter suppression depth (right column).

4.4 Discussion

Suppression was measured in a range of adult participants with abnormal binocular vision with noiseless luminance (L), luminance-modulated noise (LM) and contrast-modulated noise (CM) stimuli in localised areas within the central circular 24 deg of the visual field. For the majority of participants, suppression was present with clinical tests (see Table 4.1). Participants were either strabismic or microstrabismic. Amblyopia is not male or female specific (Attebo et al., 1998) and therefore suppression extent or depth was not influenced by having only female participants.

4.4.1 Depth and extent of suppression

4.4.1.1 Strabismics

Participants with strabismus, i.e. deviation greater than 6 prism dioptres, showed deep suppression for L stimuli. Suppression extent was asymmetric in these participants, in agreement with previous studies finding scotomata extending from the central to the fixation point, i.e. corresponding point to the non-amblyopic, non-strabismic eye fovea (Harms, 1937; Travers, 1938; Jampolsky, 1955; Herzau, 1980; Sireteanu and Fronius, 1981; Sireteanu, Fronius, and Singer, 1981; see section 4.2). This is most clearly evident with LM stimuli for participant CMc (Figure 4.15), who showed the deepest suppression of all participants across the whole visual field (corresponding to greatest inter-ocular visual acuity difference). Pratt-Johnson and Tillson (1983) suggested that suppression of the whole strabismic eye's binocular field occurred in those with no fusion, offering an explanation for CMc's results with L and CM stimuli. However, suppression areas may have been summated in that study due to large (3.4 deg) targets used with the Adapted Lees Screen method, giving spurious results. Suppression of LM stimuli for participant CMc was asymmetric (deeper in the left hemifield). This also suggests that LM stimuli may be more appropriate to assess suppression in those with deep amblyopia, as display contrast resolution limits the range of measurable suppression with L and CM stimuli.

For the majority of strabismics (though not microstrabismics), suppression of luminance-defined modulation increment sectors was deeper than decremental sectors. In a contrast discrimination task, Zele, Wood and Girgenti (2010) found amblyopes to have better decrement than increment discriminability, also observed in participants with normal binocular vision (Anstis and Ho, 1998; Baker et al., 2012; Lu and Sperling, 2012). This combined with local adaptation to luminance modulation decrement rings may give shallower measured suppression. A previous study using the same stimulus types also found deeper increment than decrement suppression for L stimuli for normal observers with monocular ND filters (see Chapter 3, Experiment 2). Some observers in Babu et al.'s (2013) study also showed deeper increment than decrement suppression. Differential suppression not observed with inter-ocular blur (see Chapter 2, Experiment 1) may be due to the reduction of contrast with the blurring lenses. ND filters, which reduce the luminance of one eye's input, therefore simulate the central suppression scotoma in strabismic amblyopic viewing during a modulation matching task using luminance-modulated noise stimuli.

4.4.1.2 Microstrabismics

Suppression was shallower for microstrabismics than strabismics. For first-order stimuli (L and LM), suppression was localised to central sectors (within 1.5 deg of the fovea), with no suppression seen outside of this area. This suggests that the fovea is being suppressed in microstrabismics, in agreement with previous studies (Sireteanu and Fronius, 1981; Sireteanu et al. 1981; Hallden, 1982). Campos (1982) and Mehdorn (1989; see Chapter 1, Section 1.4.2 for review) found no suppression in microstrabismics. These studies explain their lack of measured suppression as being due to harmonious abnormal retinal correspondence (hARC), and that suppression is not required in the presence of hARC. However, different tasks used to measure suppression within these studies also showed some suppression.

Suppression found in the present study could therefore be attributed to a different method of measuring suppression. Harmonious ARC occurs when one eye's fovea fuses with an extra-foveal retinal point in the other eye to give

single clear vision in spite of ocular deviation (Bagolini, 1967). Suppression of the fovea in this condition would be highly favourable to prevent diplopia. Due to the large cortical representation of the fovea, it may be expected that central suppression would be localised in this area to prevent the fovea of the deviated eye from contributing to perception (i.e. diplopia), as in the present study.

Joosse et al. (1997) investigated both depth and extent of suppression in microstrabismics (defined as less than 8 deg, approximately 14 prism dioptres) within the central 20 deg horizontal by 25 deg vertical visual field (see Chapter 1, Section 1.4.2 for review of the study). The task was near threshold, differing from the suprathreshold inter-ocular contrast matching task used in the present experiment, and may explain the lack of suppression scotomata found in the majority of their microstrabismics. Their method had a resolution of 2.5 deg, lower than the central resolution of the present experiment (0.75 deg for L and LM, 1.3 deg for CM), possibly causing larger suppression scotomata to be measured in the five participants where it was present (5-30 deg centred around the deviating eye fixation point). The size of the fixation and test lights is also not mentioned, and this may also have affected suppression measured.

In summary, strabismics generally showed asymmetric suppression maps, as well as central suppression. With L stimuli microstrabismics showed central suppression only. Babu et al. (2013) performed a similar task with similar L stimuli, and found central symmetric suppression for all participants, which included four microstrabismics, six strabismics, and four anisometropes (see Chapter 1, Section 1.4.2 for review). However, the authors did not investigate suppression asymmetry in their study. If data were reanalysed in a similar fashion to the present experiment, a similar asymmetry may have been uncovered, as the individual suppression maps for strabismics in that study suggest. That mild suppression occurred across the visual field for four normal participants in Babu et al.'s study suggests bias in the experimental design, though ocular dominance may have contributed to this suppression measured in normals (Li et al., 2010; Zhang et al., 2011).

4.4.2 Comparing suppression depth with clinical findings

Larger inter-ocular acuity differences between the eyes correlates with deeper suppression for all stimulus types (Figure 4.10), agreeing with previous studies (Sireteanu and Fronius, 1981; Agrawal et al., 2006; Li et al., 2011, 2013; Narasimhan et al., 2012). Correlation between suppression and inter-ocular acuity difference in amblyopia does not prove a causal relationship. However, present results do contradict a previous suggestion that weak suppression is required to prevent diplopia in deep amblyopia (Holopigian et al., 1988; see Chapter 1, Section 1.1). Furthermore, the present study is inconsistent with recent studies showing no suppression in amblyopes (Barrett, Panesar, Scally and Pacey, 2012, 2013). Those studies did not correct ocular deviation, therefore stimulation of corresponding retinal points is not achieved likely causing the conflict with the present results.

Recent models that suggest an imbalance in inhibitory and excitatory interactions between amblyopic and non-amblyopic eyes (e.g. Meese et al., 2006; Ding et al., 2013a) explain the data of the present study well. Deeper amblyopia is related to a greater imbalance in inter-ocular interactions. Specifically, more inhibition is exerted on the weaker eye by the stronger in terms of amblyopic eye input. The stronger eye dominated perception, until input is equalised across the eyes, i.e. weaker eye modulation is increased, and both eyes contribute more equally to perception. In the present study this occurs in local areas of the visual field.

Suppression depth averaged across all sectors showed a negative correlation with stereosensitivity (Figure 4.12) for all stimulus types, similar to Li et al.'s (2011) study. A reduction in stereoacuity may be due to one eye being suppressed. There were significant positive correlations between red filter suppression and suppression mapping depth. This suggests that red filter suppression in the central field can give an idea of suppression averaged across the visual field. However, more participants would strengthen these conclusions.

Participants AR and DM both showed no suppression with the Worth 4-Dot test similar to previous studies where no suppression in ARC was found (Bagolini, 1967; Campos, 1982; Mehdorn, 1989). However, foveal suppression was demonstrated in the present study, suggesting sensitivity to even small areas of suppression found with ARC (Herzau, 1996). Alternatively, poor discriminability due to binocular lustre may have been responsible for the deeper central suppression. This is unlikely as error bars were not very large for the areas of deeper central suppression (see Figures 4.17 and 4.19 for participants AR and DM, respectively), suggesting normal discriminability of the stimuli.

4.4.3 Suppression with the addition of noise to luminance-defined stimuli

For strabismics, the addition of noise reduced suppression whilst retaining the same hemifield asymmetry. Differential suppression of increment and decrement luminance modulation sectors was also reduced (analogous to Chapter 3, Experiment 2). As suppression of L stimuli reached the maximum measurable level (mainly with strabismics), the use of LM stimuli to measure patterns of suppression across the visual field of those with a higher degree of amblyopia is indicated over L stimuli. Suppression in microstrabismics was similar with LM and L stimuli, showing that noise did not have an effect on microstrabismic suppression. This suggests that microstrabismic and strabismic suppression are different, possibly due to different development of each condition.

Introduction of motion or flicker, similar to dynamic noise, breaks down suppression in amblyopia (e.g. Scheiman and Wick, 2008), perhaps in a similar way to continuous flash suppression (Wolfe, 1986; Tsuchiya and Koch, 2005; Yang and Blake, 2012). Adding stimulus noise to amblyopic eyes, that have more internal noise than non-amblyopic eyes (Baker, Meese and Hess, 2008; Levi and Klein, 2003), may have a weaker effect on amblyopic eye suppression. This leads to less of an inter-ocular difference in stimulus strength for LM compared with L stimuli, and LM stimuli would therefore have to be adjusted to a lesser degree to achieve an inter-ocular perceptual match. This may have contributed to lower suppression measures found for LM compared to L stimuli.

4.4.4 Luminance- and contrast-modulated noise stimuli suppression

For all but one participant (DM), suppression was deeper with CM compared with LM stimuli. Data from previous human fMRI (Larsson et al., 2006), and cat (Mareschal and Baker, 1998) and monkey (Baker et al., 2013; Li et al., 2014) electrophysiological studies show activity in V2 when viewing CM stimuli, which implicates V2 as a site for some stages of CM processing. Neurons in V2 are binocular and show reduced activation to strabismic eyes of monkeys (Bi et al., 2011). Deeper suppression measured for CM compared to LM stimuli may require a greater CM than LM signal increase in the amblyopic eye to achieve balanced binocular input.

Deeper CM than LM suppression may also reflect greater extrastriate than striate deficits in amblyopia, in agreement with Zhou, Huang, and Hess (2013). A larger deficit in monocular second- compared to first-order sensitivity, as found in previous studies (Wong, Levi and McGraw, 2001, 2005; Simmers et al., 2003; Mansouri, Allen and Hess, 2005; Chung, Li and Levi, 2006) may indicate that suppressed CM stimuli need to be increased to a relatively greater degree than LM stimuli to be detected. This may have confounded measured CM suppression with reduced CM detectability, although this is unlikely as all stimuli were suprathreshold.

For microstrabismics, suppression of LM stimuli was centrally localised, but changed to a more widespread, possibly hemispheric pattern, across the visual field with CM stimuli. If CM stimuli are processed in areas receiving predominantly binocular input, disruption to binocularity may cause reduced sensitivity to CM stimuli regardless of visual field location. Therefore, general CM suppression across the visual field is expected with microstrabismics. The generally deeper CM suppression in strabismics could also be explained by the above reasoning. Suppression of CM stimuli also extended across a larger central area than LM stimuli for strabismics. Larger CM than LM spatial summation areas have been found previously (Sukumar and Waugh, 2007), possibly explaining the greater extent of CM than LM suppression scotomata. Furthermore, CM envelope extraction occurs in an extrastriate area, with larger

receptive fields, e.g. V2 (Gattass, Gross and Sandell, 1981; Foster, Gaska, Nagler and Pollen, 1985; Kennedy, Martin, Orban and Whitteridge, 1985; Gattass, Sousa and Gross, 1988), compared to those found in V1.

4.4.5 Blur and ND filters as models for amblyopia

As discussed in a companion study (see Chapter 2, Experiment 1), previous investigations have shown that dioptrically blurring normals is a good model for anisometropic amblyopia, both with monocular and binocular viewing. Due to the preponderance of studies investigating strabismic over anisometropic suppression across the visual field, comparisons of monocular blur with normals and anisometropic amblyopia are limited. Experiment 1 showed that blur appears to cause general suppression across the visual field, whereas anisometropes show symmetric suppression in the central binocular visual field (Sireteanu and Fronius, 1981; Babu et al., 2013). However, as the anisometropic participants in the present study have or have had strabismus, comparisons would need to be drawn with pure anisometropes to obtain a more definitive answer.

Neutral density (ND) filters appear to model amblyopic suppression well, as central suppression was found for normal participants of Experiment 2 with monocular ND filters (see Chapter 3) and with the present experiment participants. For L stimuli, the majority of participants with binocular disturbance showed central suppression. Those with strabismus, in addition to a central suppression scotoma, showed asymmetric suppression, which was not simulated with ND filter in normals. Furthermore, strabismics in the present study and normals from Experiment 2 (with inter-ocular retinal illuminance difference) showed deeper suppression of modulation increments compared to decrements for luminance-defined (L or LM) sectors. Therefore, monocular ND filters during binocular viewing best simulates suppression across the central visual field of anisometropes found in the aforementioned studies, and the central suppression present in strabismics. The hemispheric effect in strabismics cannot be demonstrated in normals with ND filters, indicating that that strabismic suppression is associated with a true neural deficit.

4.5 Conclusion

Inter-ocular suppression in those with abnormal binocular vision varies across the visual field, and depth is correlated positively with the amount of inter-ocular difference in visual acuity and negatively with stereosensitivity. Those with strabismus show asymmetric suppression extending from the central point to the periphery. Microstrabismics show central suppression only, although with CM stimuli, more widespread deeper suppression is measured. Suppression is reduced when stimuli are weakened with addition of dynamic binary noise to luminance-defined (first-order) stimuli for strabismics. Microstrabismic suppression was unaffected by the addition of noise, suggesting the existence of distinct differences in suppression development for microstrabismics and strabismics. The inclusion of dynamic noise can be useful for quantifying deeper suppression found in greater degrees of amblyopia. Suppression of contrast-modulated noise is deeper than that measured for luminance-modulated noise stimuli, in both strabismics and microstrabismics. This result suggests that the use of contrast-modulated noise stimuli allows for more sensitive suppression quantification in mild amblyopes and those with amblyogenic factors, i.e. disturbance to binocularity. As participants in the present study all have some binocular disturbance, results are in agreement with previous studies that suggest some stages of contrast-modulated stimulus processing occurs in areas receiving predominantly binocular input.

4.6 Appendix

4.6.1 Suppression scotomata for each participant

Table 4.4: Suppression characteristic for each stimulus type for each participant, with clinical details including visual acuity. Strab. – strabismic, alt. int. – alternating intermittent, aniso. – anisometrope, SOT – esotrope, XOT – exotrope, micro. – microstrabismus

Participant	L Suppression	LM Suppression	CM Suppression
AH - Strab. (alt., int.) aniso., R 6/9.5+2, L 6/6+2	Left hemifield	Left hemifield	Mild across entire field
CMa - Strab. (26 LSOT), R 6/4.8-1, L 6/15	Deeper central, left hemifield	Deeper central	Deeper central
CMc - Strab. (7LXOT), R 6/6+3, L 6/19+2	Deep across entire field	Left hemifield	Deep across entire field
JB - Strab. (corrected by surgery) aniso., R 6/15, L 6/6+2	Deeper central	Deeper central	Deeper central
AW - Micro. (manifest 6 LSOT), R 6/4-2, L 6/5-1	Mild central only	Mild central only	Mild across entire field
AR - Micro., R 6/4.8-1, L 6/6-1	Moderate central only	Moderate central only	Mild across entire field
DM - Micro., R 6/4.8-1, L 6/6-1	Deep central only	Deep central only	Deep across entire field
IR - Micro., R 6/7.5, L 6/6	Mild central only	No suppression	Mild central
NS - Micro., R 6/7.5-1, L - 6/3.8	Moderate central only	Mild across entire filed	Moderate across entire field

4.6.2 Strabismic suppression maps

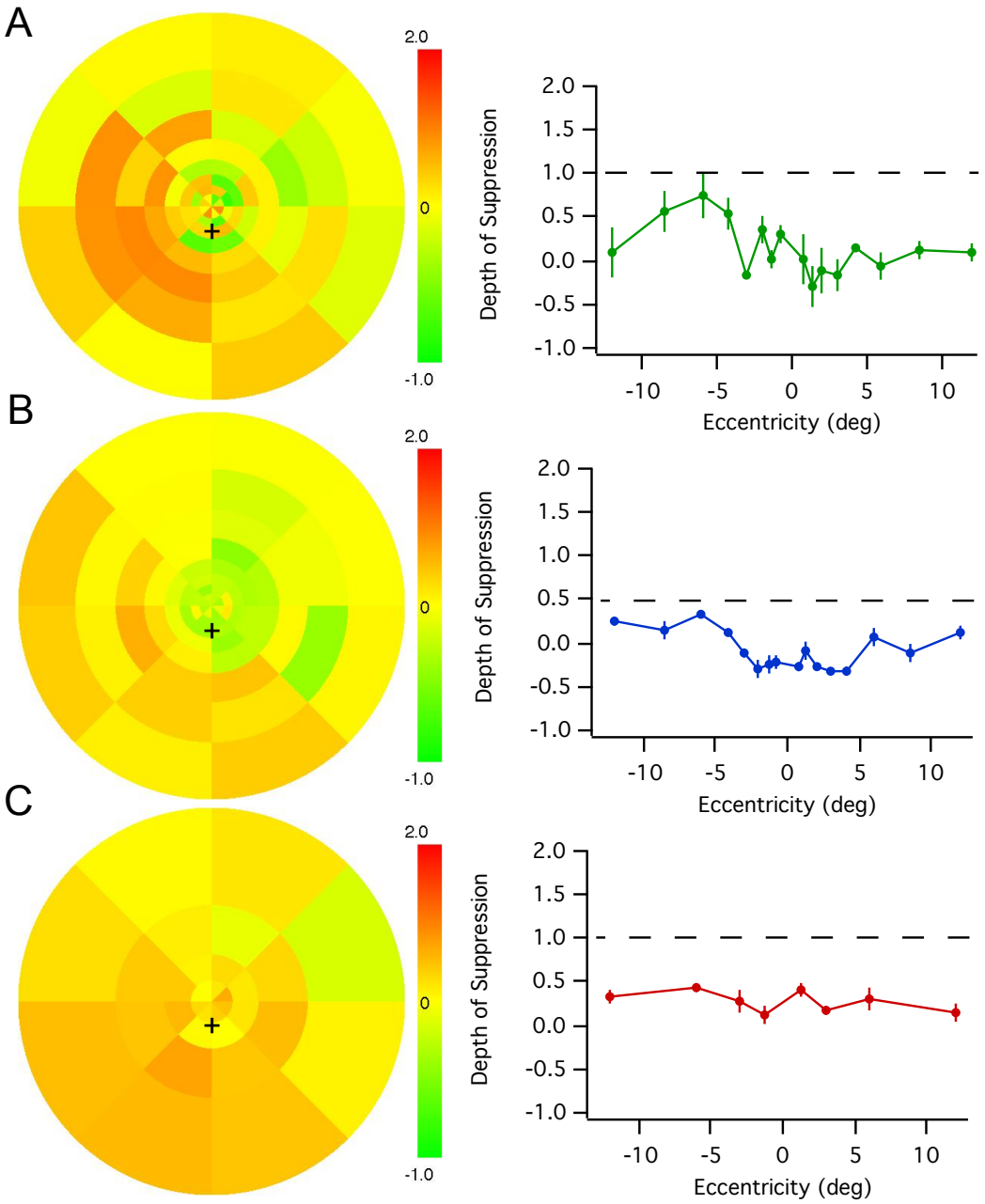

Figure 4.13. Data for participant AH, an alternating intermittent exotrope with anisometropia. Visual acuity: R 6/9.5+2, L 6/6+2. Coloured suppression maps are shown in the left column (details as described in section 3.1 of this Experiment). The right column shows suppression averaged across each orientation for each hemifield. A, B, and C depict L, LM, and CM stimuli respectively. The black cross denotes location of the suppressing eye fovea. This suppression map is a true representation of the participant's visual field, i.e. no re-ordering of hemispheres as in the main analysis. Dashed lines for maximum adjustable suppression. Error bars show standard error across orientations.

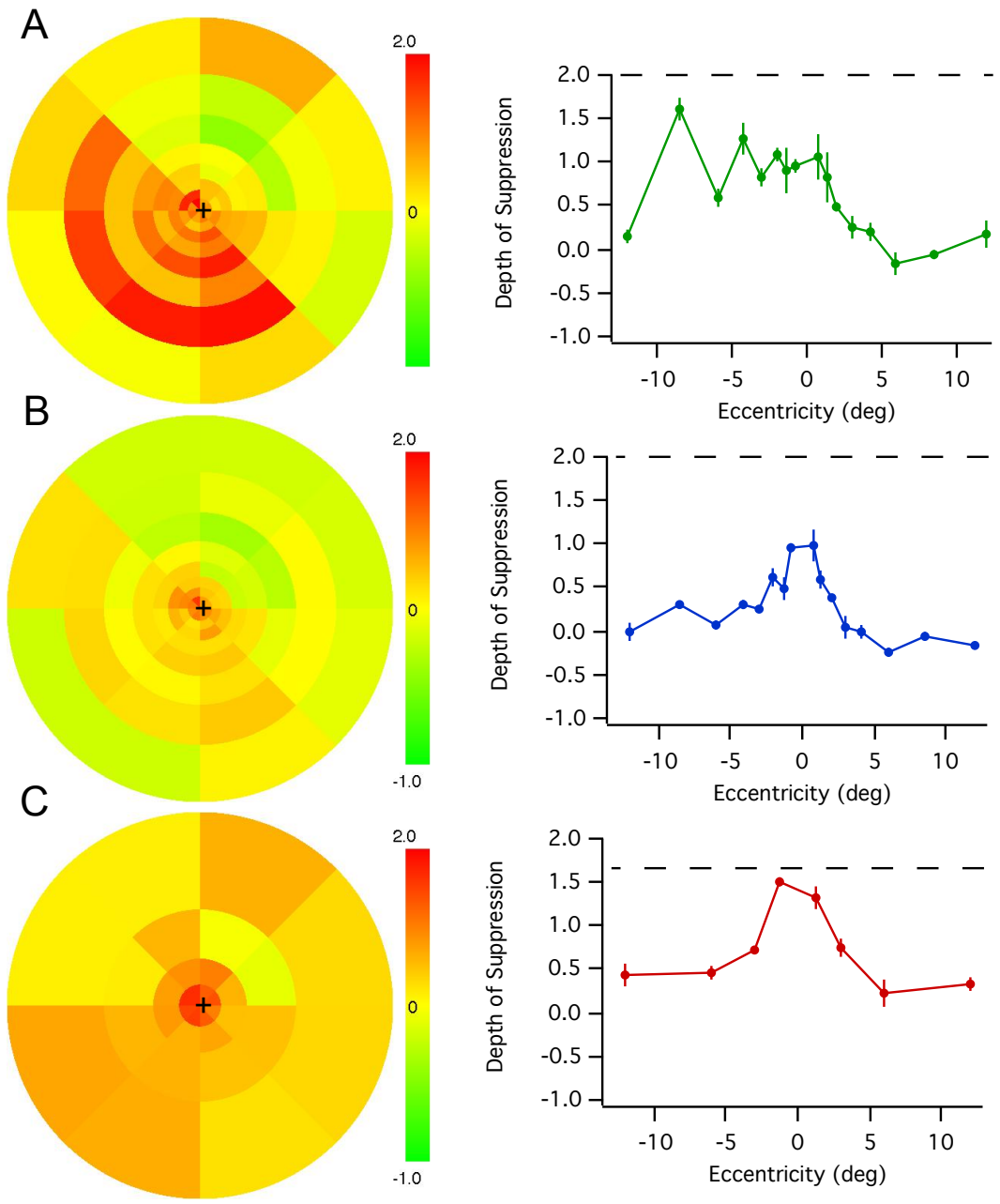

Figure 4.14. Participant CMa has a constant left esotropia. Visual acuity R 6/4.8-1, L 6/15. All other details as in previous Figure.

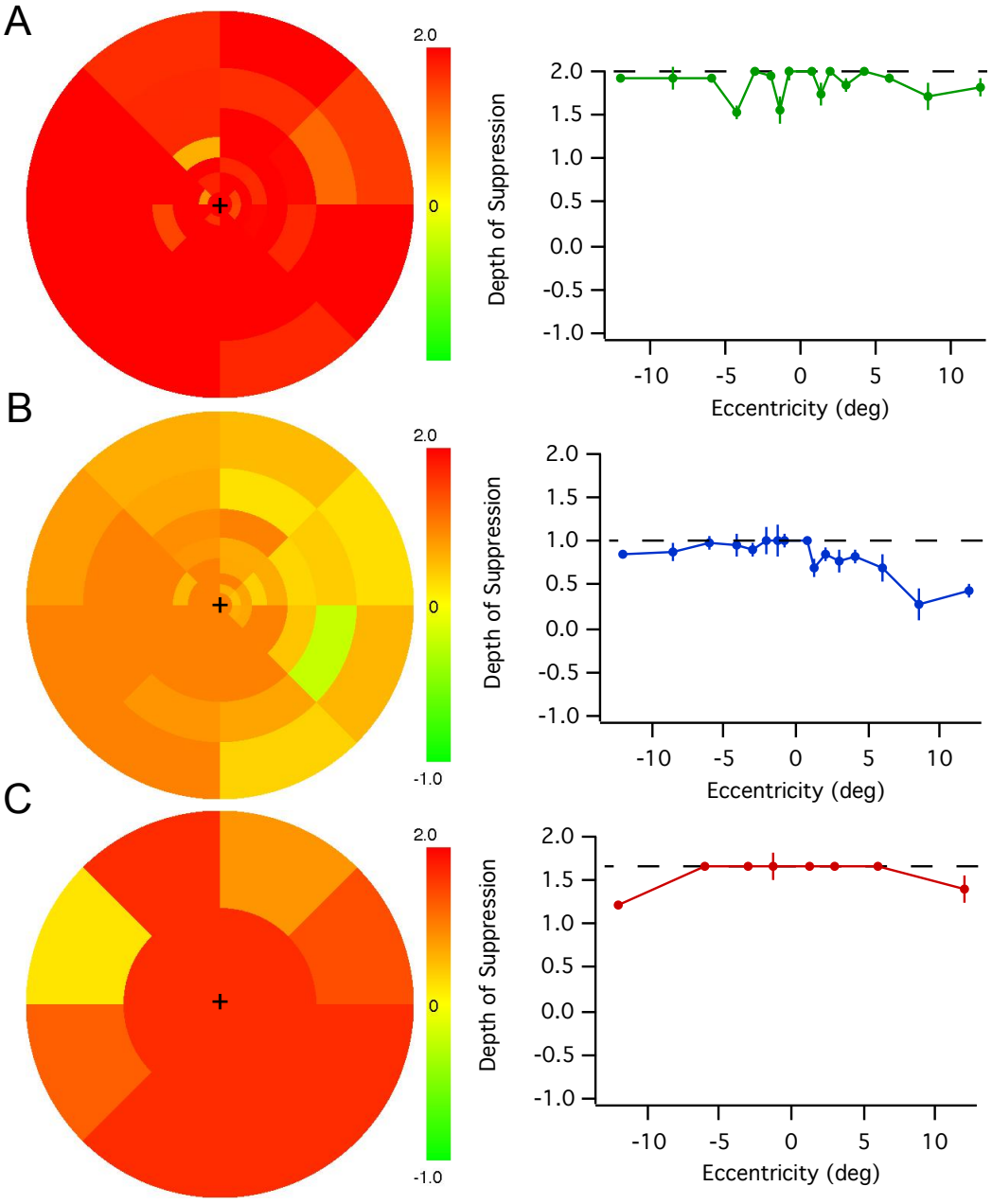

Figure 4.15. Participant CMc has a consecutive left exotropic strabismus. Visual acuity R 6/6+3, L 6/19+2. All other details as in previous Figure.

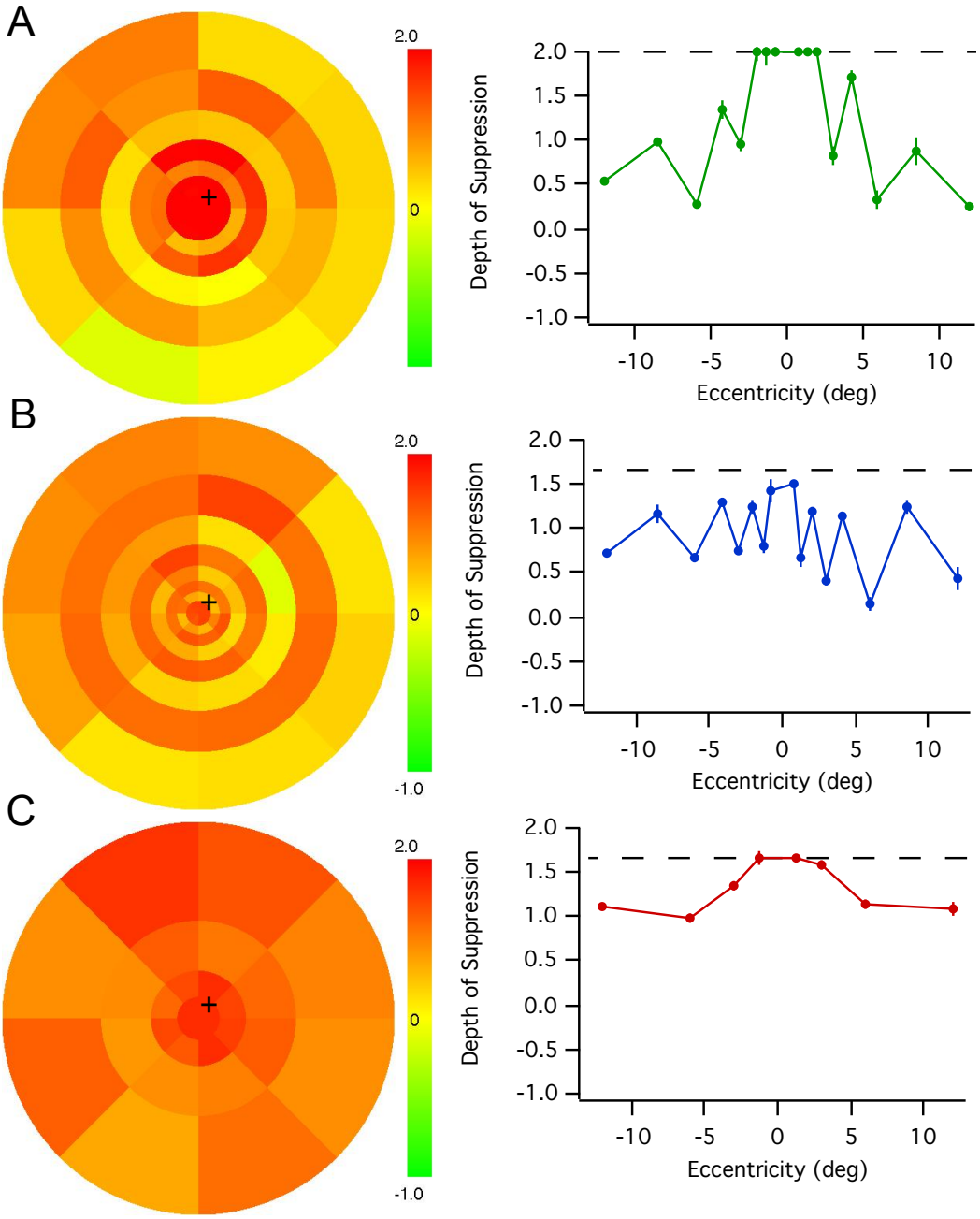

Figure 4.16. Participant JB is an anisometrope with a history of strabismus surgery. Visual acuity R 6/15, L 6/6+2. All other details as in previous Figure.

4.6.3 Microstrabismic suppression maps

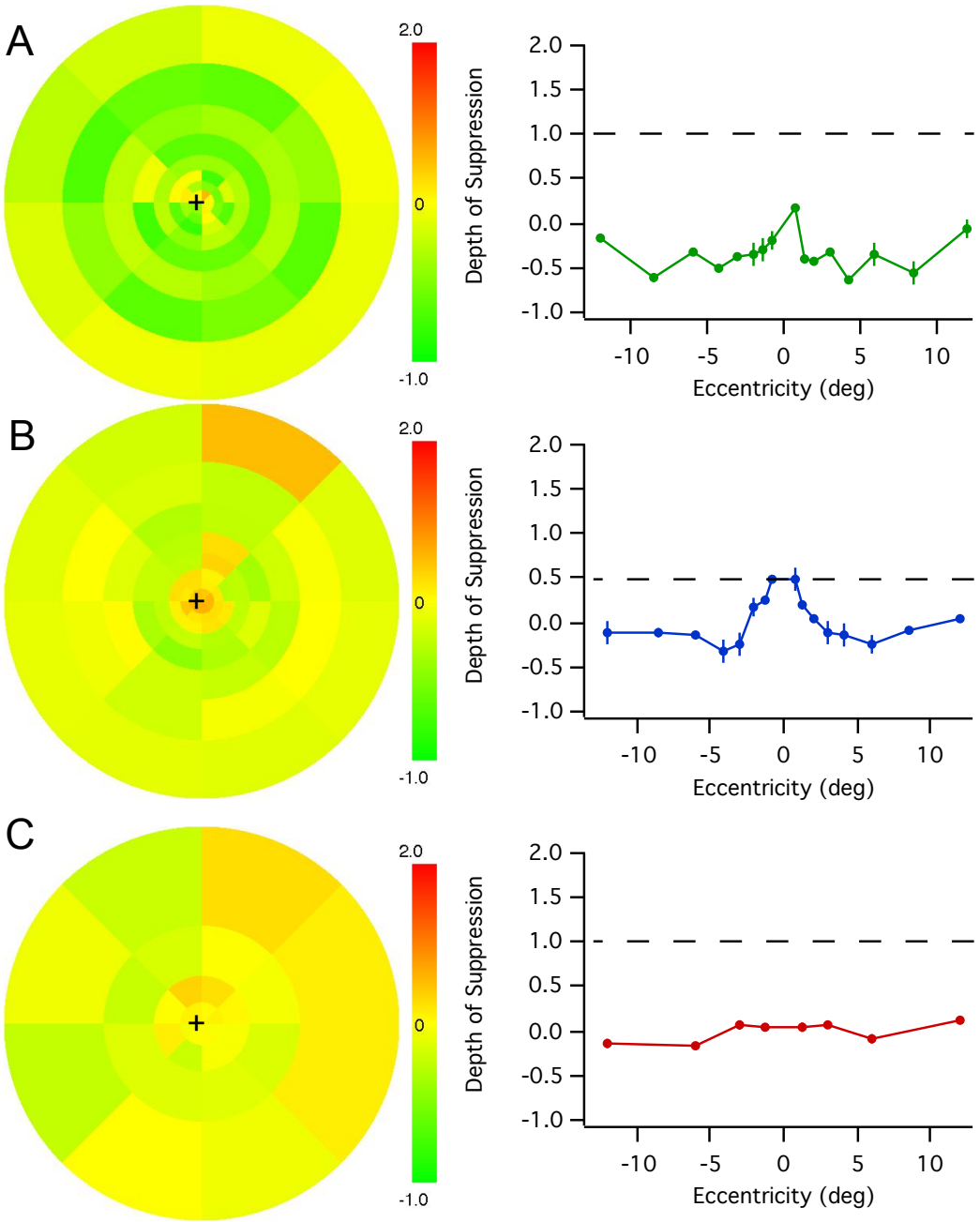

Figure 4.17. Participant AR has anisometropia with LE eccentric fixation and reduced stereoacuity (120''). Visual acuity R 6/4.8-1, L 6/6-1. All other details as in previous Figure.

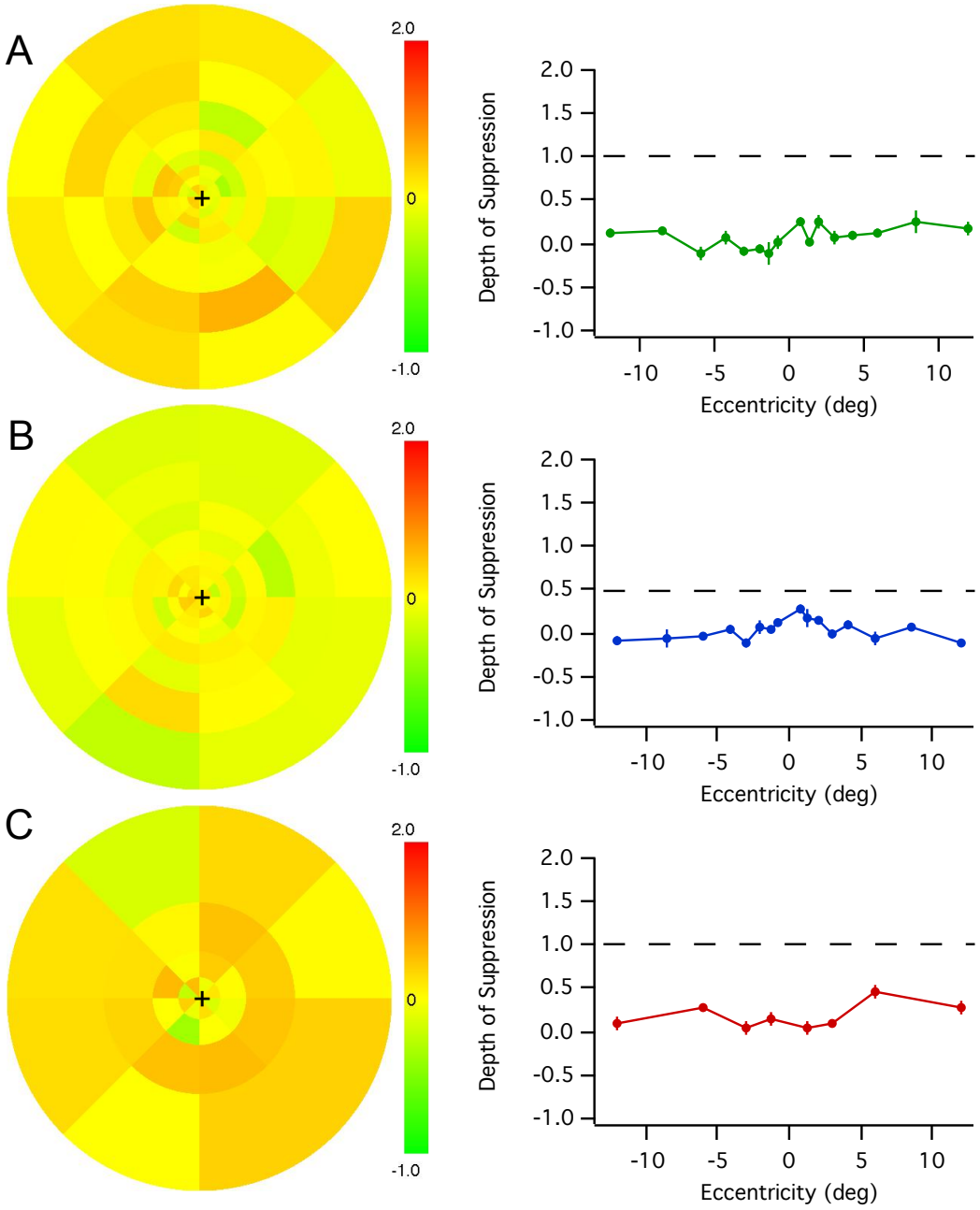

Figure 4.18. Participant AW has a constant manifest 6 prism dioptre left esotropia. Visual acuity R 6/4-2, L 6/5-1. All other details as in previous Figure.

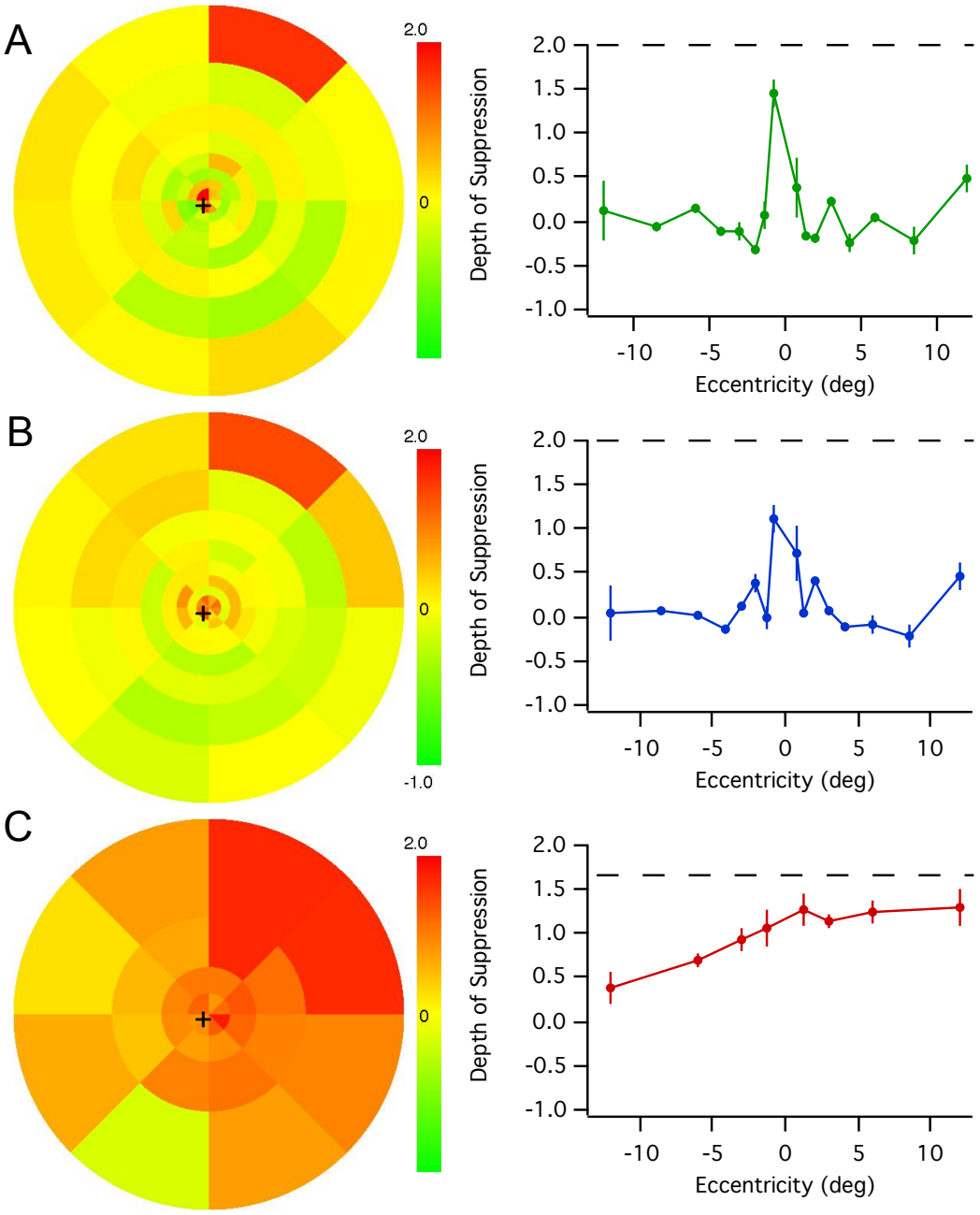

Figure 4.19. Participant DM has no manifest deviation, though has LE temporal eccentric fixation with reduced stereoacuity (120''). Visual acuity R 6/4.8+3, L 6/6-1. All other details as in previous Figure.

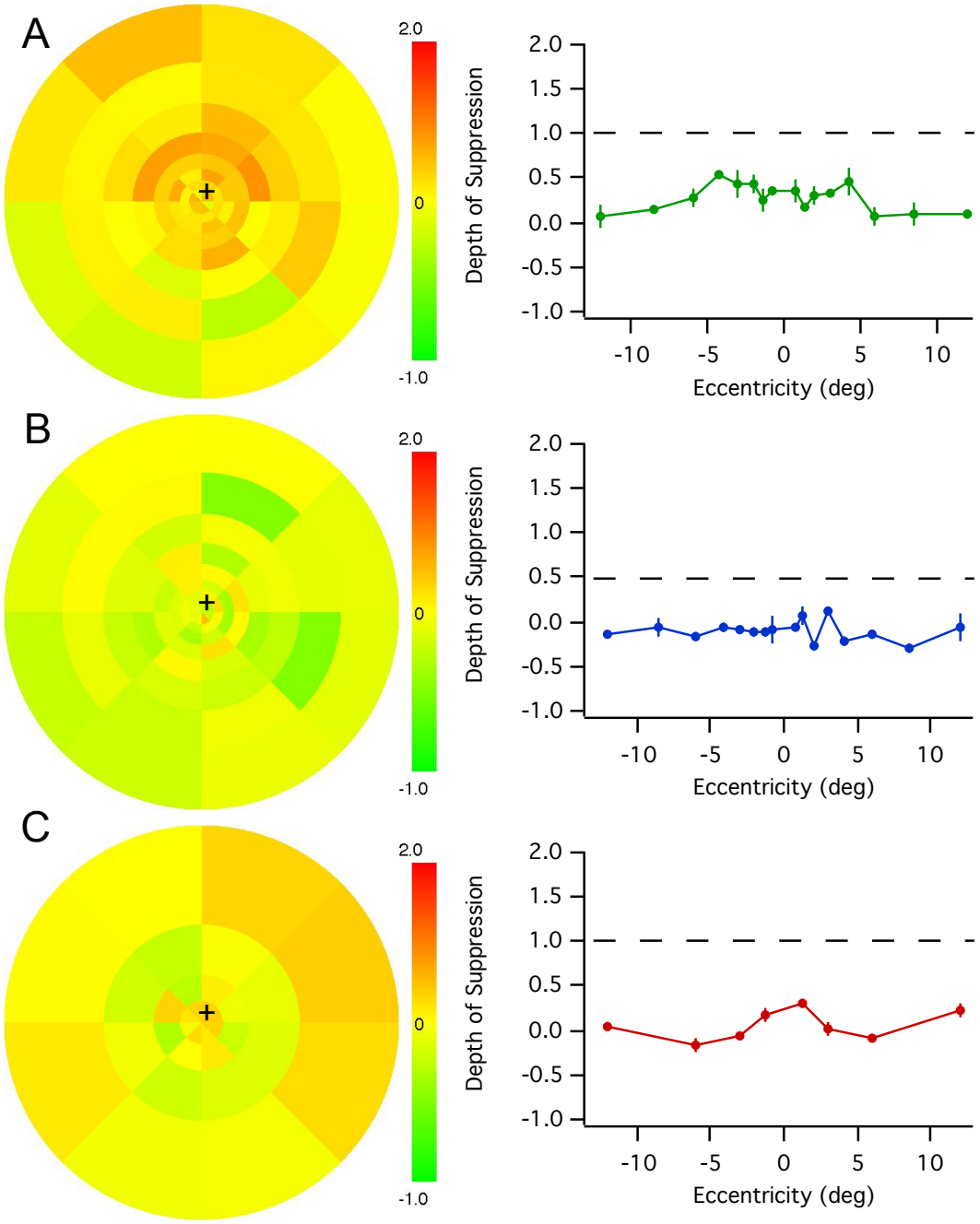

Figure 4.20. Participant IR is an anisometrope with reduced stereoacuity (120'') with no manifest deviation, though had RE eccentric fixation. Visual acuity R 6/7.5, L 6/6. All other details as in previous Figure.

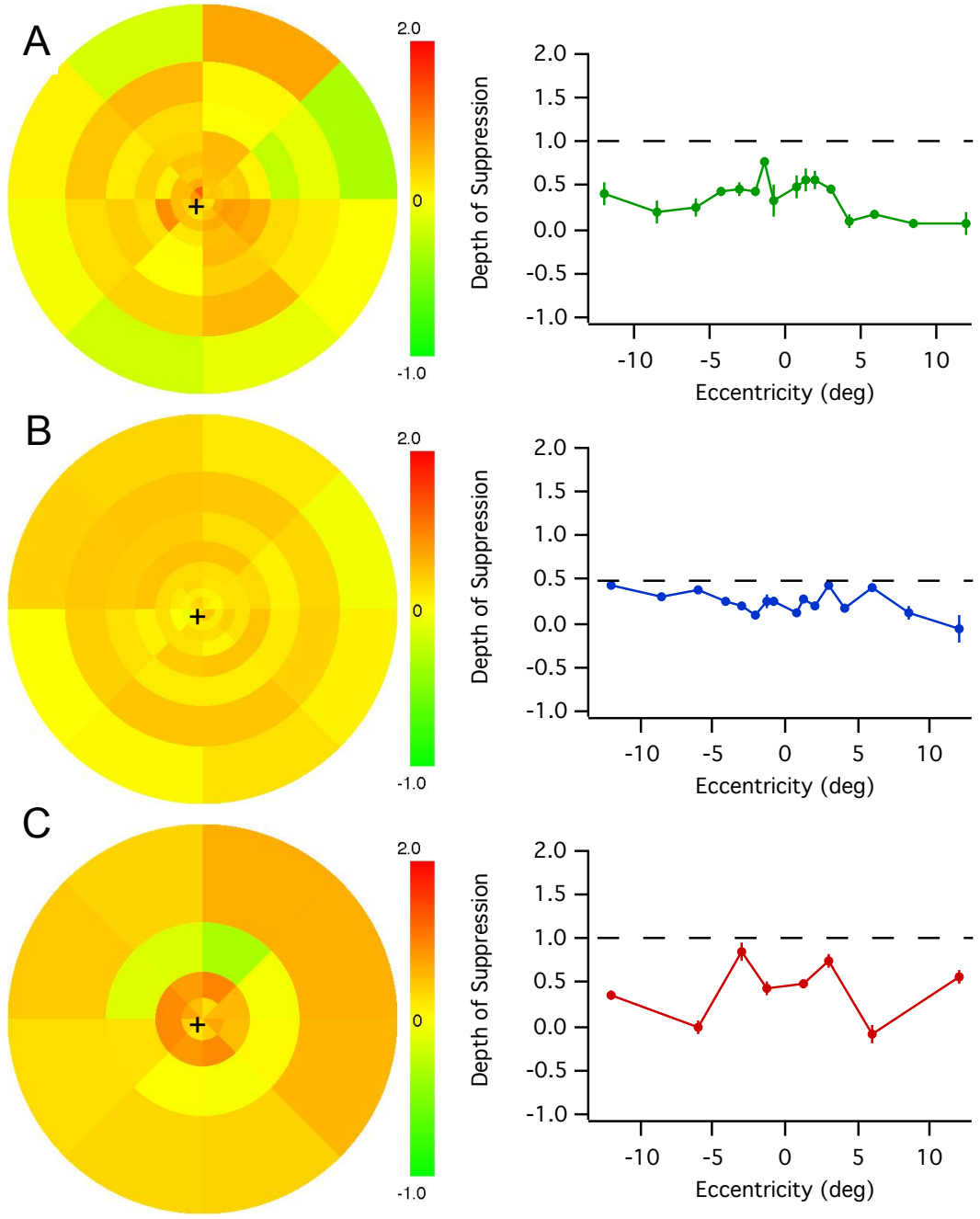

Figure 4.21. Participant NS has reduced stereoacuity (240'') with no manifest deviation with correction (20 prism dioptre right esotropia without correction). Visual acuity R 6/7.5-1, L 6/3.8. All other details as in previous Figure.

CHAPTER 5
SUMMARY OF RESULTS AND CONCLUSIONS

5.1 Results and conclusions

Depth and extent of inter-ocular suppression is measured in three participant groups: in normals with differential inter-ocular blur, normals with inter-ocular luminance difference, and participants with binocular abnormalities. Suppression of noiseless luminance (L), luminance-modulated (LM) and contrast-modulated (CM) noise stimuli is measured for all three groups. The following sections address the specific research aims introduced at the beginning of this thesis (see Chapter 1, Section 1.6).

5.1.1 Developing a suppression mapping tool

One main aim was to develop an accurate and easy to use suppression mapping tool. In Experiments 1 and 2, suppression depth is measured in normal participants with increasing inter-ocular difference caused by monocular blur and monocular ND filters, respectively. Similarly in Experiment 3, a larger inter-ocular acuity difference in participants with abnormal binocular vision shows deeper suppression, comparable to results found in previous studies (Sireteanu and Fronius, 1981; Agrawal et al., 2006; Li et al., 2012; Narasimhan et al., 2012; Babu et al., 2013; Li et al., 2013). In addition, localised suppression scotomata are quantified, and show different patterns across eccentricity similar to those found in previous studies between microstrabismic observers (Sireteanu, et al., 1981; Campos, 1982; Mehdorn, 1989; Babu et al., 2013) and strabismic observers (Travers, 1938; Irvine, 1948; Jampolsky, 1955; Sireteanu et al., 1981; see Chapter 1, 1.4.2 for discussion). These repeatable differences in suppression depths and patterns between participant groups suggest that an accurate method of suppression mapping with a simple paradigm has been successfully developed. The method can therefore be applied to other unilateral pathologies to investigate the extent and depth of suppression scotomata during habitual binocular viewing, e.g. cataract, optic neuritis, and retinal pathologies.

5.1.2 Inter-ocular blur suppression

In Experiment 1, inter-ocular suppression is demonstrated in normals with monocular blur during binocular viewing of all stimulus types, and extends across the visual field with no localised areas within the central circular 24 deg. As inter-ocular blur difference increases, so does suppression depth, suggesting that deeper suppression is required to prevent confusion of the blurred and unblurred images. Figure 5.1 illustrates this for first-order luminance-defined stimuli with luminance-modulated noise (LM – blue) and noiseless luminance (L – green) stimuli with box and whisker plots for each stimulus type. Suppression depth increases at a greater rate with L than LM stimuli. The rate of suppression increase per dioptre of inter-ocular blur (taken as a linear slope fit to data averaged across all participants for each stimulus type) is 0.15±0.042 and 0.11±0.049 for L and LM stimuli, respectively. Therefore, adding dynamic noise reduces measured suppression and reduces the sensitivity of LM stimuli to changes in inter-ocular blur. Suppression is significantly deeper and also deepens at a greater rate with increasing blur for CM stimuli (0.19±0.005) compared with LM stimuli (0.11±0.049) across all levels of blur. Differences in suppression between stimulus types cannot be attributed to variation in stimulus visibility, noise characteristics, or differential effects of blur on stimulus discriminability.

Processing of CM stimuli is thought to be subject to the filter-rectify-filter model (Chubb and Sperling, 1988). Here, a first stage linear filter in V1 detects the luminance noise carrier, and then the CM envelope is rectified before being detected by a second linear filter. Some stage of this model may be served by specific non-linear mechanisms (i.e. rectification), possibly located in an extrastriate area that receives predominantly binocular input. These are different from early striate areas that can process luminance-defined stimuli receiving monocular input only (Zhou and Baker, 1993; Mareschal and Baker, 1998; Baker and Mareschal, 2001). Reduced monocular input with dioptric blur provides an inter-ocular difference that is a suboptimal stimulus for binocular mechanisms, and therefore stimulus strength is increased to a greater degree in CM compared with LM stimuli to break suppression.

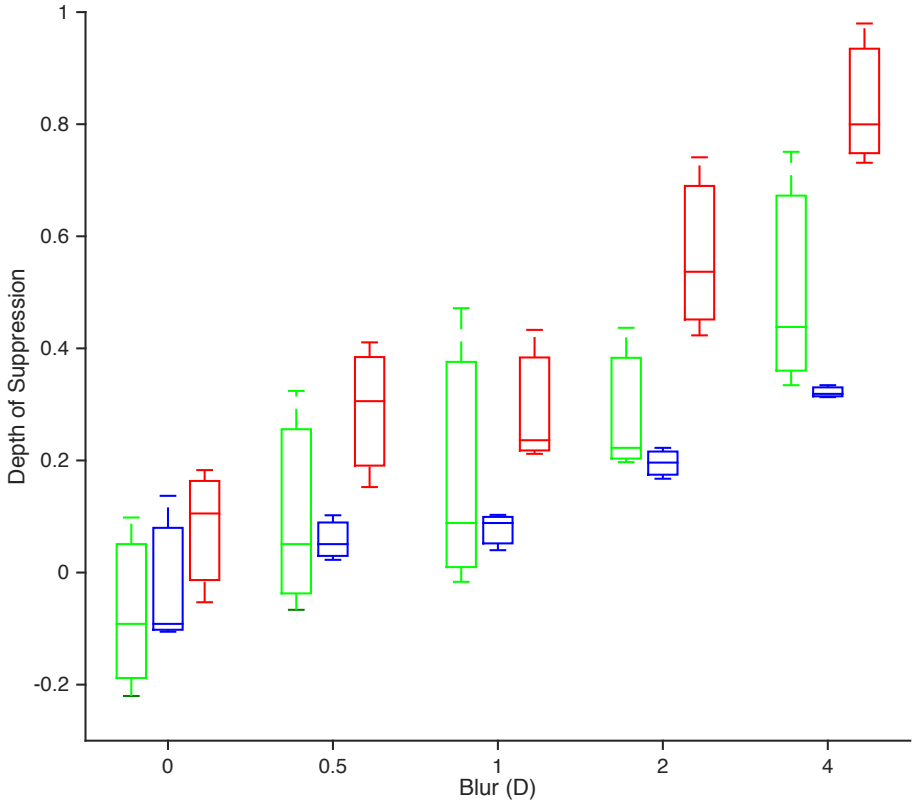

Figure 5.1: Box and whisker plots for L (green), LM (blue), and CM (red) stimulus types for each blur level. Box tops and bottoms show 75th and 25th percentiles, respectively, while the centre line shows the median. Whiskers show maximum and minimum extreme values.

5.1.3 Inter-ocular ND suppression

Similar to the results of Experiment 1, in Experiment 2 measured suppression deepens in normal vision in response to inter-ocular differences in luminance adaptation (by increasing monocular ND strength) for all stimulus types. This is shown in Figure 5.2, where suppression depth is averaged across the visual field and plotted against ND strength for each stimulus type, averaged across participants in box and whisker plots. Suppression deepens at a greater rate (measured by taking the gradient linear functions fit to 0-2 ND data) with L (0.23±0.01) compared to LM stimuli (0.04±0.03), and CM (0.21±0.06) compared to LM stimuli (0.04±0.03) per unit of inter-ocular ND. However, in contrast to inter-ocular blur, measured suppression varies systematically with visual field eccentricity. For all stimuli, deeper suppression is measured centrally compared

to that measured in the periphery. In addition, for L and LM stimuli only, measured suppression is deeper for modulation increment (lighter) compared to modulation decrement (darker) rings. This result suggests that adaptation to ND filters (i.e. attenuated luminance) results in greater sensitivity to local luminance decrements than increments (Kingdom and Whittle, 1996). Similar to blur suppression, adding noise (LM) to noiseless (L) stimuli reduces the measured suppression depth, but also differential increment/decrement suppression is reduced, further suggesting that dynamic noise breaks down suppression.

Due to there being localised areas of suppression measurable with ND filters, unlike the diffuse suppression across the visual field measured with inter-ocular blur, the extent of LM and CM suppression could be compared. Central suppression is spread over a larger area for CM than LM stimuli, and this is true after accounting for differential suppression to LM increments and decrements (there was no difference in suppression between CM increments and decrements). This is thought to be due to larger receptive fields in extrastriate areas that may serve CM envelope extraction (Gattass et al, 1981; Foster et al., 1985; Kennedy et al., 1985; Gattass et al., 1988), compared with earlier, smaller receptive fields for LM extraction.

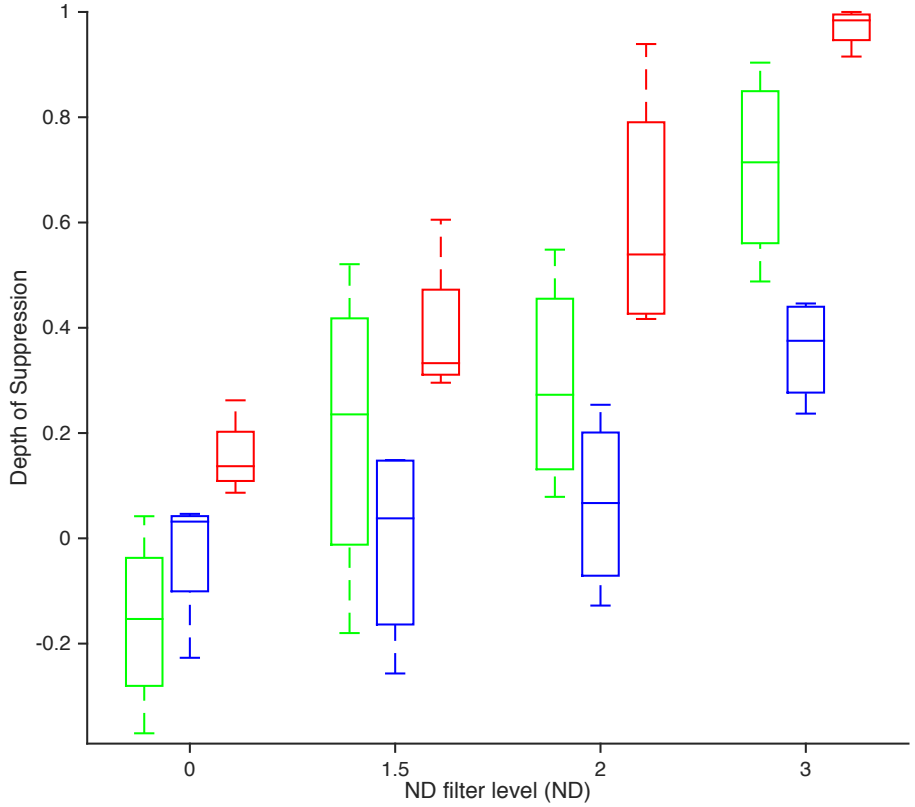

Figure 5.2: Box and whisker plots for L (green), LM (blue), and CM (red) stimulus types for each ND level. Box tops and bottoms show 75th and 25th percentiles, respectively, while the centre line shows the median. Whiskers show maximum and minimum extreme values.

5.1.4 Suppression in binocularly abnormal participants

In the third and final experiment, suppression is measured in participants with microstrabismus and strabismus. Microstrabismic participants show central suppression for L and LM stimuli, agreeing with some previous studies (Sireteanu and Fronius, 1981; Sireteanu et al., 1981; Hallden, 1982) using a variety of techniques, but not others (Campos, 1982; Mehdorn, 1989). This disagreement is most likely due to the level of dissociation of the eyes during the specific suppression test, such that the least dissociation (as with the present suppression mapping tool) causes the greatest (and most comparable to habitual viewing) extent of suppression scotoma to be measured.

Strabismic participants also show central suppression, in addition to deeper suppression measured in one hemifield, agreeing with previous studies (Harms, 1937; Travers, 1938; Jampolsky, 1955; Herzau, 1980; Sireteanu and Fronius, 1981; Sireteanu, Fronius, and Singer, 1981). Similar to the results of Experiments 1 (blur) and 2 (ND filters), addition of noise to first-order noiseless (L) stimuli to give LM stimuli, reduces measured suppression for strabismics participants and suppression is deeper with CM compared with LM stimuli for both strabismic and microstrabismic participants.

For microstrabismic participants, CM suppression is deeper and spread over a larger area than that measured using LM stimuli. Extra stages of processing serving CM stimuli that may occur in areas receiving predominantly binocular input, do not receive correlated binocular information in the participants with abnormal binocular vision, due to their inherent binocular abnormality. It is suggested that due to this abnormal binocular vision, measured CM stimulus suppression is deeper than LM stimuli. Furthermore, larger receptive field sizes responsible for detection of the CM than LM envelope may also be responsible for the greater extent of CM than LM suppression.

5.1.5 Blur and ND filters as models of amblyopic suppression

Suppression maps for both microstrabismic and strabismic participants are compared to those measured in normal participants with different levels of inter-ocular blur and ND across eight eccentricities (Figure 5.3). Only LM and CM stimuli are compared due to different numbers of L sectors between experiments (64 for Experiments 1 and 3, 32 for Experiment 2).

With 1 D inter-ocular blur, a similar average level of suppression across the visual field is seen compared to that measured in the microstrabismic group (Figure 5.3A – open circles versus closed squares, respectively). However, central suppression is not simulated, as suppression with blur is equal across the visual field measured. True central LM suppression would also be deeper than that plotted for microstrabismic participants in Figure 5.3A, as adjacent sectors for microstrabismics and blurred normals are averaged across 16

eccentricities (still covering the central 24 deg, i.e. smaller sectors). In contrast to inter-ocular blur, suppression caused by inter-ocular illuminance difference (open triangles) is deeper in the centre of the visual field. However, measured ND suppression depth is lower than that measured for the microstrabismic group in the periphery, and suppression measured for inter-ocular ND filter suppression is deeper for increments than decrements, as can be seen in the "zig-zag" shape of the suppression curve across the visual field for 1.5 ND. The "ziz-zag" pattern of suppression is not seen in microstrabismic participants.

The diffuse central CM suppression (spread over a larger central area than for LM stimuli) for the microstrabismic group is similar to a 1 D blur and 1.5 ND (Figure 5.3B), suggesting that either of these are good models for CM microstrabismic suppression extent across the visual field. However, measured suppression depth is lower for microstrabismics than normals with 1 D inter-ocular blur. Moreover, slight hemispheric CM suppression is seen with microstrabismic participants, but not in normal participant with inter-ocular blur or inter-ocular ND filter suppression in degraded normal vision.

Strabismic participants (Figure 5.3C and D, closed diamonds) show a pattern of asymmetric suppression across the visual field when measured with LM stimuli, that could not be simulated with either blur or ND filters. The central LM suppression pattern is similar with 2 ND inter-ocular filter difference (Figure 5.3C), although measured suppression is not as deep in normals with ND filters, as it was for the strabismic group. Furthermore, deeper increment than decrement suppression measured with ND filters in normal vision is not seen in microstrabismics. Suppression depth is similar in one half of the visual field with 4 D blur, although as there is no variation in depth across the visual field, central strabismic suppression simulation with ND filters is more accurate than with inter-ocular blur.

Strabismic participants show deeper central CM suppression than microstrabismic participants. This pattern is mimicked well with 2 ND inter-ocular difference in normal vision, although the measured suppression is not as deep as strabismic participants. Inter-ocular 4 D blur in normal participants

show no localised areas of CM suppression. Therefore, strabismic suppression measured with CM stimuli can be simulated more accurately with ND filters inter-ocular difference (above 2 ND) in participants with normal vision.

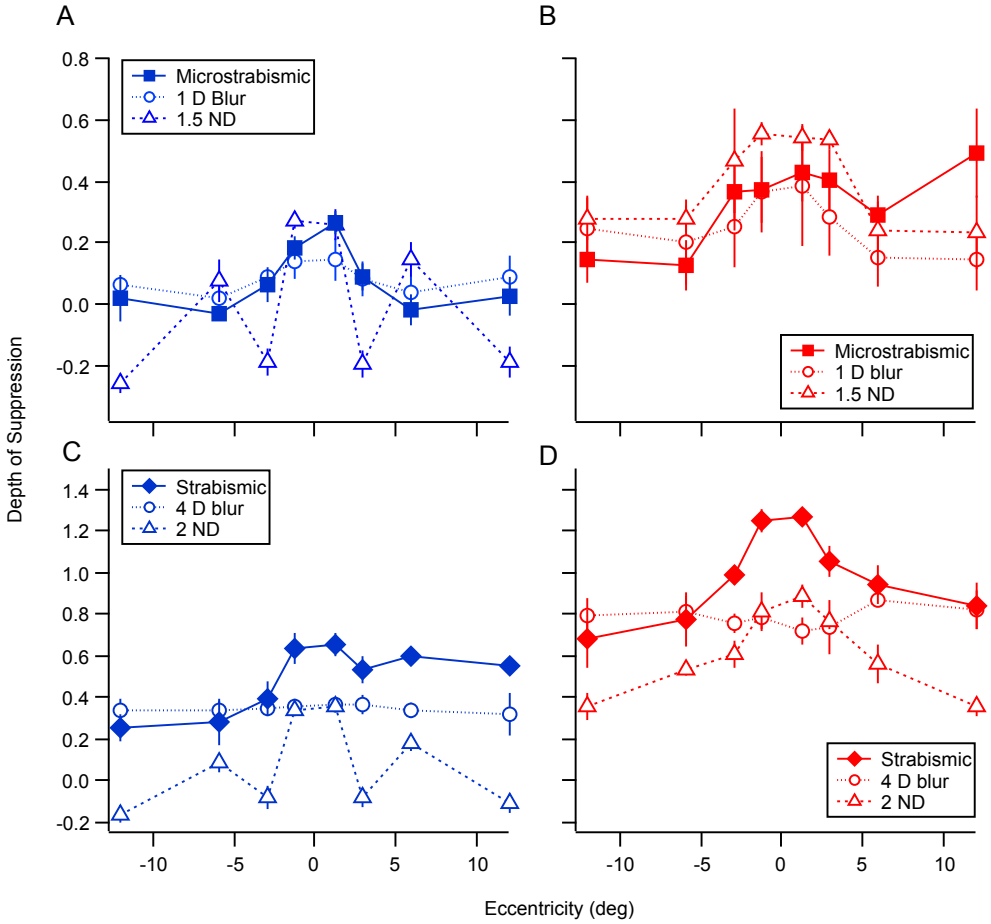

Figure 5.3: Plots of blur (open circles) or ND (open triangles) giving the most similar patterns to microstrabismics (closed squares) with LM (A) or CM (B) stimuli, and strabismics (closed diamonds) with LM (C) or CM (D) stimuli. Data are averaged across four orientations (at each of the eight eccentricities) to represent the horizontal visual field (0 deg is the central visual field).

To assess change in overall suppression depth (averaged across the visual field) with change in inter-ocular visual acuity differences across the experiments, slope values were compared (Figure 5.4). Slope values are obtained by plotting the depth of suppression against inter-ocular acuity difference caused by either inter-ocular blur, inter-ocular retinal illuminance adaptation difference, or by binocular abnormalities. Results are shown in Figure 5.4. Higher slope values indicate that suppression deepens at a greater

rate for L than LM, and CM than LM stimuli for all Experiments (blur, ND filters, and binocular abnormalities). The smallest rate of change occurred with increasing inter-ocular blur, probably due to blur having a large effect on visual acuity (i.e. filtering high spatial frequencies), though less of an effect on the inter-ocular modulation matching task. Slope values were larger for ND than blur, showing deeper suppression for the same inter-ocular visual acuity difference. The greatest rate of change in suppression depth for all stimulus types occurs with amblyopes. This suggests that the degree of amblyopia (i.e. the cortical deficit) contributes more to measured inter-ocular suppression than the normal participants with induced inter-ocular difference (either inter-ocular blur or luminance difference).

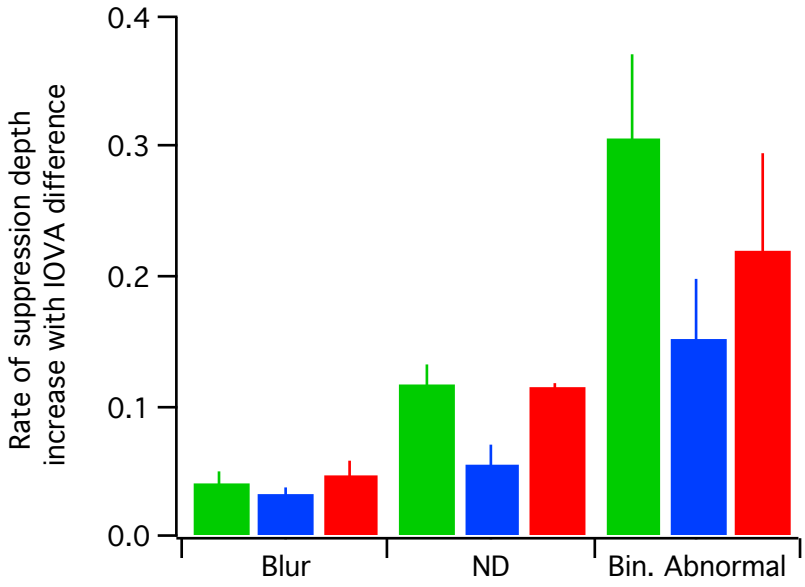

Figure 5.4: Slope values for L (green), LM (blue), and CM (red) stimuli for Experiment 1 (blur), 2 (ND), and 3 (binocularly abnormal). Slope values represent rate of change in suppression depth with increasing inter-ocular visual acuity (IOVA) difference.

As inter-ocular blur in normal participants does not show similar suppression depth to participants with abnormal binocular vision, dioptric blur may not be an appropriate model to mimic anomalous binocular vision, at least for the clinical participants for the dichoptic modulation matching task used in the present study. The results of Experiment 1 can, however, be applied to monovision

contact lens wear, showing that blur within the central 24 deg visual field is suppressed with large inter-ocular acuity differences (up to 4 D). Inter-ocular luminance differences in normal vision (with ND filters) show similar patterns of central suppression to that previously reported in anisometropic amblyopia (as described by other investigators), and also the central suppression of strabismics in the present study. Thus inter-ocular ND filters in normal vision provide a good model for central inter-ocular suppression in strabismic, central microstrabismic suppression, and also central anisometropic amblyopic suppression.

5.1.6 LM versus CM suppression

Deeper suppression measured using CM, compared with LM, stimuli evidenced in the present study's participants with binocular abnormalities, illustrates that suppression differs at different stages of the spatial vision pathway. Both induced (in normals) and inherent binocular abnormalities cause deeper suppression to be measured with CM than with LM stimuli. This lends further support to the supposition that CM stimuli undergo a stage of processing served by binocular mechanisms, with a possible physiological substrate located in extrastriate area V2, similar to that found in cat (Mareschal and Baker, 1998) and monkey (Li et al., 2014a) physiological studies. Therefore, CM stimuli can be employed as a more sensitive detector of suppression in amblyopia, or in those with amblyogenic factors, where binocular abnormality is suspected. Deep suppression in those with larger degrees of amblyopia can also be quantified with LM stimuli, as overall suppression depth is reduced but the pattern of suppression is generally retained. In addition, L stimulus decrements showed shallower suppression than increments, and could thus also be used to quantify deep suppression.

5.2 Future work

Translating the findings of this project to a clinical setting is the principle direction I wish future work to take. A main goal is to carry out suppression mapping on a larger range of those with binocular disruption, namely those who

are clinically defined as amblyopic. This will further current understanding of suppression patterns specific to amblyopia with different aetiologies. Additionally, a larger cohort of amblyopes will reveal whether suppression depth is related to degree of amblyopia. Although this would not prove a causal link, it can point to reducing suppression as a treatment of amblyopia, as is currently being developed. Current methods use repetition of suppression measurements that equate visual input between the two eyes (Hess, Mansouri and Thompson, 2010b; Black et al., 2011; Narasimhan, Harrison and Giaschi, 2012; Li et al., 2014b). However, as the present results show localised suppression areas in the amblyopic visual field, suppression can be targeted locally by repeatedly measuring suppression in these areas.

Recent work has shown effective treatment of suppression in adult amblyopes (Hess, Mansouri and Thompson, 2010b; Black et al., 2012; Ooi, Su, Natale and He, 2013; Mansouri et al., 2014). Although this is a worthy goal for future work, adapting the present suppression mapping technique into a treatment method for child amblyopes is another primary aim. Adaptation would involve changing the technique into a game format to keep the child attentive, ensuring compliance and success of the treatment. Furthermore, the binocular visual field could potentially be measured in those with unilateral conditions, e.g. cataract, diabetic retinopathy, glaucoma, and macular degeneration.

The suppression mapping technique can be adapted to measure suppression of different stimulus types. For example, orientation-modulation and texture suppression could be measured, as well as first- and second-order motion stimuli, in line with other more recent studies measuring suppression with stimuli served by different processing mechanisms. Whereas these studies focus on foveal suppression, or global suppression over a larger area, suppression of different stimuli could be measured in localised areas. This would allow further understanding of visual processing, e.g. suppression and spatial summation areas. Another valuable avenue of future work would be to combine the current suppression mapping technique with electrophysiological recording, monitoring visual evoked potentials as suppression in broken down, i.e. when an inter-ocular modulation match is made.

REFERENCES

Abrahamsson, M. and Sjöstrand, J., 1988. Contrast sensitivity and acuity relationship in strabismic and anisometropic amblyopia. *The British Journal of Ophthalmology*, 72(1), pp.44–49.

Agrawal, R., Conner, I.P., Odom, J., Schwartz, T.L. and Mendola, J.D., 2006. Relating binocular and monocular vision in strabismic and anisometropic amblyopia. *Archives of Ophthalmology*, 124(6), pp.844-850

Albright, T.D., 1992. Form-cue invariant motion processing in primate Visual cortex. *Science*, 255(5048), pp.1141–1143.

Allard, R. and Faubert, J., 2006. Same calculation efficiency but different internal noise for luminance- and contrast-modulated stimuli detection. *Journal of Vision*, 6(4), pp.322–334.

Allard, R. and Faubert, J., 2007. Double dissociation between first- and second-order processing. *Vision Research*, 47(9), pp.1129–1141.

Anderson, R.S. and Thibos, L.N., 1999a. Relationship between acuity for gratings and for tumbling-E letters in peripheral vision. *Journal of the Optical Society of America*, 16(10), pp.2321–2333

Anderson, R.S. and Thibos, L.N., 1999b. Sampling limits and critical bandwidth for letter discrimination in peripheral vision. *Journal of the Optical Society of America,* 16(10), p.2334–2342

Anstis, S.M., 2000. Monocular lustre from flicker. *Vision Research*, 40(19), pp.2551–2556.

Anstis, S.M. and Ho, a, 1998. Nonlinear combination of luminance excursions during flicker, simultaneous contrast, afterimages and binocular fusion. *Vision Research*, 38(4), pp.523–539.

Attebo, K., Mitchell, P., Cumming, R., Smith, W., Jolly, N. and Sparkes, R., 1998. Prevalence and causes of amblyopia in an adult population. *Ophthalmology*, 105(1), pp.154–159.

Aulhorn, E., 1966. Phase difference haploscopy. A new method for the separation of optic impressions of both eyes. *Klinische Monatsblätter für Augenheilkunde*, 148(4), pp.540–544.

Babu, R.J., Clavagnier, S.R., Bobier, W.R., Thompson, B. and Hess, R.F., 2013. The regional extent of suppression: strabismics versus nonstrabismics. *Investigative Ophthalmology and Visual Science*, 54(10), pp.6585–6593.

Back, A., Grant, T. and Hine, N., 1992. Comparative Visual performance of three presbyopic contact lens corrections. *Optometry and Vision Science*, 69(6), pp.474–480.

Bagolini, B., 1967. Anomalous correspondence: Definition and Diagnostic Methods. *Documenta Ophthalmologica. Advances in Ophthalmology*, 23(1), pp.346–386.

Baker, C.L., 1999. Central neural mechanisms for detecting second-order motion. *Current Opinion in Neurobiology*, 9(4), pp.461–466.

Baker, C.L., Li, G., Wang, Z., Yao, Z., Yuan, N., Talebi, V., Tan, J., Wang, Y. and Zhou, Y., 2013. Second-order neuronal responses to contrast modulation stimuli in primate visual cortex. *Journal of Vision*, 13(9), p.41.

Baker, C.L. and Mareschal, I., 2001. Processing of second-order stimuli in the Visual cortex. *Progress in Brain Research*, 134, pp.171–191.

Baker, D.H., Meese, T.S. and Georgeson, M.A., 2007. Binocular interaction: contrast matching and contrast discrimination are predicted by the same model. *Spatial Vision*, 20(5), pp.397–413.

Baker, D.H., Meese, T.S. and Hess, R.F., 2008. Contrast masking in strabismic amblyopia: attenuation, noise, interocular suppression and binocular summation. *Vision Research*, 48(15), pp.1625–1640.

Baker, D.H., Meese, T.S., Mansouri, B. and Hess, R.F., 2007. Binocular summation of contrast remains intact in strabismic amblyopia. *Investigative Ophthalmology and Visual Science*, 48(11), pp.5332–5338.

Baker, D.H., Wallis, S., Georgeson, M.A. and Meese, T.S., 2012. Nonlinearities in the binocular combination of luminance and contrast. *Vision Research*, 56, pp.1–9.

Banks, M.S. and Salapatek, P., 1978. Acuity and contrast sensitivity in 1-, 2-, and 3-month-old human infants. *Investigative Ophthalmology and Visual Science*, 17(4), pp.361–365.

Barbeito, R., Bedell, H.E., Flom, M.C. and Simpson, T.L., 1987. Effects of luminance on the Visual acuity of strabismic and anisometropic amblyopes and optically blurred normals. *Vision Research*, 27(9), pp.1543–1549.

Barlow, H., 2003. The role of single-unit analysis in the past and future of neurobiology. *The Visual Neurosciences*, pp.14–30.

Barlow, H.B., 1953. Summation and inhibition in the frog's retina. *The Journal of Physiology*, 119(1), p.69–88.

Barnes, G.R., Hess, R.F., Dumoulin, S.O., Achtman, R.L. and Pike, G.B., 2001. The cortical deficit in humans with strabismic amblyopia. *The Journal of Physiology*, 533(1), pp.281–297.

Barrett, B.T., Panesar, G.K., Scally, A.J. and Pacey, I.E. 2012. A limited role for suppression in the central field of individuals with strabismic amblyopia. *PloS One*, 7(5), p.e36611.

Barrett, B.T., Panesar, G.K., Scally, A.J. and Pacey, I.E. 2013. Binocular Summation and Other Forms of Non-Dominant Eye Contribution in Individuals with Strabismic Amblyopia during Habitual Viewing. *PloS One*, 8(10), p.e77871.

Bedell, H.E. and Flom, M.C., 1981. Monocular spatial distortion in strabismic amblyopia. *Investigative Ophthalmology and Visual Science*, 20(2), pp.263–268.

De Belsunce, S. and Sireteanu, R., 1991. The time course of interocular suppression in normal and amblyopic subjects. *Investigative Ophthalmology and Visual Science*, 32(9), pp.2645–2652.

Bethune, G., 1846. The Disease Known as Morbid Sensibility of the Retina, Illustrated by Cases. *Boston Medical Journal*, 35, pp.341–343.

Bhola, R., Keech, R. V, Kutschke, P., Pfeifer, W. and Scott, W.E., 2006. Recurrence of amblyopia after occlusion therapy. *Ophthalmology*, 113(11), pp.2097–2100.

Bi, H., Zhang, B., Tao, X., Harwerth, R.S., Smith, E.L. and Chino, Y.M., 2011. Neuronal responses in Visual area V2 (V2) of macaque monkeys with strabismic amblyopia. *Cerebral cortex,* 21(9), pp.2033–2045.

Black, J.M., Hess, R.F., Cooperstock, J.R., To, L. and Thompson, B., 2012. The measurement and treatment of suppression in amblyopia. *Journal of Visualized Experiments*, (70), p.e3927.

Black, J.M., Thompson, B., Maehara, G. and Hess, R.F., 2011. A compact clinical instrument for quantifying suppression, *Optometry and Vision Science*, 88(2), pp.E334–343.

Blake, R., O'Shea, R.P. and Mueller, T.J., 1992. Spatial zones of binocular rivalry in central and peripheral vision. *Visual Neuroscience*, 8(5), pp.469–478.

Bradley, A. and Freeman, R.D., 1981. Contrast sensitivity in anisometropic amblyopia. *Investigative Ophthalmology and Visual Science*, 21(3), pp.467–476.

Brainard, D.H., 1997. The Psychophysics Toolbox. *Spatial Vision*, 10(4), pp.433–436.

Burian, H., 1947. Sensorial retinal relationship in concomitant strabismus. *Archives of Ophthalmology*, pp.373–494.

Campbell, F.W. and Green, D., 1965. Monocular versus Binocular Visual Acuity. *Nature*, 208, pp.191-192

Campbell, F.W. and Robson, J., 1968. Application of Fourier analysis to the visibility of gratings. *The Journal of Physiology*, 197, pp.551–566.

Campos, E., 1982. Binocularity in comitant strabismus: binocular visual fields studies. *Documenta Ophthalmologica*, 53(3), pp.249–281.

Chalmers, D.J., 1995. Facing up to the problem of consciousness. *Journal of Consciousness Studies*, 2(3), pp.200-219.

Chima, A.S., Formankiewicz, M.A., and Waugh, S.J., 2015. Investigation of interocular blur suppression using luminance- modulated and contrast-modulated noise stimuli. *Journal of Vision*, 15(3), pp.1–22.

Chubb, C. and Sperling, G., 1988. Drift-balanced random stimuli: a general basis for studying non-Fourier motion perception. *Journal of the Optical Society of America. A, Optics and Image Science*, 5(11), pp.1986–2007.

Chung, S.T.L., Li, R.W. and Levi, D.M., 2006. Identification of contrast-defined letters benefits from perceptual learning in adults with amblyopia. *Vision Research*, 46(22), pp.3853–3861.

Cohen, A.H., 1981. Monocular fixation in a binocular field. *Journal of the American Optometric Association*, 52(10), pp.801–806.

Collins, M. and Goode, A., 1994. Interocular blur suppression and monovision. *Acta Ophthalmologica*, 72(3), pp.376–380.

Conner, I.P., Odom, J.V., Schwartz, T.L. and Mendola, J.D., 2007. Retinotopic maps and foveal suppression in the visual cortex of amblyopic adults. *The Journal of Physiology*, 583(Pt 1), pp.159–173.

Cooper, E.A., Jiang, H., Vildavski, V., Farrell, J.E. and Norcia, A.M., 2013. Assessment of OLED displays for vision research. *Journal of Vision*, 13(12), pp.1–13.

Crawford, M.L.J., Smith, E.L., Harwerth, R.S. and Von Noorden, G.K., 1984. Stereoblind monkeys have few binocular neurons. *Investigative Ophthalmology and Visual Science*, 25(July), pp.1983–1985.

Curcio, C.A., Sloan, K.R., Kalina, R.E. and Hendrickson, A.E., 1990. Human photoreceptor topography. *The Journal of comparative neurology*, 292(4), pp.497–523.

Daniel, P. and Whitteridge, D., 1961. The representation of the visual field on the cerebral cortex in monkeys. *The Journal of Physiology*, 159(2), pp.203–221.

Daw, N.W., 2006. *Visual development*. 2nd ed. *Medicine*, New York: Springer, p.268.

Ding, J., Klein, S. and Levi, D.M., 2013a. Binocular combination in abnormal binocular vision. *Journal of Vision*, 13(2), pp.1–31.

Ding, J., Klein, S. and Levi, D.M., 2013b. Binocular combination of phase and contrast explained by a gain-control and gain-enhancement model. *Journal of Vision*, 13(2), pp.1–37.

Ding, J. and Levi, D.M., 2014. Rebalancing binocular vision in amblyopia. *Ophthalmic and Physiological Optics,* 34(2), pp.199-213

Ellemberg, D., Allen, H. and Hess, R.F., 2004. Investigating local network interactions underlying first- and second-order processing. *Vision Research*, 44(15), pp.1787–1797.

Ellemberg, D., Allen, H. and Hess, R.F., 2006. Second-order spatial frequency and orientation channels in human vision. *Vision Research*, 46(17), pp.2798–2803.

Evans, B.J.W., 2007. Monovision: a review. *Ophthalmic and Physiological Optics,* 27(5), pp.417–439.

Fahle, M., 1983. Non-fusable stimuli and the role of binocular inhibition in normal and pathologic vision, especially strabismus. *Documenta Ophthalmologica*, 55(4), pp.323–340.

Farivar, R., Thompson, B., Mansouri, B. and Hess, R., 2011. Interocular suppression in strabismic amblyopia results in an attenuated and delayed hemodynamic response function in early visual cortex. *Journal of Vision*, 11(14), pp.1–12.

Fink, W.H., 1938. The dominant eye: Its clinical significance. *Archives of Ophthalmology*, 19(4), p.555–582.

Fiorentini, A., Maffei, L., Pirchio, M. and Spinelli, D., 1978. An electrophysiological correlate of perceptual suppression in anisometropia. *Vision Research*, 18(12), pp.1617–1621.

Flom, M.C. and Neumaier, R., 1966. Prevalence of amblyopia. *Public Health Reports*, 81(4), pp.329–342.

Flom, M.C., Weymoth, F.W. and Kahneman, D., 1963. Visual Resolution and Contour Interaction. *Journal of the Optical Society of America*, 53(9), pp.1026-1032.

Formankiewicz, M. a and Waugh, S.J., 2013. The effects of blur and eccentric viewing on adult acuity for pediatric tests: implications for amblyopia detection. *Investigative Ophthalmology and Visual Science*, 54(10), pp.6934–6943.

Foster, K.H., Gaska, J.P., Nagler, M. and Pollen, D., 1985. Spatial and temporal frequency selectivity of neirones in visual cortical areas V1 and V2 of the macaque monkey. *Journal of Physiology*, 365, pp.331–363.

Gao, Y., Reynaud, A., Tang, Y., Feng, L., Zhou, Y. and Hess, R.F., 2014. The amblyopic deficit for 2nd order processing: Generality and laterality. *Vision Research*. [Epub ahead of print].

Gattass, R., Gross, C.G. and Sandell, J.H., 1981. Visual topography of V2 in the macaque. *The Journal of comparative neurology*, 201(4), pp.519–539.

Gattass, R., Sousa, a P. and Gross, C.G., 1988. Visuotopic organization and extent of V3 and V4 of the macaque. *The Journal of Neuroscience*, 8(6), pp.1831–1845.

Geisler, W.S. and Albrecht, D.G., 1997. Visual cortex neurons in monkeys and cats: detection, discrimination, and identification. *Visual Neuroscience*, 14(5), pp.897–919.

Georgeson, M.A. and Schofield, A.J, 2011. Binocular functional architecture for detection of luminance- and contrast-modulated gratings. *Journal of Vision*, 11(11), pp.305–305.

Glickstein, M. and Whitteridge, D., 1987. Tatsuji Inouye and the mapping of the visual fields on the human cerebral cortex. *Trends in Neurosciences*, 10(9), pp.350–353.

Godts, D., Trau, R. and Tassignon, M.-J., 2006. Effect of refractive surgery on binocular vision and ocular alignment in patients with manifest or intermittent strabismus. *The British Journal of Ophthalmology*, 90(11), pp.1410–3.

Goodman, L.K., Black, J.M., Phillips, G., Hess, R.F. and Thompson, B., 2011. Excitatory binocular interactions in two cases of alternating strabismus. *Journal of AAPOS*, 15(4), pp.345–349.

Goodwin, R.T. and Romano, P.E., 1985. Stereoacuity degradation by experimental and real monocular and binocular amblyopia. *Investigative Ophthalmology and Visual Science*, 26(7), pp.917–23.

Gottlob, I., Charlier, J. and Reinecke, R.D., 1992. Visual acuities and scotomas after one week levodopa administration in human amblyopia. *Investigative Ophthalmology and Visual Science*, 33(9), pp.2722–278.

Von Graefe, A., 1856. Ueber die Untersuchung des Gesichtsfeldes bei amblyopischen Affectionen. *Archiv für Ophthalmologie*, 2(2), pp.258 – 298.

Le Gros Clark, W. and Penman, G., 1934. The Projection of the Retina in the Lateral Geniculate Body. *Proceedings of the Royal Society of London,* 114(788), pp.291–313.

Guillery, R.W., 1967. Patterns of fiber degeneration in the dorsal lateral geniculate nucleus of the cat following lesions in the visual cortex. *The Journal of Comparative Neurology*, 130(3), pp.197–221.

Hairol, M.I. and Waugh, S.J., 2010. Lateral facilitation revealed dichoptically for luminance-modulated and contrast-modulated stimuli. *Vision Research*, 50(23), pp.2530–2542.

Hallden, U., 1982. Suppression scotomata in concomitatnt. *Acta Ophthalmologica*, 60(5), pp.828–834.

Harms, H., 1937. Ort und Wesen der Bildhemmung bei Schielenden, *Archiv für Ophthalmologie*, 138(1-2), pp.149–210.

Harrad, R.A., 1996. Psychophysics of suppression. *Eye (London, England)*, 10 (Pt 2), pp.270–273.

Harrad, R.A., Sengpiel, F. and Blakemore, C., 1996. Physiology of suppression in strabismic amblyopia. *The British Journal of Ophthalmology*, 80(4), pp.373–377.

Harwerth, R.S., Smith, E.L. and Levi, D.M., 1980. Suprathreshold binocular interactions for grating patterns. *Attention, Perception, and Psychophysics*, 27(1), pp.43–50.

Held, R., Birch, E. and Gwiazda, J., 1980. Stereoacuity of human infants. *Proceedings of the National Academy of Sciences*, 77(9), pp.5572–5574.

Helmholtz, H., 1925. *Treatise on physiological optics. III. The perceptions of vision.* New York: Thoemmes, pp.512–516.

Helveston, E.M. and von Noorden, G K. Microtropia: A newly defined entitiy. *Archives of Ophthalmology*, 78(3), pp.272–281.

Hendry, S. and Reid, R., 2000. The koniocellular pathway in primate vision. *Annual Review of Neuroscience*, 23, pp.127–153.

Henson, D.B. and Williams, D.E., 1980. Depth perception in strabismus. *British Journal of Ophthalmology*, 64(5), pp.349–353.

Heravian-Shandiz, J., Douthwaite, W.A. and Jenkins, T.C.A., 1991. Binocular interaction with neutral density filters as measured by the visual evoked responses. *Optometry and Vision Science*, 68(10), pp.801–806.

Herzau, V., 1980. Untersuchungen über das binokulare Gesichtsfeld Schielender. *Documenta Ophthalmologica*, 284, pp.221–284.

Hess, R.F., 2001. Amblyopia: site unseen. *Clinical and Experimental Optometry*, 84(6), pp.321–336.

Hess, R.F., Babu, R.J., Clavagnier, S.R., Black, J., Bobier, W.R. and Thompson, B., 2014. The iPod binocular home-based treatment for amblyopia in adults: efficacy and compliance. *Clinical and Experimental Optometry*, 97(5), pp.389–398.

Hess, R.F., Campbell, F. and Zimmern, R., 1980. Differences in the neural basis of human amblyopias: the effect of mean luminance. *Vision Research*, 20(4), pp.295–305.

Hess, R.F. and Howell, E.R., 1977. The threshold contrast sensitivity function in strabismic amblyopia: evidence for a two type classification. *Vision Research*, 17(9), pp.1049–55.

Hess, R.F. and Jacobs, R., 1979. A preliminary report of acuity and contour interactions across the amblyope's visual field. *Vision Research*, 19(12), pp.1403–1408.

Hess, R.F., Li, X., Mansouri, B., Thompson, B. and Hansen, B.C., 2009a. Selectivity as well as sensitivity loss characterizes the cortical spatial frequency deficit in amblyopia. *Human brain mapping*, 30(12), pp.4054–4069.

Hess, R.F., Mansouri, B. and Thompson, B., 2010a. A binocular approach to treating amblyopia: antisuppression therapy. *Optometry and Vision Science : official publication of the American Academy of Optometry*, 87(9), pp.697–704.

Hess, R.F., Mansouri, B. and Thompson, B., 2010b. A new binocular approach to the treatment of amblyopia in adults well beyond the critical period of visual development. *Restorative Neurology and Neuroscience*, 28(6), pp.793–802.

Hess, R.F., Mansouri, B., Thompson, B. and Gheorghiu, E., 2009b. Latent stereopsis for motion in depth in strabismic amblyopia. *Investigative Ophthalmology and Visual Science*, 50(10), pp.5006–5016.

Hess, R.F., Pointer, J.S., Simmers, A.J. and Bex, P., 2003. Border distinctness in amblyopia. *Vision Research*, 43(21), pp.2255–2264.

Hess, R.F., Thompson, B., Gole, G. and Mullen, K.T., 2009c. Deficient responses from the lateral geniculate nucleus in humans with amblyopia. *The European Journal of Neuroscience*, 29(5), pp.1064–1070.

Von der Heydt, R., Peterhans, E. and Baumgartner, G., 1984. Illusory contours and cortical neuron respones. *Science*, 224(4654), pp.1260–1262.

Holopigian, K., 1989. Clinical suppression and binocular rivalry suppression: the effects of stimulus strength on the depth of suppression. *Vision Research*, 29(10), pp.1325–1333.

Holopigian, K., Blake, R. and Greenwald, M., 1988. Clinical suppression and amblyopia. *Investigative Ophthalmology and Visual Science*, 29(3), pp.444-451.

Horton, J.C. and Hocking, D.R., 1996. Pattern of ocular dominance columns in human striate cortex in strabismic amblyopia. *Visual Neuroscience*, 13(4), pp.787–795.

Huang, C., Zhou, J., Lu, Z., Feng, L. and Zhou, Y., 2009. Binocular combination in anisometropic amblyopia. *Journal of Vision*, 9(3), pp.1–16.

Hubel, D. and Wiesel, T., 1977. Ferrier lecture: Functional architecture of macaque monkey visual cortex. *Proceedings of the Royal Society of London*, 198(1130), pp.1–59.

Hubel, D.H. and Wiesel, T.N., 1959. Receptive Fields of Single Neurones in the Cat's Striate Cortex. *Journal of Physiology*, 148(3), pp.574–591.

Hubel, D.H. and Wiesel, T.N., 1960. Receptive fields of optic nerve fibres in the spider monkey. *The Journal of physiology*, 154(3), pp.572–580.

Hubel, D.H. and Wiesel, T.N., 1965. Binocular interaction in striate cortex of kittens reared with artificial squint. *Journal of Neurophysiology*, 28(6), pp.1041–1059.

Hubel, D.H., Wiesel, T.N. and LeVay, S., 1977. Plasticity of ocular dominance columns in monkey striate cortex. *Philosophical transactions of the Royal Society of London. Series B, Biological Sciences*, 278(961), pp.377–409.

Irvine, S., 1948. Amblyopia ex anopsia. Observations on retinal inhibition, scotoma, projection, light difference discrimination and visual acuity. *Transactions of the American Ophthalmological Society*, 46, pp.527–575.

Jain, S., Arora, I. and Azar, D.T., 1996. Success of Monovision in Presbyopes : Review of the Literature and Potential Applications to Refractive Surgery. *Survey of Ophthalmology*, 40(6), pp.491–499.

Jalie, M., 2003. *Ophthalmic lenses and dispensing*. 2nd ed. Oxford: Butterworth-Heinemann.

Jampolsky, A., 1955. Characteristics of Suppression in Strabismus. *Archives of Ophthalmology*, 54(5), pp.683–696.

Johannsdottir, K.R. and Stelmach, L.B., 2001. Monovision: a review of the scientific literature. *Optometry and Vision Science,* 78(9), pp.646–651.

Johnson, W., 1893. Suppression of the Visual Image. *Transactions of the American Ophthalmological*, 6, pp.551–559.

Joly, O. and Frankó, E., 2014. Neuroimaging of amblyopia and binocular vision: a review. *Frontiers in Integrative Neuroscience*, 8(62), pp.1–10.

Joosse, M. V, Simonsz, H.J. and Jong, de P.T.V.M., 2000. The visual field in strabismus: a historical review of studies on amblyopia and suppression. *Strabismus*, 8, pp.135–149.

Joosse, M. V, Simonsz, H.J., van Minderhout, E.M., Mulder, P.G. and de Jong, P.T., 1999. Quantitative visual fields under binocular viewing conditions in primary and consecutive divergent strabismus. *Albrecht von Graefes Archiv für Klinische und Experimentelle Ophthalmologie*, 237(7), pp.535–545.

Joosse, M. V, Simonsz, H.J., van Minderhout, H.M., de Jong, P.T., Noordzij, B. and Mulder, P.G., 1997. Quantitative perimetry under binocular viewing conditions in microstrabismus. *Vision Research*, 37(19), pp.2801–2812.

Kandel, E., Schwartz, J. and Jessell, T., 2000. *Principles of Neural Science*. 4th ed. *Beijing: Publishing House of Beijing Medical University,* New York: McGraw-Hill.

Kennedy, H., Martin, K.A., Orban, G.A. and Whitteridge, D., 1985. Receptive field properties of neurones in visual area 1 and visual area 2 in the baboon. *Neuroscience*, 14(2), pp.405–415.

Kilwinger, S., Spekreijse, H. and Simonsz, H.J., 2002. Strabismic suppression depends on the amount of dissimilarity between left- and right-eye images. *Vision Research*, 42(16), pp.2005–2011.

Kingdom, F.A. and Whittle, P., 1996. Contrast discrimination at high contrasts reveals the influence of local light adaptation on contrast processing. *Vision Research*, 36(6), pp.817–829.

Kiorpes, L., Kiper, D.C., O'Keefe, L.P., Cavanaugh, J.R. and Movshon, J.A., 1998. Neuronal Correlates of Amblyopia in the Visual Cortex of Macaque Monkeys with Experimental Strabismus and Anisometropia. *Journal of Neuroscience*, 18(16), pp.6411–6424.

Kirschen, D.G., Hung, C. and Nakano, T., 1999. Comparison of suppression, stereoacuity, and interocular differneces in visual acuity in monovision and Acuvue Biforcal Contact Lenses. *Optometry and Vision Science*, 76(12), pp.832–837.

Knowles, E.J. and Griffiths, H.J., 2003. Evaluation of the Sbisa bar for the measurement of sensory fusion. *The British Journal of Ophthalmology,* 60, pp.45–48.

Knox, P.J., Simmers, A.J., Gray, L.S. and Cleary, M., 2012. An exploratory study: prolonged periods of binocular stimulation can provide an effective treatment for childhood amblyopia. *Investigative Ophthalmology and Visual Science*, 53(2), pp.817–824.

Kukkonen, H., Rovamo, J. and Näsänen, R., 1995. Masking potency and whiteness of noise at various noise check sizes. *Investigative Ophthalmology and Visual Science*, 36(2), pp.513–518.

Lang, J., 1971. Binocular Amsler's charts. *The British Journal of Ophthalmology*, 55, pp.284–286.

Lang, J., 1974. Management of microtropia. *The British Journal of Ophthalmology*, 58(3), pp.281–292.

Larsson, J., Landy, M. and Heeger, D., 2006. Orientation-selective adaptation to first- and second-order patterns in human visual cortex. *Journal of Neurophysiology*, 95(2), pp.862–881.

Leaney, J., Klistorner, A., Arvind, H. and Graham, S.L., 2010. Dichoptic suppression of mfVEP amplitude: effect of retinal eccentricity and simulated unilateral visual impairment. *Investigative Ophthalmology and Visual Science*, 51(12), pp.6549–6555.

Lee, B.B., Smith, V.C., Pokorny, J. and Kremers, J., 1997. Rod inputs to macaque ganglion cells. *Vision Research*, 37(20), pp.2813–2128.

Legge, G.E., 1984. Binocular contrast summation--II. Quadratic summation. *Vision Research*, 24(4), pp.385–394.

Legge, G.E. and Foley, M., 1980. Contrast Masking in Human Vision. *Journal of the Optical Society of America*, 70(12), pp.1458–1470.

Legge, G.E. and Kersten, D., 1987. Contrast discrimination in peripheral vision. *Journal of the Optical Society of America*, 4(8), pp.1594–1598.

Legge, G.E. and Rubin, G.S., 1981. Binocular interactions in suprathreshold contrast perception. *Perception and Psychophysics*, 30(1), pp.49–61.

Leonards, U. and Sireteanu, R., 1993. Interocular suppression in normal and amblyopic subjects : The effect of unilateral. *Perception*, 54(1), pp.65–74.

Levelt, W.J., 1965. Binocular Brightness Averaging and Contour Information. *British Journal of Psychology*, 56(1965), pp.1–13.

Levelt, W.J., 1968. *On binocular rivalry*. Soesterberg, The Netherlands: Institute for Perception RVO-TNO, pp.1-110.

Leventhal, A.G., Wang, Y., Schmolesky, M.T. and Zhou, Y., 1998. Neural correlates of boundary perception. *Visual Neuroscience*, 15(6), pp.1107–1118.

Levi, D.M., Hariharan, S. and Klein, S., 2002. Suppressive and facilitatory spatial interactions in amblyopic vision. *Vision Research*, 42(11), pp.1379–1394.

Levi, D.M. and Harwerth, R.S., 1977. Spatio-temporal Interactions In Anisometropic and Strabismic Amblyopia. *Investigative Ophthalmology and Visual Science*, 16(1), pp.90–95.

Levi, D.M., Harwerth, R.S. and Manny, R.E., 1979. Suprathreshold spatial frequency detection and binocular interaction in strabismic and anisometropic amblyopia. *Investigative Ophthalmology and Visual Science*, 18(7), pp.714–25.

Levi, D.M., Harwerth, R.S. and Smith, E.L., 1980. Binocular Interaction in Normal and Anomalous Binocular Vision. *Documenta Ophthalmologica*, 49, pp.303–324.

Levi, D.M. and Klein, S., 1982a. Differences in vernier discrimination for grating between strabismic and anisometropic amblyopes. *Investigative Ophthalmology and Visual Science*, 23(3), pp.398–407.

Levi, D.M. and Klein, S., 1982b. Hyperacuity and amblyopia. *Nature*, 298, pp.268–270.

Levi, D.M. and Klein, S., 1985. Vernier acuity, crowding and amblyopia. *Vision Research*, 25(7), pp.979–91.

Levi, D.M. and Klein, S., 1990a. Equivalent intrinsic blur in amblyopia. *Vision Research*, 30(12), pp.1995–2022.

Levi, D.M. and Klein, S., 1990b. Equivalent intrinsic blur in spatial vision. *Vision Research*, 30(12), pp.1971–1993.

Levi, D.M. and Klein, S., 2003. Noise provides some new signals about the spatial vision of amblyopes. *The Journal of Neuroscience*, 23(7), pp.2522–2526.

Levi, D.M., Klein, S. and Aitsebaomo, A., 1985. Vernier acuity, crowding and cortical magnification. *Vision Research*, 25(7), pp.963–977.

Levi, D.M., Klein, S. and Yap, Y., 1987. Positional uncertainty in peripehral and amblyopic vision. *Vision Research*, 21(4), pp.581–597.

Levi, D.M., McKee, S.P. and Movshon, J.A., 2011. Visual deficits in anisometropia. *Vision Research*, 51(1), pp.48–57.

Li, G., Yao, Z., Wang, Z., Yuan, N., Talebi, V., Tanb, J., Y, W., Zhou, Y. and Baker, C.L., 2014. Form-Cue Invariant Second-Order Neuronal Responses to Contrast Modulation in Primate Area V2. *Journal Neuroscience*, 34(36), pp.12081–12092.

Li, J., Hess, R.F., Chan, L.Y.L., Deng, D., Yang, X., Chen, X., Yu, M. and Thompson, B., 2013. Quantitative Measurement of Interocular Suppression in Anisometropic Amblyopia: A Case-Control Study. *Ophthalmology*, 120(8), pp.1–9.

Li, J., Lam, C.S.Y., Yu, M., Hess, R.F., Chan, L.Y.L., Maehara, G., Woo, G.C. and Thompson, B., 2010. Quantifying sensory eye dominance in the normal visual system: a new technique and insights into variation across traditional tests. *Investigative Ophthalmology and Visual Science*, 51(12), pp.6875–6881.

Li, J., Thompson, B., Ding, Z., Chan, L.Y.L., Chen, X., Yu, M., Deng, D. and Hess, R.F., 2012. Does partial occlusion promote normal binocular function? *Investigative Ophthalmology and Visual Science*, 53(11), pp.6818–6827.

Li, J., Thompson, B., Lam, C.S.Y., Deng, D., Chan, L.Y.L., Maehara, G., Woo, G.C., Yu, M. and Hess, R.F., 2011. The role of suppression in amblyopia. *Investigative Ophthalmology and Visual Science*, 52(7), pp.4169–4176.

Li, X., Dumoulin, S.O., Mansouri, B. and Hess, R.F., 2007. Cortical deficits in human amblyopia: their regional distribution and their relationship to the contrast detection deficit. *Investigative Ophthalmology and Visual Science*, 48(4), pp.1575–1591.

Liu, G.T., Atushi, M., Goldsmith, Z., van Erp, T.G.M., Francis, E., Quinn, G., Modestino, E.J., Bonhomme, G.R. and Haselgrove, J.C., 2002. Eye Dominance in the Visual Cortex Using Functional MRI at 1.5 T: An Alternative Method. *Journal of AAPOS*, 6(1), pp.40–48.

Livingstone, M. and Hubel, D.H., 1988. Segregation of Form, Color, Movement and Depth : Anatomy, Physiology, and Perception. *Science*, 240, pp.740–749.

Lovasik, J. V and Szymkiw, M., 1985. Effects of aniseikonia, anisometropia, accommodation, retinal illuminance, and pupil size on stereopsis. *Investigative Ophthalmology and Visual Science*, 26(5), pp.741–750.

Lu, Z. and Sperling, G., 2012. Black – white asymmetry in visual perception. *Journal of Vision*, 12(10), pp.1–21.

Ludvigh, E., 1941. Extrafoveal visual acuity as measured with Snellen test-letters. *American Journal of Ophthalmology*, 25(3), pp.303-310.

MacMillan, E.S., Gray, L.S. and Heron, G., 2007. Visual adaptation to interocular brightness differences induced by neutral-density filters. *Investigative Ophthalmology and Visual Science*, 48(2), pp.935–942.

Maehara, G., Thompson, B., Mansouri, B., Farivar, R. and Hess, R.F., 2011. The perceptual consequences of interocular suppression in amblyopia. *Investigative Ophthalmology and Visual Science*, 52(12), pp.1–39.

Maguire, G.W., Smith, E.L., Harwerth, R.S. and Crawford, M.L., 1982. Optically induced anisometropia in kittens. *Investigative Ophthalmology and Visual Science*, 23(2), pp.253–264.

Mallett, R., 1988. *Techniques of investigation of binocular vision anomalies*. *Optometry*, London: Butterworths, pp.238–284.

Mansouri, B., Allen, H.A., and Hess, R.F., 2005. Detection, discrimination and integration of second-order orientation information in strabismic and anisometropic amblyopia. *Vision Research*, 45(18), pp.2449–2460.

Mansouri, B., Thompson, B. and Hess, R.F., 2008. Measurement of suprathreshold binocular interactions in amblyopia. *Vision Research*, 48(28), pp.2775–2784.

Mansouri, B., Singh, P., Globa, A. and Pearson, P., 2014. Binocular training reduces amblyopic visual acuity impairment. *Strabismus*, 22(1), pp.1–6.

Mareschal, I. and Baker, C.L., 1998. Temporal and spatial response to second-order stimuli in cat area 18. *Journal of Neurophysiology*, 80(6), pp.2811–2823.

McIlhagga, W. and Peterson, R., 2006. Sinusoid = light bar + dark bar?, *Vision Research*, 46(12), pp.1934–1945.

McKee, S.P., Levi, D.M. and Movshon, J.A., 2003. The pattern of visual deficits in amblyopia. *Journal of Vision*, 3(5), pp.380–405.

Meese, T.S., Georgeson, M.A. and Baker, D.H., 2006. Binocular contrast vision at and above threshold. *Journal of Vision*, 6(11), pp.1224–1243.

Mehdorn, E., 1989. Suppression scotomas in primary microstrabismus--a perimetric artefact. *Documenta Ophthalmologica*, 71(1), pp.1–18.

Millodot, M., 2014. *Dictionary of Optometry and Visual Science*. Seventh ed. Oxford, UK: Butterworth-Heinemann, p.450.

Millodot, M., Johnson, C. a, Lamont, a and Leibowitz, H.W., 1975. Effect of dioptrics on peripheral visual acuity. *Vision Research*, 15(12), pp.1357–1362.

Mower, G.D., Christen, W.G., Burchfiel, J.L. and Duffy, F.H., 1984. Microiontophoretic bicuculline restores binocular responses to visual cortical neurons in strabismic cats. *Brain Research*, 309(1), pp.168–172.

Narasimhan, S., Harrison, E.R. and Giaschi, D.E., 2012. Quantitative measurement of interocular suppression in children with amblyopia. *Vision Research*, 66, pp.1–10.

Von Noorden, G. and Campos, E., 2002. *Binocular vision and ocular motility: theory and management of strabismus*. 6th ed. MIssouri: Mosby.

Von Noorden, G.K., 1974. Factors involved in the production of amblyopia. *The British Journal of Ophthalmology*, 58(3), pp.158–164.

Von Noorden, G.K., 1985. Amblyopia: a multidisciplinary approach. Proctor lecture. *Investigative Ophthalmology and Visual Science*, 26(12), pp.1704–1716.

Von Noorden, G.K. and Leffler, M.B., 1966. Visual Acuity in Strabismic Amblyopia Under Monocular and Binocular Conditions. *Archives of Ophthalmology*, 76(2), pp.172–177.

Norcia, A.M., Tyler, C.W. and Hamer, R.D., 1990. Development of contrast sensitivity in the human infant. *Vision Research*, 30(10), pp.1475–1486.

Nordmann, J.P., Freeman, R.D. and Casanova, C., 1992. Contrast sensitivity in amblyopia: masking effects of noise. *Investigative Ophthalmology and Visual Science*, 33(10), pp.2975–2985.

Ooi, T.L., Su, Y.R., Natale, D.M. and He, Z.J., 2013. A push-pull treatment for strengthening the 'lazy eye' in amblyopia. *Current Biology* , 23(8), pp.R309–310.

Pardhan, S. and Gilchrist, J., 1990. The effect of monocular defocus on binocular contrast sensitivity. *Ophthalmic and Physiological Optics*, 10(1), pp.33–36.

Pardhan, S., Gilchrist, J., Douthwaite, W. and Yap, M., 1990. Binocular inhibition: Psychophysical and electrophysiological evidence. *Optometry and Vision Science*, 67(9), pp.688–691.

Patel, A.S. and Jones, R.W., 1968. Increment and Decrement Visual Thresholds. *Journal of the Optical Society of America*, 58(5), pp.696–699.

Peichl, L. and Wässle, H., 1983. The structural correlate of the receptive field centre of alpha ganglion cells in the cat retina. *The Journal of Physiology*, 341, pp.309–324.

Peli, E., 1990. Contrast in complex images. *Journal of the Optical Society of America*, 7(10), pp.2032–2040.

Pelli, D.G., 1997. The VideoToolbox software for psychophysics: transforming numbers into movies. *Spatial Vision*, 10(4), pp.437–442.

Peterhans, E. and Von der Heydt, R., 1989. Mechanisms of contour perception in monkey visual cortex. II. Contours bridging gaps. *The Journal of Neuroscience*, 9(5), pp.1749–1763.

Pianta, M.J. and Kalloniatis, M., 1998. Characteristics of anisometropic suppression, *Perception and Psychophysics*, 60(3), pp.491–502.

Poggio, G. and Talbot, W., 1981. Mechanisms of static and dynamic stereopsis in foveal cortex of the rhesus monkey. *The Journal of Physiology*, 315, pp.469–492.

Pointer, J. and Hess, R.F., 1989. The contrast sensitivity gradient across the human visual field: with emphasis on the low spatial frequency range. *Vision Research*, 29(9), pp.1133–1151.

Pratt-Johnson, J.A. and Tillson, G., 1983. Suppression in strabismus and the hemiretinal trigger mechanism. *Archives of Ophthalmology*, 101(2), pp.218–224.

Pugh, M., 1954. Foveal vision in amblyopia. *The British Journal of Ophthalmology*, 38(6), pp.321-331.

Purpura, K., Kaplan, E. and Shapley, R.M., 1988. Background light and the contrast gain of primate P and M retinal ganglion cells. *Proceedings of the National Academy of Sciences of the United States of America*, 85(12), pp.4534–4537.

Ransom-Hogg, A. and Spillmann, L., 1980. Perceptive field size in fovea and periphery of the light- and dark-adapted retina. *Vision Research*, 20(3), pp.221–228.

Rorden, C. and Karnath, H.-O., 2004. Using human brain lesions to infer function: a relic from a past era in the fMRI age? *Nature Reviews Neuroscience*, 5(10), pp.813–819.

Rovamo, J. and Kukkonen, H., 1996. The effect of noise check size and shape on grating detectability. *Vision Research*, 36(2), pp.271–279.

Rovamo, J., Virsu, V. and Näsänen, R., 1978. Cortical magnification factor predicts the photopic contrast sensitivity of peripheral vision. *Nature*, 271(5), pp.54–56.

Rowe, F.J., 2012. *Clinical Orthoptics*. Oxford: Blackwell Science, p.468.

Scheiman, M. and Wick, B., 2008. *Clinical Management of Binocular Vision: Heterophoric, Accommodative, and Eye Movement Disorders*. 3rd ed. Philadelphia: Lippincott Williams and Wilkins, p.748.

Schira, M.M., Tyler, C.W., Breakspear, M. and Spehar, B., 2009. The foveal confluence in human visual cortex. *The Journal of Neuroscience*, 29(28), pp.9050–9058.

Schofield, A.J. and Georgeson, M.A., 1999. Sensitivity to modulations of luminance and contrast in visual white noise: separate mechanisms with similar behaviour. *Vision Research*, 39(16), pp.2697–2716.

Schofield, A.J. and Georgeson, M.A., 2003. Sensitivity to contrast modulation: the spatial frequency dependence of second-order vision. *Vision Research*, 43(3), pp.243–259.

Schofield, A.J. and Georgeson, M.A., 2011. Functional architecture for binocular summation of luminance- and contrast-modulated gratings. *Perception*, 40, p.17.

Schor, C.M., 1977. Visual stimuli for strabismic suppression. *Perception*, 6, pp.583–593.

Sengpiel, F. and Blakemore, C., 1996. The Neural Basis of Suppression and Amblyopia in Strabismus. *Eye*, 10, pp.250–258.

Sengpiel, F., Blakemore, C., Kind, P. and Harrad, R.A., 1994. Interocular suppression in the Visual Cortex of Strabismic cats. *Journal of Neuroscience*, 14(11), pp.6855–6871.

Sengpiel, F., Jirmann, K.-U., Vorobyov, V. and Eysel, U.T., 2006. Strabismic suppression is mediated by inhibitory interactions in the primary visual cortex. *Cerebral cortex*, 16(12), pp.1750–1758.

Simmers, A.J., Ledgeway, T., Hess, R.F. and McGraw, P. V, 2003. Deficits to global motion processing in human amblyopia. *Vision Research*, 43(6), pp.729–738.

Simpson, T.L., 1991. The suppression effect of simulated anisometropia. *Ophthalmic and Physiological Optics,* 11(4), pp.350–358.

Simpson, T.L., 1992. Monocular Acuity in the Presence and Absense of Fusion. *Optometry and Vision Science*, 69(5), pp.405–410.

Sireteanu, R. and Fronius, M., 1981. Naso-temporal asymmetries in human amblyopia: consequence of long-term interocular suppression. *Vision Research*, 21(7), pp.1055–1063.

Sireteanu, R., Fronius, M. and Singer, W., 1981. Binocular interaction in the peripheral visual field of humans with strabismic and anisometropic amblyopia. *Vision Research*, 21(7), pp.1065–1074.

Smith, A.T. and Ledgeway, T., 1997. Separate detection of moving luminance and contrast modulations: fact or artifact? *Vision Research*, 37(1), pp.45–62.

Smith, A.T. and Ledgeway, T., 1998. Sensitivity to second-order motion as a function of temporal frequency and eccentricity. *Vision Research*, 38(3), pp.403–410.

Smith, E.L., Chino, Y.M., Ni, J., Cheng, H., Crawford, M.L. and Harwerth, R.S., 1997. Residual binocular interactions in the striate cortex of monkeys reared with abnormal binocular vision. *Journal of Neurophysiology*, 78(3), pp.1353–1362.

Smith, E.L., Harwerth, R.S. and Crawford, M.L., 1985. Spatial contrast sensitivity deficits in monkeys produced by optically induced anisometropia. *Investigative Ophthalmology and Visual Science*, 26(3), pp.330–342.

Smith, E.L., Harwerth, R.S., Duncan, G.C. and Crawford, M.L.J., 1986. A comparison of the spectral sensitivities of monkeys with anisometropic and stimulus deprivation amblyopia. *Behavioural Brain Research*, 22(1), pp.13–24.

Smith, E.L., Levi, D.M., Manny, R. and Harwerth, R.S., 1985. The relationship between binocular rivalry and strabismic suppression. *Ophthalmology and Visual Science*, pp.80–87.

Song, S., Levi, D.M. and Pelli, D.G., 2014. A double dissociation of the acuity and crowding limits to letter identification, and the promise of improved visual screening. *Journal of Vision*, 14(5), pp.1–37.

Sukumar, S. and Waugh, S.J., 2007. Separate first- and second-order processing is supported by spatial summation estimates at the fovea and eccentrically. *Vision Research*, 47(5), pp.581–596.

Teller, D.Y. and Galanter, E., 1967. Brightnesses, luminances, and Fechner's paradox. *Perception and Psychophysics*, 2(7), pp.297–300.

To, L., Thompson, B., Blum, J.R., Maehara, G., Hess, R.F. and R, J., 2011. A game platform for treatment of amblyopia. *IEEE Transactions on Neural Systems and Rehabilitation Engineering*, 19(3), pp.280–289.

Du Toit, R., Ferreira, J. and Nel, Z., 1998. Visual and nonvisual variables implicated in monovision wear. *Optometry and Vision Science*, 75(2), pp.119–125.

Tong, F., Nakayama, K., Vaughan, J.T. and Kanwisher, N., 1998. Binocular rivalry and visual awareness in human extrastriate cortex. *Neuron*, 21(4), pp.753–759.

Tong, F., Meng, M. and Blake, R., 2006. Neural bases of binocular rivalry. *Trends in Cognitive Sciences*, 10(11), pp.502–511.

Travers, T.A.B., 1938. Suppression of vision in squint and its association with retinal correspondence and amblyopia. *The British Journal of Ophthalmology*, 22(10), pp.577–604.

Tsuchiya, N. and Koch, C., 2005. Continuous flash suppression reduces negative afterimages. *Nature Neuroscience*, 8(8), pp.1096–1101.

De Valois, R., Morgan, H. and Snodderly, D., 1974. Psychophysical studies of monkey Vision-III. Spatial luminance contrast sensitivity tests of macaque and human observers. *Vision Research*, 14, pp.75–81.

Wade, N., 1998. Early studies of eye dominance. *Laterality: Asymmetries of Body, Brain and Cognition*, 3(2), pp.97–108.

Wallace, D., Lazar, E., Melia, M., Birch, E., Holmes, J.M., Hopkins, K., Kraker, R.T., Kulp, M.T., Pang, Y., Repka, M.X., Tamkins, S.M. and Weise, K.K., 2011. Stereoacuity in children with anisometropic amblyopia. *Journal of AAPOS*, 15(5), pp.455–461.

Wensveen, J.M., Smith, E.L. and Harwerth, R.S., 2001. Clinical suppression in monkeys reared with abnormal binocular visual experience. *Vision Research*, 41(12), pp.1593-1608.

Westendorf, D.H. and Fox, R., 1977. Binocular detection of disparate light flashes. *Vision Research*, 17(6), pp.697–702.

Whittle, P., 1986. Increments and decrements: Luminance discrimination. *Vision Research*, 26(10), pp.1677–1691.

Wick, B., Wingard, M., Cotter, S.A. and Scheiman, M., 1992. Anisometropic amblyopia: is the patient ever too old to treat? *Optometry and Vision Science*, 69(11), pp.866–878.

Wiesel, T.N. and Hubel, D.H., 1963a. Effects of Visual Deprivation on Morphology and Physiology of cells in the Cat's Lateral Geniculate Body. *Journal of Neurophysiology*, 26, pp.978–993.

Wiesel, T.N. and Hubel, D.H., 1963b. Single-cell responses in striate cortex of kittens deprived of vision in one eye. *Journal of Neurophysiology*, 26(1003), pp.1003–1017.

Wiesel, T.N. and Hubel, D.H., 1966. Spatial and Chromatic Interactions in the Lateral Geniculate Body of the Rhesus Monkey. *Journal of Neurophysiology*, pp.1115–1156.

Wilcox, L.M. and Hess, R.F., 1996. Is the site of non-linear filtering in stereopsis before or after binocular combination? *Vision Research*, 36(3), pp.391–399.

Wilson, H.R., 1991. Model of peripheral and amblyopic hyperacuity. *Vision Research*, 31(6), pp.967–982.

Wolfe, J.M., 1986. Briefly presented stimuli can disrupt constant suppression and binocular rivalry suppression. *Perception*, 15(4), pp.413–417.

Wong, A.M.F., Burkhalter, A. and Tychsen, L., 2005. Suppression of metabolic activity caused by infantile strabismus and strabismic amblyopia in striate visual cortex of macaque monkeys. *Journal of AAPOS*, 9(1), pp.37–47.

Wong, E.H. and Levi, D.M., 2005. Second-order spatial summation in amblyopia. *Vision Research*, 45(21), pp.2799–2809.

Wong, E.H., Levi, D.M. and McGraw, P. V, 2001. Is second-order spatial loss in amblyopia explained by the loss of first-order spatial input? *Vision Research*, 41(23), pp.2951–2960.

Wong, E.H., Levi, D.M. and McGraw, P. V, 2005. Spatial interactions reveal inhibitory cortical networks in human amblyopia. *Vision Research*, 45(21), pp.2810–2819.

Wood, I.C., 1983. Stereopsis with spatially-degraded images. *Ophthalmic and Physiological Optics*, 3(3), pp.337–340.

Wunderlich, K., Schneider, K. a and Kastner, S., 2005. Neural correlates of binocular rivalry in the human lateral geniculate nucleus. *Nature Neuroscience*, 8(11), pp.1595–1602.

Yang, E. and Blake, R., 2012. Deconstructing continuous flash suppression. *Journal of Vision*, 12(3), pp.1–14.

Yang, E., Blake, R. and McDonald, J.E., 2010. A new interocular suppression technique for measuring sensory eye dominance. *Investigative Ophthalmology and Visual Science*, 51(1), pp.588–593.

Yap, Y.L., Levi, D.M. and Klein, S., 1987. Peripheral hyperacuity: three-dot bisection scales to a single factor from 0 to 10 degrees. *Journal of the Optical Society of America*, 4(8), pp.1554–1561.

Zele, A.J., Wood, J.M. and Girgenti, C.C., 2010. Magnocellular and parvocellular pathway mediated luminance contrast discrimination in amblyopia. *Vision Research*, 50(10), pp.969–976.

Zhang, P., Bobier, W.R., Thompson, B. and Hess, R.F., 2011. Binocular balance in normal vision and its modulation by mean luminance. *Optometry and Vision Science : official publication of the American Academy of Optometry*, 88(9), pp.1072–1079.

Zhou, J., Georgeson, M.A. and Hess, R., 2014. Linear binocular combination of responses to contrast modulation: Contrast-weighted summation in first-and second-order vision. *Journal of Vision*, 14, pp.1–19.

Zhou, J., Huang, P. and Hess, R.F., 2013. Interocular suppression in amblyopia for global orientation processing. *Journal of Vision*, 13(5), pp.1–14.

Zhou, J., Jia, W., Huang, C. and Hess, R.F., 2013. The effect of unilateral mean luminance on binocular combination in normal and amblyopic vision. *Scientific Reports*, 3, p.2012.

Zhou, J., Liu, R., Zhou, Y. and Hess, R.F., 2014. Binocular Combination of Second-Order Stimuli. *PLoS One*, 9(1), p.e84632

Zhou, Y. and Baker, C.L., 1993. A Processing Stream in Mammalian Visual Cortex Neurons for Non-Fourier Responses. *Science*, 261(5117), pp.98–101.

Zhou, Y., Huang, C., Xu, P., Tao, L., Qiu, Z., Li, X. and Lu, Z.-L., 2006. Perceptual learning improves contrast sensitivity and visual acuity in adults with anisometropic amblyopia. *Vision Research*, 46(5), pp.739–750.

Zilles, K. and Amunts, K., 2010. Centenary of Brodman's map - conception and fate. *Nature Reviews Neuroscience*, 11(2), pp.139–146.